KILLING OF MYCOBACTERIA BY MACROPHAGE CATHEPSIN D

by

MAYURI JUGMOHAN

BSc Biochemistry Honours, University of KwaZulu-Natal

Submitted in partial fulfilment of the requirements for the degree of

MASTER OF SCIENCE IN BIOCHEMISTRY

University of KwaZulu-Natal

Pietermaritzburg

January 2011

Preface

The experimental work described in this dissertation was carried out in the School of Biochemistry, Genetics and Microbiology, University of KwaZulu-Natal, Pietermaritzburg, South Africa, from January 2008 to January 2011, under the supervision of Dr. Edith Elliott.

These studies represent original work by the author (candidate) and have not otherwise been submitted in any form for any degree or diploma to any tertiary institution. Where use has been made of the work of others it was duly acknowledged in the text.

Supervisor signature: ..... Date: .....

Dr. Edith Elliott

Candidate signature: ..... Date: .....

Ms Mayuri Jugmohan

Declaration – Plagiarism

I, ..., declare that

(i) The research reported in this dissertation, except where otherwise indicated, is my original work.

(ii) This dissertation has not been submitted for any degree or examination at any other university.

(iii) This dissertation does not contain other persons‟ data, pictures, graphs or other information, unless specifically acknowledged as being sourced from other researchers.

(iv) This dissertation does not contain other persons‟ writing, unless specifically acknowledged as being sourced from other researchers. Where other written sources have been quoted, then:

a) their words have been re-written but the general information attributed to them has been referenced;

b) where their exact words have been used, their writing has been placed inside quotation marks, and referenced.

(v) Where I have reproduced a publication of which I am an author, co-author or editor, I have indicated in detail which part of the publication was actually written by myself alone and have fully referenced such publications.

(vi) This dissertation does not contain text, graphics or tables copied and pasted from the Internet, unless specifically acknowledged and the source being detailed in the dissertation and in the references sections.

Candidate Signed:

Abstract

Tuberculosis (TB) is the fifth largest cause of death in South Africa, with one in ten cases being resistant to treatment due to the development of multidrug-resistance and extensively drug-resistance in the agent responsible for this disease, *Mycobacterium tuberculosis*. This pathogen has developed mechanisms to evade killing by immune cells such as macrophages. *Mycobacterium smegmatis*, a non-pathogen, that does not evade killing by the macrophage, is often used to gain a better insight into the bacteriocidal pathways used to kill mycobacteria, and those potentially blocked by *M.tuberculosis*. In such studies nitric oxide and "lysosomal" proteases have emerged as major bacteriocidal pathways. Studies on the role of aspartic protease, cathepsin D, in killing green fluorescent protein- (GFP-) tagged-*M.smegmatis* in J774 macrophages required antibodies that would not cross-react with mycobacterial antigens. These were raised in chickens, using alum and saponin as adjuvants, and porcine and human cathepsin D. Using such antibodies, quantitative colocalization analysis using ImageJ and the JACoP colocalization plugins showed a greater degree of colocalization between cathepsin D and LysoTracker Red DND-99 in *M.smegmatis*-infected J774 macrophages than in uninfected cells. This indicates the possible presence of active, bacteriocidal cathepsin D in acidic, and hence matured phagosomes. A higher colocalization between cathepsin D and LAMP-1 and cathepsin D and LAMP-2 in uninfected cells possibly indicates the recycling of these two markers from vesicles not containing killed bacteria. Propidium iodide (PI) labelling and loss of GFP fluorescence appeared reliable indicators of *M.smegmatis* death or viability, respectively, as myobacteria that took up PI also lost green fluorescence, while *M.smegmatis* that exhibited green fluorescence (viable) were not observed to take up propidium iodide (dead). Faint colocalization between cathepsin D, LAMP-1 and -2 with dead, and to a lesser extent with live *M.smegmatis* occurred. Besides intensity correlation values other colocalization programs indicate the absence of colocalization between these markers and dead *M.smegmatis*, but, together with *in vitro* killing experiments (cathepsin D, 0.0098 units/ml resulting in 59% killing in 4 h) these appear to indicate a possible role of cathepsin D in killing of *M.smegmatis*.

Acknowledgements

Education is one of the greatest gifts that God has given to me and without God‟s love I would not have been able to have achieved all that I have. Om Namah Shivaya, thank you God for pulling me through my darkest days.

During the course of my studies I was fortunate to have been helped and supported by many wonderful people. I would like to thank:

Dr. Edith Elliott, my supervisor, for taking me on as a student, for pushing me to develop into an independent thinker, for teaching me to question and understand aspects of both science and life in general and for always putting the well-being of her students before her own.

Dr. Celia Snyman, for her patience in teaching me difficult techniques such as cell culture and sectioning. I also appreciate her willingness to help solve problems that were both of a scientific and personal nature and for always encouraging me.

Priscilla Donnelly, Patricia Joubert, Tutuzwa Xuma and Shirley Mackellar, the staff of the Electron Microscopy Unit for teaching and assisting me with transmission electron and confocal microscopy work.

Prof. Anderson, Prof. Coetzer, Prof. Goldring, Dr. Niesler, Dr. Che Pillay, Jessica Subramani and Yegan Pillay for their advice and interest in my work.

Robyn Hillebrand, Charmaine Ahrens, Richard Shabalala and Agnes Zondi for general assistance.

Adushan Pillay, Candice Crouch, Jocelyne Mwabi, Daniel Bohnen, Blessing Mkhwanazi, Cherise Dunn, Bongiwe Xulu and Louis Buzwani, my fellow lab mates, for creating a wonderful atmosphere in the lab and for sharing their knowledge and expertise with me.

Richard Kangethe, Davita Pillay, Lorelle Bizaare, Phillia Vukea, Laurelle Jackson, Kayleen Brien, Hlumani Ndlovu, Sabelo Hadebe, Hermogenes Mucache, Cara-Lesley Bartlett, Bridgette Cumming, Dennis Lin, David Choveaux, Jacqueline Foster Viljoen, Melissa Govender, Ramona Hurdayal, Kyle Goetsch, Scott Driscoll and Ike Achilonu, my fellow students, for their support, help and friendship.

Thashni Chetty, Andrea Pillay and Kaitlin Koorbanally, my wonderful friends/ sisters for their love and support.

Benice Sivparsad, Mark Pillay and Kumar Bridgmohan, for the fun and memorable times that we‟ve shared.

Perina Vather, Avrashka Govender and Rosandya Govender, my diva sisters, for their love, friendship and encouragement and for making even the toughest days a bit brighter.

My Nana and Nanie, Mr and Mrs G.D Raghubir, my Ma and Aja, Veena and Suresh Ramsundar, Githa Monie, Pro Kaka, Kunthi Ma and Nokupiwe Shezi for their love and concern.

Sayog and Shericha, my siblings, for always being there for me and for their constant love and encouragement especially during my difficult moments.

My parents Pete and Mickey Jugmohan, I know that I have driven you two insane with my ups and downs especially during my studies. I would like to thank you for never letting me quit and for always pushing me to try my best. Thank you for your emotional and financial support and for putting up with all the tears, I love you both unconditionally and I dedicate this thesis to the both of you.

Table of Contents

List of Figures

List of Tables

List of abbreviations and symbols

ε	extinction coefficient
λ	wavelength
%	percentage
ºC	degrees Celsius
~	approximately
μm	micrometer (10^{-6} meter)
AMPs	antimicrobial peptides
AP	adaptor protein
APCs	antigen presenting cells
ASMase	acid sphingomyelinase
ATP	adenosine triphosphate
β_2M	β_2-microglobulin
BCG	bacillus Calmette-Guérin
BCIP	5-bromo-4-chloro-3-indolyl phosphate
BLAST	basic local alignment tool
BSA	bovine serum albumin
C3	third component of complement
CBB	Coomassie brilliant blue
CDR	complementary determining regions
CFU	colony forming units
C_H	immunoglobulin heavy chain constant region
C_L	immunoglobulin light chain constant region
CLIP	class II-associated Ii peptide
Cm	centimeter

CR	complement receptors
CTL	cytotoxic T lymphocyte
CY3	cyanine 3
CY5	cyanine 5
DAB	3,3‟-diaminobenzidine
dH_2O	distilled water
DMEM	Dulbecco‟s modified Eagle‟s medium
DMF	dimethylformamide
EDTA	ethylene diamine tetraacetic acid
EEA1	early endosome antigen 1
EGF	epidermal growth factor
EGFP	enhanced green fluorescent protein
EGTA	ethylene glycol-bis(β-aminoethyl ether) *N*,*N*,*N*‟,*N*‟-tetra acetic acid
ELISA	enzyme linked immunosorbent assay
EM	electron microscopy
ER	endoplasmic reticulum
Fc	fragment crystallizable
FcγR	receptors binding the Fc region of the indicated Ig molecule (γ forIgG)
FCA	Freund‟s complete adjuvant
FCS	foetal calf serum
FIA	Freund‟s incomplete adjuvant
FITC	fluorescein isothiocyanate
FSG	fish skin gelatine
g	relative centrifugal force
GFP	green fluorescent protein
GTPases	guanosine triphosphatase
h	hour(s)

HBSS	Hank‟s Balanced Salts
Hck	hematopoietic cell kinase
HEPES	*N*-2-hydroxy-piperazine-*N*‟-2 ethane sulfonic acid
H_2O_2	hydrogen peroxide
HRP	horseradish peroxide
HIV	human immunodeficiency virus
HLA-DM	human leukocyte antigen-DM
HOCl	hypochlorous acid
ICA	intensity correlation analysis
ICCB	intensity correlation coefficient-based
ICQ	intensity correlation quotient
IFN-γ	interferon-γ
IgG, IgY, IgA, IgM, IgE	immunoglobulins G, Y, A, M and E
IGF-1	insulin-like growth factor-1
Ii	invariant chain
IL	interleukin
iNOS	inducible NO synthase
ITAMs	immunoreceptor tyrosine-based activation motifs
IPTG	isopropyl β-D-1-thiogalactopyranoside
JACoP	Just Another Co-localization Plugin
k_1 and k_2	overlap coefficients expressed as two parameters
kDa	kiloDalton(s)
l	litre(s)
LAMP(s)	lysosomal associated membrane proteins
LR	London Resin
LSM	laser scanning microscope

LYAAT	lysosomal amino acid transporter
mA	milliAmp
MAPK	mitogen activated protein kinase
MHC	major histocompatibility complex
MIIC	MHC class II-containing compartment
min	minute(s)
M6P	mannose-6-phosphate
M6PRs	mannose-6-phosphate-receptors
M6PR-46	cation-dependent mannose-6-phosphate-receptor-46
M6PR-300	cation-independent mannose-6-phosphate- receptor-300
MVBs	multivesicular bodies
MWM	molecular weight marker
NADPH	nicotinamide adenine dinucleotide phosphate (reduced form)
NBT	nitroblue tetrazolium
NK	natural killer
nm	nanometer (10^{-9} meter)
NO	nitric oxide
NOS	NO synthase
NOD1	Nucleotide-binding oligomerization domain- containing protein1
Nramp	natural resistance associated macrophage protein
O_2^-	superoxide
$OH^{\cdot}$	hydroxyl radical
PAGE	polyacrylamide gel electrophoresis
PAMPs	pattern-associated molecular patterns
PBS	phosphate buffered saline

PEG	polyethylene glycol
PFA	paraformaldehyde
PHEM	PIPES, HEPES, EGTA and $MgCl_2$ buffer
PI	propidium iodide
PMTS	photo-multiplying tubes
PIPES	piperazine-*N*,*N*‟-bis (2-ethanesulfonic acid)
Ponceau S	3-hydroxy-4-[2-sulfo-4(sulfo-phenylazo) phenylazo]2,7-naphthalene disulfonic acid
PRRs	pattern-recognition receptors
PVDF	polyvinylidene difluoride
(*r*)	Pearson‟s correlation coefficient
RER	rough endoplasmic reticulum
RGB	red-green-blue
RNIs	reactive nitrogen intermediates
r.p.m	revolutions per minute
RT	room temperature
s	second(s)
SDS	sodium dodecyl sulfate
SNARE	soluble N-ethylamaleimide-sensitive factor attachment protein receptor
SRP	signal recognition particle
TAP	transporter associated with antigen processing
TB	tuberculosis
TBS	tris-buffered saline
TCA	trichloroacetic acid
TEM	transmission electron microscopy
TEMED	*N,N,N',N'*-tetramethyl ethylenediamine

T_H1	T-helper cell type 1
T_H2	T-helper cell type 2
tif	tagged image file
TLR	toll-like receptor
TNF	tumour necrosis factor
tris	2-amino-2-(hydroxymethyl)-1,3-propandiol
TNF-α	tumor necrosis factor
TPP	three-phase partitioning
V	volts
V-ATPase	vacuolar –ATPase
V_H	immunoglobulin heavy chain variable region
V_L	immunoglobulin light chain variable region

CHAPTER ONE

INTRODUCTION

Members of the mycobacteria group of bacteria may be divided into non-pathogenic, opportunistic and pathogenic mycobacteria. Non-pathogenic mycobacteria include *Mycobacterium smegmatis* (a saprophytic mycobacterial species) whereas *Mycobacterium fortuitum* is considered an opportunist pathogen and species such as *Mycobacterium bovis, Mycobacterium aviam*, *Mycobacterium marinum* and *Mycobacterium tuberculosis* which infect cows, birds, fish and humans, respectively, are considered pathogenic (Bohsali *et al*., 2010; Kaufmann, 2010; Martino *et al*., 2005; Novotny *et al*., 2010; Rennie *et al*., 2010; Tell *et al*., 2001). In humans Tuberculosis (TB), caused by *M. tuberculosis*, is the fifth largest cause of mortality in South Africa. This is a particularly serious health problem as one in ten cases of this disease is resistant to treatment, resulting in treatment-resistant forms of TB such as multidrug-resistant- and extensively drug-resistant TB (McGaw *et al*., 2008; Migliori *et al*., 2010).

Macrophages are one of the main cell types involved in killing *M. tuberculosis*. Although much progress has been made with regards to understanding the mechanisms by which macrophages kill mycobacteria, there are still many aspects which are poorly understood. Several pathogenic mycobacterial species such as *M. tuberculosis* have been shown to alter the bactericidal mechanisms of host macrophages so as to evade killing and subsequently promote their survival within these cells (Clemens and Horwitz, 1995; Russell, 2001; Xu *et al*., 1994). Improving the understanding of macrophage killing and latency, (a condition in which an individual is able to control a *M.tuberculosis* infection maintaining sub-clinical symptoms while not able to eradicate the pathogen), would allow for a better understanding of how 10% of humans who carry *M.tuberculosis* develop the disease while 90% of the infected population do not. It is possible that a reactivation of latent infections may result when the immune system of the individual is compromised, for example, in individuals infected with the human immunodeficiency virus (HIV). An understanding of how macrophages kill mycobacteria is vital for the development of mycobacterial therapies and approaches that may be used to enhance the natural killing activity of macrophages, hence the

current study on macrophages and non-pathogenic mycobacteria such as *M.smegmatis* (Anes *et al*., 2006; Chan and Flynn, 2004; Flynn and Chan, 2001a; Flynn and Chan, 2001b; Lawn *et al*., 2010; Tufariello *et al*., 2003).

1.1. Macrophages

The term "macrophage" originates from the Greek translation for "big eater" and was first used by Elie Metchnikoff more than 100 years ago to describe large mononuclear phagocytic cells (Chang, 2009). Macrophages are usually between 10 and 30 μm in diameter and have a nucleus that is between 6 and 12 μm. Their cytoplasm contains granules and vacuoles that, depending on the physiological and macrophage activation state may be seen using phase contrast microscopy (Elhelu, 1983). Macrophages originate in the bone marrow from pluripotent hematopoietic stem cells (Figure 1.1). These undergo differentiation as a result of exposure to local cytokines such as granulocyte-macrophage colony-stimulating factor and interleukin (IL)-3 that are produced by a variety of cells including T cells, endothelial cells and fibroblasts upon receiving various stimuli (Shi *et al*., 2006). This exposure results in haemopoetic myeloid precursor cells leaving the bone marrow to enter the blood stream where they are referred to as monocytes (Figure 1.1). While in the blood, monocytes come into contact with an abundance of stimulatory and regulatory molecules. These determine subsequent differentiation, final cell type, phenotypic characteristics as well as the location of the cells (Figure 1.1) (Haskó *et al*., 2007; Janeway *et al*., 2005b; Unanue, 1976). Macrophages have several functions including the phagocytosis and elimination of microorganisms, antigen presentation and secretion of biologically active substances whose effects range from inducing cell growth to cell death (Brode and Macary, 2004; Nathan, 1987). Activated macrophages also secrete several cytokines such as interleukin (IL)-1β, tumour necrosis factor-α (TNF-α), IL-6, CXCL8 and IL-12 that have been observed to have local and systematic effects that are ultimately aimed at assisting the host in handling infections. Some of these effects include the induction of fever brought about by the secretion of TNF-α, IL-1β and IL-6 that transmit a pyrogenic message to the hypothalamus where fever is regulated, the activation of natural killer cells, B and T lymphocytes, brought about by the secretion of IL-12, the recruitment of neutrophils, basophils and T cells to an infection site by the secretion of CXCL8 (also known as IL-

8) (Blatteis, 2000; Coma *et al*., 2006; Patterson *et al*., 2002; Russell *et al*., 2009). The focus of the current research, however, is on the role of cathepsin D in killing in the phagosome. For this reason phagocytosis and the events in the phagosome, though complex, form a focus.

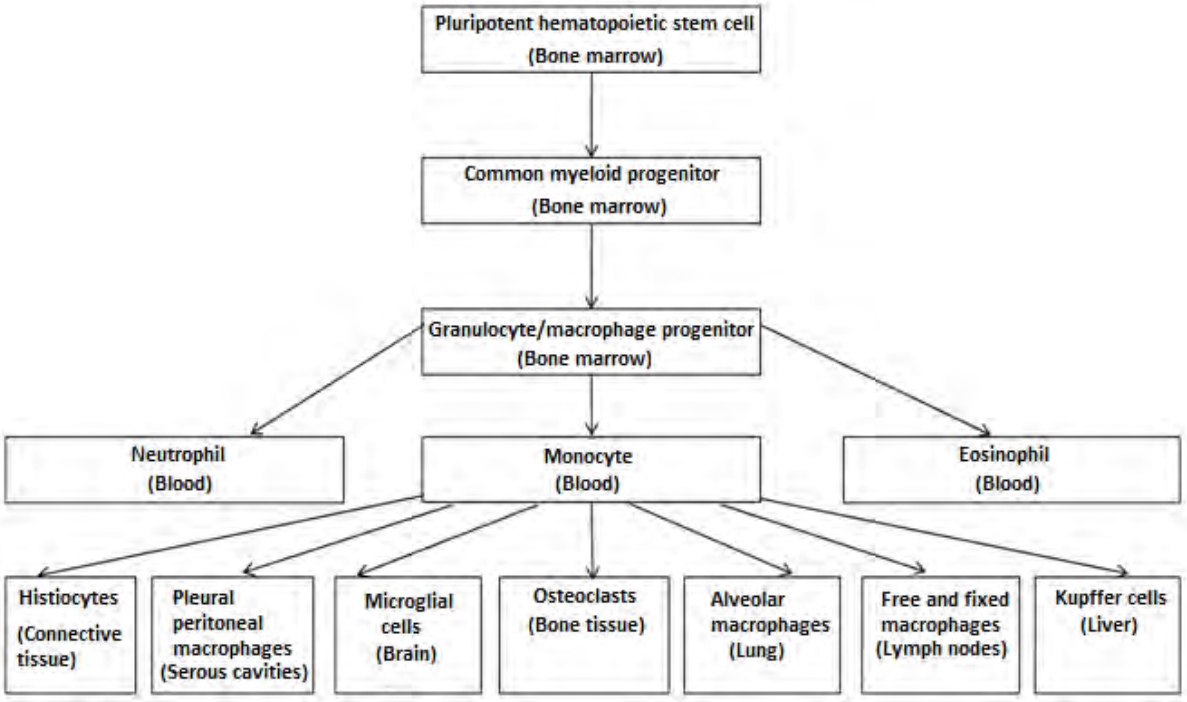

Figure 1.1: The different stages of differentiation of pluripotent hematopoietic stem cells which lead to the formation of macrophages in various locations.

Pluripotent hematopoietic stem cells which are found in the bone marrow undergo several steps of differentiation to form macrophages. Firstly, they differentiate to form common myeloid progenitor cells followed by differentiation into granulocyte/macrophage progenitor cells which are also found in the bone marrow. This leads to the formation of neutrophils, monocytes and eosinophils which are located in the blood. Monocytes thereafter differentiate to form resident macrophages which are named according to their locations (adapted from Janeway *et al*., 2005b; Unanue, 1976).

1.2. Phagocytosis

Macrophages, together with various other cells such as dendritic, mast and neutrophils play vital roles in immunity and the killing of microorganisms. These cells are capable of engulfing foreign material such as bacteria so that further steps may be taken by the immune system to eliminate infection (Bedoui *et al.*, 2010; Dale *et al.*, 2008; Rocha-de-Souza *et al.*, 2008). This process of engulfment is referred to as phagocytosis and is defined as an innate immune response that is triggered by the interaction of various receptors and usually involves the internalization of large particles (generally greater than 0.5 μm in diameter) into a body referred to as a phagosome (May and Machesky, 2001; Wilkinson, 1976).

Besides the engulfment of foreign organisms, phagocytosis is required for antigen presentation, homeostasis, tissue remodeling and inflammation (García-García and Rosales, 2002). Although phagocytosis is a complex process, it may be broken down into several key steps. Firstly, the uptake of the foreign particle is brought about by the interaction of the macrophage surface receptors with specific ligands found on the particle surface (Henneke and Golenbock, 2004). This is followed by the stimulation of actin-polymerization. Thereafter, actin-rich pseudopods extend, "zipper" their membranes around the particle and divide the resultant vacuole from the cell membrane (Figure 1.2). This results in the internalization of the particle and the formation of a phagosome (Allen and Aderem, 1996b; Greenberg, 1999; Huynh *et al*., 2007b). Once internalization is complete, the phagosome undergoes a maturation process (referred to as phagosomal maturation (Figure 1.2) and discussed in Section 1.4) which involves a series of fusion and fission events with various vesicle populations. During these events, the phagosome receives a number of proteins which include hydrolytic enzymes, proton-, vacuolar-ATPases (V-ATPase, which cause the acidification of the phagosome) and antimicrobial peptides which transform the phagosome into a microbicidal organelle (Huynh *et al*., 2007b; Vieira *et al*., 2002). Due to the fact that a portion of the cell membrane is involved in the internalization process and is ultimately internalized, the surface areas of most phagocytic cell membranes decrease after phagocytosis. However, this is not the case with macrophages as quantitative spectroscopic and electrophysiological measurements have shown that their cell surfaces actually remain

the same size or increase slightly after phagocytosis. This is believed to be due to the replacement of the membrane by membranes which are derived from an intracellular reserve i.e. via membrane recycling from internally fused vesicles. Recycling is also associated with antigen processing and cycling of MHC-antigen complexes to the cell surface for antigen presentation (Huynh *et al*., 2007b).

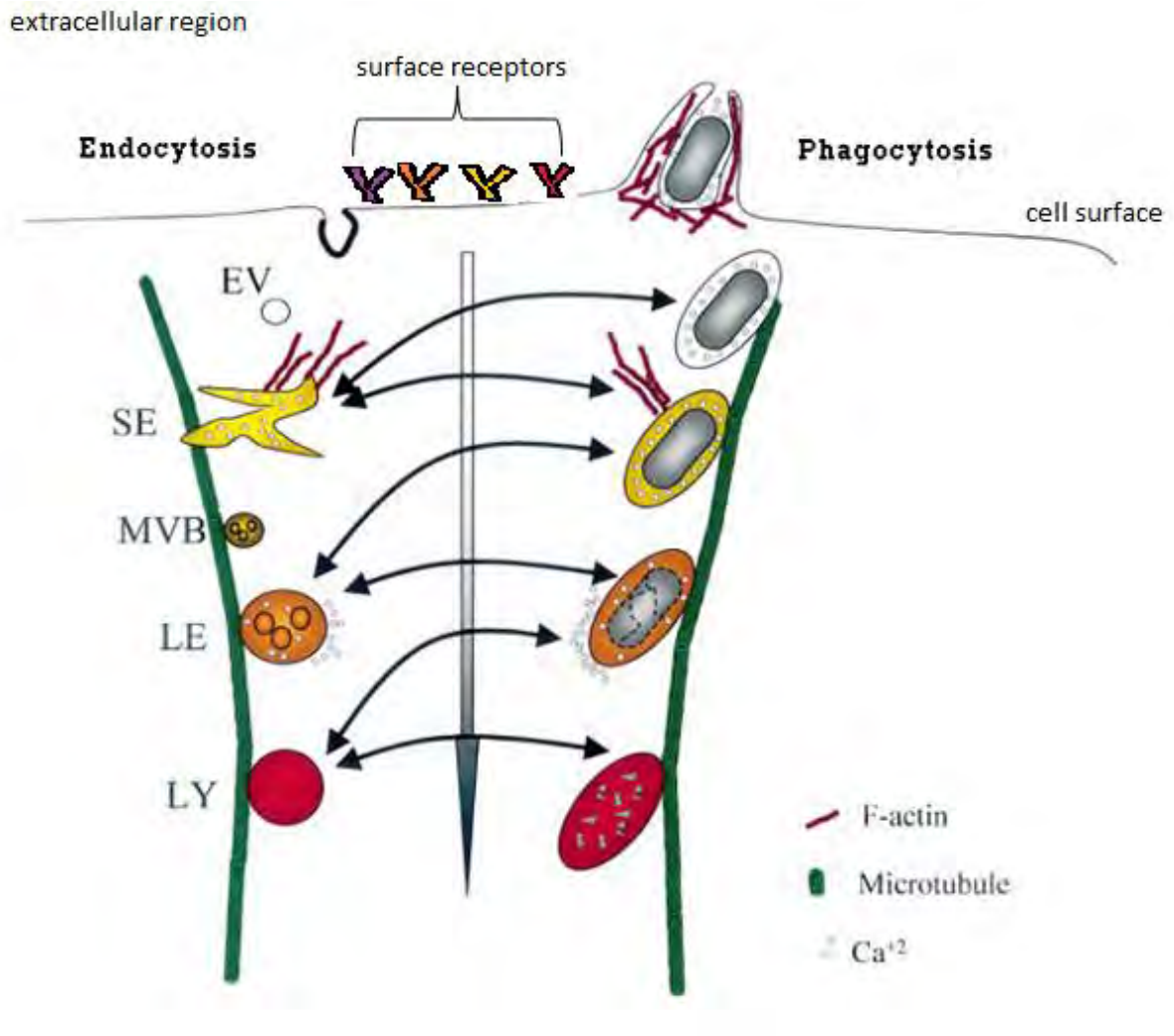

Figure 1.2: The association between the endocytic pathway and phagosomal maturation.

The process of phagosomal maturation involves the organelles of the endocytic pathway and ultimately results in the formation of a "phagolysosome" which has several microbicidal properties. During the initial stages of phagocytosis, actin-rich pseudopods extend, "zipper" their membranes around the foreign particle and divide the resultant vacuole from the cell membrane. The fusion of phagosomes with organelles of the endocytic pathway is indicated by the connecting arrows. The presence of calcium is also illustrated and has been shown to be required for the activation of phagocyte respiratory burst, production of nitric oxide, secretion of microbicidal granule constituents, production of proinflammatory mediators such as TNF-α and is also believed to be necessary for phagosome-lysosome fusion. At the various stages of maturation, endosomes, lysosomes and phagosomes are believed to bind to microtubules. EV = endocytic vesicle, SE = sorting endosome, LE = late endosome, LY = lysosome (adapted from Vieira *et al*., 2002).

1.3 Macrophages and bacterial antigen presentation

Antigen presentation usually involves the introduction of a specific antigen in the form of a peptide bound to a major histocompatibility complex (MHC) molecule (either class I or II) on the surface of an activated antigen presenting cell (APC) to a "cytotoxic" $CD8^+$ or a "helper" $CD4^+$ T cell. Dendritic cells are considered as the major primary APCs, though some macrophages and B cells are also capable of performing this function (Brode and Macary, 2004).

MHC molecules, which provide a means of recognition of antigens by T cells, are divided into two types, MHC class I and II. These molecules contain a polymorphic binding site made up of a β-pleated sheet that is flanked by two α helixes, which form a groove that allows for the binding of a peptide ligand (Singh *et al*., 1997). MHC class I molecules present such peptide fragments that are produced as a result of the degradation of intracellular pathogens. In the case of virally infected cells or intracellular bacteria that escape from the phagosome into the cytoplasm, the peptides formed as a result of the degradation may be presented to naïve (uncommitted or undifferentiated) T cells triggering differentiation to a natural killer or $CD8^+$ T cell, if presented with the peptide fragments (generated by the proteosome), bound to MHC class I molecules. If the antigen is from an extracellular source, it is usually brought into the cell via an endosome or phagosome and presented together with MHC class II molecules to naïve T cells, triggering their differentiation to T-helper cell type 1 (T_H1) or T-helper cell type 2 (T_H2) cells which assist in activation of committed natural killer $CD8^+$ T cells or committed B cells, respectively (Janeway *et al*., 2005a). Committed B cells that are further stimulated by their target antigen will divide and differentiate into plasma or stimulated B cells which will divide and begin to release specific antibodies to that antigen and $CD8^+$ T cells stimulated by mycobacterial antigens may subsequently kill cells infected with mycobacteria, or other pathogens, that may otherwise survive unharmed in infected macrophages (Brode and Macary, 2004; Collins *et al*., 2009; Hewitt, 2003; Smith *et al*., 2008; Yamamoto, 2006).

MHC class I molecules are heterodimers that are made up of a heavy chain which is a type I integral membrane glycoprotein and a β_2-microglobulin (β_2M) soluble protein. The folding and assembly of MHC class I molecules takes place in the lumen of the endoplasmic reticulum (ER) and is aided by the ER chaperone proteins ERP57, calnexin and calreticulum (Figure 1.3). Binding of the processed peptide to the MHC class I molecule is an important part of the assembly process, thus the transportation of processed peptides to the lumen of the ER is needed and this requirement is met by the transporter associated with antigen processing (TAP). TAP also provides a scaffold for the stage in which binding of the peptide to the MHC class I molecule takes place. During this stage, TAP binds to the MHC class I molecule in a complex that also includes the ER chaperones calreticulum and ERP57. For this interaction to occur, tapasin, a transmembrane glycoprotein acts as a bridging molecule between TAP and the MHC class I molecule/chaperone complex. Tapasin also aids the binding of peptides to the MHC class I molecule and once this binding process is complete, the MHC class I molecule/peptide complex dissociates from TAP, clusters at the ER membrane and is selectively transported via cargo vesicles to the Golgi apparatus (Figure 1.3). The MHC class I molecule/ peptide complex is trafficked through the Golgi apparatus to the cell membrane for presentation to committed $CD8^+$ T cells, triggering them to kill the cell containing the cytoplasmic antigen (Hewitt, 2003).

Although it is generally accepted that peptides brought into the cell via phagocytosis/ endocytosis are presented on MHC class II molecules at the cell surface, antigens from intracellular pathogens including phagosomal-mycobacteria, have been observed to also bring about MHC class-I-dependent $CD8^+$ T-cell responses, via a process known as cross-presentation (Belizaire and Unanue, 2009; Houde *et al*., 2003). In a study conducted by Guermonprez *et al*. (2003), this was shown to occur via a fusion event between the phagosome and the ER, resulting in the formation of an "ER-phagosome mix compartment". ER-phagosome fusion allows mycobacterial peptides to be loaded on ER located MHC class I molecules and MHC class I presentation to occur (Savina *et al*., 2006).

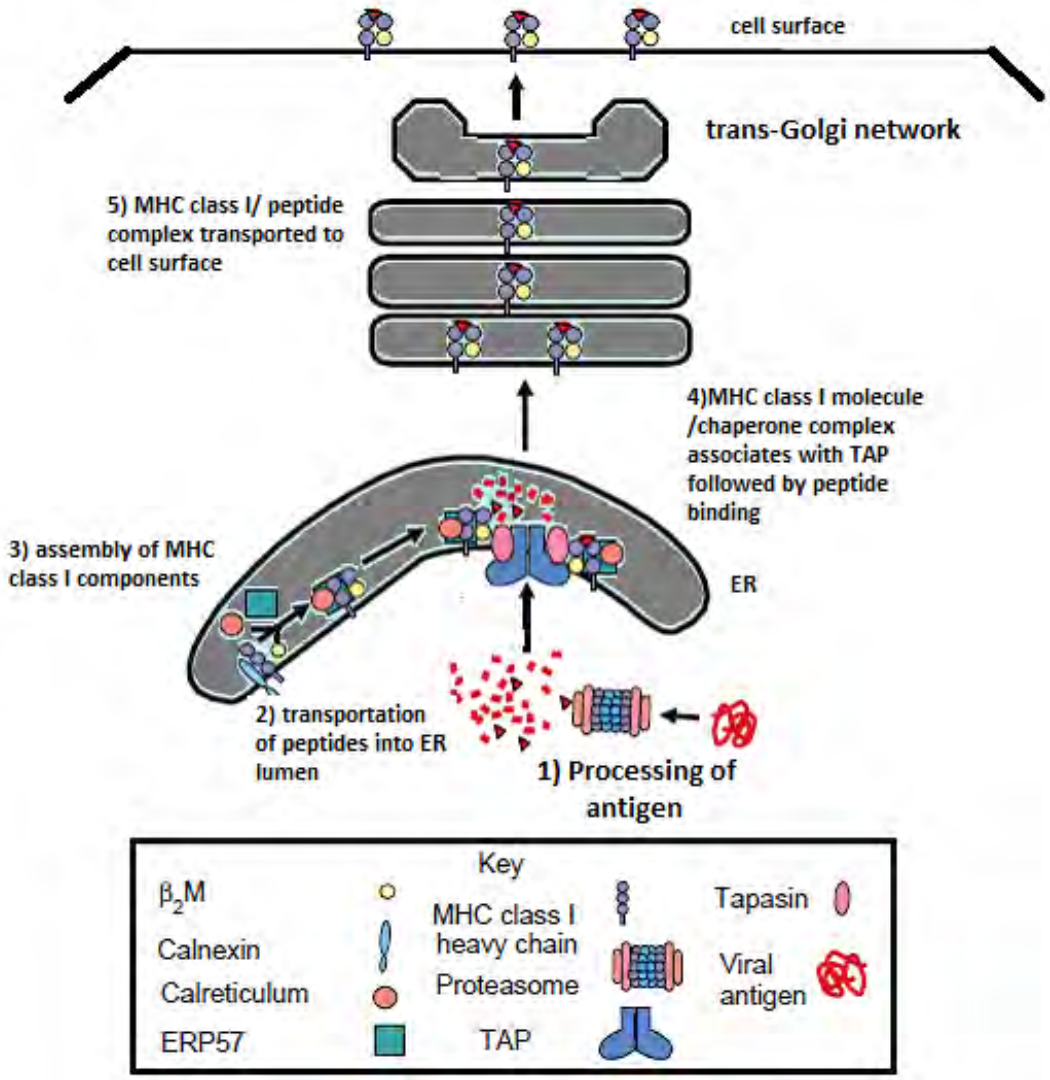

Figure 1.3: Presentation of cytosolic peptides bound to MHC class I molecules.

(1) The proteins that are processed in the cytosol by the proteosome are transported into the lumen of the ER via TAP (2). (3) ER chaperone proteins calnexin, calreticulum and ERP57 bring about the folding and assembly of MHC class I components (heavy chain and β_2M) in the lumen of the ER. (4) The MHC class I molecule/ chaperone complex links with TAP and the binding of the peptide fragment to the MHC class I molecule/ chaperone/ TAP complex is brought about by tapasin. (5) MHC class I molecule/ peptide complex dissociates from TAP and is transported to the Golgi apparatus and subsequently to the cell surface (adapted from Hewitt, 2003).

MHC class II molecules, on the other hand, present peptide fragments, derived from exogenous proteins, to committed $CD4^+$ T cells. These exogenous proteins are usually brought into the APC by endocytosis (where they are contained within an endosome) or phagocytosis. In the case of phagocytosed bacteria, breakdown of the microorganism to potentially antigenic peptides takes place within mature phagosomes (via a series of degradation mechanisms). The loading of peptides onto MHC class II molecules takes place in a special MHC class II-containing compartment referred to as MIIC, a late endosome-like compartment that fuses with the phagosome or endocytic vesicles bringing in antigens (Rocha and Neefjes, 2008).

MHC class II molecule assembly takes place in the ER and the movement of the molecule is assisted by the invariant chain (Ii) (Figure 1.4). Once the Ii has guided the MHC class II molecule to the MIIC, it is processed by cathepsin S to the class II-associated Ii peptide (CLIP) (Figure 1.4). Prior to peptide binding, CLIP occupies the peptide binding groove of the MHC class II molecule and by doing this it prevents premature peptide binding. CLIP is thereafter released in a process which involves the catalytic effect of the class II-related molecule, human leukocyte antigen-DM (HLA-DM) to allow the antigenic peptide to bind to a MHC class II molecule (Figure 1.4) (Ferrante *et al*., 2008; Sendide *et al*., 2005; Singh *et al*., 2006). The antigenic peptide which is bound to the MHC class II molecule is thereafter taken to the surface of the APC where it is presented to committed $CD4^+$ T cells or B cells which then begin to stimulate the production of target antigen-specific antibodies.

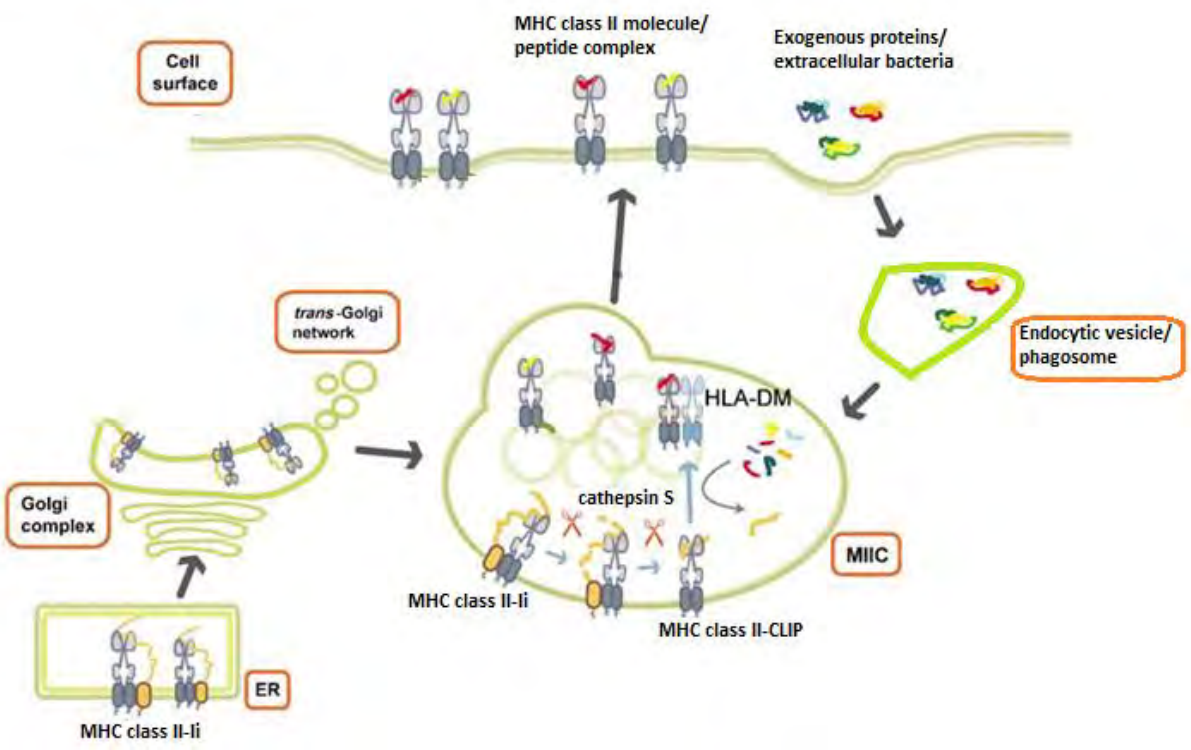

Figure 1.4: Presentation of endosomal/phagosomal peptides bound to MHC class II molecules.

Exogenous proteins/ extracellular bacteria are brought into the cell by endocytosis and phagocytosis respectively. The exogenous proteins/ extracellular bacteria are subsequently broken down by a series of degradation mechanisms. MHC class II molecules are assembled in the ER and guided out by the Ii through the Golgi complex and trans-Golgi network to the MIIC. Ii is subsequently processed by the endosomal protease cathepsin S into the class II-associated Ii peptide (CLIP). This peptide prevents premature peptide binding by occupying the peptide binding groove of the MHC class II molecule. Prior to peptide binding, CLIP is released in a process which involves the catalytic effect of HLA-DM. The MHC class II molecule/ peptide complex is thereafter transported to the surface of the APC where it is presented to $CD4^+$ T cells (adapted from Rocha and Neefjes, 2008).

1.4. Phagosome maturation

The plasma membrane-derived intracellular phagosome which contains an internalized foreign particle undergoes a modification process which is brought about by a series of fission and fusion events with various organelles containing enzymes that assist in killing and digestion and this results in changes in the phagosome membrane as well as in the contents of the phagosome. This modification process is referred to as phagosome maturation and involves organelles of the endocytic pathway including the early and late endosomes, lysosomes and other vesicle populations and results in the formation of an organelle called the "phagosome-lysosome", which has several microbicidal properties (Griffiths, 2004; Vieira *et al*., 2002).

Since phagosome maturation involves organelles of the endocytic pathway, an understanding of this pathway and the interactions of its organelles with the phagosome is necessary. During endocytosis, solutes, membrane-bound ligands and transmembrane proteins are contained in small vesicles which are derived from the plasma membrane (Figure 1.2). These endocytic vesicles are targeted to sorting endosomes (also referred to as early endosomes) which organise and re-route the molecules that have been internalised. Sorting endosomes are usually characterized based on the presence of Rab5 or early endosome antigen 1 (EEA1). Rab5 is one of the best characterized Rab proteins of the early endocytic pathway. It controls the transfer of cargo from the plasma membrane to the sorting/ early endosome, the production of phosphatidylinositol-3-phosphate lipid which is found in high concentrations on early endosomes and the movement of early endosomes on actin and microtubule tracks (Jovic *et al*., 2010).

The lumen of sorting/ early endosomes is mildly acidic (pH ~ 5.5-6.5) and has been observed to contain small but functionally relevant amounts of some lysosomal enzymes (Claus *et al*., 1998; Jovic *et al*., 2010; Killisch *et al*., 1992; Ludwig *et al*., 1991; Piguet *et al*., 1999). One such lysosomal enzyme is cathepsin H, that has been observed to have its greatest concentration (with regards to the endocytic pathway) in early endosomal compartments (Claus *et al*., 1998). The cargo contained within the sorting/ early endosome is moved to recycling endosomes or late endosomes. Recycling endosomes are often located in the juxtanuclear region, close to the microtubule-organizing centre, have a higher pH (pH ~ 6.5) and are distinguished by the presence of Rab 11 (Barbieri *et al.*, 1996; Lemmon and Traub, 2000; Mohrmann and van der Sluijs, 1999; Mukherjee *et al.*, 1997; Riezman *et al.*, 1997; Vieira *et al.*, 2002; Woodman, 2000).

The molecules which are to be degraded are usually transported to late endosomes which are classically defined as more acidic (pH ~ 4.5-5.5) and have more proteases than sorting endosomes. These organelles contain small intraluminal vesicles and are further distinguished by the presence of Rab7 and 9, mannose-6-phosphate receptor and lysosomal associated membrane proteins (LAMPs) (Mukherjee *et al.*, 1997; Somsel Rodman and Wandinger-Ness, 2000; Vieira *et al.*, 2002). The manner in which cargo is transported to the late endosome is an issue which has caused much debate. Two models

to explain this process have been proposed: the vesicle shuttle model and the maturation model. The first model states that sorting endosomes are stable organelles from which transport intermediates referred to as multivesicular bodies (MVBs) are formed. These MVBs transport cargo from the sorting endosome to the late endosome, while the maturation model suggests that sorting endosomes are in fact temporary organelles which mature into MVBs and ultimately form late endosomes (Gruenberg, 2001; Gruenberg and Maxfield, 1995; Gu and Gruenberg, 1999; Thilo *et al.*, 1995; Vieira *et al.*, 2002).

Lysosomes are organelles which are part of the latter portion of the endocytic pathway. Their specific definition has varied amongst cell biology experts. Amongst these definitions, lysosomes are defined as organelles which contain many acidic hydrolases and lysosomal glycoproteins (Vieira *et al.*, 2002). They have been observed to be ~ 0.2-0.5 μm in diameter with an electron-dense matrix. They may be distinguished from late endosomes as they do not have mannose-6-phosphate receptors (Bright *et al.*, 1997). "Lysosomes" have also been shown to be positive for lysosomal associated membrane proteins-1, -2 and -3 (LAMP-1, -2 and -3) (LAMP-3 is also referred to as tetraspanin CD63) (van Meel and Klumperman, 2008). These absolute definitions of lysosomes, however, seem to be cell type specific as they do not seem to hold true for the macrophage where different types of "lysosome" populations have been described (Anes *et al*., 2006; Claus *et al*., 1998). In cells such as J774 macrophages, lysosomes have been divided into two broad categories: organelles that are similar to late endosomes and functionally distinct organelles that are found further along the endocytic pathway (Anes *et al*., 2006). In the study conducted by Anes *et al*. (2006) an attempt was made to describe late endocytic organelles and later small "lysosomal" storage organelles by performing a detailed analysis on the acquisition of different late endocytic markers by *M.smegmatis*-containing phagosomes. These markers included LAMP-1, vacuolar–ATPase (V-ATPase), LYAAT (a membrane transporter that transports apolar amino acids out of „lysosomes"), LAMP-3/ CD63, Hck (a Src-family tyrosine kinase associated with secretory lysosomes), LysoTracker Red DND-99 (a flurophore that contains a weak basic amine that selectively accumulates in acidic compartments and is used to identify organelles with a pH below 5.5-6) and an

indigestible gold content marker (labelling the late endosome-lysosome compartments) (Anes *et al*., 2006; Freundt *et al*., 2007; Sagné *et al*., 2001). By doing this, four different types of late endocytic-lysosome-like organelles were identified by analyzing the extent to which these organelles delivered their contents to the phagosome, one possibly involved in antigen presentation, an early event and containing lysosomal enzymes, such as cathepsin D, and gold at a moderate pH of 5.5-6 and LAMP-1 positive, another LAMP-1 negative containing the gold marker, the other later-fusing vesicles containing a V-ATPase or a lysosomal amino acid transporter (LYAAT) were distinguished (Anes *et al*., 2006).

At the various stages of maturation, these endosomes, lysosomes and phagosomes are believed to bind to microtubules (Figure 1.2) and are involved in a series of fusion events. It is believed that phagosomes are involved in temporary and incomplete fusion with endocytic organelles, a process referred to as "kiss and run" (Desjardins, 1995; Jahreiss *et al.*, 2008). According to this hypothesis, phagosomes fuse with endocytic organelles, allowing for the transfer of membrane as well as luminal contents ("the kiss"). Thereafter, a fission event occurs ("the run") and the two organelles separate, sometimes taking back their luminal content of lysosomal proteases (Desjardins, 1995).

These temporary fusions between phagosomes and early endosomes have been shown to involve N-ethylmaleimide-sensitive factor-attachment protein receptors (SNAREs) and Rab GTPases. SNAREs on vesicles are able to interact with similar SNAREs on target membranes which results in the formation of a very stable complex, allows for the close contact of the two membranes and subsequently promotes the fusion of the interacting membranes (Vieira *et al.*, 2002). Lysosomes, in this way, are now thought to function as storage organelles, fusing and delivering lysosomal enzymes when required and retrieving and storing lysosomal enzymes when not needed for digestion.

Rab proteins are considered as important for membrane trafficking as they have specific organelle distribution and because they promote the selective tethering and subsequent fusion of vesicles with target organelles (Zerial and McBride, 2001). There are several Rab GTPases which have been shown to be involved in the endocytic pathway. These include Rab-4, -11, -7 and -5. Rab-4 and -11 have been observed to be associated with

recycling endosomes while Rab7 has been observed to be localized to late endosomes and has been reported to be responsible for delivery of cathepsin D to the phagosome (Seto *et al*., 2009; Vieira *et al*., 2002). Rab5 (which is one of the best characterized endosomal Rab GTPases) has mostly been associated with the sorting endosome and the temporary fusion between the sorting endosome and the phagosome.

1.4.1. Phagosomal acidification during maturation

The luminal fluid contained within a phagosome is made up of extracellular fluid which becomes entrapped during the initial formation of the phagosome. The entrapped fluid is at first slightly alkaline but undergoes acidification and usually reaches a pH value less than 5.5 as seen in the study by Anes *et al*. (2006). The acidification of the phagosomal lumen has been reported to have several functions including its negative effect on bacterial growth, providing pH sensitive enzymes requiring an acidic pH with an environment in which they are optimally active and may also be directly involved in phagosomal maturation by regulating membrane traffic events (Steinberg *et al.*, 2007).

The acidification of the phagosomal lumen is primarily dependent on a multimeric enzyme complex called V-ATPase which associates with the phagosomal membrane (Lukacs *et al.*, 1990; Steinberg *et al.*, 2007). The V-ATPase which is an active pump transforms the energy of ATP hydrolysis into the transport of protons across the phagosome membrane. This enzyme is made up of two main complexes, a cytoplasmic V_1 complex which hydrolyses ATP as well as a V_0 complex which is membrane-embedded and through which protons flow (Steinberg *et al.*, 2007). The V_1 complex is made up of three main parts, a globular headpiece, a central rotational stalk and a peripheral stalk each of which contain several subunits. The V_0 complex also contains several subunits which form a ring structure (Beyenbach and Wieczorek, 2006). The energy that is released from the hydrolysis of ATP brings about the rotation of the ring structure of the V_0 complex which in turn brings about the transmembrane displacement of protons.

The importance of phagosomal acidification in the elimination of microorganisms has been highlighted by the observation that some species of mycobacteria such as *M. avium* and *M. tuberculosis* avoid acid-mediated degradation by preventing the insertion

of V-ATPase pumps into phagosomal membranes (Hackam *et al.*, 1997; Sturgill-Koszycki *et al.*, 1994). This mechanism together with the fact that some species of mycobacteria such as *M.tuberculosis* prevent phagosome-lysosome fusion are believed to be ways in which mycobacteria avoid killing (Clemens and Horwitz, 1995). How this is achieved has been an intense focus of research (Raja, 2004; Sun *et al*., 2010; Vergne *et al*., 2004). Recent research, however, has shown that the activation of macrophages by the cytokine IFN-γ enables the macrophage to overcome the prevention of phagosome-lysosome fusion as well as the prevention of phagosomal acidification. This is believed to be one of the ways in which macrophages attempt to regain control with regards to mycobacteria which inhibit phagosomal maturation and hence killing of microorganisms (Schaible *et al*., 1998; Vandal *et al*., 2008). In the study by Anes *et al*. (2006), however, acidification initially seemed to encourage growth of *M.smegmatis*.

1.5. Macrophage receptors involved in phagocytosis

The large number of macrophage surface receptors that are involved in phagocytosis may be divided into two main groups based on the specific ligands to which they bind. These two groups are referred to as opsonin-dependent receptors and pattern-recognition receptors (PRRs) (García-García and Rosales, 2002; Krishnan *et al*., 2007).

1.5.1. Opsonin-dependent receptors

Opsonin-dependent receptors require foreign particles to be coated by an opsonin so that these particles may be recognized. There are various types of opsonins but the best characterized examples include IgG and fragments of the third component of complement (C3). The opsonin-dependent receptors which bind to these ligands include Fc receptors (which bind to the Fc domain of various subclasses of IgG) and the complement receptors (CR1, -3, -4) (which bind to several isotypes of C3). Both types of receptors are located on the macrophage surface (Table 1.1) (Adams and Hamilton, 1984).

The Fc receptors which recognise the Fc region of IgG are made up of three distinct classes, Fcγ-RI, Fcγ-RII and Fcγ-RIII (Indik *et al.*, 1995). Although IgG is considered as a major opsonin, other Igs such as IgA and IgE have also been observed with their

corresponding receptors Fcα-R and Fcε-R, respectively (Table 1.1) (May and Machesky, 2001; van Egmond *et al.*, 1999; Yokota *et al.*, 1992).

FcγRs belong to the immunoreceptor class of receptor tyrosine kinases. These receptors contain immunoreceptor tyrosine-based activation motifs (ITAMs) within their cytoplasmic regions. This motif is made up of two pairs of tyrosines and leucines within the consensus sequence D/E-X_7-D/E- X_2-Y-X-X-L-X_7-Y-X-X-L and has been observed to be important for signal transduction (Sánchez-Mejorada and Rosales, 1998). When FcγRs bind to IgG molecules, they create a clustering/cross-linking effect which induces phosphorylation of certain tyrosine residues within the ITAMs (Swanson and Hoppe, 2004). These phosphorylated motifs have been observed to have a high-affinity for members of the Syk family of tyrosine kinases which play a vital role in transmitting the phagocytic signal once bound to ITAMs (Greenberg, 1999). The process of phosphorylation of ITAMs has been shown to be essential for FcγR-mediated actin assembly (which requires the activation of the GTPases Rac1 and Cdc42) and is thus essential for Fc-receptor mediated phagocytosis (DeMali and Burridge, 2003; Greenberg, 1999). The clustering/cross-linking effect of FcγRs also results in bactericidal activity and the production and secretion of lymphokines and inflammatory mediators such as arachidonate metabolites and histamine (Sánchez-Mejorada and Rosales, 1998).

Table 1.1: Well characterized opsonin-dependent receptors and their specific ligands (adapted from Heale and Speert, 2002).

Receptor	Ligand
CR1(CD35)	C3b
CR3(CD11b/CD18)	iC3b
CR4(CD11c/CD18)	iC3b
C1q receptor	Mannose-binding protein
SPR210	Lung surfactant protein A
CD14	LPS-binding protein
Fcγ-RI (CD64)	IgG1, IgG3, IgG4, IgG2
Fcγ-RII(CD32)	IgG1, IgG3, IgG4, IgG2
Fcγ-RIII(CD16)	IgG1 and IgG3
Fcα-R(CD89)	IgA
Fcε-R	IgE

The process of complement-receptor-mediated phagocytosis is different from phagocytosis that is mediated by Fc receptors. Particles which have been opsonized by complement "sink" into the phagocyte, the phagocyte membrane is minimally altered and the internalization process does not usually result in an inflammatory response or oxidative burst (May and Machesky, 2001). The complement system, which is made up of approximately thirty proteins, can be activated by microbial molecules, for example, carbohydrates or by binding to antibodies such as IgM and IgG which are found on the surface of the microorganism.

During complement activation C3 is converted to C3b which contains a highly reactive thioester group. This reactive group can covalently bind to hydroxyl and amino groups on the surface of microorganisms. The bound C3b acts as an opsonin and is recognised by complement receptor 1 (CR1, also known as CD35). Once C3b is further converted to iC3b by plasma factors H and I, it may then be recognised by complement receptor -3 (CR3, also known as CD11b/CD18) or -4 (CR4 also known as CD11c/CD18) (Table 1.1) (May and Machesky, 2001; Nishida *et al.*, 2006; van Lookeren Campagne *et al.*, 2007).

iC3b-opsonized particles are only phagocytosed if the macrophage has been activated, for instance, by inflammatory cytokines or by attaching to the extracellular matrix (Brown, 1986; May and Machesky, 2001; Pommier *et al*., 1983). This results in a conformational change in the complement receptor which brings about a clustering of receptors (necessary for binding of the foreign particle) and allows for the transduction of the phagocytic signal and subsequent internalization of the foreign particle (Allen and Aderem, 1996a; Detmers *et al.*, 1987; May and Machesky, 2001; Oxvig *et al.*, 1999).

1.5.2. Pattern recognition receptors

PRRs are those receptors which recognize conserved pathogen-associated molecular patterns (PAMPs). PAMPs play a crucial role in the activation of macrophages as they provide one of the two signals that are required for the activation process to occur.

One of the first signalling cytokines is interferon-γ (IFN-γ) (produced early in the immune response by innate immune cells such as natural killer (NK) cells). As the immune response proceeds, a second source of IFN-γ is provided by antigen-specific T_H1 T cells (Young, 2006). The second signal is stimulated via the interaction of PAMPs with PRRs such as toll-like receptors. This leads to the induction of tumour necrosis factor (TNF) production by macrophages, and the combination of TNF and IFN-γ results in activated macrophages inducing a strong microbicidal response that involves a complex repertoire of metabolic reactions (Silva and Faccioli, 1992; Van Ginderachter *et al*., 2006; Zhang and Mosser, 2008).

PRRs are not just limited to the cell membrane of immune cells, they may also be secreted into the extracellular environment, located on intracellular vesicles or found in the cytoplasm. Secreted PRRs are able to mediate opsonization, activate complement pathways and transfer PAMPs to other PRRs. Intracellular PRRs are capable of inducing cellular apoptosis and activating cytokine secretion. Well known cell surface PRRs include toll-like receptor (TLRs) -1, -2, -4 and -5, the mannose receptor (MR) and CD36 (Table 1.2) (Zhang and Mosser, 2008).

Table 1.2: Well characterized pattern recognition receptors (PRRs), their specific ligands and their various locations (adapted from Zhang and Mosser, 2008).

Receptor	Ligand
TLR1	Tri-acyl lipoprotein
TLR2	Gram-positive peptidoglycan and lipoteichoic acid, fungi zymosan
TLR3	Virus double-stranded RNA, poly C, poly I
TLR4	Gram-negative LPS, MMTV envelope proteins
TLR5	Bacteria flagellin
TLR6	Mycoplasma di-acyl lipopeptides
TLR7	Virus single-stranded RNA
TLR8	Virus single-stranded RNA
TLR9	Bacterial and viral unmethylated CpGDNA, malaria pigment haemozoin
CD36	Apoptotic cells, collagen types I and IV, erythrocyte membrane protein 1, oxidized LDL, platelet-agglutinating protein p37
MARCO	Lipopolysaccharide (LPS), LTA (lipoteichoic acid), uteroglobin-related protein 1
Mannose receptor (MR)	Mannose, fucose and *N*-acetyl glucosamine
Dectin-1	Fungal β-glucans, zymosan
Nucleotide-binding oligomerization domain-containing protein 1 (NOD1)	*Chlamydia*, enteroinvasive *E.coli*
NOD2	*L.monocytogenes, Salmonella flexneri*

Although phagocytosis results in the formation of a phagosome, not all phagosomes may share exactly the same maturation process. The fate of a phagosome usually depends on the receptor-ligand interactions which precede its formation (Vieira *et al.*, 2002). This has been supported by the observation that phagosomes containing *Mycobacterium tuberculosis* derived from Fc-receptor-mediated phagocytosis fuse with lysosomes. Those phagosomes formed after certain complement-receptor-mediated phagocytosis events do not seem to fuse, however, this is believed to be possibly due to the inhibition of complement receptor-mediated Ca^{2+} signalling (Figure 1.2) that is required for the activation of phagocyte respiratory burst, production of nitric oxide, secretion of microbicidal granule constituents and the production of proinflammatory mediators such as TNF-α by *M.tuberculosis*. This alteration in macrophage activation may contribute to the prevention of phagosome-lysosome fusion and in turn promote mycobacterial survival (Malik *et al.*, 2000). This level of complex extracellular signalling was ignored in the current study, as phagocytosis was performed in decomplemented foetal calf serum in a manner similar to that reported by Anes *et al*. (2006) and many other researchers (Kaniuk *et al*., 1992; Scully and Lehner, 1979).

1.6. Macrophage killing mechanisms

The killing mechanisms used by macrophages in dealing with microbial infection ultimately results in the production of an environment which is toxic or uninhabitable for the microorganism (Appelberg, 2006). These mechanisms may be divided into two categories, oxygen-dependent and oxygen-independent mechanisms (Lowrie and Andrew, 1988).

1.6.1. Oxygen-dependent macrophage killing mechanisms

Activated macrophages undergo a process known as respiratory burst in which a temporary increase in oxygen consumption occurs (Forman and Torres, 2002). This process is caused by the reduced nicotinamide adenine dinucleotide phosphate (NADPH) oxidase complex which assembles at the phagosomal membrane (Hampton *et al*., 1998). During respiratory burst, macrophages oxidize glucose through the dehydrogenase of the hexose monophosphate shunt, resulting in the reduction of NADP to NADPH (Allen, 1994). Upon oxidation of cytoplasmic NADPH, electrons are transferred to molecular oxygen located on the phagosomal side of the membrane. This

brings about the formation of superoxide (O_2^-) which can go on to form hydrogen peroxide (H_2O_2) (Forman and Torres, 2002). Oxidative burst is a critical microbicidal mechanism, the importance of which became obvious in people with a susceptibility to infections due to inactive NADPH oxidase resulting in a condition known as chronic granulomatous disease (Smith and Curnutte, 1991).

Hydrogen peroxide that is produced in macrophages has been observed to interact with myeloperoxidase and a halide, usually chloride, to produce a potent antibacterial substance called hypochlorous acid (HOCl) within phagosomes (Dale *et al.*, 2008; Harrison and Schultz, 1976). In acidic conditions such as those that may occur in the phagosome, HOCl can react with excess chloride to form molecular chlorine (Cl_2) which is able to target microorganisms at several chemical sites such as oxidizable groups for example sulfhydryl groups, iron-sulfur centres and sulfur-ether groups. The oxidation of these groups can result in the loss of microbial membrane transport as well as the suppression of microbial DNA synthesis (Hampton *et al*., 1998; Klebanoff, 2005).

Phagocytes are also capable of producing hydroxyl radicals ($OH^{\cdot}$) which have membrane damaging bactericidal potential. These radicals can be produced via two potential mechanisms. The first involves a superoxide-driven Fenton reaction between hydrogen peroxide and a transition metal catalyst. The second involves a reaction with hypochlorous acid (HOCl) and superoxide. These bactericidal radicals are capable of killing intracellular microoganisms (Hampton *et al*., 1998).

1.6.2. Oxygen-independent macrophage killing mechanisms

The production of reactive nitrogen intermediates (RNIs) such as nitric oxide (NO) in response to pathogen-derived molecules is also an important microbicidal pathway in macrophages. NO is usually formed when the guanidino nitrogen of L-arginine is oxidized by NO synthase (NOS). The bactericidal effects of NO are due to its ability to deaminate and directly damage bacterial DNA by generating strandbreaks. NO and other RNIs may also modify lipids at the microbial surface as well as intracellularly, hence gaining access to bacterial DNA by first damaging the membranes of the bacteria (Chan *et al.*, 2001).

The production of bactericidal peptides is another mechanism used by macrophages to deal with bacterial infections. These peptides are often referred to as antimicrobial peptides (AMPs) and are usually classified according to their structural characteristics. Although AMPs have a variety of structural characteristics they do share some common features. Most of these peptides are less than 60 amino acids in length and have an overall positive charge. AMPs also have the ability to take on an amphipathic shape in which a number of hydrophobic and hydrophilic amino acids segregate (Diamond *et al*., 2009; Zasloff, 2002; Zasloff, 2007). These usually dissolve into and disrupt the bacterial membrane, and subsequently bring about bacterial cell death (Pálffy *et al*., 2009). A group of AMPs referred to as defensins are one of the best characterized macrophage AMPs. Mammalian defensins are cationic, arginine-rich, non-glycosylated and contain six cysteine residues which form three intramolecular disulfide bridges. Defensins may be divided into three classes based on the alignment of their disulfide bridges and their overall molecular structure. These include α-defensins, θ-defensins and β-defensins (Bals, 2000). Other proteins which have antimicrobial properties include lysozyme, collagenase and elastase (Lehrer and Ganz, 1990; Unanue *et al.*, 1976).

It is believed that macrophages may also create a hostile environment for engulfed microorganisms by restricting their access to vital substances needed for survival (Appelberg, 2006). One such substance is iron which is required for the optimal growth of microbes within host cells. During infection macrophages, which are involved in the recycling of iron from erythrocytes, limit the release of recycled iron and thus they lower the extracellular iron concentration. The influence of cytokines also causes infected macrophages to move iron from phagosomes to cytoplasmic ferritin (a major iron storage protein). This in turn inhibits the multiplication of intracellular microbes. There are, however, some microbes which have evolved mechanisms that allow them to obtain iron from iron containing host proteins including haemoglobin and transferrin (a protein which binds to iron). Such microorganisms have iron uptake systems that rely on high-affinity receptors for these iron containing host proteins (Perkins-Balding *et al*., 2004). Some microorganisms have also been found to specifically interfere with iron-sequestering host mechanisms by altering the expression of iron storage proteins and by degrading cytoplasmic ferritin (Ganz, 2009). Microorganisms such as *Neisseria*

meningitides gain access to iron by processes such as disseminated intravascular coagulation in which haemoglobin is released into the bloodstream by mechanical shearing of erythrocytes and this is followed by the subsequent acquisition of iron from the released haemoglobin (Dyer *et al*., 1987). Another mechanism which some microbial species such as *Neisseria gonorrhoeae* may use to obtain iron for survival is to compete with proteins such as transferrin for the opportunity to bind to iron (Mickelsen and Sparling, 1981).

Recently, the solute carrier family 11 member1, Slc11a1, natural resistance associated macrophage protein (Nramp) 1 has been identified in many host organisms. This integral membrane protein is believed to control the intraphagosomal replication of pathogenic microorganisms such as *M.tuberculosis* as it acts as a divalent cation pump and is thus able to regulate the divalent cation concentrations within the phagosome (Govoni and Gros, 1998; Wagner *et al*., 2005). These divalent cations amongst others include Fe^{2+} and are important in monocytes, macrophages and neutrophils as they are involved in the generation of reactive oxygen intermediates during respiratory burst. An example of this is the interaction between hydrogen peroxide, generated by respiratory burst with Fe^{2+}/Fe^{3+} to produce reactive hydroxyl and superoxide radicals that play a vital role in early defence against intracellular microorganisms (Agranoff *et al*., 1999).

In human monocytes and macrophages, Nramp1 has been observed on the membrane of some endosomal and „lysosomal" compartments and upon phagocytosis, it has also been observed to be recruited to the phagosomal membrane where it remains for the maturation of the phagosome to the phagosome-lysosome. This suggests that it is associated with the control of the internal environment of the phagosome (Gruenheid *et al*., 1999; Wagner *et al*., 2005). Nramp1 acts as a divalent cation pump and it is believed to also promote vesicle fusion which may result in the recruitment of V-ATPase (Barton *et al*., 1999; Hackam *et al*., 1998). This implies that Nramp1 may improve the fusing ability of mycobacteria-containing phagosomes (Wagner *et al*., 2005). A second homologue Nramp2 (also referred to as DCT1/DMT1) has also been identified in mammals. Unlike Nramp1 which is specific to macrophages and monocytes, Nramp2 is expressed in many different cells. This protein is a transporter of divalent cations including Fe^{2+}, Zn^{2+} and Mn^{2+}. In macrophages, Nramp2 is localized to recycling

endosomes and to the plasma membrane and in both locations it has been found to colocalize with transferrin (Gruenheid *et al*., 1999). Interestingly, Nramp2 has been observed to behave as a mediator for microtubule-dependent phagosome and „lysosome" transport (Wagner *et al*., 2005).

Bacterial Nramp homologues have also been identified and the conservation of protein sequences between prokaryotes and eukaryotes is considerably high (Agranoff *et al*., 1999; Cellier *et al*., 2001; Reeve *et al*., 2002; Wagner *et al*., 2005). The homologues that have been identified in *M.tuberculosis* and other mycobacteria are referred to as Mramp and are pH-dependent divalent cation transporters with broad specificity. Some ions that are transported by Mramps include Fe^{2+} and Zn^{2+} (Agranoff *et al*., 1999). In a study conducted by Agranoff *et al*., (1999), *Mycobacterium bovis* bacillus Calmette-Guérin (BCG) Mramp mRNA was detected in infected THP1 (human macrophage cell line) phagocytes and is believed to assist survival of pathogenic mycobacteria in cells such as macrophages. It is believed that both mycobacteria and macrophages utilize Nramp homologues to compete for intraphagosomal metal ions (Agranoff *et al*., 1999).

A sequence of killing events in macrophages has recently been described in detail by Anes *et al*. (2006) who described the killing of *Mycobacterium smegmatis* by J774 macrophages as a dynamic process. Anes *et al.* (2006) suggested that the killing process involves periods of initial killing, followed by bacterial growth, and, thereafter, two additional killing phases. During the first phase, NO synthesis and release into the phagosome takes place and was responsible for killing during the first 2 hours after infection, but is usually stopped during this phase (less than 2 hours, Figure 1.5). The assembly of phagosomal actin and the fusion of the phagosome with late endocytic organelles also occurs in the first killing phase as well as in the third (Figure 1.5), facilitating fusion with late endosome-like structures. As a result of the fusion of the phagosome with late endocytic-like organelles, lysosomal proteases are delivered to the phagosome. These lysosomal proteases have been shown to contribute to the killing of *M.smegmatis* by J774 macrophages. This was demonstrated by Anes *et al*. (2006) who used a cocktail of lysosomal protease inhibitors, and demonstrated a reduction in the killing of *M.smegmatis* by J774 macrophages during the first killing phase (1-4 hours after infection). The first killing phase was followed by a period of bacterial growth as

well as a recycling of phagosomal membrane and its contents, LAMP-1 and rhodamine-labelled gold, (a late endosome-lysosome marker), respectively, back to late endosomes (Figure 1.5) implying a loss of lysosomal enzymes also. The second killing phase took place between nine and twelve hours post infection, and involved two disctinct compartments, one containing LYAAT (a lysosomal amino acid transporter) and another containing the V-ATPase-enriched structures (responsible for the pH below 5.5), distinct from LAMP-1 labelled or gold-containing late endosomal compartments. This suggests that the fusion between phagosomes and LAMP-1 labelled or gold-containing late endosomal compartments must have taken place prior to this second killing phase. These compartments (which were negative for LAMP-1 and a gold marker) are believed to be different from the usual late endosomes and lysosomes as most of the gold marker and LAMP-1 had been recycled out of the phagosome by this time, and LAMP-1 and gold content marker were only re-obtained during the third killing phase (Anes *et al*., 2006). This could represent the MHC class II containing-compartment (MIIC) in which cathepsin D has been associated with antigen processing as a V-ATPase has previously been reported in such a compartment (Benes *et al*., 2008; Singh *et al*., 2006).

The third killing phase occurred between twelve and twenty-four hours post infection and it was during this phase that almost all live *M.smegmatis* were killed though this phase was associated with the fusion of LAMP-1 and gold markers. The associated killing activity seemed no longer to be associated with the activity of lysosomal enzymes as lysosomal protease inhibitors no longer affected killing.

During this phase, phagosomal actin assembly occurred and fusion of late endosome-like organelles also took place as demonstrated by the reaquisition of the LAMP-1 and gold content marker. During this phase most of the phagosomes were strongly acidic due to the fusion of a late endosomal population containing the V-ATPase and the endosomal population containing the lysosomal amino acid transporter (LYAAT) fused also at this time, possibly to assist export of amino acids of degraded proteins (Figure 1.5). This study, conducted by Anes *et al*. (2006), demonstrated that the successful killing mechanisms employed by J774 macrophages are used at specific periods and not continuously and that iNOS was responsible for initial killing (0-1 hours after

infection), lysosomal enzymes (cysteine, serine or aspartyl proteases such as cathepsin D) were responsible for killing in the first killing phase (1-4 hours after infection) based on inhibitor evidence and that initial and later fusion events are MAP kinase p38-and actin-mediated and that *M.smegmatis* are able to manipulate p38 levels to their own advantage, down regulating levels at the end of the first killing phase (1-4 hours after infection) allowing bacterial growth (Figure 1.5).

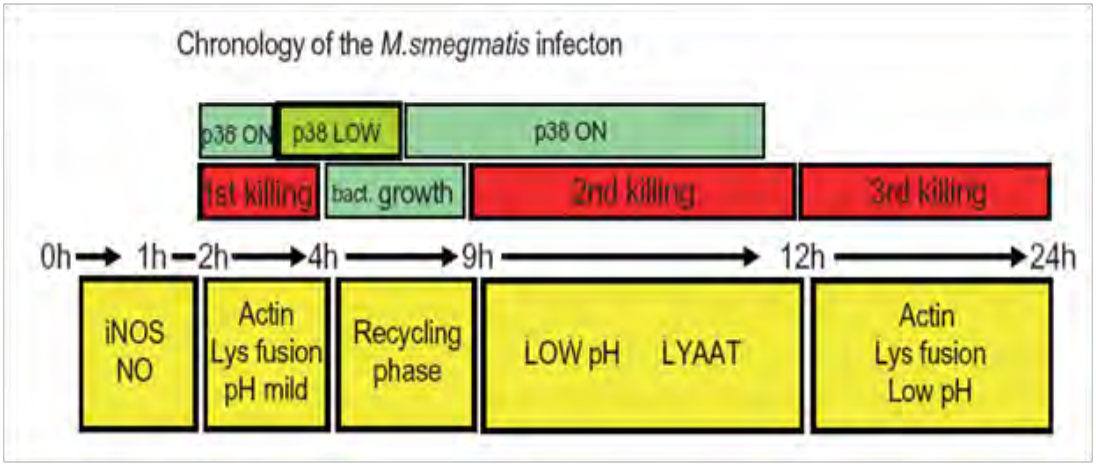

Figure 1.5: Representation of the mechanisms involved in the killing of *M.smegmatis* by J774 macrophages.

The killing of *M.smegmatis* is a dynamic process which involves initial killing periods followed by bacterial growth and thereafter by two other killing stages. NO synthesis was an early killing mechanism and was only involved in the first killing phase. The assembly of phagosome actin and fusion with late endocytic organelles took place in the first and last killing phases. The phagosomal membrane as well as its contents were recycled at the same time as the period of bacterial growth. The acidification of the phagosome coincided with the second and third killing phases. Map kinase p38 was a vital regulator of most processes except that of NO synthesis (Anes *et al.*, 2006). Abreviations: p38 = map kinase p38, NO = nitric oxide, iNOS = inducible NO synthase, LYAAT = lysosomal amino acid transporter, Lys = lysosome (adapted from Anes *et al*., 2006).

Even though much progress has been made in understanding the mechanisms used by macrophages in eliminating microorganisms, this complex area of research is not fully understood. Over the years, there has been much interest expressed in the antimicrobial properties of lysosomal proteases, in particular the cathepsins. The term “cathepsin” was first used by Willstätter and Bamann, (1929) to describe an intracellular proteinase of animal origin that was active at a weak, acidic pH (Zamecnik and Stephenson, 1945).

This term now describes a group or lysosomal proteases which are divided into three different families based on their catalytic mechanisms. These include; cathepsins B, C, F, L, K, S, H, O, V, W and Z which are cysteine proteases, cathepsins D and E which are aspartic proteases and cathepsins A and G which are serine proteases (Gacko *et al*., 2007; Garwicz *et al*., 1998; Ohshita and Hiroi, 2006; Turk *et al*., 2001; Yanagawa *et al*., 2007). Several researchers have studied the microbicidal properties of cathepsins in order to gain a better understanding of their involvement in killing microorganisms. In a study conducted by Thorne *et al*. (1976), it was shown that cathepsins B, D and G were able to lyze lysozyme resistant *Staphylococcus aureus* as well as make Acinetobacter 199A more susceptible to lysozyme.

Cathepsin D has also been shown to play a role in the elimination of *Listeria monocytogenes* (a food-borne pathogen) in both macrophages and fibroblasts via a nonoxidative bactericidal mechanism (del Cerro-Vadillo *et al*., 2006). The indirect importance of cathepsin D in eliminating *Listeria monocytogenes* has been demonstrated in TNF- and INF-γ-responsive acid sphingomyelinase (ASMase) deficient mice. ASMase produces a product known as ceramide which activates cathepsin D. It has been observed that ASMase deficient mice are more susceptible to *L.monocytogenes* than wild-type mice (Utermöhlen *et al.*, 2003). Cathepsin D–containing phagosomes were also observed to have a greater reduction in *L.monocytogenes* viability than those which did not contain this protease (Prada-Delgado *et al.*, 2001). Cathepsin D is believed to eliminate *L.monocytogenes* by targeting its main virulence factor, listeriolysin O (del Cerro-Vadillo *et al*., 2006).

Singh *et al.* (2006) observed that in mycobacteria-containing phagosomes of macrophages, the presence of a V-ATPase was required for the processing of an immunodominant antigen of *Mycobacterium tuberculosis*, Ag85B, via a cathepsin D–dependent mechanism. This was observed in H37Ra (attenuated strain of *M.tuberculosis*) and to a lesser extent in H37Rv (virulent strain of *M.tuberculosis*) infected macrophages. According to Ramachandra *et al*. (2001), once this antigen is processed it is able to prime Ag85B-specific CD4 Th1 cells through the MHC class II pathway showing that cathepsin D processing of the mycobacterial antigen and MHC II

presentation could be mainly responsible for cell death in the second killing phase as reported by Anes *et al*. (2006).

M.smegmatis is an ideal model for studying the mechanisms used by macrophages in killing non-pathogenic bacterial species. This non-pathogenic bacterial species is known to be killed within phagosomes by a combination of factors such as lysosomal proteases, RNIs and other possible factors which have yet to be identified (Anes *et al*., 2006; Gutierrez *et al*., 2008). On the other hand pathogenic mycobacteria such as *M.tuberculosis* and *Mycobacterium avium* have been observed to block many of these mechanisms including, phagosome-late endosome-lysosome fusion, phagosome acidification and NO release, and are thus capable of growing within phagosomes, which do not mature due to the lack of proinflammatory responses and the prevention of the formation of a microbicidal-phagosome (Clemens and Horwitz, 1995; Gutierrez *et al*., 2008; Schaible *et al*., 1998). Seto *et al*. (2009) also showed that Rab-7-dependent fusion of a late endosomal compartment was required for the delivery of cathepsin D to phagosomes and that this was blocked by *M.tuberculosis* enabling survival.

In summary, in order to conduct a study on how pathogenic microorganisms avoid killing, a detailed study on the mechanisms by which non-pathogenic microorganisms are killed by phagocytes such as macrophages needs to be conducted. For this, a well established model system is required and one such model which has been used by several researchers involves the killing of *M.smegmatis* by J774 murine macrophages (Anes *et al*., 2006; Fabrino *et al*., 2009; Gutierrez *et al*., 2008).

In the study conducted by Anes *et al.* (2006) the role of lysosomal proteases (contained in late endosomes and lysosomes) was indicated by the fact that inhibition of these proteases, by a cocktail of lysosomal protease inhibitors, in early and not late fusion events, impacted negatively on the killing of *M.smegmatis* by J774 murine macrophages. In early fusion events, in which lysosomal protease-containing late endosomal compartments (which are Rab7 positive and indicated in the study by Anes *et al*. (2006) by the acquisition of gold and LAMP-1 markers) were shown to fuse with the *M.smegmatis*-containing phagosome, the cocktail of inhibitors consisting of leupeptin, aprotinin and pepstatin, which inhibit cysteine proteases, serine proteases and

aspartyl proteases, respectively, prevented killing in early killing events (Gacko *et al*., 2007; Garwicz *et al*., 1998; Ohshita and Hiroi, 2006; Yanagawa *et al*., 2007). Studies on *M.tuberculosis* showed that cathepsin D delivery was Rab7-dependent (late endosome fusion-dependent) and infection caused dissociation of Rab7 from the *M.tuberculosis*-containing phagosome, inhibiting delivery of cathepsin D and subsequent phagosomal maturation and killing (Seto *et al*., 2009). This implies that the late endosome fusion and delivery of cathepsin D, or other lysosomal proteases, may be required for killing of *M.tuberculosis* and other mycobacteria as has been seen for other bacterial species such as *Listeria monocytogenes* and *Staphlococcus aureus* (del Cerro-Vadillo *et al*., 2006; Thorne *et al*., 1976).

Cathepsin D and its possible antimicrobial properties were, therefore, adopted as a focus for this study, using the approach and model system used by Anes *et al*. (2006) as this represents the most detailed study performed to date on the mechanisms used by J774 macrophages in the killing of *M.smegmatis*.

Several approaches were considered for establishing a possible role of cathepsin D in killing *M. smegmatis*. The use of confocal and other visualization studies seemed to be the most suitable and informative option. These studies required the use of anti-cathepsin D antibodies which did not cross-react with *M.smegmatis* so that cathepsin D could be detected in *M.smegmatis*-containing phagosomes. This prompted the raising of anti-cathepsin D antibodies with an adjuvant that did not contain mycobacterial antigens (Chapter three).

Classical "lysosomes" or organelles in which cathepsin D is believed to be stored in its active form, have been observed to have certain characteristics. These include a particular size which is estimated to be approximately 0.2-0.5 μm in diameter, an electron-dense matrix, an acidic luminal pH as well as its lack of mannose-6-phosphate receptors (Bright *et al.*, 1997; Sun-Wada *et al.*, 2003). In the studies of Anes *et al*., (2006) and Seto *et al*. (2009), however, LAMP-1 labelled compartments containing lysosomal enzymes and Rab7-dependent delivery of cathepsin D seem to be involved in killing and LAMP-2 seems to be required for undisturbed cathepsin D trafficking (Eskelinen, 2006).

To gain a better understanding of the possible involvement of cathepsin D in killing and investigate which cathepsin D-containing organelles may be involved in killing, organelles which contain cathepsin D needed to be characterized. This was done by determining if such organelles were positive for the lysosomal associated membrane proteins-1 and 2 (LAMP-1 and -2) (using previously raised commercial monoclonal antibodies against LAMP-1 and -2). These organelles were also characterized in terms of acidity using LysoTracker Red DND-99 (Freundt *et al*., 2007).

Infection studies involving J774 murine macrophages and *M.smegmatis* have also been conducted using Green Fluorescent Protein (GFP) tagged-*M.smegmatis*. These studies are described in Chapter four.

The possible bactericidal properties of cathepsin D were also determined using an *in vitro* killing assay in which cathepsin D was directly added to *M.smegmatis* to determine its effect on the viability of the microorganism. This is also described in detail in Chapter four.

1.7. Summary of objectives of this study

From the many lysosomal proteases that are believed to play a role in killing *M.smegmatis* by J774 macrophages, cathepsin D was chosen as the subject of this study, based on the approach of Anes *et al*. (2006). Confocal and other visualization studies were chosen as the best approaches for this study and for this antibodies which do not cross-react with mycobacteria were required. Antibodies against cathepsin D were raised in chickens using saponin as the adjuvant of choice as contents of the conventionally used Freund‟s complete adjuvant, namely heat-killed and dried mycobacteria would have generated cross-reacting antibodies to *M.smegmatis* during infection studies (Stills, 2005). This process is described in Chapter three after a detailed description of any common methods is given in Chapter two.

The organelles which contained cathepsin D were also characterized using the lysosomal associated membrane proteins-1 and 2 (LAMP-1 and -2) and LysoTracker which is used to indicate acidity, and, where colocalized with cathepsin D, the activity of cathepsin D. The characterization of these organelles involved colocalization studies

using the image processing software ImageJ (French *et al.*, 2008). This is described in Chapter four.

Infection studies involving *M.smegmatis* and J774 macrophages were also conducted and the visualization of infection was made possible by the use of GFP-tagged *M.smegmatis*. The presence of GFP also made it possible to conduct colocalization studies between the microorganism, LAMP-1 and -2, cathepsin D and LysoTracker. This is described in Chapter four.

One of the challenges of this study was finding a way in which dead *M.smegmatis* could be distinguished from live *M.smegmatis*. Propidium iodide, was explored as an indicator of dead cells, and to distinguish live, (GFP-fluorescent) and dead *M.smegmatis* (non GFP-fluorescent), allowing the colocalization of dead *M.smegmatis* with cathepsin D and LAMP-1 and -2, and acidity to be explored in Chapter four (Lahiri *et al*., 2005; Shi *et al*., 2007; Unal Cevik and Dalkara, 2003). The final discussion and suggested future work is given in Chapter five.

CHAPTER TWO

GENERAL MATERIALS AND METHODS

The common chemicals and biochemical techniques used during the current study are described in this chapter. The following chapters will describe more specialized techniques that are relevant to the specific chapters.

2.1 General reagents

The acrylamide, ammonium persulfate, calcium chloride, glutaraldehyde [25% (m/v)], glycine, hydrochloric acid, hydrogen peroxide [30% (v/v)], sodium dihydrogen phosphate, potassium chloride, sodium azide, sodium chloride, sodium hydroxide and paraformaldehyde (PFA) were from BDH (Poole, England). The sodium dodecyl sulfate (SDS) was from Boehringer Mannheim (Mannheim, Germany). The tris base [2-amino-2-(hydroxymethyl)-1,3-propandiol (Tris)] was purchased from MP Biomedicals (Eschwege, Germany). The D (+) glucose, glacial acetic acid, potassium dihydrogen phosphate, methanol and magnesium chloride were from Saarchem (Wadeville, South Africa). Page Ruler Prestained Protein ladder was from Inqaba Biotechnical Industries LTD (Pretoria, South Africa). The glycerol was from AR-Associated Chem. Enterprises (Glenvista, South Africa). The 2-mercaptoethanol was purchased from Merck Schuchardt, OHG (Munich, Germany). The Ponceau S was acquired from Searle (High Wycombe, Bucks, United Kingdom). The Elite milk powder was from Clover SA (Pty) Ltd (Roodepoort, South Africa). The monoclonal antibodies against lysosomal-associated membrane proteins (LAMPs), LAMP-1 and -2, were acquired from the Developmental Studies Hybridoma Bank (University of Iowa, Iowa City, Iowa, USA). The LysoTracker Red DND-99 was purchased from Molecular Probes (Eugene, USA). The 5-bromo-4-chloro-3-indolyl phosphate (BCIP) and nitroblue tetrazolium (NBT) were from Roche (Indianapolis, Indiana). The copper (II) chloride dihydrate, *N,N,N',N'*-tetramethyl ethylenediamine (TEMED) and polyethylene glycol (PEG 6 kDa) were purchased from Merck (Darmstadt, Germany). Hybond-C-Extra nitrocellulose membrane was from Amersham Biosciences (Buckinghamshire, England). The LR White resin was purchased from London Resin (London, United Kingdom). The

Multidishes (24 well) and Nunc Easy Flasks were acquired from Nunc Intermed (Roskilde, Denmark). The dimethylformamide (DMF) was from Fluka (Seelze, Germany). The Whatman No. 1 filter paper was from Whatman International Ltd (Maidstone, England). The bisacrylamide (N,N‟-methylene-bisacrylamide), bisbenzimide H33342 trihydrochloride (Hoechst), bovine serum albumin (BSA), Coomassie brilliant blue (CBB) G-250, 3,3'-diaminobenzidine (DAB), Dulbecco‟s modified Eagle‟s medium (DMEM), fish skin gelatin (FSG), goat anti-rat IgG (whole molecule) fluorescein isothiocyanate, Hanks‟ balanced salts (HBSS), L-glutamine, phosphorylase B (M_r 97.4 kDa), propidium iodide, rabbit anti-chicken IgG (whole molecule) FITC conjugate, saponin, and sodium bicarbonate, sodium chloride, soybean trypsin inhibitor (M_r 21.5 kDa), trypsin-EDTA solution (x 10) (Sigma Chemical Co.) were purchased from Sigma (St. Louis, Missouri). The donkey anti-chicken (IgY) CY3 conjugate, donkey anti-rat (IgG) CY5 conjugate and donkey anti-chicken (IgY) CY5 conjugate were acquired from Jackson Immuno Research Pharmaceuticals (West Grove, Pennsylvania). The foetal calf serum (FCS) was purchased from Gibco (Paisley, UK). The protein A-gold was from the Department of Cell Biology, University of Utrecht, Netherlands. Difco Middlebrook 7H9 Broth, Difco Middlebrook OADC Enrichment and Difco Middlebrook 7H10 Agar was from Becton Dickinson and Company (Sparks, USA). The Hygromycin B was acquired from Invitrogen (Carlsbad, USA).

2.2 Cell culture

The J774 macrophage cell line is a murine cell line that was established from a tumor in a female BALB/c mouse (Segura and Gottschalk, 2002). This cell line is a well established model system in cell biology as well as in immunology due to it being easily genetically manipulated and maintained (Lam *et al*., 2009). J774 cells are capable of phagocytosis and secretion of lymphocyte-activating factors and they have also been found to have Fc and C3 receptors (Dietz and Cole, 1982). These cells also display properties of adherence and are capable of antibody-dependent lysis of target cells (Ralph and Nakoinz, 1977; Zabrenetzky and Gallin, 1988). J774 macrophages have been observed to contain a number of proteases associated with classical lysosomes including cathepsin D (Claus *et al*., 1998; Pitt *et al*., 1992). Due to these favourable characteristics, the J774 macrophage cell line was used as a model system for the study

of phagocytosis of *M.smegmatis* and the potential microbicidal properties of cathepsin D.

2.2.1 Reagents

Dulbecco‟s modified Eagle‟s medium (DMEM) (with L-glutamine and 1000 mg/l glucose). was prepared according to the manufacturer‟s instruction with L-glutamine (0.58 g) and sodium bicarbonate (3.7 g) added to the medium.

HBSS (without calcium chloride, magnesium sulphate, phenol red and sodium bicarbonate). was also prepared according to the manufacturer‟s instruction with an additional 0.35 g sodium bicarbonate added to the solution.

1 x Trypsin-EDTA solution [with 0.5 g porcine trypsin, 0.2 g EDTA and 0.09 g NaCl]. 10 x Trypsin-EDTA (1ml) was diluted in HBSS (9 ml) and warmed to 37ºC just before use.

Decomplemented FCS. Aliquots of commercially available FCS were incubated at 56ºC for 30 min to denature the complement component and subsequently stored at -20ºC before use.

2.2.2 Procedure

J774 cells were cultured in DMEM with 10% (v/v) decomplemented FCS at 37ºC with 5% CO_2 in a Nuaire US Autoflow CO_2 water-jacketed incubator. When cells were approximately 70% confluent, they were washed in HBSS and adherent cells were trypsinized with 1 x trypsin-EDTA solution. The cells were usually split in a ratio of 1:3.

2.3 SDS-PAGE

Electrophoresis has been used by many researchers over the years as a means of separating protein mixtures so that their individual components may be identified. This technique is useful for confirming the similarity or differences between protein samples and may also serve as a means of semi-preparatively purifying proteins for use in other applications. Polyacrylamide has been used as a successful matrix for gel electrophoresis. During polyacrylamide gel electrophoresis (PAGE), proteins move

through pores in a polyacrylamide gel matrix as a result of an electric field (Gallagher, 2006).

The pore size of the gel may be altered by varying the amounts of acrylamide and the cross-linking agent used in PAGE, *N*,*N*'-methylene bisacrylamide. Proper polymerization is brought about by a free radical chain system produced either by photolysis of a labile compound or by the chemical decomposition of a labile compound. Most PAGE methods involve the use of TEMED and ammonium persulfate, di-sulfate ester of hydrogen peroxide that readily homolyzes into unstable $\bullet SO_4$- radicals. These radicals react with TEMED, a tertiary amine, to form TEMED free radicals which thereafter react with acrylamide to bring about polymerization. Initially, the migration rate of proteins in PAGE is determined by a combination of factors including the pore size of the gel and the charge, size and shape of the protein (Gallagher, 2006; Ninfa and Ballou, 1998; Ornstein, 1964). Larger proteins usually undergo a greater frictional force when passing through a gel with a given pore size and thus migrate slower than smaller proteins (Switzer and Garrity, 1999).

The use of sodium dodecyl sulfate-polyacrylamide gel electrophoresis (SDS-PAGE) in protein analysis was first introduced by Shapiro *et al*. (1967). The original SDS-PAGE method was later modified by Laemmli, (1970) and this modified version has become one of the most popularly used PAGE methods (Dennison, 2003b). This type of PAGE, involves the use of the detergent SDS which interacts with the respective protein molecules. The protein sample preparation involves the boiling of the protein in the presence of SDS resulting in its denaturation or linearization of the protein. The interaction between SDS molecules and proteins results in the formation of rod-like complexes which have a constant ratio of 1.4 mg of SDS per mg of protein (Dennison, 2003b; Garfin, 1990; Pitt-Rivers and Impiombato, 1968). Within these rod-like complexes, the negative charge of SDS is able to disguise the charge of the protein and this results in all proteins having the same charge/mass ratio as well as an anodic migration (Dennison, 2003b; Weber and Osborn, 1969).

During SDS-PAGE, two polyacrylamide gel compositions referred to as the stacking gel and the running/resolving gel are used in a single electrophoresis system. Protein

samples are prepared according to post SDS-PAGE analysis requirements. In the case of reducing SDS-PAGE, the protein sample preparation involves the addition of 2-mercaptoethanol as well as boiling of the sample which reduces disulfide linkages and results in breaking up of the quaternary protein structure. While the protein sample preparation for non-reducing SDS-PAGE, does not involve boiling or addition of a reducing agent such as 2-mercaptoethanol. This type of SDS-PAGE is necessary if the preservation of the protein native structure is important for further analysis such as for determining enzyme activity usually demonstrated using zymograms (Dennison, 2003b; Heussen and Dowdle, 1980). After protein sample preparation an appropriate voltage is applied and this is followed by the subsequent carrying of current throughout the gel (Switzer and Garrity, 1999).

When glycine (contained within the tank buffer which is added to the gel system prior to the loading of samples) enters the low pH (6.8) of the stacking gel, it is mostly in the neutral zwitterionic form with approximately only 1% in the negative glycinate form. Due to this, glycine is prevented from being an effective carrier of current and has very little mobility. However, chloride ions contained within the stacking gel are more effective carriers of current and move ahead of proteins, and due to their full negative charge and small size they also experience a relatively low frictional force. The proteins (which have a negative charge due to their association with SDS molecules) experience a larger frictional force due to their mass and they migrate through the stacking gel slower than the chloride ions but faster than the largely uncharged group of glycine molecules.

This migratory pattern causes the protein molecules to build up ahead of the advancing glycine front and finally stack into narrow, concentrated bands at the interface between the running and stacking gel (Ninfa and Ballou, 1998; Switzer and Garrity, 1999). The chloride ions at this point readily migrate from the stacking gel into the running gel. The running gel contains a high concentration of buffer with a pH of 8.8 as well as a relatively high concentration of acrylamide (which results in a decreased gel pore size). The high pH buffer brings about a greater negative charge to the glycine ions and this combined with the relatively small size of the glycine ions result in them overtaking the protein molecules as they migrate through the system. The reduced gel pore size brings

about an increase in the frictional force which in turn affects protein molecule mobility. The equal charge/mass ratio of the protein molecules that was brought about their association with the SDS molecules now forces the proteins to migrate through the gel based on their size. Larger proteins which experience a greater frictional force, migrate slower than smaller proteins and are thus restricted to positions found relatively higher than smaller proteins. To determine the approximate size of the proteins, a mixture of proteins of known molecular weights, often referred to as a molecular weight marker is included during the electrophoretic process. The relative mobility of the proteins contained within the molecular weight marker may be determined and plotted as log molecular weight versus relative mobility and the resultant standard curve that is produced can be used together with the relative mobilities of the unknown proteins to estimate their molecular weights (Switzer and Garrity, 1999).

2.3.1 Reagents

Acrylamide/bisacrylamide monomer stock solution [30% (m/v) acrylamide, 2.7% (m/v) bisacrylamide]. Acrylamide monomer (73 g) and *N,N'*–methylenebisacrylamide (2 g) were dissolved and made up to 250 ml with dH_2O. The solution was filtered through Whatman No.1 filter paper and stored in an amber bottle at 4ºC.

4 x Separating gel buffer [1.5 M Tris-HCl buffer, pH 8.8]. Tris (45.37 g) was dissolved in approximately 200 ml of dH_2O, adjusted to pH 8.8 with HCl and made up to 250 ml with dH_2O. The buffer was filtered through Whatman No.1 filter paper and stored at 4ºC.

4 x Stacking gel buffer [500 mM Tris-HCl, pH6.8]. Tris (3 g) was dissolved in 40 ml of dH_2O and the pH of the solution was adjusted to 6.8 with HCl. The solution was thereafter made up to 50 ml with dH_2O.

SDS stock solution [10% (m/v) in dH_2O]. SDS (10 g) was dissolved in dH_2O and made up to 100 ml with dH_2O. The solution was stored at room temperature (RT).

Ammonium persulfate initiator solution [10% (w/v) in dH_2O]. Ammonium persulfate (0.1 g) was dissolved in dH_2O (1 ml) just before use. This solution was kept at 4ºC for no longer than 1 week.

Tank buffer [250 mM Tris-HCl, 192 mM glycine, 0.1% (m/v) SDS, pH 8.3]. Tris (3 g) and glycine (14.4 g) were dissolved in dH_2O and made up to 1 l. Prior to use, SDS stock solution (2.5 ml) was added to 250 ml of tank buffer.

Reducing treatment buffer [125 mM Tris-HCl buffer, 4% (m/v) SDS, 20% (v/v) glycerol, 10% (v/v) 2-mercaptoethanol, pH 6.8].4 x Stacking gel buffer (2.5 ml), SDS stock solution (4 ml), glycerol (2 ml) and 2-mercaptoethanol (1 ml) were combined and made up to 10 ml with dH_2O.

2.3.2 Procedure

The Hoefer® Mighty Small SDS-PAGE electrophoresis unit was assembled according to the instructions specified by the manufacturer. The aluminium and glass plates, plastic combs and spacers were rinsed in dH_2O, 70% ethanol and thereafter rinsed in dH_2O once more and dried. These components were assembled in a gel caster as per the manufacturer‟s instructions.

Table 2.1: Reagent proportions for Laemmli running and stacking gels of different acrylamide concentrations.

Reagent	Running gel (%) 15%	Stacking gel (%) 15%
Acrylamide/bisacrylamide monomer stock solution (ml)	6.25	0.94
4 x running gel buffer (ml)	3.75	0
4 x Stacking gel buffer (ml)	0	1.750
SDS stock solution (µl)	150	70
Ammonium persulfate (initiator) (µl)	75	35
dH_2O (ml)	3.5	4.3
TEMED (µl)	7.5	15

The acrylamide/bisacrylamide monomer stock solution, running gel buffer, SDS stock solution and dH_2O were combined with the ammonium persulfate initiator solution and TEMED according to the volumes specified in (Table 2.1). The resultant solution was mixed well and loaded into the assembled gel caster unit, overlaid with dH_2O to prevent exposure to oxygen and left to polymerise (1 h). Once polymerization was complete, the overlaid dH_2O was poured out and the stacking gel solution which was prepared according to the volumes specified in Table 2.1 was poured in up to the notch of the aluminium plate and a 10 or 15 well comb was inserted into the stacking gel and

polymerization was allowed to take place (30 min). The combs were thereafter removed, the resultant wells were rinsed with dH_2O and the gels were placed onto the electrophoresis units. SDS stock solution (2.5 ml) was added to tank buffer (250 ml) and this solution was poured into the upper and lower electrode compartments of the electrophoresis unit. Protein sample preparation usually involved the addition of the reducing treatment buffer to the protein sample and the resultant solution was boiled for 90 s prior to the addition of the marker dye, bromophenol blue (5µl, 0.1% (m/v) in dH_2O). Protein samples at appropriate concentrations were loaded into the wells of the stacking gel. The electrophoresis unit was connected to a power pack and run at 18 mA per gel, unlimited voltage, until the bromophenol blue marker dye was about 0.5 cm from the bottom of the running gel. During electrophoresis, the gels were cooled using a circulating water bath (4ºC). Once electrophoresis was complete, the gels were further developed for either western blotting or staining for protein visualization.

2.4 Staining techniques used to detect proteins in SDS-PAGE gels

There are various methods which may be used to detect the presence of proteins in SDS-polyacrylamide gels after electrophoresis. The most common method involves the use of an appropriate stain to visualize the proteins that are present. When choosing a staining method, one should take several factors into consideration, including the nature of the possible proteins present, the required sensitivity of the detection and the intended analytic procedures which follow the electrophoretic process (Steinberg, 2009; Switzer and Garrity, 1999). Several types of staining methods have been used by researchers over the years including fluorescence staining, Fast green staining, Amido black staining, Coomassie brilliant blue (CBB) staining and copper staining (Merril, 1990). In this study, the proteins that were separated on SDS-PAGE gels were detected using the Coomassie brilliant blue (CBB) method.

2.4.1 Coomassie brilliant blue staining

Coomassie brilliant blue (CBB) binds to the proteins in a gel. Its interaction with proteins is mainly via arginine residues, though weak interactions with tryptophan, tyrosine, phenylalanine, histidine and lysine also occur. If conducted properly, CBB staining will detect a protein band containing as little as 0.1 to 0.5 µg of protein

(Switzer and Garrity, 1999). One of the first types of CBB stains to be introduced was Coomassie brilliant blue R-250. The "R" stands for a reddish hue while the number "250" is a dye strength indicator. This was later followed by the introduction of Coomassie brilliant blue G-250 (CBB G-250) in which the "G" stands for the greenish hue associated with this dye. CBB G-250 may be used as a colloidal dispersion which does not penetrate gels and this allows for the rapid staining of proteins without unwanted background. For successful CBB staining, acidic conditions are required so that an electrostatic attraction between the dye molecules and the amino groups of proteins may be formed. Van der Waal‟s forces along with the ionic attraction binds the dye-protein complex together. These dye molecules have been observed to interact with the basic groups in polypeptides as it has been established that there is a strong correlation between the intensity of CBB staining and the number of basic amino acid residues contained within a protein (Merril, 1990). The CBB staining procedure involves the use of a dye solution which contains acetic acid, methanol and dH_2O. The methanol and acetic acid are used to fix the proteins within the gel and this allows for the CBB dye to bind to these proteins. This is followed by the "destaining" of the gel with the same aqueous solution used for staining except without the inclusion of the dye. This is necessary for the removal of excess dye from areas of the gel which did not contain any proteins. Proteins on the gel are visualized as dark blue bands (Switzer and Garrity, 1999).

2.4.1.1 Reagents

Coomassie Brilliant blue G-250 solution [0.02% (m/v) Coomassie Brilliant blue G250, 2% (w/v) phosphoric acid, 5% (m/v) aluminium sulphate, 10% (v/v) ethanol.

Coomassie Brilliant blue G-250 dye (0.2 g) and $Al_2(SO_4)_3.(H_2O)_{15}$ (50 g) were dissolved in 86% (v/v) phosphoric acid (24 ml) and ethanol (100 ml) and made up to 1 l with 876 ml dH_2O. The solution was stirred (5 min) and stored at RT.

2.4.1.2 Procedure

Once electrophoresis was concluded, the gel was placed into a clean plastic container and covered with staining solution (4 h). The stain was thereafter removed and rinsed with dH_2O before being placed into a clean container containing dH_2O. The gel was

thereafter photographed using a VersaDoc 4000 Imager (BioRad, California, USA) and analyzed using Quantity One software. The gel was thereafter stored in a sealed plastic bag containing dH_2O at 4ºC.

2.5 Western blotting

Western blotting which is also referred to as immunoblotting is a commonly used method that was pioneered by Towbin *et al*. (1979) and is used to verify the expression of a protein, the relative amount of protein in a pure or impure solution as well as to test the specificity of antibodies raised against a particular protein. During western blotting, a target protein which may be contained in a pure or crude solution is detected with a specific primary antibody. Prior to this process, protein separation according to molecular weight is achieved by SDS-PAGE. The proteins are then electrophoretically transferred to a membrane and this is followed by probing with a specific primary antibody, detection with a specific secondary antibody and finally the developmental stage usually involves a chemiluminescent or colorimetric system (Penna and Cahalan, 2007).

There are several types of western blotting systems available including the vertical type which has a large buffer reservoir and platinum electrodes as well as the horizontal, semi-dry type which has graphite plate electrodes (Dunn, 1989; Kyhse-Andersen, 1984; Pettegrew *et al*., 2009). The composition of the transfer buffer is one of the important factors that determines the efficiency of the protein transfer process. The most commonly used type of buffer was developed by Towbin *et al*. (1979) and includes Tris base and glycine at a pH of 8.3 (Dunn, 1989). Methanol is usually added to this buffer in the case of SDS gels as it promotes the dissociation of SDS from the proteins and also improves the adsorption of proteins onto transfer membranes in the presence of SDS (Pettegrew *et al*., 2009).

Several types of transfer membranes are available however the most commonly used is nitrocellulose, pore size 0.45 µm for proteins larger than 15 kDa and 0.2 µm for proteins smaller than 15 kDa. Positively charged nylon membranes have also been used as they have a higher protein binding capacity of approximately 480 µg cm^{-2} as compared to nitrocellulose whose protein binding capacity is approximately 80 µg cm^{-2}. However the

use of nylon membranes has often been associated with problems during protein visualization (Dunn, 1989). Polyvinylidene difluoride (PVDF) membranes have also been observed to be successful transfer membranes as they have high mechanical strength. They have also been reported to have a higher protein binding capacity as well as a greater ability to retain bound proteins after exposure to washing and blocking reagents as compared to nitrocellulose and nylon membranes (Dunn, 1989; Pettegrew *et al*., 2009).

Prior to the probing process, the unoccupied binding sites of the transfer membrane need to be blocked. Several blocking solutions have been used by researchers, each of them including a solution of protein such as bovine serum albumin (BSA), ovalbumin, haemoglobin or gelatin. It has, however, been observed that some proteins included in the blocking solution may not always be unreactive during the probing process and this may result in background staining (Dunn, 1989). A blocking solution containing non-fat milk powder has been successfully used by many researchers as its use usually results in very low background staining (Dunn, 1989; Schalkwijk *et al*., 1992). Once probing with the specific primary antibody has taken place, a detection system is necessary for the visualization of the possible reaction between the primary antibody and the specific protein with which it reacts. For this purpose, indirect sandwich techniques using second or third ligands have been developed. These techniques are commonly used for immunodetection as they usually increase the sensitivity and specificity of the immunoblot technique. Detection systems commonly used usually involve either fluorescence such as fluorescein isothiocyanate, radiolabels for example ^{125}I or enzyme reactions such as peroxidise and alkaline phosphatase. In the case of enzyme reactions, reagents are conjugated to these enzymes and are used in conjunction with a suitable substrate to produce a detectable signal (Dunn, 1989). Examples of such enzyme reactions include the use of horseradish peroxidase (HRP) in the presence of substrates such as 3,3‟-diaminobenzidine (DAB) and 4-chloro-1-naphthol (Conyers and Kidwell, 1991; Straus, 1982).

2.5.1 Reagents

Transfer buffer [25mM Tris-HCl and 192mM glycine-HCl buffer, 20% (v/v) methanol, 0.01% (m/v) SDS, pH 8.3]. Tris base (6.05 g) and glycine (28.8 g) were dissolved in 1.6 l of dH_2O. Methanol (400 ml) was added and the solution was stored at 4ºC. Prior to use, 10% (m/v) SDS (10 ml) was added to 1 l of the solution.

Ponceau S protein staining solution [0.1% (w/v) Ponceau S in 1% (m/v) acetic acid]. Glacial acetic acid (1 ml) was diluted to approximately 90 ml with dH_2O. Ponceau S (1 g) was added to the solution, dissolved and the solution was made up to 100 ml with dH_2O. The solution was stored at RT.

Tris-buffered saline (TBS) [20 mM Tris-HCl, 200 mM NaCl, pH 7.4]. Tris (2.42 g) and NaCl (11.68 g) were dissolved in approximately 900 ml of dH_2O. The solution was titrated to pH 7.4 with HCl and made up to 1 l.

Blocking solution [5% (m/v) non-fat milk powder in TBS]. Elite non-fat milk powder was dissolved in TBS (100 ml). This solution was made up just before use.

Alkaline phosphatase substrate buffer [50mM Tris-HCl buffer, 5 mM $MgCl_2$, pH 9.5]. Tris (6.05 g) and $MgCl_2$ (1.0 g) were dissolved in 980 ml of dH_2O. The pH was adjusted to 9.5 with HCl and the solution was made up to 1 l with dH_2O. The solution was stored at 4ºC.

5-Bromo-4-chloro-3-indolyl phosphate (BCIP) stock solution. BCIP (150 mg) was dissolved in DMF (3 ml). The solution was stored at -20ºC in an amber bottle that was covered with foil.

Nitroblue tetrazolium (NBT) stock solution. NBT (300 mg) was dissolved in DMF [70 % (v/v)] (2.1 ml) and the solution was made up to 3 ml with dH_2O. The solution was stored at -20ºC in an amber bottle that was covered with foil.

Alkaline phosphatase substrate solution [0.015% (m/v) BCIP, 0.03% (m/v) NBT in substrate buffer]. BCIP stock solution (30 µl) and NBT stock solution (30 µl) were dissolved in alkaline phosphatase substrate buffer (10 ml) just before use.

0.2 M Tris buffer, pH 7.6. Tris base (24.2 g) was dissolved in dH_2O (800 ml), the pH of the solution was adjusted to 7.6 with 1M HCl and made up to a final volume of 1 l.

3,3'-diaminobenzidine (DAB) substrate solution. DAB (2.5 mg) was dissolved and made up to 5 ml in 0.2 M tris buffer, pH 7.6; just before use, 30% H_2O_2 (15 µl) was added to the solution. When working with DAB, extra precaution was necessary as it is a potential carcinogen; thus gloves were worn and special care was taken to avoid inhalation of DAB powder. All contaminated glassware, spills or waste solutions were decontaminated in a solution of hypochlorite.

4-Chloro-1-naphthol substrate solution [0.06% (m/v) 4-chloro-1-naphthol, 0.0015% (v/v) H_2O_2]. 4-chloro-1-naphthol (0.03 g) was dissolved in methanol (10 ml). Two ml of this solution was then diluted to 10 ml with TBS. 30% H_2O_2 (4 µl) was added to the solution just before use.

2.5.2 Procedure

Just before the completion of SDS-PAGE, 1 sheet of Hybond^{TM}– C Extra nitrocellulose hybridization transfer membrane (0.45 µm) and 8 sheets of Whatman filter paper which were cut to a suitable size were carefully placed into transfer buffer before being totally immersed so as to avoid the creation of air bubbles. After SDS-PAGE (Section 2.3), the gel was removed, placed squarely on top of the transfer membrane and a sandwich which was composed of 4 sheets of Whatman filter paper on the respective sides of the transfer membrane and the gel was assembled. The sandwich was, thereafter, placed in between two pieces of Scotchbrite foam and placed into the transfer cassette (Bio-Rad Mini Trans-Blot® Electrophoretic Transfer Cell). The cassette was positioned into the electrophoresis tank in such a manner that the transfer membrane was closest to the anode. The tank was thereafter filled with transfer buffer and stirred with a magnetic stirrer bar throughout the transfer process which was performed at 300 V, 150 mA for 16 h. After the transfer process, the gel and nitrocellulose transfer membrane were removed from the cassette and the gel outline was marked on the nitrocellulose. Excess nitrocellulose membrane was trimmed and thereafter the membrane was placed into Ponceau S protein staining solution to allow for the visualization of the molecular weight marker as well as to determine the efficiency of the protein transfer. The proteins

contained within the molecular weight marker were marked using light pencil lines. The stain was removed by washing the nitrocellulose membrane in dH_2O. The membrane was thereafter air dried between sheets of filter paper before the probing process could begin. At the beginning of the probing process, the nitrocellulose membrane was placed into the blocking solution (1 h, RT) so that free sites contained within the membrane could be blocked, thus preventing the non-specific adsorption of antibodies. The membrane was thereafter washed with TBS (3 x 5 min) and incubated with the respective primary antibody that had been diluted in blocking solution (2 h, RT or overnight, 4ºC). The membrane was then washed with TBS (3 x 5 min) and incubated with the appropriate enzyme conjugated secondary antibody that had also been diluted with the blocking solution (1 h, RT). Thereafter the membrane was washed in TBS (3 x 5 min) and placed into the appropriate substrate solution and developed in the dark until distinct bands were observed. The membrane was then rinsed with dH_2O, dried between filter paper and photographed using a VersaDoc 4000 Imager (BioRad, California, USA) and analyzed using Quantity One software.

2.6 Mycobacterial culture

The study of pathogenic mycobacteria such as *M.tuberculosis* is crucial to the understanding of its pathogenesis. However, the direct study of this pathogenic organism is not always possible or convenient for two main reasons. Firstly many pathogenic species of mycobacterium such as *M.tuberculosis* are category three human pathogens and require a biosafety level three laboratory and animal facilities as well as extensive training prior to its culture. Secondly, *M.tuberculosis* is a slow growing microorganism and doubles every twenty two hours in liquid culture. Between two and three weeks are required for its colony formation and this results in prolonged experimental time. Many researchers have thus chosen non pathogenic mycobacterial model organisms to gain a better insight into how non-pathogens are killed, before the pathogen is studied and the mechanisms allowing for the survival of the pathogen are distinguished. One such model microorganism is *M.smegamtis*, a saprophytic (obtaining nourishment from dead or decaying organic matter) mycobacterial species that usually lives in soil. This mycobacterial species is generally non-pathogenic and is used as a model organism as it is fast growing, with a doubling time of approximately four hours

and colony generation occurring between two to three days and it also shares many features with pathogenic mycobacteria such as *M.tuberculosis* (He and De Buck, 2010; Shiloh and DiGiuseppe Champion, 2010).

The culturing of *M.smegamtis* has been simplified by the availability of the Middlebrook 7H9 broth medium and 7H10 agar base (Difco^{TM}) which support the growth of many mycobacterial species (Middlebrook and Cohn, 1958). The Middlebrook 7H9 broth base is usually supplemented with glycerol and further enriched with the Middlebrook OADC Enrichment solution (Difco^{TM}) which contains oleic acid, albumin, dextrose, sodium chloride and catalase. *M.smegamtis* is usually grown at 37ºC with shaking (Chacon *et al*., 2002; Takayama and Kilburn, 1989).

In this current study, *M.smegmatis* mc2155 harbouring a p19-(long-lived) EGFP was cultured according to Blokpoel *et al*. (2005) and Anes *et al*. (2006) with minor modifications.

2.6.1 Reagents

Middlebrook 7H9 broth. Middlebrook 7H9 broth (0.47 g) and glycerol (0.2 ml) was dissolved in dH_2O (90 ml). The broth medium was thereafter autoclaved (121ºC) and after it was cooled, Middlebrook OADC Enrichment solution (10 ml) and hygromycin [50 µg/ml] (0.25 ml) (used to stabilize GFP expression) was added to the broth medium under sterile conditions.

Middlebrook 7H10 agar. Middlebrook 7H10 agar powder (1.9 g) and glycerol (0.5 ml) was added to dH_2O (90 ml) and dissolved by heating the solution with gentle agitation until the powder was completely dissolved. The broth medium was thereafter autoclaved (121ºC) and after it was cooled, Middlebrook OADC Enrichment solution (10 ml) and hygromycin [50 µg/ml] (0.25 ml) (used to stabilize GFP expression) was added to the agar solution under sterile conditions.

2.6.2 Procedure

Middlebrook 7H9 broth medium was inoculated with a single *M.smegmatis* mc2155 colony under sterile conditions. The culture was grown at 37ºC with shaking (200 r.p.m) in a New Brunswick Scientific controlled environment incubator shaker.

2.7 Fluorescent immunocytochemistry, confocal microscopy and colocalization

Fluorescence may be defined as the ability of some atoms and molecules to absorb light at a particular wavelength and after a short period of time, emit light at a longer wavelength. For fluorescence to occur, an outside source of energy is required. The light that is emitted is usually in the form of electromagnetic radiation. Since the introduction of fluorescent microscopy, the number of its applications has increased greatly. One of its major applications is its use in immunocytochemistry (Herman, 1998c). The technique of immunocytochemistry involves the use of antibodies which recognize particular antigens in cells and this recognition is usually visualized with the aid of labelled molecules (Polak and Van Noorden, 1997).

Immunofluorescence is a technique that brings together the specificity of antibodies with the sensitivity of fluorescence and is useful for observing specific cell and tissue components. The antibodies used in immunofluorescence are labelled with fluorescent molecules that ultimately enable the visualization of the interaction between the specific antibody and the antigen. Two methods have been usually used in immunofluorescence and these are referred to as direct and indirect immunofluorescence. Direct immunofluorescence refers to the labelling of an antibody with a fluorescent molecule and the recognition of the appropriate antigen by this antibody. This method, although highly specific (due to the fact that one antigen may only bind to a few antibodies as long as the antibody is specific) may also result in a weak overall fluorescent signal. During indirect immunofluorescence, the antigen is first incubated with the suitable antibody that is unlabelled. This is followed by the introduction of a second antibody that is labelled with a fluorescent molecule. This second antibody was raised using the first antibody as an antigen. This method of immunofluorescence produces a greater overall fluorescence signal compared to the direct method due to the fact that each

antigen is able to bind to multiple antibodies thus providing more binding sites for secondary antibody interaction (Herman, 1998a). When conducting immunofluorescence, it is important to make sure that the concentrations of the primary and secondary antibodies are not too high as this would lead to non-specific fluorescence. Thus it is essential that one optimizes the concentrations of the primary and secondary antibodies to minimize non-specific fluorescence. Non-specific fluorescence may result from tissue components in tissue samples with a naturally occurring fluorescence and this is referred to as autofluorescence (Herman, 1998a). Autofluorescence may also result from the presence of fixatives, such as glutaraldehyde used during the sample preparation which form aromatic fluorescing compounds upon reacting with cells or fixation of antibodies to tissues (Baschong *et al*., 2001; Herman, 1998a). There are a number of steps that may be taken to reduce the amount of non-specific fluorescence. These include using non-fluorescent fixatives such as paraformaldehyde, thorough washing between the various steps of the immunofluorescence procedure and the use of a mounting medium which contains components that prevent photobleaching (the irreversible fading of a fluorescent label upon exposure to excitation light) or improve fluorescence. The blocking of unreactive sites with solutions that include bovine serum albumin as well as the quenching of free aldehyde (which would otherwise react with primary and or secondary antibodies) using glycine are also methods of decreasing non-specific fluorescence. The proper storage of the fluorescently labelled antibodies is also important for successful immunofluorescence as frequent freeze-thawing may result in disruption of covalent bonds between the fluorescent molecule and the antibody (Herman, 1998a).

When choosing a fluorophore, one should choose one that associates specifically with the structure of interest, it should also provide a strong signal, photobleach minimally and be nontoxic. When using a fluorophore for laser scanning confocal microscopy, one should also take into consideration the laser lines available and the excitation and emission spectra of the probe. The chosen fluorophore should be excited by the existing laser lines, and its absorption maximum should also be at or close to one of the available wavelengths. If more than one fluorophore is used in the same procedure, the fluorophores should have well separated excitation and emission spectra, emission

overlap should be minimal. It is also important to check that the available confocal beam splitters are able to collect the emission spectra of the fluorophore efficiently (Cullander, 1999).

Laser scanning confocal microscopy, used extensively in this current study, has emerged as a powerful imaging tool that allows for the visualization of fluorescently labelled molecules using laser beams which have particular wavelengths. The original design of the confocal microscope was introduced by Marvin Minsky in 1955 (Minsky, 1988). In this original design, a stationary light beam was used to scan across a specimen that was moved on a vibrating stage. This original design has since evolved and for purposes of viewing biological specimens, an alternative method of scanning specimens has been developed in which the specimen is stationary and the light beam scans across it, referred to as beam scanning. There are two main methods of beam scanning; multiple-beam scanning and single-beam scanning, the latter of which is used more often. Single beam scanning is employed by laser scanning confocal microscopes (Paddock, 1999). Laser scanning confocal microscopes consist of a laser light source and an intermediate optical system that is coupled to an objective lens and a photodetector. Some of the popular lasers associated with laser scanning confocal microscopes include the low power argon ion laser and the argon-krypton mixed gas laser (Table 2.2) (Sheppard and Shotton, 1997b).

Table 2.2: Emission wavelengths of lasers that are commonly used in laser scanning confocal microscopy (adapted from Sheppard and Shotton, 1997b).

Laser	Wavelength (nm)			
	Ultraviolet	**Blue**	**Green**	**Red**
Helium-cadmium	325	442		
Helium-cadmium (Red Green Blue)		442	534, 538	636
Low power argon ion		488	514	
Water-cooled argon ion	351, 364	457, 488	514, 528	
Argon-krypton mixed gas		488	568	647
Helium-neon (green)			543	
Helium-neon (red)				633

Laser scanning confocal microscopy and other types of confocal microscopy are able to create sharp images of a sample specimen which would appear blurred if the specimen was viewed using a conventional microscope. By eliminating light from out of focus planes and minimizing the superimposition of detail, confocal microscopy is able to produce images that are incredibly detailed and free from blur. The way in which confocal microscopy illuminates a single point of the specimen with a focussed beam so that images from above and below the plane of focus are eliminated is achieved by placing a pinhole aperture in the way of the emitted light and just before the detector photo-multiplying tube (PMT) allowing for the illumination of only a specific depth of the sample specimen to be collected (Figure 2.1). A single fraction-limited spot of light

is projected onto the sample specimen using a high numerical aperture objective lens and the light that is subsequently reflected or fluoresced by the specimen is collected by the objective and is either allowed or prevented from passing through a second pinhole aperture. The light that originates from above and below the image plane strikes the pinhole but is not transmitted to the detector known as the photomultiplier tubes (PMT), while the light that makes it through the pinhole is measured by this detector (Figure 2.1) (Herman, 1998d). Laser scanning confocal microscopes usually have sets of beam splitters and mirrors which are used to direct the beam path of light emitted by the laser source. There are three main types of beam splitters that are used in confocal microscopy; the broad spectrum, the polarizing and the dichroic beam splitter (Cogswell and Larkin, 1995).

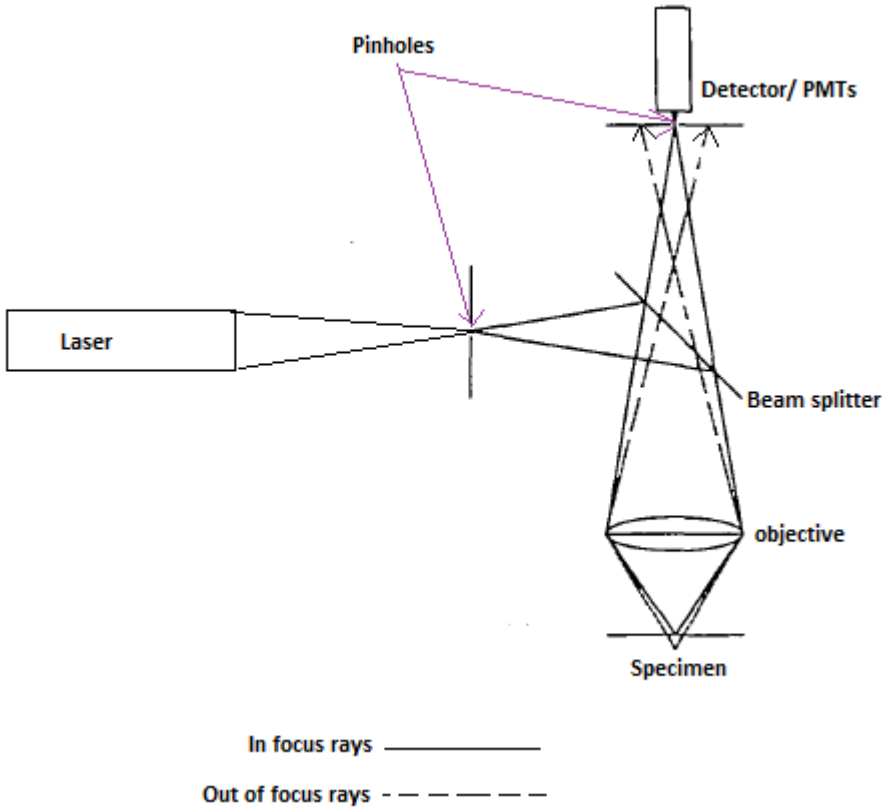

Figure 2.1: A schematic representation of the beam path in a confocal microscope.

In laser scanning confocal microscopes, a laser beam passes through a pinhole that is placed in the beam path of a laser source. The path of this beam is directed by beam splitters and mirrors and illuminates a single point on the specimen. A second pinhole is placed in front of the detector system (PMTs). This pinhole excludes light that originates from above and below the image plane thus preventing it from being detected by the PMTs (adapted from Shotton, 1989).

With confocal microscopy, a complete image of the specimen is never achieved because, at any point in time, only one point is observed. Thus, to enable visualization of a complete image, the detector is attached to a computer which assembles the image one pixel at a time. The image that is generated by a confocal microscope is of a thin planar region (involving two dimensions) of the specimen. This is referred to as optical sectioning. By gathering the optical section images at regular intervals along the optical axis, it is possible using specialized software to combine these two dimensional images to create a three dimensional image (Sheppard and Shotton, 1997a; Wilson, 1995).

The generation of sharp optical sections by confocal microscopy is largely due to the rejection of out of focus light by pinholes and thus the size of the pinhole is a very

important aspect to consider when imaging using a confocal microscope (Wilson, 1995). The size of the pinhole dictates light intensity and the thickness of the optical section, thus for confocal microscopes with a variable pinhole, an optimum pinhole size should be chosen to provide the best combination of brightness and optical section thickness (Herman, 1998d). To obtain an optimal image of a focal plane, the diameter of the pinhole should be equal to that of the central disk of the Airy diffraction pattern of the image of the illuminated point, referred to as 1 Airy unit. To understand the concept of an Airy diffraction pattern, it is important to understand that the image of a small illuminated object point is not infinitely small but is a circularly Airy diffraction image with a central bright disk surrounded by concentric circles that decrease in light intensity as the distance from the central disk increases (Inoue, 1995). The diameter of the Airy disc is dependent on the numerical aperture, or resolving power of the objective used and the wavelength of the excited light (Herman, 1998b).

Using immunofluorescence, one is able to study the interaction of intracellular antigens by performing colocalization studies. Colocalization, in terms of fluorescence, may be defined as the degree to which two or more fluorophores can be detected within the same defined location. These fluorophores are usually conjugated to antibodies which ultimately recognize specific antigens and thus, the detection of these fluorophores and subsequent colocalization studies usually indicate a relationship between the respective antigens. Colocalization between two or more antigens may indicate that these antigens share common structural and functional characteristics (Zinchuk *et al*., 2007).

The ability to visualize the specific locations of proteins within cells is important as the location and physiological function of a protein are closely related and thus, by being able to visualize the location of proteins, one may gain a better understanding of their involvement in biological processes. Immunofluorescence microscopy has been used by many researchers to determine the localization of proteins using well-characterized markers. This technique, which involves the use of fluorophore-conjugated antibodies and other fluorophore-conjugated markers, has also enabled researchers to visualize the relationship between various proteins using colocalization studies in which the localization of a protein in relation to another is visualized and analyzed. At present only the colocalization of one fluorescent label against another i.e. two fluorophores at a

time is possible in colocalization studies. Conventionally, one of the fluorophores is designated a red colour while the other is usually green. Colocalization studies are extremely useful as the colocalization between proteins usually indicates that they share common structural and functional characteristics (Bolte and Cordelières, 2006; Zinchuk *et al*., 2007).

Colocalization between proteins is said to occur when two proteins bind to the same spatial compartments (Costes *et al*., 2004). In terms of multichannel fluorescence microscopy images, colocalization can be defined as the existence of more than one signal at the same pixel location (Zinchuk *et al*., 2007). Over the years, the image representation and analysis methods used during colocalization studies have caused much debate amongst researchers. The large number of colocalization representation and analysis methods and the complexity associated with some of them make it difficult to choose and implement an appropriate method. In addition to this, not all colocalization methods fit all circumstances as the contents of cells have various morphologies such as Golgi stacks, vesicles, and cytoskeletons. Thus, colocalization studies often requires a customized rather than a standard approach (Bolte and Cordelières, 2006; Costes *et al*., 2004; Li *et al*., 2004).

The representation of colocalization by means of visualization is often the starting point for colocalization studies and usually involves a basic overlay method which is made up of the different colours/channels. These channels (green and red), representing two different molecules within a dual-coloured/channel image, are overlayed and subsequently give rise to yellow regions at points where the two molecules of interest are present in the same pixel. The presence of these yellow regions is dependent on the relative signal intensity collected in both channels. This overlay method of visualizing colocalization is only reliable when both colours/channels within a dual-coloured/ channel image exhibit the same grey value properties (Bolte and Cordelières, 2006). Grey value refers to the brightness/intensity of a pixel, where each pixel is associated with a value representing its luminosity from black to white. These values range from 0 to 255/0 to 256 for 8-bit images, with 0 being black and 255/256 being white (Oberholzer *et al*., 1996). The probability, however, of an image where two fluorophores with different signal strengths exhibiting similar grey level properties is

very rare. Another limitation of representing colocalization using the overlay method is that it is not suitable for quantification purposes as this method can result in a misrepresentation and misinterpretation of the relative proportion of molecules. To overcome the problems encountered with the overlay method of colocalization representation, image analysis is required. There are two main methods of analyzing colocalization; the first of which involves a global statistical approach in which intensity correlation coefficient-based (ICCB) analyses are conducted and the other involves an object-based approach (Bolte and Cordelières, 2006).

ICCB analysis involves the statistical analysis of the relationship between the intensity values of the green and red pixels in a dual-coloured/channel image. This analysis involves the use of correlation coefficients which measure the strength of the linear relationship between the intensity values of the green and red pixels. The most commonly used correlation coefficient is the Pearson‟s correlation coefficient which may be understood if one represents the correlation of the pixel intensities of the channels of a dual-coloured/channel image in a two-dimensional histogram/scatter plot where the intensity of a given pixel in the green channel is used as the x-coordinate of the scatter plot. Similarly the intensity of the corresponding pixel in the red channel is used as the y-coordinate. If the labelling of both fluorophores that are represented by the channels are proportional to each other and the detection of the channels are carried out in a linear range, the resulting scatter plot pattern should be a line which has a slope that reflects the relative stoichiometry of both the fluorphores based on their relative detection efficiencies. In the case of complete colocalization between the two channels, the dots that appear on the scatter plot should be centred on a line. The nature of the distribution of these dots with reference to the fitted line is determined by calculating the Pearson‟s correlation coefficient (r) (Bolte and Cordelières, 2006). This correlation coefficient describes the correlation of the intensity distributions between the different channels in a dual-coloured/channel image and only takes into consideration the similarity of the shapes of the channels (Manders *et al*., 1992).

It is calculated using the formula:

$$r = \frac{\sum_i (R_i - R_{aver}) \cdot (G_i - G_{aver})}{\sqrt{\left[\sum_i (R_i - R_{aver})^2 \cdot \sum_i (G_i - G_{aver})^2\right]}}$$

R_i and G_i are the grey values of voxel (volume pixel) i of the red and green components of a dual-coloured/channel image respectively. R_{aver} and G_{aver} are the average grey values of R_i and G_i, respectively. Since R_{aver} and G_{aver} are subtracted from R_i and G_i respectively when calculating Pearson‟s correlation coefficient, the value of this coefficient ranges from -1 to 1 with -1 showing negative correlation between the colours of a dual-coloured image and 1 for complete positive correlation between the colours (Bolte and Cordelières, 2006; Manders *et al*., 1992). It has been established that values from 0.5 to 1 indicate colocalization while values from -0.1 to 0.5 indicate an absence of colocalization (Table 2.3) (Zinchuk and Zinchuk, 2008). When R_{aver} and G_{aver} are not subtracted from R_i and G_i, a new coefficient referred to as the Manders‟ Overlap Coefficient is established and calculated using the following equation:

$$r = \frac{\sum_i R_i \cdot G_i}{\sqrt{\left[\sum_i (R_i)^2 \cdot \sum_i (G_i)^2\right]}}$$

This coefficient indicates the actual overlap of the channels that make up a dual-channel image and has values that range between 0 and 1. It is not sensitive to differences in signal intensities between the components of an image which usually arise as a result of different labelling with fluorophores and photo-bleaching range (Manders *et al*., 1992). If an overlap coefficient of 0.5 is calculated for a dual-coloured/channel image, it implies that 50% of the pixels of both channels overlap while a coefficient of 0 indicates that there are no overlapping pixels. Values between 0.6 and 1 indicate colocalization

while values from 0 to 0.6 indicate an absence of colocalization (Table 2.3) (Zinchuk and Zinchuk, 2008).

The degree of colocalization may also be expressed by means of two separate parameters using Overlap coefficients k_1 and k_2 which describe the differences in intensities of the green and red colours of a dual-image. The values for k_1 and k_2 are calculated using formulas which depend on the sum of the products of the red and green intensities. These formulas are expressed as:

$$k_1 = \frac{\sum_i R_i \cdot G_i}{\sum_i R_i^2} \qquad k_2 = \frac{\sum_i R_i \cdot G_i}{\sum_i G_i^2}$$

The k_1 coefficient is sensitive to differences in the intensity of the green channel while k_2 is sensitive to differences in the intensity of the red channel. Colocalization between the two colours/channels occurs if the values for k_1 and k_2 are close to each other (Table 2.3), for example if the value for k_1 is 0.5 and that of k_2 is 0.6. (Manders *et al*., 1992; Zinchuk and Zinchuk, 2008).

Based on the expression of colocalization as two separate parameters, two other coefficients, M_1 and M_2 were defined. Unlike k_1 and k_2, M_1 and M_2 are not dependent on the intensities of the two channels. These coefficients are calculated using the following formula:

$$M_1 = \frac{\sum_i R_{i,\text{coloc}}}{\sum_i R_i} \quad M_2 = \frac{\sum_i G_{i,\text{coloc}}}{\sum_i G_i}$$

The M_1 and M_2 coefficients range from 0 to1 with 0 indicating no overlap/ synchronization between the colours of a dual-colour image and 1 indicating a 100% colocalization between them. These coefficients are proportional to the amount of fluorescence of the colocalizing regions in each channel of a dual-coloured/channel image relative to the total fluorescence in the particular channel and they may be determined even when the signal intensities in the two channels differ to a large degree (Manders *et al*., 1992). Values for M_1 and M_2 greater than 0.5 indicate colocalization while values less than 0.5 indicate an absence of colocalization (Table 2.3) (Zinchuk and Zinchuk, 2008) .

The M_1 and M_2 coefficients are very sensitive to noise within images (the presence of colour dots or specks in places where they should not exist). To overcome this sensitivity, M_1 and M_2 should be calculated by setting a threshold value for each colour channel which is based on the estimated value of noise/background (Bolte and Cordelières, 2006; Manders *et al*., 1992). The setting of a threshold value is used as a "cut-off" to distinguish between specific and non-specific staining where the overlapping regions between both channels that are determined using these threshold values are considered as colocalized regions. The contributions of the channels within these defined colocalized regions are defined as colocalized coefficients. The downfall of this technique is that the threshold values are usually set based on a visual estimation of the images or they may be set based on a segmentation algorithm and this results in inconsistent results (Bolte and Cordelières, 2006; Costes *et al*., 2004). An approach to overcome this was introduced by Costes *et al*. (2004) and is referred to as the Costes" approach. This approach uses the amount of correlation in the various regions of a scatter plot to automatically estimate thresholds. It also involves a statistical significance test to determine the probability (P-value) that the measured Pearson"s coefficient (*r*) established from the correlation of the two colours/channels of a dual coloured/channel image, referred to as r_{obs}, is significantly greater than the values of *r* that would be calculated if there was only random overlap. To calculate the P-value, the pixel blocks of the image are scrambled and the *r* value for this image is calculated and compared to the *r* value of the original, unscrambled image. In doing so, the two spatial distributions become independent and this enables contribution to the correlation of

random overlap to be measured. By repeatedly scrambling and measuring the correlation of random overlap, one is able to determine the probability distribution of the amounts of random overlap for the two channels. This distribution is centred on 0. If one compares the *r* value for the unscrambled image with this probability distribution, it is then possible to determine if significant colocalization exists (Bolte and Cordelières, 2006; Costes *et al*., 2004). According to Costes *et al*. (2004), a P-value greater than 95% indicates that the calculated Pearson‟s coefficient is true and not due to random overlap. Li *et al*. (2004) also developed a method of colocalization analysis in an approach which discriminates between actual colocalization and coincidental events. Using this approach, it is assumed that the overall difference of pixel intensity from the mean intensity of a single colour/ channel of a dual-coloured/channel image is equal to zero. To express this, Li *et al*. (2004) formulated the equations $\sum_{n\ pixels} (A_i - a) = 0$ and $\sum_{n\ pixels} (B_i - b) = 0$. With regards to the respective channels/ colours, A_i and B_i refer to the current pixel‟s intensity and a and b refer to the current channels mean intensity. In order to present and interpret the data generated using this approach, Li *et al*. (2004), also introduced the concept of an intensity correlation quotient (ICQ) which is defined as the ratio of positive $(A_i - a)(B_i - b)$ products divided by the overall products subtracted by 0.5. The ICQ of a dual-coloured/channel image ranges from 0.5 to -0.5. Positive values less than 0.5 indicate colocalization while negative values greater than -0.5 indicate exclusion/ non-colocalization. Images which have too much noise/ random staining will have an ICQ that is approximately equal to zero (Table 2.3) (Bolte and Cordelières, 2006; Li *et al*., 2004).

Table 2.3: Summary of values of coefficients that are used to indicate the presence or absence of colocalization (adapted from Zinchuk and Zinchuk, 2008; Li *et al*., 2004).

Coefficient	Values indicating colocalization	Values indicating an absence of colocalization
Pearson's correlation coefficient	From 0.5 to 1	From -1 to 0.5
Overlap coefficient according to Manders	From 0.6 to 1	From 0 to 0.6
Overlap coefficients k_1 and k_2	Values that are close to each other for example if k_1 is 0.5 and k_2 is 0.6.	Values that are distant, for example if k_1 is 0.5 and k_2 is 0.9.
Colocalization coefficients M_1 and M_2	More than 0.5	Less than 0.5
Intensity correlation quotient (ICQ)	Positive values less than 0.5	Negative values greater than -0.5

Several programs have been developed for the purpose of image processing and colocalization analysis including:

- Imaris (www.bitplane.com/go/products/imaris),
- Volocity (www.improvision.com/products/volocity),
- Imagesurfer (www.imagesurfer.org)
- ImageJ (http://rsbweb.nih.gov/ij/)

(Bolte and Cordelières, 2006; Feng *et al*., 2007; Huang *et al*., 2008; Rueden and Eliceiri, 2007).

During the course of this current study the publically available image processing program ImageJ was used for image processing and colocalization analysis. ImageJ

(available at http://rsbweb.nih.gov/ij/), a program that was developed at the National Institute of Health (NIH), is a java-based, public-domain image processing and analysis program (Girish and Vijayalakshmi, 2004). This program is used in a large number of scientific fields including engineering, medical imaging, material sciences and microscopy. ImageJ has several add-on programs (that add to the core program‟s functionality) which are either written in Java (where they are referred to as plugins) or in ImageJ‟s macro programming language (where they referred to as macros) (Collins, 2007; Schmid *et al*., 2010).

ImageJ‟s success as an image processing program is due to its incorporation of several useful image processing tools including histogram manipulations tools, standard image filters (including mean and median), a background subtraction tool that is able to handle uneven backgrounds and a deconvolution tool that reduces out of focus fluorescence (Collins, 2007; Gammon *et al*., 2006; McNally *et al*., 1999). One of the most important features of ImageJ, in terms of this current study, is its ability to perform colocalization analyses. This program has several plugins for colocalization analyses, the most useful being JACoP (Just Another Co-localization Plugin) (http://rsb.info.nih.gov/ij/plugins/track/jacop.html). JACoP groups the most essential ICCB tools and enables the user to compare the data generated using these tools in one easy step (Bolte and Cordelières, 2006). This plugin was used for the current study to determine Pearson‟s correlation coefficients, Manders‟ Overlap coefficients, overlap coefficients when expressed as two separate parameters (k_1 and k_2), M_1 and M_2 coefficients, intensity correlation quotients (ICQs) and was also used to implement the Coste‟s approach for colocalization analysis.

2.7.1 Procedure

The overlay method was initially used to visualize areas of colocalization within confocal laser scanning microscope (LSM) images that had been exported in a Tagged Image File (tif) format with yellow regions indicating areas of colocalization. This method of colocalization representation was not easily visible, thus LSM images were exported into ImageJ as Red-Green-Blue (RGB) images where they were split into their respective red, green and blue image components using the menu command: *“Image → Colour → Split channels.”* Two resultant components of interest were selected and the

ImageJ colocalization highlighter tool was used to indicate regions of colocalization in white. This was done by selecting the menu command: "*Plugins→ Colocalization analysis→ Colocalization Highlighter."* Thereafter the menu command "*Plugins→ JACoP"* was selected. The following colocalization analysis tools: *"Pearson's coefficient, M_1 and M_2 coefficients, Overlap coefficients (k_1 and k_2), Costes' automatic threshold, Costes' randomization* and *Li's intensity correlation analysis (ICA)* were then chosen. The "*Analyze"* option was thereafter selected. After colocalization analysis, the components of the RGB images were converted into 8-bit black and white images so that they could be displayed more easily. This was done by selecting the respective component image and the menu command "*Image→type→8-bit.*

2.8 Electron microscopy, embedding in LR White resin and immunogold labelling

During the course of this study, the main electron microscopy (EM) techniques used were transmission electron microscopy (TEM) of ultrathin resin sections and immunogold labelling. Over the years, several researchers have used EM in various areas of research as it is one of the best methods for visualizing the ultrastructure of cells and tissues as well as the localization of proteins at high resolution (Cortese *et al*., 2009; Giepmans, 2008; Stahlberg and Walz, 2008).

When one embarks on using electron microscopy for the analysis of biological specimens and for immunocytochemical analysis, one should consider the method of fixation, the technique of tissue processing and the choice of embedding agent as these play a major role in retaining tissue reactivity to antibodies as well as the ultrastructure of the biological specimen (Newman and Hobot, 1987). Biological specimens are made up of about 80% water, thus sample preparation requires the sample to be prepared in such a way that prevents structural collapse upon dehydration in the vacuum of the electron microscope (Stahlberg and Walz, 2008). An important aspect to consider prior to specimen preparation is the choice of embedding medium in which the particular biological specimen is embedded. Embedding media may be divided into two broad categories, temporary/ resin free media and permanent embedding media. Examples of temporary media include techniques that involve the use of polyethylene glycol (PEG)

and poly-methylmethacrylate while examples of permanent embedding media include epoxy resins and acrylic resins.

For successful embedding, the embedding medium and the procedure used to process the specimen should possess certain characteristics as well as adhere to certain guidelines. The embedding medium should have the ability to infiltrate biological samples easily and it should be able to harden uniformly without major swelling or shrinking. It should also have a good combination of hardness and plasticity which will allow for smooth ultrathin sectioning, as thin as 100 nm. Other desirable qualities of the embedding media include a monomer viscosity that is neither too low, which usually results in shrinking of the specimen during polymerization, or too high, which tends to prevent rapid and uniform penetration of the specimen by the embedding mixture, also the density of the polymerized medium should be low enough so that proper imaging is not negatively affected. Steps leading up to the infiltration process, the infiltration itself, polymerization as well as the sectioning process should not negatively affect the ability of the of antigens at the surface level from being recognized by antibodies and it should also not adversely affect or modify the fine structure of the specimen. Once the labelling process is complete, the ultrathin sections should be dried before being placed into the electron microscope and this process should not adversely affect the fine structure of the specimen. The sections and specimens contained within them should also be resistant to radiation by the electron beam of the electron microscope. When sections are viewed, they should be processed in such a way that adequate contrast is achieved and the clear recognition of the specimen‟s ultrastructure should be possible. It is also important that different batches of the same embedding medium be consistent in terms of their quality as this is important for reproducible results (Griffiths, 1993a; Hayat, 2000b). There are several different types of resin that are suitable for EM, each with their own advantages and disadvantages which need to be considered before they are used. Some well known examples include acrylic resins such as LR White, LR Gold and Lowicryl resins, and epoxy resins such as Araldite, Epon and Spurr (Goping *et al*., 1996; Griffiths, 1993a). The resin chosen for the current study was LR White.

LR White, produced by the London Resin (LR) company, is a polyhydroxy-aromatic acrylic resin that is composed of a hydrophilic mixture of acrylic monomers. This resin

has low toxicity as it contains only monomers that are used in medicine and dentistry, thus a fumehood is not required during its use (Hayat, 2000b). LR White has low viscosity, thus, it requires tissue dehydration with ethanol before polymerization (Cameron and Toner, 1992; Griffiths, 1993a; Palmieri and Kiss, 2005). Polymerization of this resin may be brought about by one of three ways; (1) by heat (50ºC), (2) ultraviolet light and (3) using a chemical process that involves the use of an aromatic tertiary amine accelerator (Cameron and Toner, 1992; Griffiths, 1993a). Unlike epoxy resins which are impermeable to most aqueous solutions (such as immunoglobulins, colloidal gold and lectins) due to their hydrophobic characteristics, LR White is permeable to such solutions due to its hydrophilic nature (Goping *et al*., 1996; Hayat, 2000b). Monomeric LR White is largely insoluble in water (though approximately 12% (v/v) is miscible). Sections of polymerized resin are hydrophilic, however, and this quality gives LR White an advantage in that etching of sections for immunocytochemistry is not necessary. Heavily cross linked hydrophobic resins such as epoxy, however, require etching to introduce hydropillic groups to allow access of the antibody to the antigen but this negatively affects delicate tissue antigens. LR White is also a preferable resin as it is associated with minimal nonspecific staining. Like other resins, however, immunogold staining is limited to the surface of the section (Hayat, 2000b).

Although opinions vary on whether LR White results in good preservation of organelle structure and antigenicity, modifications such as the addition of 2% phosphotungstic acid to 70% ethanol during the dehydration process have been reported to improve such properties (Mutasa, 1989; Palmieri and Kiss, 2005; Sakai *et al*., 2005). Another important aspect to consider when embedding samples for electron microscopy is the choice of fixative. All fixation methods for immunocytochemistry at the electron microscopy level aim to: (1) to keep antigens in their original locations within tissues and (2) to maintain the ultrastructural morphology of the tissue while preserving antigenicity. These two goals are often difficult to achieve, thus the best compromise between the two is generally sought (Merighi, 1992). Several fixation methods are available for electron microscopic immunocytochemistry. Of these fixation methods, chemical fixation is the most widely used method for the preservation of biological

samples. Over the years aldehyde fixation has been observed to provide satisfactory preservation of ultrastructure and the choice of aldehyde for such studies is usually glutaraldehyde (Hayat, 2000a). Glutaraldehyde is a five-carbon aliphatic dialdehyde which forms colourless crystals that are very soluble in water, ethanol and most organic solvents (Griffiths, 1993b; Hayat, 2000a). Aqueous solutions of glutaraldehyde are relatively stable and have a moderately acidic pH (Griffiths, 1993b). Although glutaraldehyde is not extremely toxic, its use has sometimes been associated with skin irritations (Griffiths, 1993b; Reifenrath *et al*., 1985). The use of glutaraldehyde as a fixative for electron microscopy studies was introduced by Sabatini *et al*. (1963) and since then it has become the most popularly used fixative for preserving fine structure. This results from its ability to crosslink proteins rapidly, effectively and irreversibly (Hayat, 2000a). In solution glutaraldehyde is uncharged and is thus able to cross all biological membranes in a short space of time. This fixative is able to generate intracellular cross-linking within seconds resulting in a large, three-dimensional network of irreversible cross-links throughout the cytoplasm in a matter of seconds. The cross-linked structures that form are due to the interaction between glutaraldehyde and nucleophiles in the cells, the majority of which are amines. In addition to these amines, sulfhydral groups from cysteine and imidazole side chains of histidine also take part in cross-linking reactions. The ratio of the concentration of glutaraldehyde to the concentration of amines in the tissue sample is important as it determines the kinetics, size and nature of the cross-linking products formed. The highest degree of cross-linking as determined by the size of the cross-linked products has been observed when the ratio of glutaraldehyde to free amines is 2:1. When the concentration of glutaraldehyde is too high, the formation of rapid cross-links is actually inhibited and this can lead to the occurrence of aldol condensation reactions. When proteins are below a certain concentration, very little cross-linking takes place. The interaction between amines and glutaraldehyde initially results in a significant drop in pH which can potentially affect the fixation process and should be dealt with by adequate buffering. However, the buffers which are sometimes used for EM studies do not cross cell membranes in satisfactory amounts as they are composed of charged molecules. Although the use of glutaraldehyde usually ensures a high degree of preservation of tissue ultrastructure, its impressive ability to cross-link sometimes results in a loss of

antigenicity. If one considers the other well known fixative formaldehyde for immunocytochemistry, one may achieve better preservation of antigenicity due to its lower cross-linking potential (Griffiths, 1993b). Formaldehyde, a water soluble fixative is commercially available as formalin and contains methanol, which is used as a stabilizer to prevent breakdown to formic acid (a breakdown contaminant that often forms in solutions of formalin at room temperature) (Hayat, 2000a). As a result of its low cross-linking potential, however, the use of this fixative often results in poor preservation of ultrastructure. A combination fixative composed of paraformaldehyde (usually between 1 and 4%) (m/v) and glutaraldehyde (usually between 0.05% and 2%) (m/v) has been used by many researchers to achieve a satisfactory compromise between the preservation of fine ultrastructure and antigenicity (Bendayan *et al*., 1987; Bohn, 1978; Eldred *et al*., 1983; Karttunen *et al*., 1989; Roberg and Ollinger, 1998; Sisson and Vernier, 1980). When preparing a combination fixative such as that composed of paraformaldehyde and glutaraldehyde, it is important to optimize the concentration of the components for each individual antigen as the optimum concentrations are dependent on several factors such as the nature of the particular antigen and the tissue sample as a whole (Lamberts and Goldsmith, 1986).

The choice of buffers used during the fixation process is also extremely crucial. Besides stabilizing the acid-base balance during fixation, the buffer also has an impact on the osmotic pressure of the environment in which the fixative acts. The pH of the buffer also influences the cross-linking potential of glutaraldehyde and the rate at which cross-linking takes place (Hayat, 2000a). It is also important to consider the pKa of the chosen buffer which should be within 0.5 pH units of the required pH so that its buffering capacity may be maximized. The buffer should also be chemically stable and should also have a high degree of solubility in water. One should also ensure that the chosen buffer does not react with fixative nor should it be prone to forming complexes with metal ions that are needed to stabilize intracellular structures. If one uses glutaraldehyde as a fixative, the buffer that is used in conjunction with it should have sufficient buffering capacity to minimize the lowering of the pH that occurs due to the interaction of glutaraldehyde with tissue amines (Hayat, 2000a). Some common buffers used in EM include cacodylate (pKa 6.2) and carbonate (pKa 6.4), however, these buffers are not

suitable as their pKa values are too low for most fixation purposes. Phosphate buffers are also quite commonly used for EM and even though they have suitable pKa values, they have limited solubility in the presence of divalent cations. The buffers introduced by Good *et al*. (1966) are considered more suitable for fixation and include PIPES, HEPES and MOPS (Griffiths, 1993b). For this current study, the buffer used during the fixation process contained a combination of PIPES, HEPES, EGTA and $MgCl_2$ as described in Santama *et al*. (1998) and Chugani *et al*. (1993).

Most biological specimens are too thick in their natural state to be penetrated by an electron beam and thus thin sections are required. In order to obtain an electron micrograph of high quality, the thin section should be able to withstand both the high vacuum environment as well as the electron bombardment. The thin sections should also be of uniform thickness and free from chatter, wrinkles breaks and folds. To obtain thin sections, the use of an ultramicrotome is required. There are several factors that influence the quality of sections including the quality of the ultramicrotome, the cutting edge of the knife, the knife angle, the cutting speed, the embedding material, the face of the specimen block and the fluid in the trough in which sections are collected. Ideally, sectioning should be done in a room free from noise, dust, wind and vibration (Hayat, 2000c). The quality of knives used for sectioning is extremely important if one wants to obtain high quality, thin sections. Glass or diamond knives are usually used for sectioning with the former being used for this current study. The use of glass knives for sectioning was first introduced by Latta and Hartmann (1950). The suitability of glass as a material for the production of knives for ultrathin sectioning is due to certain characteristics that it possesses. Glass is homogeneous, lacks specific shape, is hard and not excessively fragile. It also has no well-defined slip planes in its structure and is extremely strong (its theoretical strength is approximately 1-2 x 10^6 pounds per square inch). Usually a glass edge is smoother and sharper than a steel edge, however, the edge of a glass knife is not infinitely sharp as the diagonal break is never true. Plate glass is usually used for the production of glass knives as it can be fractured by simple breaking methods and has sufficient cutting strength. Due to the fact that plate glass is not uniform in its consistency, a clean break is sometimes not achieved. One can overcome this by applying controlled and equal forces on both sides of the score line which results

in the fracture running continuously along the path of stress that is caused by these forces. The affordability of glass knife production usually results in these knives being used more often than diamond knives. Knife making has become an easier task due to the availability of knife makers such as the Leica Knife maker, LKB Knifemaker and the Messer Knifemaker. Glass knives that are used for resin sectioning have a limited lifespan as edges become blunt due to the fluid nature of glass which the thin cutting edge of glass knives are particularly susceptible to. If glass knives are to be stored, this should be done in a careful manner, as dust particles can damage the cutting edge. Thus it is advisable to prepare knives immediately before sectioning (Hayat, 2000c). Once sections are cut, they are usually stored on formvar- (which usually provides support for the section) coated copper grids (Kempf, 1973).

During EM studies involving immunocytochemistry, sections are usually incubated with Protein A from *Staphylococcus aureus*, a ligand which binds to antigen-antibody complexes (via the Fc region of antibodies, in particular IgG molecules) and is usually conjugated to ferritin or peroxidase or bound to colloidal gold for detection and localization of particular antigens in a cell section by EM (Roth, 1982; Roth *et al*., 1978). Protein A is able to bind to the antibodies from many, but, not all species. Its affinity for antibodies from different species also varies and it has been found to have a particular affinity for IgG molecules from rabbits. It is also important to note that protein A does not show substantial affinity for chicken antibodies (Griffiths, 1993c). This was important to consider for this current study as some of the antibodies used were raised in chickens. Due to this, the use of a linker antibody was required and the linker antibody, rabbit anti-chicken IgY was chosen.

2.8.1 Embedding of J774 and *M.smegmatis* cells in LR White resin for electron microscopy studies

2.8.1.1 Reagents

2 x PHEM buffer [130 mM PIPES, 60 mM HEPES, 20 mM EGTA, 4 mM $MgCl_2$, pH 7.3]. PIPES (9 g), HEPES (2.68 g) EGTA (1.875 G) and $MgCl_2.6H_2O$ (0.163 g) were dissolved in 180 ml of dH_2O. The pH of the solution was adjusted to 7.3 with NaOH, made up to 200 ml, aliquoted and stored at -20ºC.

1 x PHEM buffer [65 mM PIPES, 30 mM HEPES, 10 mM EGTA, 2 mM $MgCl_2$, pH 7.3]. 2 x PHEM (50 ml) was diluted with dH_2O (45 ml). The pH of the solution was adjusted to 7.3 and made up to 100ml.

Glutaraldehyde-PHEM [1% (v/v) in PHEM, pH 7.3]. Glutaraldehyde (100 µl) [(25% (v/v)] was added to 2 x PHEM buffer (1.25 ml) and made up to 2.5 ml with dH_2O.

Gelatin-PHEM [10% (m/v) in PHEM, pH 7.3]. Gelatin (10 g) was added to 100 ml 1 x PHEM and dissolved by heating. The volume was made up to 100 ml with dH_2O.

2.8.1.2 Procedure

J774 cells were grown to 70% confluence as described in Section 2.2.2 and *M.smegmatis* was cultured until an $O.D_{600}$ of 0.2 was reached (Section 2.6.2). J774 cells were fixed using glutaraldehyde-PHEM in equal volumes of 1 x PHEM buffer and DMEM supplemented with 10% decomplemented FCS (2 h, RT). The cells were scraped off using a rubber scraper, collected in a 15 ml tube and centrifuged (1000 x g, 4 min). *M.smegmatis* cultures were centrifuged (1000 x g, 5 min), washed with PBS and centrifuged again (1000 x g, 5 min). The *M.smegmatis* pellets were fixed using glutaraldehyde-PHEM in equal volumes of 1 x PHEM buffer and sterile Middlebrook 7H9 broth medium (2 h, RT). Pellets were washed with PBS and centrifuged twice (1000 x g, 3 min).

Both J774 cell and *M.smegmatis* pellets were then washed with PBS (3 x 3 min) and treated with gelatine-PHEM (30 min, 36ºC). The cell pellets were then separated into smaller pieces using a sterile blade, washed in dH_2O (2 x 2 min) and dehydrated

systematically in several ethanol concentrations (25%, 50%, 70%, 90% and 100%) (v/v), 15 min per concentration. The cell pellets were introduced into increasing concentrations of LR White resin in ethanol [(1:2 resin to ethanol (30 min), 1:1 resin to ethanol (30 min) and 100% resin (x 2) (30 min), 100% resin (1 h)]. Cell pellets were left in LR white resin overnight and thereafter placed into resin-filled gelatin capsules and placed in a hot air oven (48 h, 57 ºC).

2.8.1.3 Production of glass knives

Glass knives were produced on a LKB 7800 glass knife maker modified as described by Moorewood *et al*. (1992). A glass strip was cleaned with dH_2O and 70% ethanol, allowed to dry and fractured on a LKB 7800 glass knife maker in order to produce triangular knives. Knife edges were examined and those that were suitable were selected for ultrathin sectioning. Troughs made of aluminium foil tape were assembled onto the knives and sealed with nail varnish to prevent water leakage. Ultrathin resin sections (90-110 nm) were cut using a Reichert-Jung Ultracut ultramicrotome, floated onto the water contained within the watertight troughs and collected on formvar- coated copper grids.

2.8.2 Immunolabelling of J774 and *M.smegmatis* LR White ultrathin sections

2.8.2.1 Reagents

PBS, pH 7.2. NaCl (8 g), KCl (0.2 g), $Na_2HPO_4.2H_2O$ (1.15 g) and KH_2PO_4 (0.2 g) were dissolved in 1 l of dH_2O.

Glutaraldehyde fixative [1% (v/v) in PBS]. Glutaraldehyde [1 ml of a 25% (v/v) stock solution] was diluted to 25 ml with PBS.

BSA-PBS [1% (m/v) in PBS, pH 7.4]. BSA (1 g) was dissolved in PBS (100 ml).

Glycine-PBS [20 mM in PBS]. Glycine (0.15 g) was dissolved in PBS and made up to 100 ml.

Fish skin gelatine (FSG)-BSA [1% (v/v) FSG, 0.8% (m/v) BSA in 20 mM glycine-PBS]. FSG [1.11 ml of a 45% (v/v) solution] and BSA (0.4 g) were dissolved in 50 ml

of glycine-PBS. The solution was centrifuged (10 000 x g, 2 h, 4ºC) so that insoluble debris could be removed. The solution was aliquoted and stored at -20 ºC.

Uranyl acetate [2% (m/v) in dH_2O]. Uranyl acetate (1 g) was dissolved in 50 ml of dH_2O and stored at 4ºC.

Lead citrate [0.2% (m/v) in dH_2O]. Lead citrate (0.1 g) was dissolved in 50 ml dH_2O and stored in a sealed glass bottle at 4ºC.

2.8.2.2 Procedure

Immunogold labelling of embedded J774 cells was performed on ultrathin sections that had been collected onto formvar coated copper grids. The grids were incubated on droplets of the various reagents on parafilm at RT (Table 2.4). Once the procedure was completed and the grids were air dried, the immunogold labelling was viewed using a Phillips CW 120 Biotwin TEM at 80-100 kV.

Table 2.4: Procedure for immunogold labelling of embedded J774 cells.

Procedure	Incubation time
Blocking in non-specific binding sites with BSA-PBS (20 µl).	10 min
Blocking and aldehyde quenching using FSG-BSA (20 µl)	4 x 1 min
Incubated in primary antibody that was diluted in FSG-BSA (10 µl)	1 h
Washed in PBS (20 µl)	5 x 4 min
Incubated in rabbit anti-IgY linker antibody (10 µl)	1 h
Washed in PBS (20 µl)	5 x 4 min
Incubated in Protein-A gold probe (10 nm) that was diluted in FSG-BSA (10 µl)	1 h
Washed in PBS (20 µl)	5 x 4 min
Fixed in glutaraldehyde fixative (10 µl)	5 min
Washed in dH_2O (100 µl)	5 x 4 min
Stained in Uranyl acetate (30 µl)	10 min
Washed in dH_2O (100 µl)	5 x 4 min
Stained in Lead citrate (30 µl)	4 min

Controls were performed with the substitution of pre-immune antisera (used at the same concentration as the primary antibody) and *M.smegmatis* ultra thin sections.

CHAPTER THREE

ANTI-CATHEPSIN D ANTIBODIES FOR STUDIES ON MACROPHAGE-MYCOBACTERIAL INTERACTIONS

3.1 Cathepsin D

Cathepsin D is a glycoprotein and is part of the A1 family of aspartyl proteases which also includes cathepsin E and pepsin A (Minarowska *et al*., 2007a). This protease is a lysosomal endopeptidase, is found in nearly all cells except in mature lysosome-free erythrocytes and has been observed to play a role in several physiological functions such as protein degradation, apoptosis and autophagy. It has also been associated with conditions such as Alzheimer‟s disease, neuronal ceroid lipofuscinosis and mycobacterial antigen processing (Minarowska *et al*., 2008; Thorne *et al*., 1976; Zaidi *et al*., 2008).

3.1.1 Synthesis of cathepsin D

In humans, the cathepsin D gene is located at the end of the short arm of chromosome 11 in the p15.5 region and is close to the H-*ras* oncogene. Cathepsin D expression is regulated by steroid hormones, growth factors such as insulin-like growth factor-1 (IGF-1), tumor necrosis factor (TNF-α) and epidermal growth factor (EGF), as well as by retinoic acid (Minarowska *et al.*, 2008). This is usually synthesized in a preprocathepsin D form (composed of 412 amino acids) on the rough endoplasmic reticulum (RER) (Minarowska *et al*., 2008; Zaidi *et al*., 2008). Preprocathepsin D has a signal sequence (composed of 20 amino acids) which allows the nascent protein to be imported into endoplasmic reticulum (ER) lumen via binding of a signal recognition particle (SRP) which binds to an SRP receptor. Signal peptidase cleavage of the N-terminal signal sequence gives rise to soluble procathepsin D (composed of 392 amino acids, 52 kDa) in the ER lumen.

Thereafter procathepsin D undergoes several post-translation modifications including the formation of disulfide bridges, N-glycosylation and phosphorylation. The formation of disulfide bridges usually occurs between the cysteine residues Cys27-Cys96, Cys46-

Cys53, Cys222-Cys226 and Cys265-Cys302 and their locations are dependent on the enzyme protein disulphide isomerase. N-glycosylation occurs at the triad sequences Asn70-Gly71-Thr72 and Asn199-Val200-Phe201. Once oligoglycosylation chains are synthesized, they are transferred onto the asparagine residues which are contained within these triad sequences (Minarowska *et al*., 2008; Zaidi *et al*., 2008). The glycosylated procathepsin D is thereafter transported to the Golgi complex where its N-linked oligosaccharides are covalently modified and their mannose residues are phosphorylated at position six to give rise to the mannose-6-phosphate (M-6-P) groups (Zaidi *et al*., 2008). The M6P groups are recognized by mannose-6-phosphate-receptors (M6PRs). These occur in two forms, M6PR-46 (46 kDa), that is dependent on the presence of bivalent cations and traffics the procathepsin D via an early endosome and the M6PR-300 (300 kDa), a bivalent cation-independent-receptor, that traffics procathepsin D directly to the late endosome (Benes *et al*., 2008; Chao *et al*., 1990; Mathews *et al*., 2002; Minarowska *et al*., 2008; Romagnoli *et al*., 1993). As the studies of Anes *et al*. (2006) found that initial killing occurs by interaction of the mycobacterium-containing phagosome with an early, mildly acidic compartment, this compartment may be the early endosome compartment to which the M6PR-46 delivers procathepsin D, and may be where cathepsin D may be relevant in killing after cathepsins such as cathepsin L and B activate the proenzyme (Laurent-Matha *et al*., 2006; Wille *et al*., 2004). However, the form of cathepsin D present in the early endosome is unclear.

Cathepsin D is, thereafter, transported to the late endosome where it usually undergoes final processing (Diment *et al*., 1988; Minarowska *et al*., 2008; Zaidi *et al*., 2008). Firstly the low pH within this organelle (pH ~ 4.5-5.5) brings about the dissociation of the procathepsin D M6P-M6PR complex. The M6PR returns to the Golgi apparatus to transport other M6P-labelled proteins to the late endosome. The presence of the M6PR is, therefore, often used to distinguish late endosomes from lysosomes (which are considered as the organelles in which this enzyme is stored in its active form) as these receptors are not found in lysosomes (Matsuo *et al*., 2004; Minarowska *et al*., 2008; Zaidi *et al*., 2008).

Processing of human procathepsin D thereafter undergoes dephosphorylation and a proteolytic process which results in the removal of the pro-peptide (44 amino acids) and leads to the formation of an active intermediate form of the enzyme which is a single chain molecule (~ 48 kDa, 348 amino acids) (Zaidi *et al*., 2008). The 48 kDa intermediate is thereafter processed into an active mature two-chain form of cathepsin D and this is brought about by the action of cathepsin B and L (Laurent-Matha *et al.*, 2006). The two-chain form is made up of an amino terminal light chain (14 kDa) and a carboxyl-terminal heavy chain (34 kDa) which are associated with each other via hydrophobic interactions (Zaidi *et al*., 2008). Porcine cathepsin D is also synthesized and processed similarly to human cathepsin D. The intermediate form of the enzyme is approximately 43 kDa, slightly smaller than the human enzyme while the light and heavy chain of the active two chain mature form are approximately 15 and 31 kDa, respectively (Barth and Afting, 1984; Yonezawa *et al*., 1988).

An alternate transportation route of cathepsin D to "lysosomes", in which cathepsin D is transported in a membrane-associated form from the Golgi to early endosomes and subsequently to late endosomes and subsequently to "lysosomes" has been suggested. In a pulse-chase study conducted in rabbit macrophages it was observed that macrophage cathepsin D is first synthesized as an inactive, membrane-associated precursor (53 kDa) which undergoes processing to form an active, membrane-associated form (47 kDa), in an early endosomal compartment and thereafter into a soluble/non-membrane associated form (46 kDa) found in endosomes and "lysosomes" (Diment *et al*., 1988). The active membrane-associated cathepsin D form found within early endosomes may be responsible for the microbicidal effect seen by Anes *et al*. (2006), though the presence of a membrane-associated form of cathepsin D in human and mouse macrophages has not been investigated.

3.1.2 Catalytic mechanism of cathepsin D

Cathepsin D usually cleaves peptide bonds that are found inside polypeptide chains. These bonds are generally formed by carboxyl groups of hydrophobic amino acids in particular those of aromatic amino acids (Minarowska *et al.*, 2008). The catalytic site of cathepsin D is made up of two aspartic residues located in the triad sequences Asp33-Thr34-Gly35 and Asp231-Thr232-Gly233 (Gacko *et al.*, 2007; Minarowska *et al.*,

2008). These aspartic residues work together with water to bring about the hydrolysis of peptide bonds. Upon the attachment of cathepsin D to a substrate in an acidic environment, the ionized Asp33 residue activates a water molecule and subsequently brings about the detachment and transfer of a proton onto the peptide bond of the substrate (Figure 3.1) (Gacko *et al.*, 2007). This coincides with the transfer of a proton that is derived from the Asp231 residue onto the oxygen of the substrate‟s carbonyl group (Figure 3.1) (Minarowska *et al.*, 2008). This brings about the formation of a tetrahedral intermediate which is sensitive to the action of the activated water molecule and which is eventually broken down (Minarowska *et al.*, 2008; Veerapandian *et al.*, 1992). Since the catalytic reactions involve the ionizing groups of cathepsin D, its activity is pH dependent. It has been observed that the optimum pH for cathepsin D activity is between 3.5-5.5 (Barrett, 1970; Dorer *et al.*, 1978; Minarowska *et al.*, 2008). Hence cathepsin D should only be active in organelles with a pH within this range i.e. organelles such as the late endosome (pH ~ 4.5-5.5) or a more acidic digestive body (Matsuo *et al*., 2004; Minarowska *et al*., 2008).

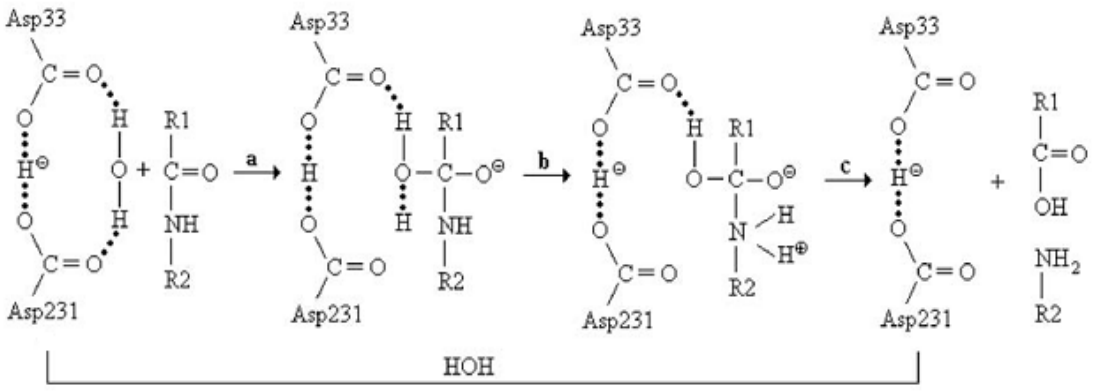

Figure 3.1: The mechanisms involved in the breakdown of substrates by cathepsin D.

Cathepsin D is usually active in acidic environments where its mode of catalytic action involves the transfer of protons. (a) When cathepsin D attaches to a substrate, the ionized Asp33 residue activates a water molecule and this leads to the detachment and transfer of a proton onto the peptide bond of the substrate. Simultaneously, a proton from the Asp231 residue is transferred onto the oxygen of the substrate‟s carbonyl group. This brings about the formation of a tetrahedral intermediate (b) which is sensitive to the action of the activated water molecule and which is eventually broken down (c) (adapted from Minarowska *et al*., 2008).

3.1.3 Substrate specificity of cathepsin D

Cathepsin D, like other aspartyl proteases, has been observed to recognize peptide substrates comprising as many as seven amino acid residues, while those that are made up of five amino acid residues or less have not been shown to be cleaved by this protease (Minarowska *et al.*, 2008). It has thus been suggested that the specificity of this protease may be dependent, not only on the amino acid residues that flank the scissile bond, but also on the primary or even higher order protein structural features of the substrate. This may, in turn, be affected by pH (which varies in the various compartments i.e. pH of the early endosome is between 5.5-6.5 while the pH of the late endosome is between 4.5-5.5 (Killisch *et al*., 1992; Lee, 2010; Matsuo *et al*., 2004; Minarowska *et al*., 2008; Piguet *et al*., 1999).

Cathepsin D has been shown to have a preference for peptides that have hydrophobic amino acid residues that flank the cleaved peptide bond, in positions P1 and P1' (Schechter and Berger, 1967) (Figure 3.2). Leucine and aromatic residues, that are hydrophobic, are particularly favoured in the P1 position. A hydrophobic residue in the P2 position and a charged residue usually one that is basic is favoured in positions P2' and P5' (Figure 3.2). These preferences were established by van Noort and van Drift (1989) from the analysis of digested products that were rapidly released from a protein substrate. These sites were not the only peptide bonds that were subject to cleavage by cathepsin D as other peptides were also released under the same conditions, in smaller amounts, however (van Noort and van der Drift, 1989).

One of the aims of the current study was to determine if cathepsin D is involved in the killing of *M.smegmatis*, and if so, whether this protease has a direct or indirect role in the killing process. Though the target on the surface of the bacteria is difficult to predict this would be a protein with a cleavage site favoured by cathepsin D. A direct role may possibly be determined, therefore, by adding cathepsin D directly to *M.smegmatis* in an environment that is suitable for cathepsin D activity i.e. under acidic conditions. Should the enzyme itself show no bacteriocidal activity on *M.smegmatis*, then the bactericidal activity could be indirect, via activation of another protease. Studies on the possible direct involvement of cathepsin D will be reported in Chapter four.

The direct bacteriocidal activity of cathepsin D may also be implied by demonstrating the presence of the enzyme in the phagosome where killed bacteria are found. In order to locate cathepsin D in the phagosome, a specific antibody that does not cross-react with *M.smegmatis* was needed to be raised as most commercial polyclonal antibodies cross-react with *M.smegmatis* due to the use of adjuvants containing bacterial products. To raise such an antibody, a pure cathepsin D antigen with the least homology (most foreign) to that of the cathepsin D antigen of the animal to be inoculated is needed. An adjuvant or vehicle for injection to prolong the release of the antigen is also required. This adjuvant should not cause cross-reactivity with mycobacteria by containing bacterial products and the immune system needs to be exploited and maximally stimulated.

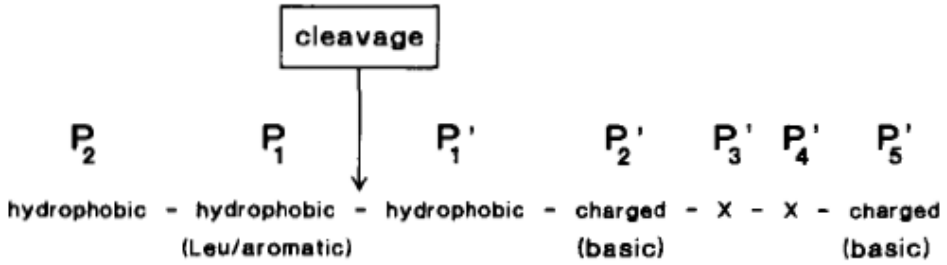

Figure 3.2: The pattern of amino acid residues which are found at sites that are preferentially cleaved by cathepsin D.

Cathepsin D has been observed to have a preference for peptides which have hydrophobic amino acid residues that flank the cleaved peptide bond, in positions P1 and P1'. The presence of leucine or hydrophobic aromatic residues are particularly favoured in position P1. A hydrophobic residue in the P2 position and a charged residue usually one which is basic is favoured in positions P2' and P5' (adapted from van Noort and van der Drift, 1989).

For the generation of antibodies, it is, therefore, important to understand the immune system of mammals and how antibody production is induced.

3.2 The immune response and antibody production

There are two main types of immunity; adaptive immunity and innate immunity (Dai *et al*., 2009; Lippolis, 2008). The innate immune system is described as nonspecific in nature and present at birth. Innate immunity is the first line of defence against invading

pathogens. Some pathogens are, however, able to evade detection and clearance by this type of immunity and this is when adaptive immunity comes into play. The adaptive immune system is usually responsible for dealing with ever-changing pathogen challenge and adapting to dynamic-antigen specific pathogen recognition using various systems, in which pathogen-recognition is primarily based on the characteristic of being foreign (Lippolis, 2008). This type of immunity has a high level of specificity. It responds slower than the innate immune system, however. The main components of the adaptive immune system are B (or bursal or bone marrow-derived) lymphocytes and T (or thymus-derived) lymphocytes. B cells have B cell receptors or immunoglobulins on their surfaces and T cells have equivalent antigen and costimulatory receptors on their cell surfaces (Cooper *et al*., 1967; Hau and Hendriksen, 2005; Kersey and Gajl-Peczalska, 1975; Lippolis, 2008; Moura *et al*., 2008; Rabb, 2002; Savino *et al*., 1992).

During the early stages of B lymphocyte development, immunoglobulin (Ig) genes (variable (V), diverse (D) and joining (J) gene segments) are rearranged and this is one of the ways in which a large repertoire of B cells is formed (Foreman *et al*., 2007).

Immunoglobulins produced by B cells are composed of two identical, heavy and light chains that are linked to each other by disulfide bridges. The first 100-110 amino acids of the amino-terminal region of the light and heavy chain vary greatly amongst immunoglobulins and these regions are referred to as variable light (V_L) for light chains, and variable heavy (V_H) for heavy chains. The carboxyl-terminal region of the light and heavy chains are fairly constant and are termed constant (C) regions, C_L for light chains, and C_H for heavy chains (Figure 3.3). The differences in immunoglobulins arise from areas within the V regions called Complementary Determining Regions (CDRs) which are found on both light and heavy chains. These regions make up the antigen binding site of the antibody molecule. There are two types of CDRs found within light chains and these are referred to as kappa (κ) and lambda (λ). Each immunoglobulin molecule contains only one type of light chain CDR, either κ or λ. The heavy chain is responsible for determining the class of the immunoglobulin. Five known heavy chain constant region sequences exist and these are referred to as μ, δ, γ, ε and α. Thus in humans, there are five main classes of antibodies, IgM (μ), IgD (δ), IgG (γ), IgE (ε) and IgA (α). Each of these classes of antibodies differ in terms of structure and function (Moura *et*

al., 2008). In chickens and other avian species, there are three main classes of Igs, IgA, IgM and IgG. The most abundant of these classes is IgG which is referred to as IgY when found in the egg yolk (Hau and Hendriksen, 2005).

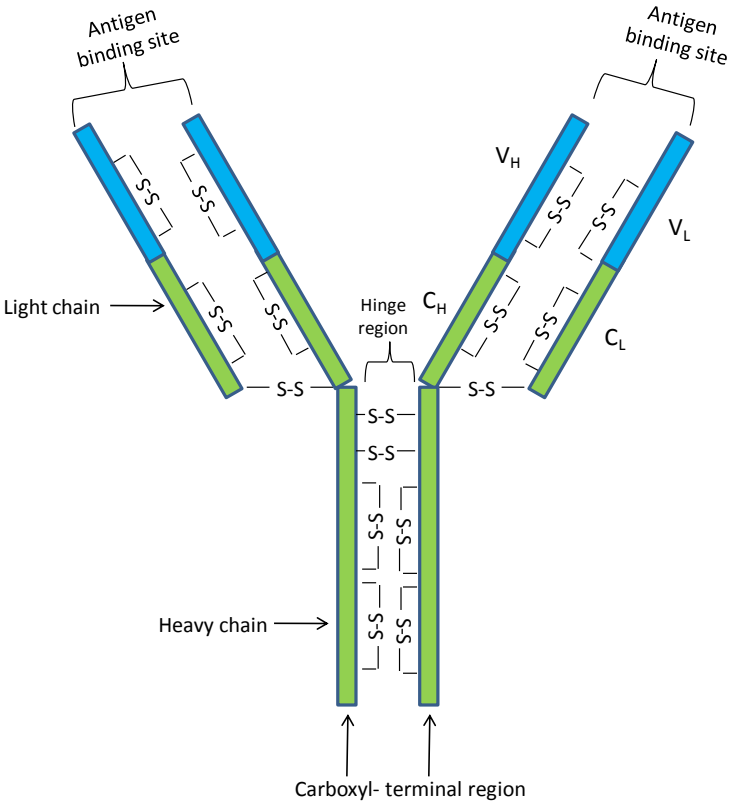

Figure 3.3: Immunoglobulin structure.

Immunoglobulins are composed of two identically, linked heavy chains and two identical light chains that are linked together by disulfide bridges. Both heavy and light chains contain variable and constant regions. Variable regions in light chains (V_L) and heavy chains (V_H) contain areas referred to as Complementary Determining Regions (CDRs) which make up the antigen binding site of the immunoglobulin molecule. The carboxyl-terminal region of the heavy and light chains contain constant regions, (C_H) and (C_L), respectively (adapted from Roitt, 2006).

During the early stage of B lymphocyte development, the immature B cell has an antigen-receptor in the form of a cell-surface IgM which enables it to interact with

antigens in its environment. Those immature B cells that interact strongly with self molecules are eliminated via negative selection thus reducing the possibility of self-reactivity and possible auto-immune reactions (Crowley *et al*., 2008; Parsons *et al*., 2009). This loss of cells from the B cell repertoire is referred to as clonal deletion (Bolland, 2008). After negative selection, surviving immature B cells mature to express IgD in addition to IgM and subsequently move into the periphery lymphoid organs where they are capable of being activated by an interaction with their specific foreign antigen. Once activated, B cells proliferate and differentiate into antibody-secreting plasma cells and memory cells (Moura *et al*., 2008).

During T cell development, bone marrow derived T cell precursors which lack most surface molecules characteristic of mature T cells migrate to the thymus. The most common surface markers that are used to identify T cells are CD4 and CD8 T cell receptors. These early T cells lack both CD4 and CD8 surface molecules and are referred to as double negative thymocytes (Hu *et al*., 2010). These cells subsequently undergo a process in which their T cell receptor gene segments (namely the V, D and J gene segments) are rearranged (Bandyopadhyay *et al*., 2007). There are two known types of T cell receptors: α:β T cell receptors and γ:δ T cell receptors (Chien and Bonneville, 2006). T cells that have α:β T cell receptors undergo developmental stages that results in their expression of both CD4 and CD8 surface molecules. At this stage they are referred to as double positive thymocytes (Veillette *et al*., 1989; Wang and Bosselut, 2009). These double positive thymocytes undergo a process referred to as positive selection (Fu *et al*., 2010). During this process, T cells are selected based on their ability to recognize self-MHC molecules that are presented on the surface of thymic cortical epithelial cells (Arens and Schoenberger, 2010; Hu *et al*., 2010; Viret and Janeway, 1999). Double positive thymocytes go on to lose their ability to express either CD4 or CD8 surface molecules, i.e. they differentiate into $CD4^+$/ $CD8^-$ or $CD8^+$/ $CD4^-$ T cells (Wang and Bosselut, 2009). Several suggestions have been made to describe the factors that influence this differentiation process. One theory suggests that the strength of the T cell receptor signal directs this differentiation process where stronger signals are induced by MHC class II signalling than by MHC class I signalling, thus favouring CD4 differentiation over CD8 differentiation. It has also been suggested

that the duration of the intrathymic T cell receptor signal may influence the differentiation of double positive thymocytes where longer, more persistent signals promote CD4 lineage differentiation and shorter, transient signals encourage the differentiation into CD8 T cells (Liu and Bosselut, 2004). Thymocytes also undergo negative selection in which those cells that are capable of binding to self peptide fragments bound to MHC molecules (that are presented by medullary thymic epithelial cells) are eliminated. This process results in the elimination of T cells that could be involved in autoimmune reactions. After the selection processes, the T cells migrate from the thymus to become part of the peripheral T cell repertoire (Arens and Schoenberger, 2010; Bandyopadhyay *et al*., 2007).

The distinction of "self" from "non-self" is one of the core aspects of immunology, more specifically antibody production. This should be given careful consideration before embarking on raising antibodies (Langman and Cohn, 2000). It is common practice amongst researchers to determine if the antigen against which they intend on raising antibodies is, therefore, sufficiently different from the host animal‟s proteins. This is so that the immune system of the host animal recognizes the respective antigen as being foreign and will elicit an immune response in the form of antibody production. (To this end, many researchers perform sequence alignments between the specific antigen and host animal‟s proteins, using appropriate software (such as basic local alignment tool (BLAST) software), in order to predict the possible immunogenicity of the specific antigen (Landowski *et al*., 2001; Lindskog *et al*., 2005)).

After T cells have completed their development within the thymus they migrate to peripheral lymphoid organs as naïve T cells where they may encounter a specific antigen bound to an MHC molecule found on the surface of an antigen presenting cell (APC) that has similarly been selected for a lack of self-reacting receptors (Noble, 2000). Dendritic cells, macrophages and B cells are all capable of serving as APCs with dendritic cells being the most important APC with regards to T cells (Arens and Schoenberger, 2010; Stockwin *et al*., 2000). Most APCs are able to ingest various pathogens as they have pathogen recognition receptors such as toll-like receptors which recognize conserved pathogen-associated molecular patterns (Arens and Schoenberger, 2010). These APCs are similarly selected for non-self reactivity, as described for B cells

and assist in activating T and B cells. The initial encounter of naïve T and B cells with their specific antigen is referred to as activating or priming.

Naïve T and B cells need primary exposure to an antigen-MHC class I/ MHC class II complex to become a committed or effector cell. The exposure of naïve T cells to an MHC class I-antigen (of cytoplasmic origin) complex results in the commitment to $CD8^+$ T cells as well the commitment to a specific cytoplasmic antigen i.e. to become a $CD8^+$-effector killing cell that is directed against such a cytoplasmic antigen (Section 1.3). On the other hand, exposure to MHC class II-antigen complex (where antigen is derived from an exogenous source via endocytosis or phagocytosis) results in the commitment to $CD4^+$ T_H1 or $CD4^+$ T_H2 cells. $CD4^+$ T_H2 cells undergo clonal selection and induce naïve B cells to make IgM and subsequently IgG antibodies that opsonize extracellular pathogens thus allowing for their phagocytosis (Arens and Schoenberger, 2010; Fleisher, 1997). $CD4^+$ T_H1 cells, however, are necessary to supply co-stimulatory signals required for activation of $CD8^+$-effector killing cells.

Such interactions between B and T cells are important aspects in antibody production i.e. for a B and T cell to interact, the T cell must recognize a processed form of the antigen, that was originally recognized by the B cell receptor prior to its uptake and subsequent degradation, and this must be bound to an MHC class II molecule on an equivalently activated $CD4^+$ T_H2 cell (MacLennan *et al*., 1997; Ploegh, 2007; Ziegler and Unanue, 1981). This leads to the production of antibodies (Kaiko *et al*., 2008; van den Eertwegh *et al*., 1994).

Most complete adjuvants contain bacterial components to activate toll-like receptors i.e. provide pattern-associated molecular patterns (PAMPs) (Section 1.5.2) or co-stimulatory signals to boost the immune system, and oil-based or particle components that promote the slow release of the antigen to maximize immune system exposure to the antigen and hence the immune response (Section 3.3.2).

3.3 Adjuvants

The word adjuvant comes from the Latin word “adjuvare” which means to aid or enhance. Adjuvants are a group of structurally heterogenous compounds which enhance or modulate the immunogenicity of vaccine proteins or peptides which have poor immunogenic potential (Rajput *et al*., 2007). The preparation of more than one hundred adjuvants has been documented. Many of these adjuvants are rarely used due to the complexity and expense associated with their preparation as well as their toxic effects, however (Stills, 2005; Stuewart-Tull *et al*., 1976). Adjuvants may be broadly divided into two main types, those used for prophylactic purposes, mainly to produce therapeutic vaccines and those used for experimental purposes to produce antibodies needed for further studies (Casella and Mitchell, 2008; Stills, 2005). The main role of adjuvants that are used for experimental purposes is to enhance the reaction of the host‟s immune system to an antigen and thereby increase the antibody response both in terms of intensity and duration. When choosing an adjuvant, an important aspect to consider is any possible harmful effects that it might have on the host animal. The pain, distress and toxicity associated with the use of certain adjuvants have led to governmental regulations as well as the need for alternative adjuvants that are less harmful to the host animal. A good adjuvant should thus combine the ability to maximize the host antibody response as well as bring about minimal pain, distress and toxicity to the host animal (Stills, 2005).

Besides being able to improve the immunogenicity of antigens with poor immunogenic potential, adjuvants are also able to improve the speed and duration of the immune response. These substances can also modulate antibody avidity and specificity as well as decrease the dosage of antigen required (Rajput *et al.*, 2007). The mechanisms by which adjuvants bring about these effects are becoming better understood as knowledge of the molecular aspects of antigen recognition and immune response improves (Stills, 2005).

3.3.1 The mechanisms of adjuvant action

There are five main mechanisms by which adjuvants can work. These include: (1) the "depot" effect, (2) the antigen presentation effect, (3) the antigen distribution/ targeting effect, (4) the immune activation/ modulation effect, and (5) the $CD8^+$ cytotoxic T lymphocyte (CTL) induction effect (Cox and Coulter, 1997).

The "depot" effect refers to the protection of the antigen by the adjuvant from dilution and rapid degradation as well as elimination by the host. The adjuvant allows for the localization and slow release of the intact antigen thereby making it possible for the prolonged exposure of the immune system cells to a low level of antigen. This results in the continued stimulation of antibody producing cells and subsequent production of high levels of antibodies by the host (Stills, 2005). Besides providing protection to antigens, adjuvants may also preserve their conformational integrity to allow optimal presentation to antigen-presenting cells. Some adjuvants also bring about the targeting of receptors found on antigen-presenting cells such as carbohydrate adjuvants that target lectin or toll-like receptors found on dendritic cells (Cox and Coulter, 1997). Immunomodulators and immunostimulators which are usually made up of microbial cells, their cell components and other chemically modified microbial products are also contained within some adjuvants and play a role in recruiting, activating and enhancing the differentiation of some cells of the immune system. The study of mammalian toll-like receptors (TLRs) and their role in both the innate and adaptive immune response helps to provide an explanation of how microbial containing adjuvants modify the immune response. Some adjuvants may play a role in CTL induction. This requires them to mediate the incorporation of a peptide (a product which results from the processing of a particular antigen) onto an MHC class I molecule (Takagi *et al.*, 2009) (Section 1.3).

3.3.2 Types of adjuvants

Over the years various researchers have used different criteria to classify adjuvants. Some have organized adjuvants into three main groups: immunostimulatory adjuvants, carrier adjuvants and vehicle adjuvants. Adjuvants have also been characterized according to their route of administration such as mucosal or parenteral administration

(Rajput *et al.*, 2007). They have also been divided into the following groups: gel-based adjuvants, surface agents, oil emulsions, particulate adjuvants and bacterial component-containing adjuvants (Jennings *et al.*, 1998). The role of the first four groups is to prolong exposure to the antigen, while the role of the last group is to stimulate toll-like receptors and increase immune response by attracting macrophages and other antigen presenting cells, and hence promote antigen processing and presentation. From the large group of documented adjuvants, three types will be discussed in detail, Freunds adjuvants, saponin-based adjuvants and aluminium-containing adjuvants.

3.3.2.1 Freunds adjuvants

Since its original description in the 1930s, Freund‟s complete adjuvant (FCA) has been one of the most commonly used and most effective adjuvants for experimental antibody production (Opie and Freund, 1937; Stills, 2005). FCA may be classified as a water-in-oil-adjuvant as well as a bacterial component-containing adjuvant (McKee *et al.*, 2007). This adjuvant is composed of a light mineral oil, mannide monooleate (a surfactant), and heat killed and dried mycobacterial cells. FCA is usually used for initial immunizations and is almost always followed by booster injections using Freund‟s incomplete adjuvant (FIA), which lacks killed mycobacterial cells (Fikrig *et al*., 1993; Stills, 2005).

Inocula containing FCA and FIA are prepared firstly by the emulsification of an antigen in an aqueous solution with the oil, resulting in a stable water-in-oil emulsion. This step is critical for the effectiveness of both FCA and FIA as an adjuvant. The mineral oil used in Freund‟s adjuvant has been shown to have three roles: to establish an antigen depot and facilitate gradual antigen release, to provide a vehicle for antigen transport throughout the lymphatic system to immune effector cells and to facilitate interaction with antigen presenting cells. This oil is not readily metabolized or eliminated, properties shown to be necessary for continuous stimulation and this is a major factor that contributes to the success of Freund‟s ajuvants (Freund, 1956; Stills, 2005). Hydrocarbon oils which consist of short-chain hydrocarbons were the original oils used in Freund‟s adjuvants. These short-chain hydrocarbons were later shown to be responsible for acute toxicity and immunosuppression and were thereafter replaced by medium-straight chain and branched hydrocarbons which were less reactive

(Aucouturier *et al*., 2001; Shaw *et al*., 1964; Stills, 2005; Stuewart-Tull *et al*., 1976). Furthermore, the oils used in the original descriptions of Freund‟s adjuvants were produced by the acid treatment or the oleum method and were relatively crude. After 1970, however, they were produced by a single or double hydrogenation procedure which resulted in purer oils that were less toxic. Besides the differences in oil preparations, the original description of FCA also differs from current versions in terms of its mycobacterial components. The original FCA used heat-killed and dried virulent *M. tuberculosis* while most of the current commercial versions usually contain avirulent *M. tuberculosis* H37Ra and *Mycobacterium butyricum* (Stills, 2005).

Despite the great success that has been achieved with Freund‟s adjuvants in experimental antibody production, there have been many negative side effects that have been associated with their use. These include the development of lesions and necrosis (Leenaars *et al*., 1998; Rigdon and Schadewald, 1972; Steblay and Rudofsky, 1983; Stills, 2005; Tabel and Ingram, 1971). The manner in which FCA is administered may also bring about certain side effects. It has been observed that intradermal injections of FCA are associated with large granulomas that often ulcerate, while subcutaneous administration has been found to result in fistulous tracts which eventually open and drain (Broderson, 1989; Stills, 2005). Granulomas have also been observed to develop in the draining lymph nodes, spleen, lung, kidney and other organs due to the movement of minute quantities of the emulsion by the lymphatic and circulatory system following administration of the adjuvant (Pearson *et al.*, 1961; Stills, 2005). Side effects are associated with pain and distress in the host animal

These side effects are not as clearly understood. The reason for this is that it is difficult to assess pain and distress experienced by animals. Ways of accessing such feelings in immunized animals is an issue which is highly debatable. Several researchers have assumed the automatic presence of pain and distress when experimental animals presented with lesions (Jennings, 1995; Mallon *et al.*, 1991; Stills, 2005). Some researchers who have evaluated pain and distress based on the behavioural changes observed in animals injected with Freund‟s adjuvants. Morton and Griffiths (1985) and Wallace *et al*. (1990) formulated guidelines for the recognition of pain, distress and discomfort in animals used for experimental purposes. Their guidelines included the

assessment of the general appearance of the animal, its body weight, clinical signs and response to certain stimuli (Leenaars *et al.*, 1998).

In a study conducted by Halliday *et al*. (2000), no clinical or behavioral abnormalities indicative of pain or distress were observed in rabbits that were immunized with FCA even though many lesions were reported. In another study conducted by Leenaars *et al*. (1998), lesions were observed in both rabbits and mice, and similarly, no signs of pain or distress were detected in rabbits. Mice showed signs of acute pain and distress (indicated by weight loss and decrease in activity), however. Thus, although Freund‟s adjuvants are extremely potent and effective and remain the gold standard in terms of adjuvants used for experimental antibody production, the negative side effects associated with the use of these adjuvants has led to legislation banning their use in most countries (Stills, 2005). As newer adjuvants are developed and tested, it is hoped that alternatives which are as effective as Freund‟s but less harmful will become available. In this study, however, there is a more important reason for not using FCA. The reason being that such an adjuvant would and does cause cross-reactivity with *M.smegmatis* (unpublished data). At least two other adjuvants were, therefore, investigated in this study.

3.3.2.2 Saponin-based adjuvants

There has been much interest expressed in the use of saponins as adjuvants. Interest has been stimulated due to the physiological, immunological and pharmacological properties of saponins (Rajput *et al.*, 2007). Saponins which may be divided into two types, namely steroid saponins and triterpenoid saponins are found in wild and cultivated plants as well as in lower marine animals and some bacteria (Rajput *et al*., 2007; Riguera, 1997; Yoshiki *et al*., 1998). Steroid saponins have been found in plants such as oats, capsicum peppers, aubergine, asparagus, yam, fenugreek and ginseng while triterpenoid saponins have been detected in many legumes such as soybeans, beans, and peas as well as in other plants such as tea, spinach, sugar beet, quinoa, liquorices and horse chestnut (Rajput *et al.*, 2007).

Saponin-based adjuvants have been shown to modulate the cell-mediated immune system and enhance antibody production though the immuno-stimulating activity of

saponins is not clearly understood and several researchers have attempted to explain their modes of action. The use of these adjuvants is advantageous as they are able to stimulate high levels of production of antibodies to T-dependent and –independent antigens and induce CTL responses at low doses (Kensil, 1996; Oda *et al.*, 2000; Rajput *et al.*, 2007). Saponin-based adjuvants are believed to induce the production of cytokines such as interleukins and interferons which may mediate their immunostimulatory effects (Jie *et al.*, 1984; Rajput *et al.*, 2007). It has been shown that saponins intercalate into cell membranes by removing membrane cholesterol, resulting in pore formation (Bangham *et al*., 1962; Schroeder *et al*., 1998). This is speculated to be a way in which saponin-based adjuvants allow antigens to gain access to the MHC class I pathway of antigen presentation, resulting in the induction of a CTL response (Rajput *et al.*, 2007; Sjölander *et al.*, 2001).

One of the most well characterized groups of triterpenoid saponins is produced from the bark of the *Quillaja saponaria* tree, native to the Andes region. This has been found to display adjuvant activity in mice when orally administered. *Quillaja* saponins increase cell proliferation, enhanced antibody synthesis and prolong natural killer cell activity (Chavali and Campbell, 1987a; Chavali and Campbell, 1987b; Jacobsen *et al*., 1996; Kim *et al*., 2006). Two well-documented saponin fractions derived from the extract of the bark of the *Quillaja saponaria* are Quil A and QS-21 (Demana *et al.*, 2004; Kensil *et al.*, 1991). These fractions have adjuvant properties and are surface-active agents (substances that require the surface free energy of cells to bind to hydrophobic surfaces). The latter results in their immunostimulatory property (Rajput *et al.*, 2007). Quil A is composed of more than twenty three different saponins and has been successfully used for veterinary use in inducing antibody production, though it is considered too toxic for human applications (Rajput *et al.*, 2007; Willson *et al.*, 1995). The use of this saponin-type adjuvant has been associated with lesions as well as with haemolysis, however (Smith and Pettit, 2004; Sun *et al*., 2008).

QS-21 has similarly been shown to induce CTL response and T_H1 cytokines, interleukin-2 (IL-2) and IFN-γ and has also been shown to act as an adjuvant for DNA vaccines (Kensil *et al*., 1998; Rajput *et al*., 2007; Sasaki *et al*., 1998). Although QS-21 has been reported to be less toxic than Quil A, there have, however, also been reports of

lesions and haemolysis associated with the use of this saponin-type adjuvant (Buendía *et al.*, 2007; Kensil *et al.*, 1991; Pillion *et al.*, 1996; Rajput *et al.*, 2007). This adjuvant was, however, considered for the current investigation because it was previously used successfully to raise anti-human cathepsin D antibodies in chickens. The recognition displayed by these antibodies for the human cathepsin D antigen was relatively weak but were not shown to cross-react with *M.smegmatis* and as they may give better results with a different species of cathepsin D antigen, it was decided that saponin would be a suitable adjuvant for re-testing.

The other adjuvant that seems to be popular is alum.

3.3.2.3 Aluminium-containing adjuvants

Aluminium-containing compounds have been used as vaccine adjuvants for more than seventy years (Ulanova *et al.*, 2001). There are three main types of aluminium-containing adjuvants: aluminium hydroxide, aluminium phosphate and alum/potassium aluminium sulfate. Each of these types have different isoelectric points as well as other unique properties (Eickhoff and Myers, 2002). Aluminium hydroxide is a crystalline aluminium oxyhydroxide that has a positive charge at physiological pH and an isoelectric point equal to 11. Aluminium phosphate is an amorphous aluminium hydroxyphosphate that has a negative charge at physiological pH and an isoelectric point between 5 and 7. Alum is an aluminium hydroxide that contains sulfate and usually phosphate anions. Its isoelectric point depends on the precipitation process used to create the vaccine in which it is contained.

Aluminium adjuvanted vaccines may be prepared using two methods. In one of the methods, a solution of alum is added to the respective antigen to create a precipitate of protein aluminate and these are referred to as alum-precipitated vaccines. In the second method, the respective antigen is added to pre-formed aluminium hydroxide or aluminium phosphate creating an aluminium-adsorbed vaccine (Hunter, 2002; Kool *et al.*, 2008). The binding of aluminium-containing adjuvants to antigens occurs via electrostatic forces and other interactions between the adjuvant and the respective antigen such as hydrophobic interactions, van der Waals forces and hydrogen bonding (Hunter, 2002; Kool *et al*., 2008).

Aluminium-containing adjuvants have three main mechanisms of action: (1) they are able to form a depot of antigen in tissues, allowing prolonged release, (2) they produce particulate antigens that are needed for the targeting of antigen presenting cells, (3) they activate complement and stimulate macrophages (Hunter, 2002; Kool *et al*., 2008). According to most literature available, aluminium-containing adjuvants are one of the few types of adjuvants that have been approved for humans (Baylor *et al*., 2002; Hunter, 2002; Kool *et al*., 2008). These adjuvants have also been successfully used for veterinary purposes (Kenney *et al.*, 1999). Several licensed products that contain aluminium adjuvants include vaccines against Hepatitus A and B, Lyme disease, Anthrax and Rabies. Although there have been some cases of negative side effects associated with the use of these adjuvants, such as the formation of sterile abscesses and subcutaneous nodules, granulomatous inflammation and contact hypersensitivity, none of these reactions have been sufficiently recurrent to allow for major concern (Eickhoff and Myers, 2002). To date, aluminium-containing adjuvants have not been observed to induce cross-reactivity with bacterial antigens such as those present in *M.smegmatis* or mycobacteria in general, thus this adjuvant was a suitable choice for the production of anti-cathepsin D antibodies (Mannhalter *et al*., 1985).

In addition to raising antibodies to cathepsin D, classification of cathepsin D-containing vesicles according to their labelling for lysosome associated membrane proteins-1 and -2 (LAMP-1 and -2) was also an aim. These are two major markers associated with the endocytic pathway and may assist in classifying the vesicles in which cathepsin D is found. In order to check that these antibodies recognize mouse antigens and also that they do not cross-react with *M.smegmatis* (though anti-LAMP-1 and -2 antibodies should not cross react as they are monoclonal), western blots were performed. Some introduction to the LAMPs and why they were used in the current study is now given.

3.4 LAMPs

The limiting membrane of "lysosome"-like organelles, such as the acidic late endosome, is important as it mediates the transport of ions, amino acids and other solutes into such organelles and is also involved in the maintenance of an acidic luminal pH. This membrane contains a large concentration of highly glycosylated transmembrane proteins which are referred to as Lysosome Associated Membrane Proteins (LAMPs). The proteins which make up the largest percentage of this group include two type I transmembrane proteins, LAMP-1 and LAMP-2 and a tetraspanin protein LAMP-3 (also referred to as CD63) (Fukuda, 1991; Janvier and Bonifacino, 2005). For purposes of this dissertation, only LAMP-1 and -2 will be reviewed as the current study focused on these two markers, of which most is known,

3.4.1 Structure of LAMPs

LAMP-1 and -2 are homologous to each other and they share a similarity in domain structures. Both of these glycoproteins contain a polypeptide core which is ~40 kDa. A large portion of LAMP-1 and -2 are found in the lumenal side of acidic organelles. This portion is made up of two internally homologous domains which are separated by a region that is rich in proline residues. This proline rich region forms a hinge which is free to move. The hinge region of LAMP-1 molecules contains several proline and serine residues while that of LAMP-2 is enriched with proline and threonine residues. Each homologous domain of the lumenal portion of the glycoproteins contains four half cysteine residues which are highly conserved. These cysteine residues connect to each other to form four disulfide loops (Figure 3.4). The lumenal portion is connected to a transmembrane domain which goes on to form a short cytoplasmic tail. The lumenal portion contains a large number of N-glycans, some of which are complex poly-N-acetyllactosamines. It has also been reported that this portion also contains O-glycans some of which are also poly-N-acetyllactosamines (Figure 3.4) (Fukuda, 1991).

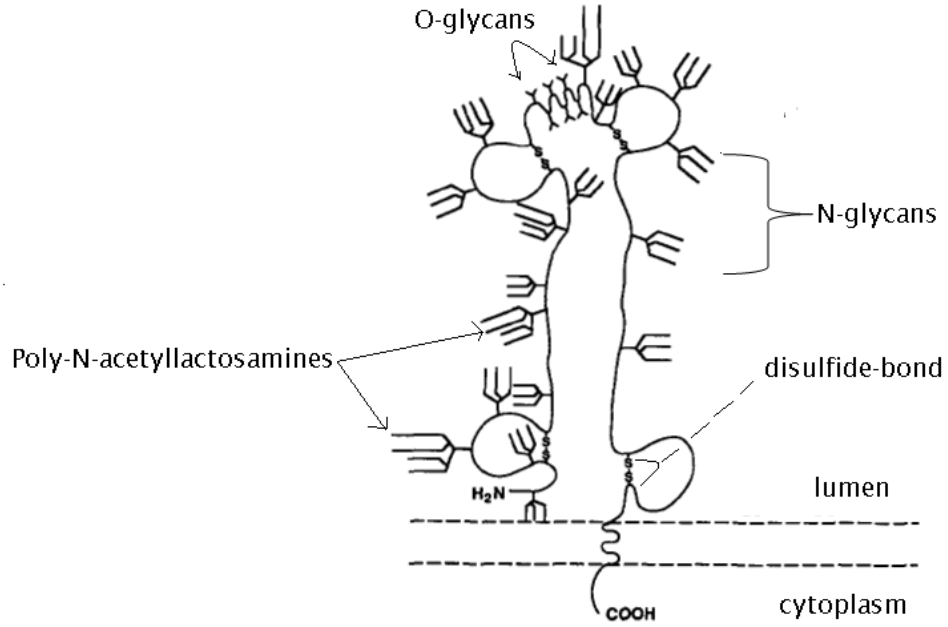

Figure 3.4: Schematic diagram depicting the structure of structure of a LAMP-1/-2 molecule.

LAMP-1 and -2 are composed of two homologous lumenal domains which are separated by a region that is rich in proline residues. Each homologous domain that is contained within the lumenal portion of the glycoproteins has four half cysteine residues which are highly conserved. These cysteine residues connect to each other to form four disulfide loops. The lumenal portion also contains a large number of N-glycans and a smaller number of O-glycans some of which are also poly-N-acetyllactosamines (adapted from Fukuda, 1991).

3.4.2 Sorting and cell trafficking of LAMPs

Two different pathways referred to as the direct and indirect pathways, have been proposed to be involved in the biosynthetic transport of LAMPs to lysosomes (Hunziker and Geuze, 1996). The direct pathway involves the transport of newly synthesized LAMPs from the trans-Golgi network to late endosomes and lysosomes. The indirect pathway involves the transport of LAMPs from the trans-Golgi network to the plasma membrane where they are internalized and delivered to a plasma membrane compartment and thereafter to late endosomes and storage "lysosomes" (Gough *et al.*, 1999). Although there is a consensus that both pathways are involved in the trafficking of LAMPs, the exact contribution of each pathway is uncertain.

An important feature which has been observed to be associated with the trafficking of both LAMP-1 and -2 is the GYXXØ motif (G-glycine, Y-tyrosine and Ø- a bulky hydrophobic amino acid) which is found within the cytoplasmic tail. This motif may be compared to the YXXØ-type motif, a tyrosine based sorting signaling motif that mediates various sorting activities in post-Golgi compartments (Bonifacino and Traub, 2003; Janvier and Bonifacino, 2005). The presence of the G, Y and Ø residues, as well as the precise placement of the motif relative to the transmembrane domain, have been observed to be vital for the efficient trafficking of LAMPs to acidic organelles. Changes in the residues or their placement relative to the transmembrane domain has been observed to result in an increase in the expression of LAMPs at the cell surface (Janvier and Bonifacino, 2005; Rohrer *et al*., 1996). The GYXXØ motif of LAMP molecules, like other YXXØ-type motifs have been observed to interact with the μ subunits (μ1, μ2, μ3 and μ4) of four heterotetrameric adaptor protein (AP) complexes, AP-1, -2, -3 and -4 (Janvier and Bonifacino, 2005; Pandey, 2009).

AP complexes are components of protein coats which interact with the cytosolic region of organelles that are part of the secretory and endocytic pathways. These complexes mediate protein sorting by bringing about the formation of coated vesicles as well as the concentration of cargo molecules within vesicles. The four AP complexes have a similar structure and are made up of two large chains, a medium chain and a small chain (Aguilar *et al*., 2001). The AP-1 complex contains β1 and γ adaptins as large chains, μ1A or μ1B as a medium chain and ζ1 as a small chain. The AP-2 complex contains β2 and α adaptins as large chains, μ2 as a medium chain and ζ2 as a small chain. The AP-3 complex has β3A or β3B and δ adaptins as large chains, μ3A or μ3B as a medium chain and ζ3 as a small chain. The AP-4 complex has β4 and ε adaptins as large chains, μ4 as a medium chain and ζ4 as a small chain (Boehm *et al.*, 2001; Shim *et al.*, 2000).

AP-1,-2 and 3 are part of vesicle coats which contain the scaffolding protein clathrin, whereas AP-4 is part of a non-clathrin coat (Janvier and Bonifacino, 2005). Clathrin is the coat protein of selective carrier vesicles as well as some secretory storage vesicles and mediates receptor-dependent endocytosis. It is also involved in the isolation of lysosomal precursors from the trans-Golgi network (Rothman and Orci, 1990). Thus the interaction of GYXXØ motifs of LAMP molecules with AP complexes brings about the

incorporation of LAMPs into coated vesicles such as those coated by clathrin and this mediates their selective transport to acidic or "lysosomal" storage organelles, via a cell surface or Golgi to late endosome, clathrin-mediated mechanism (Janvier and Bonifacino, 2005).

3.4.3 Functions of LAMP-1 and LAMP-2

Both LAMP-1 and -2 form a continuous carbohydrate lining on the inner leaflet of the membrane of acidic organelles. Thus it was originally believed that these proteins were involved in the maintenance of the structural integrity of such membranes by protecting it from the acidic luminal environment (Huynh *et al*., 2007a). However, research conducted by Kundra and Kornfeld, (1999) has shown otherwise. These researchers used endoglycosidase H to remove the Asn-linked glycans from LAMP-1 and -2 and this resulted in their rapid degradation. No measurable changes in membrane integrity were noted as a result, however. This observation suggested that LAMP-1 and -2 may have alternate functions.

The generation of LAMP-1 and -2 single and double knockout mice have been useful for the study of possible functions of these proteins. Andrejewski *et al*. (1999) observed that LAMP-1 deficient mice had phenotypes that were close to normal with no significant changes. However, these mice were also observed to have higher levels of LAMP-2 expression and it was thus suggested that this may be a mechanism used to compensate for the loss of LAMP-1.

On the other hand, LAMP-2 deficiency in mice has been shown to increase mortality of new born mice between 20 and 40 days of age (Tanaka *et al*., 2000). It has also been proposed that this protein may serve as a receptor for chaperone-meditated autophagy of cytosolic proteins (Dice, 2007). Its involvement in autophagy has also been displayed by the accumulation of autophagic vacuoles in organs such as liver, pancreas and heart in LAMP-2 deficient mice. LAMP-2 is also believed to play a role in lysosome biogenesis as LAMP-2 deficient mice have been shown to display an elevated secretion of lysosomal enzymes and incorrect cathepsin D processing (Eskelinen *et al*., 2002; Huynh *et al*., 2007a). Hence the necessity in the current study, to assess the relationship of macrophage LAMP-1 and -2 with cathepsin D to assess whether alterations in

cathepsin D association post-infection with *M.smegmatis* occurs to allow the partial escape of some *M.smegmatis* in order to escape killing. This aspect was not covered in the study by Anes *et al*. (2006) and hence represents a novel aspect of the current study.

Interestingly, LAMP-1 and -2 have also been observed to be important for phagosomal maturation. In a study conducted by Huynh *et al*. (2007a) phagocytes were generated by transfecting phagocytic receptors into immortalized embryonic fibroblasts from LAMP-deficient mice. This was necessary as the simultaneous deletion of LAMP-1 and -2 genes results in death between embryonic days 14.5 and 16.5 (Eskelinen *et al*., 2004). This research group observed that phagosomes failed to fuse with lysosomes in transfected, immortalized, embryonic fibroblasts derived from LAMP-1 and -2 deficient mice embryos.

LAMP-1 has also been associated with antigen processing involving MHC class II molecules, in an endosome-like compartment. One of the reasons that this association has been established is due to the observation of specific compartments that contain peptide-MHCII complexes, HLA-DM as well as LAMP-1 but have also been shown to lack M6PRs and several classical "lysosomal" markers, thus excluding the possibility of these being late endosomes or classical "lysosomes", respectively (Calafat *et al.*, 1994; Dani *et al.*, 2004). LAMP-2 has also been observed to facilitate MHC class II presentation of antigens. This has been demonstrated by the decrease in the presentation of antigens by MHC class II molecules in cells with a decreased expression of LAMP-2 (Zhou *et al.*, 2005). The association between LAMP-2 and MHC class II molecules has also been demonstrated by Büning *et al.* (2006) who observed that the processing and presentation of ovalbumin takes place in organelles that label positively for LAMP-2 and MHC class II molecules.

In another study conducted by Eskelinen *et al*. (2002), cells from LAMP-2 deficient mice, were observed to have a decrease in M6PRs-46 (cation-dependent mannose-6-phosphate-receptors) as compared to cells that had been isolated from normal mice. It was, therefore, suggested that LAMP-2 also plays a role in the recycling of M6PR-46. In the same study, cells from LAMP-2 deficient mice also displayed a partial mistargeting of some lysosomal enzymes such as cathepsin D and a subsequent

accumulation of autophagic vacuoles due to a decrease in lysosomal enzyme-associated degradation. This suggests that LAMP-2 plays a major role in autophagy and that this protein is mainly associated with major degradative compartments which label strongly with cathepsin D (Eskelinen, 2006).

Prior to raising antibodies against porcine cathepsin D, it was important to check the purity of the antigen against which the antibodies were raised. This was done using SDS-PAGE analysis. This was followed by checking the reactivity of the LAMP-1 and -2 as well as anti-human and anti-porcine cathepsin D antibodies for mouse macrophage antigens.

3.5 SDS-PAGE of porcine and human cathepsin D

SDS-PAGE was carried out to check the purity of both porcine and human cathepsin D proteins previously purified prior to immunization of the porcine cathepsin D with the saponin adjuvant and before characterization of a previously produced but uncharacterized anti-human cathepsin D antibody raised using an alum adjuvant (Mkhwanazi, 2009).

3.5.1 Reagents

Cathepsin D previously purified by Fortgens, (1996) from human and porcine spleen essentially according to Takahashi and Tang, (1981), but also using three-phase partitioning (TPP) prior to pepstatin affinity chromatography, was made available for this project. SDS-PAGE and Coomassie blue staining reagents are as described in Sections 2.3.1 and 2.4.1.1, respectively.

3.5.2 Procedure

Porcine and human cathepsin D sample preparation for SDS-PAGE analysis

Reducing SDS-PAGE separation of cathepsin D was conducted as described in Section 2.3.2. Human and porcine cathepsin D (1 mg/ml, 20 µl) were added to reducing treatment buffer (20 µl) and boiled for 90 s. Approximately 10 µg of treated human and porcine cathepsin D were loaded into each well of a reducing SDS-PAGE gel. After

electrophoresis, the gel was stained using Coomassie blue staining as described in Section 2.4.1.2.

3.5.3 Results

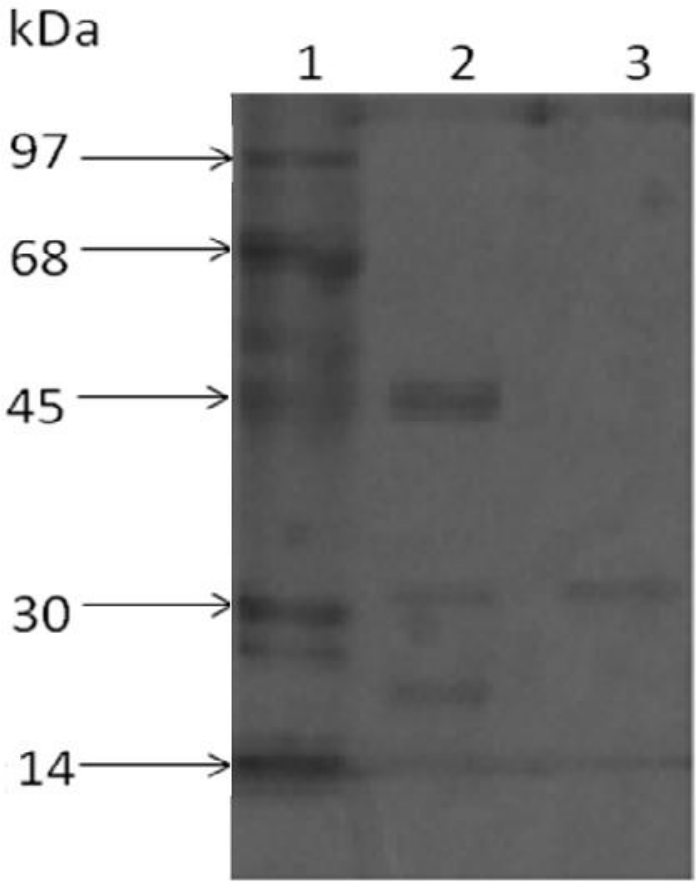

Figure 3.5: Reducing SDS-PAGE of human and porcine cathepsin D to determine purity of samples prior to immunization.

Molecular weight marker (lane 1) containing phosphorylase b, 97 kDa; BSA, 68 kDa; ovalbumin, 45 kDa; carbonic anhydrase, 30 kDa and lysozyme, 14 kDa. Human cathepsin D (lane 2, 10 µg) and porcine cathepsin D (lane 3, 10 µg) samples were prepared in reducing treatment buffer combined with bromophenol blue [5µl, 0.1% (m/v) in dH_2O] and separated on a 15% Laemmli gel and stained with Coomassie brilliant blue**.**

Three bands of approximately 45, 31 and 17 kDa were observed in the human cathepsin D sample (Figure 3.5, lane 2). The band of approximately 45 kDa is most probably the intermediate form of the enzyme although it is slightly lower than the value reported for this intermediate form of human cathepsin D which is approximately 48 kDa (Laurent-Matha *et al*., 2006; Minarowska *et al*., 2008). The second band of approximately 31 kDa is most probably the heavy chain of the active mature two chain form of the enzyme. This band is, however, slightly lower than the value reported for this form of human cathepsin D which is approximately 34 kDa (Benes *et al*., 2008; Minarowska *et al*., 2008). The third band in the human cathepsin D sample, approximately 17 kDa, is most probably the light chain of the active mature two chain form of the enzyme. This is, however, slightly higher than the value reported for this form of human cathepsin D which is approximately 14 kDa (Benes *et al*., 2008; Minarowska *et al*., 2008). A band of approximately 31 kDa was observed in the porcine cathepsin D sample (Figure 3.5, lane 3) and this is most probably the heavy chain of the active mature two chain form of the enzyme. This band corresponds to the value reported for this form of porcine cathepsin D (Barth and Afting, 1984). No contaminating bands were observed for both the human and porcine cathepsin D samples thus indicating their suitability for use in raising anti-porcine cathepsin D antibodies and checking the specificity of anti-human cathepsin D antibodies previously raised (Mkhwanazi, 2009).

3.6 Host animal for antibody production

When choosing a host for the production of antibodies, it is firstly most important to choose an animal whose proteins have the greatest sequence variation with respect to the particular antigen against which the antibodies will be produced so that this antigen has maximum antigenicity. To determine whether a target antigen to be inoculated is similar to the endogenous protein in the animal to be inoculated, sequence alignments between that of the host and the respective antigen needs to be compared and the species showing the least homology with the target antigen should be selected. Such sequence alignments may be performed using software such as BLAST (http://www/ncbi.nlm.nih.gov/Blast/) which is a sequence similarity search program that can be used to search a specified database for matches to a given query sequence. There are several BLAST tools which enable a user to compare all combinations of nucleotide

or protein queries against specified nucleotide or protein databases. BLAST based tools are able to perform alignments between sequences using specific algorithms and also provide statistical information about the significances of each alignment (Camacho *et al*., 2009; Johnson *et al*., 2008; Ye *et al*., 2006).

Other considerations that need to be taken into account when choosing an animal for antibody production include, (1) the amount of antibody production that is required, (2) the ease of harvesting the antibodies, for example, obtaining blood samples and (3) the uses of the antibodies that are produced (Leenaars and Hendriksen, 2005). The most frequently used animals for antibody production include rabbits, mice, rats, hamsters, guinea pigs, goats, sheep and chickens (Hanly *et al*., 1995; Leenaars and Hendriksen, 2005). Rabbits are usually used for antibody production because of their size, long life span, easy maintenance and handling as well as their ability to produce high titer, high affinity precipitating antiserum (Leenaars and Hendriksen, 2005). However, blood collection from rabbits is often a difficult process. An alternative to rabbits for raising antibodies are laying hens which produce antibodies that are transferred from the blood to the egg yolk (as immunoglobulin (Ig) Y) as a means of providing the embryo with protection prior to it developing a complete immune system (Polson *et al*., 1980). The most abundant immunoglobulin in the egg yolk IgG, referred to as IgY, is functionally similar to but structurally different to the mammalian IgG molecule. Besides avoiding the bleeding procedure associated with obtaining antibodies from rabbits, chickens produce ten times more IgY compared to the amount of IgG obtained from the single bleeding of a rabbit. Thus more antibodies can be obtained more easily from chickens (Hau and Hendriksen, 2005). A disadvantage of using chickens to raise antibodies is that IgY does not bind to proteins A and G, and it also does not bind mammalian complement (Hau and Hendriksen, 2005; Jensenius *et al*., 1981; Leenaars and Hendriksen, 2005). The fact that IgY does not bind to protein A may sometimes pose a problem, for example, when this is required for immunocytochemistry for location of primary antibody binding using a protein A or protein G probe. This, however, may be overcome with the use of rabbit anti-IgY linker antibodies (Carroll and Stollar, 1983).

To aid in the selection of the laboratory animal to be used in raising antibodies to cathepsin D using porcine cathepsin D, sequence alignments were performed between porcine cathepsin D and cathepsin D of possible lab animals in which antibodies may be raised. These animals included chicken, mouse, rabbit and rat.

3.6.1 Sequence Alignments between porcine cathepsin D and cathepsin D of potential host animals.

The FASTA sequence of porcine cathepsin D was obtained from the Universal Protein Resource Knowledgebase (UniProtKB) (http://www.uniprot.org/), a database which provides protein sequences and annotated data (Hinz, 2010; Jain *et al*., 2009). This sequence was used to perform a protein blast using the BLAST algorithm "blastp" (protein-protein BLAST) (http://www/ncbi.nlm.nih.gov/Blast/) so that the homology between porcine, chicken, mouse, rabbit and rat cathepsin D sequences could be determined.

3.6.2 Results

Table 3.1: Porcine cathepsin D (Q4U1U4) percentage sequence homology in chicken (Q05744), mouse (P18242), rabbit (A5HC45) and rat (Q6P6T6) species.

	Chicken cathepsin D	Mouse cathepsin D	Rabbit cathepsin D	Rat cathepsin D
Porcine cathepsin D	68%	80%	84%	80%

Porcine cathepsin D displayed the most sequence homology with rabbit cathepsin D (84%), followed by mouse and rat cathepsin D (80%) (Table 3.1). This suggests that these animals would not be suitable as host animals for the production of antibodies against porcine cathepsin D as the antigenicity of porcine cathepsin D would not be high in these animals. Porcine cathepsin D showed the lowest sequence homology with

chicken cathepsin D (68%) (Table 3.1) suggesting that chickens would be the most suitable for raising these antibodies. Thus chickens were chosen for inoculation.

3.7 Production and characterization of anti-porcine cathepsin D antibodies

As previously mentioned, for this particular study, which involves the infection of J774 macrophages with *M. smegmatis*, it is important that the adjuvant used to raise the cathepsin D antibodies does not cause cross-reactivity with *M.smegmatis* or other mycobacteria, as this would not allow the presence of cathepsin D in *M.smegmatis*-containing phagosomes to be monitored. Thus, the use of FCA (which is usually the gold standard for antibody production for many years) was not appropriate due to its microbial content (Stills, 2005). Recent legislation banning the use of this previously extensively used adjuvant now required the exploration of alternative adjuvants on which, unfortunately, there is not a large body of literature (Stills, 2005).

Previously, in our laboratory, anti-human cathepsin D antibodies have been raised using saponin and a combination of saponin and alum (Mkhwanazi, 2009). These antibodies, however, displayed poor reactivity with mouse macrophage cathepsin D. Subsequently, anti-porcine cathepsin D antibodies have been raised using alum (Lin, 2007). These antibodies also displayed weak recognition of mouse macrophage cathepsin D. It was unclear if this weak recognition was due to the adjuvant or the antigen, thus, for the current study, porcine cathepsin D and saponin were used to raise antibodies. During the current study, uncharacterized anti-human cathepsin D antibodies that were previously raised using alum (Mkhwanazi, 2009) were also characterized.

Over the years, several antibody isolation techniques have been used. These have included affinity and ion exchange chromatography and ammonium sulphate precipitation coupled with size-exclusion chromatography (Andrew and Titus, 2000). A popular method that has been used by many researchers for the isolation of IgY serum from egg yolks is polyethylene glycol (PEG 6 kDa) precipitation. PEG is a hydrophilic polymer that precipitates proteins using a dehydration exclusion mechanism, which results in proteins being concentrated and dehydrated in the extra polymer space until

they reach their solubility limit and subsequently precipitate out of solution (Bateman *et al*., 1986; Dennison, 2003a; Fahie-Wilson and Halsall, 2008; Polson *et al*., 1985). This method of IgY isolation has been used in this current study.

To check the recognition of mouse macrophage cathepsin D by previously raised chicken anti-human cathepsin D antibodies and the chicken anti-porcine cathepsin D antibodies that were raised during the current study, and select the most reactive antibodies for the current study, IgY isolation and western blot analysis using J774 cell homogenates was employed.

3.7.1 Reagents

Phosphate buffered saline (PBS), pH 7.4 [8 mM Na_2HPO_4, 1.5 mM KH_2PO_4, 137 mM NaCl, 2.7 mM KCl, 1 mM $CaCl_2.2H_2O$ and 0.5 mM $MgCl_2.6H_2O$, pH 7.4]. Na_2HPO_4 (1.145 g), KH_2PO_4 (0.2 g), NaCl (7.99), KCl (0.1998 g), $CaCl_2.2H_2O$ (0.147 g) and $MgCl_2.6H_2O$ (0.1016 g) were dissolved in 1 l of dH_2O. The pH of the solution was verified to be 7.4 before being filtered through Whatman No. 1 filter paper and autoclaved (121ºC). The solution was stored at 4ºC.

Porcine cathepsin D. Cathepsin D previously purified by Fortgens (1996) from porcine spleen, essentially according to Takahashi and Tang (1981) but using three-phase partitioning (TPP) prior to pepstatin affinity chromatography.

Saponin-PBS [0.1% (m/v) Saponin in PBS]. Saponin (1 mg) was dissolved in sterile PBS (1 ml) immediately before use.

Phosphate buffer A [100 mM sodium phosphate buffer, 0.02% (w/v) NaN_3, pH 7.6]. $NaH_2PO_4.H_2O$ (13.8 g) was dissolved in dH_2O (950 ml). The solution was titrated to pH 7.6 with NaOH and NaN_3 (0.2 g) was added to the solution before being made up to 1 l with dH_2O.

Phosphate buffer B [100 mM sodium phosphate buffer, 0.1% (w/v) NaN_3, pH 7.6]. $NaH_2PO_4.H_2O$ (13.8 g) was dissolved in dH_2O (950 ml). The solution was titrated to a pH of 7.6 with NaOH and NaN_3 (1 g) was added to the solution before being made up to 1 l with dH_2O.

J774 cell and *M.smegmatis* culture reagents were as described in Sections 2.2.1 and 2.6.1, respectively.

Western blot reagents were as described in Section 2.5.1.

3.7.2 Procedure

IgY isolated from the eggs of chickens that were to be used for the production of anti-porcine cathepsin D antibodies were tested for pre-existing antibodies against *M.smegmatis* (as chickens are often vaccinated against *Mycobacterium avium* and such endogenous antibodies would contaminate any antibodies subsequently raised against porcine cathepsin D) and two non-reactive chickens were selected for inoculation.

The porcine cathepsin D antigen was prepared in saponin-PBS in which the antigen was dissolved by gentle inversion. Approximately 250 µl of the antigen solution was injected into each breast muscle so that each chicken was administered with 40 µg of the antigen during each immunization. The initial immunization was followed by booster injections at weeks 2, 4, 6 and 8.

During the isolation of anti-porcine cathepsin D antibodies, egg yolks (from eggs collected at 0, 2, 4, 6 and 8 weeks after primary immunization) were separated from egg whites before being rinsed in dH_2O, the yolk sacs pierced and the yolk volume measured. Twice this volume of phosphate buffer A was added to the yolk in a measuring cylinder and this was mixed by inversion, sealing the open end with Parafilm. Crushed PEG [6 kDa, [3.5% (m/v)], was added and dissolved by gentle stirring. The solution was centrifuged (4420 x g, 30 min, RT), the precipitated vitellin fraction (containing lipoproteins) was pelleted and the remaining contaminating lipids were removed by filtering the supernatant fluid through cotton wool. Further PEG [6 kDa, 8.5% (m/v)], was rapidly added to the filtrate and dissolved by gentle stirring. The solution was centrifuged (12 000 x g, 30 min, RT) and the pellet dissolved in a volume

of phosphate buffer A equal to the initial yolk volume. Crushed PEG [6 kDa, 12% (m/v)], was added to the solution, mixed by gentle stirring and the solution was centrifuged (12 000 x g, 30 min, RT). The IgY pellet was dissolved in a volume of phosphate buffer B equal to $1/6^{th}$ of the original egg yolk volume. IgY yield was determined by diluting the final IgY solution in phosphate buffer B (1: 50), and using the IgY extinction coefficient ($E_{280nm}^{1\ mg/ml} = 1.25$) and the equation [IgY] = [(A_{280}/ 1.25) x 50] (mg/ml) (Goldring and Coetzer, 2003). Pre-immune IgY was similarly isolated and used as a control.

Due to the limited amount of pure antigen available, enzyme-linked immunosorbent assay (ELISA) response determinations were omitted and IgY, isolated from week eight serum, was used to probe western blots of J774 macrophage and *M.smegmatis* homogenates. This was done to check the recognition and specificity of antibody recognition of J774 macrophage cathepsin D, and a lack of cross-reactivity with *M.smegmatis*. This was carried out as described in Sections 2.2.2, 2.6.2 and 2.5.2, respectively, using primary antibodies (chicken anti-porcine cathepsin D, pre-immune IgY serums and chicken anti-human cathepsin D) at a concentration of 100 µg/ml (which was determined as the optimum antibody concentration), while the secondary antibody, rabbit anti-chicken IgY-HRP was used at 1:5000 dilution. The blot was developed using a DAB substrate solution.

3.7.3 Results

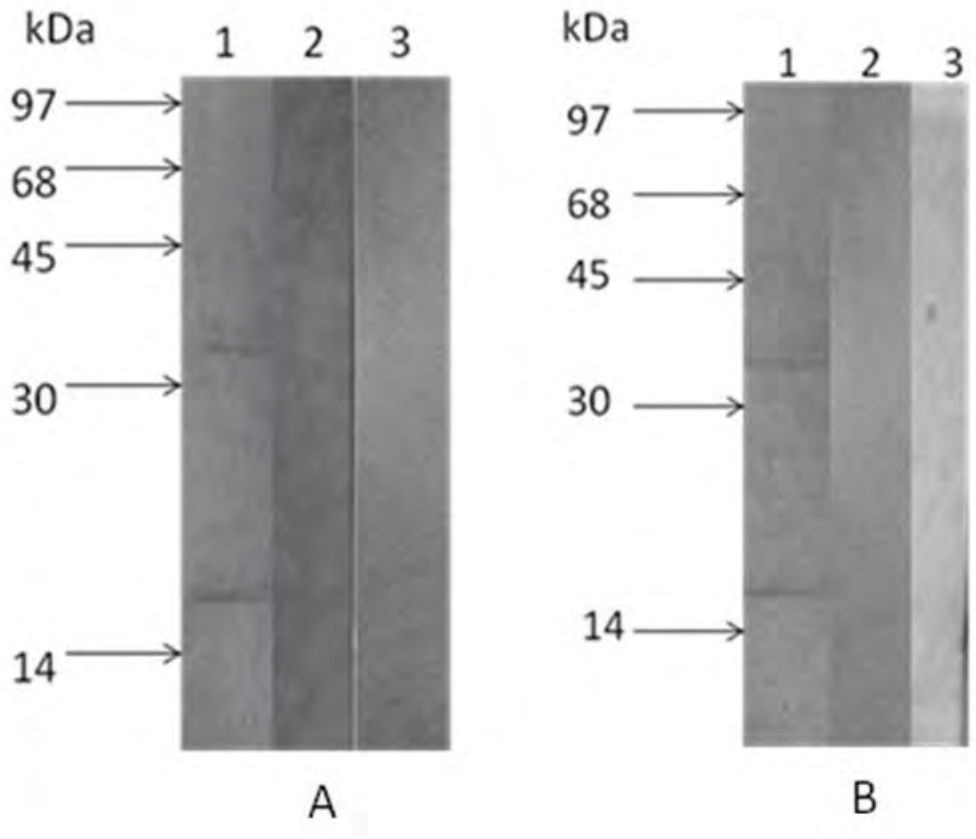

Figure 3.6: Characterization of chicken anti-porcine and chicken anti-human cathepsin D using J774 macrophage and *M.smegmatis* homogenates.

J774 homogenate (lane 1 (A and B), 20 µl) and *M.smegmatis* homogenate (lane 3 (A and B), 20 µl) were probed with chicken anti-porcine cathepsin D [100 µg/ml], (lane 1, A) and chicken anti-human cathepsin D [100 µg/ml] (lane 1, B). J774 homogenate (lane 2 (A and B), 20 µl) was probed with pre-immune IgY [100 µg/ml]. Rabbit anti-chicken IgY-HRP [1:5000] was used to for the detection process, followed by development using a DAB substrate solution after separation on a 15% reducing Laemmli gel and transfer onto nitrocellulose. MWM = phosphorylase b, 97 kDa; BSA, 68 kDa; ovalbumin, 45 kDa; carbonic anhydrase, 30 kDa and lysozyme, 14 kDa.

Chicken anti-porcine cathepsin D (Figure 3.6, A) and chicken anti-human cathepsin D antibodies (Figure 3.6, B) used to detect the presence of cathepsin D in J774 cells showed two bands of approximately 32 kDa and 17 kDa (Figure 3.6, lane 1, A), and 33 kDa and 15 kDa (Figure 3.6, lane 1, B) in the J774 macrophage homogenates. The bands of approximately 32 and 33 kDa detected in Figure 3.6, lane 1, A and B, respectively, were most probably the heavy chain of the active mature two chain form of the protease. These values are, however, slightly higher than the literature value reported for this form of mouse cathepsin D which is approximately 30 kDa (Claussen

et al., 1997). The bands of approximately 17 kDa and 15 kDa detected (Figure 3.6, lane 1, A and B, respectively), are most probably the light chain of the active mature two chain form of the protease. These are, however, slightly higher than the 14 kDa value reported in the literature for this form of mouse cathepsin D (Claussen *et al*., 1997). No bands were detected in the *M.smegmatis* homogenates (Figure 3.6, lane 3, A and B). This indicates that the antibodies raised against porcine and human cathepsin D did not cross-react with mycobacteria. The pre-immune IgY control used at the same level as the test (Figure 3.6, lane 2, A and B) displayed no non-specific bands.

3.8 Localization of cathepsin D in J774 macrophages using immunogold labelling.

To further verify the recognition of mouse cathepsin D and the lack of cross-reactivity with *M.smegmatis*, the chicken anti-porcine and anti-human cathepsin D antibodies were used in immunogold labelling studies on J774 macrophages using electron microscopy.

3.8.1 Reagents

Reagents used for the culturing of J774 and *M.smegmatis* cells were as described in Sections 2.2.1 and 2.6.1, respectively. Reagents used for fixation, embedding and immunolabelling of ultrathin sections were as described in Section 2.8.1.1. and 2.8.2.1, respectively. The chicken anti-human cathepsin D antibody (Mkhwanazi, 2009) and the chicken anti-porcine cathepsin D antibodies prepared as described in Sections 3.7.1 and 3.7.2, respectively, were also used.

3.8.2 Procedure

Culturing of J774 and *M.smegmatis* cells was described in Sections 2.2.2 and 2.6.2, respectively. Fixation and embedding of J774 and *M.smegmatis* cells were as described in Section 2.8.1.2. Protein A gold labelling of J774 and *M.smegmatis* ultrathin sections were performed with chicken anti-porcine cathepsin D [20 µg/ml] and chicken anti-human cathepsin D [20 µg/ml] as described in Section 2.8.2.2. Pre-immune IgY controls were also performed at the same level as used in the test, to check labelling specificity.

3.8.3 Results

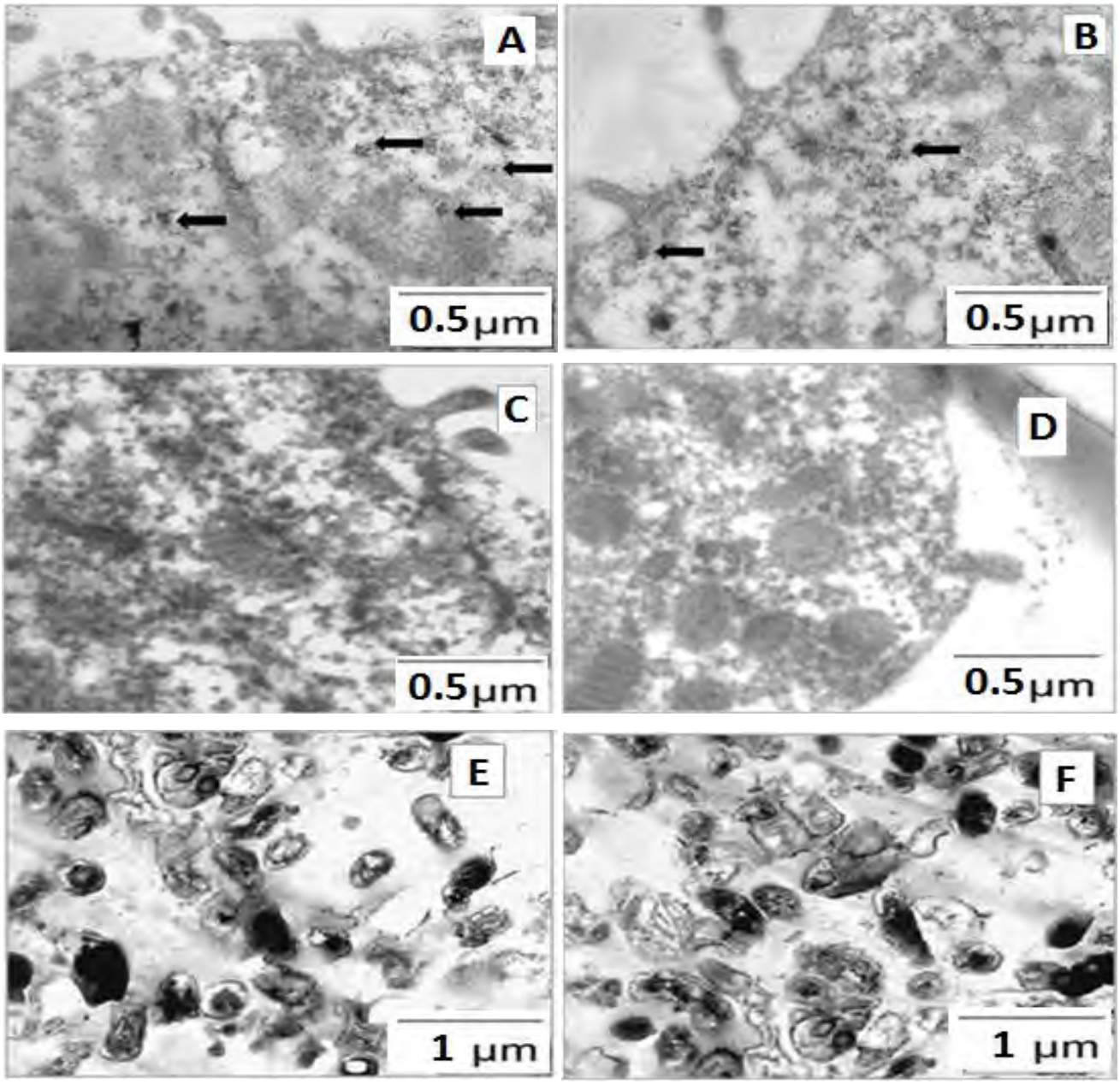

Figure 3.7: Protein A gold labelling of cathepsin D in J774 macrophages and *M.smegmatis* using chicken anti-porcine and anti-human cathepsin D.

Chicken anti-porcine cathepsin D [20 µg/ml (A and E)], chicken anti-human cathepsin D [20 µg/ml (B and F) pre-immune IgY [20 µg/ml (C and D)], a rabbit anti-chicken linker antibody [50 µg/ml] and protein-A gold probe (10 nm) were used on J774 macrophage (A, B, C and D) and *M.smegmatis* (E and F) LR White sections. LR White sections were viewed using a Philips CW 120 Biotwin TEM (80-100 kV). Cathepsin D found in electron dense vesicles were indicated using black arrows (A and B). Bar = 0.5 µm (A, B, C and D) and 1 µm (E and F).

Chicken anti-porcine cathepsin D (Figure 3.7, A) and chicken anti-human cathepsin D (Figure 3.7, B) antibodies, used to detect the presence of cathepsin D positive vesicles in J774 cell LR White ultrathin sections, labelled similar small, electron dense cathepsin D positive vesicles in the J774 cell LR White sections. Most of these vesicles appear to be approximately the same size and are also relatively close to translucent areas in the cells.

Chicken anti-porcine and chicken anti-human cathepsin D antibodies used in the labelling of LR White ultrathin sections of *M.smegmatis* showed no cross-reactivity with either antibody (Figure 3.7, E and F). Pre-immune IgY preparations (used at the same levels as the chicken anti-porcine and chicken anti-human cathepsin D antibodies labelling of J774 macrophages) showed no non-specific labelling of J774 cells (Figure 3.7, C and D). Ultrastructure of both J774 and *M.smegmatis* cells appeared to be satisfactory (Figure A-D and E-F, respectively).

3.9 Characterization of rat anti-mouse LAMP-1 and -2

Since cathepsin D trafficking and processing has been closely associated with LAMP-1 and-2 trafficking, a pattern of association was sought (Eskelinen *et al*., 2002). Western blotting was used to characterize the commercially available monoclonal antibodies, rat anti-mouse LAMP-1 and -2 using J774 cells. These monoclonal antibodies were to be used for subsequent characterization of cathepsin D-labelled-vesicles in Chapter four.

3.9.1 Reagents

Reagents used for J774 cell and *M.smegmatis* culture and western blot procedures were as described in Sections 2.2.1, 2.6.1 and 2.5.1, respectively.

Monoclonal rat anti-mouse LAMP-1 and -2 antibodies were provided by the Developmental Studies Hybridoma Bank (University of Iowa, Iowa City, Iowa, USA).

3.9.2 Procedure

J774 cell and *M.smegmatis* culture and western blot procedures were carried out as described in Sections 2.2.2, 2.6.2 and 2.5.2, respectively The primary antibodies, rat anti-mouse LAMP-1 and -2 were used at dilutions 1:800 and 1:1000, respectively, while

the secondary antibody, goat anti-rat IgG (whole molecule)-alkaline phosphatase was used at a dilution of 1:5000 and the blot was developed using an alkaline phosphatase substrate.

3.9.3 Results

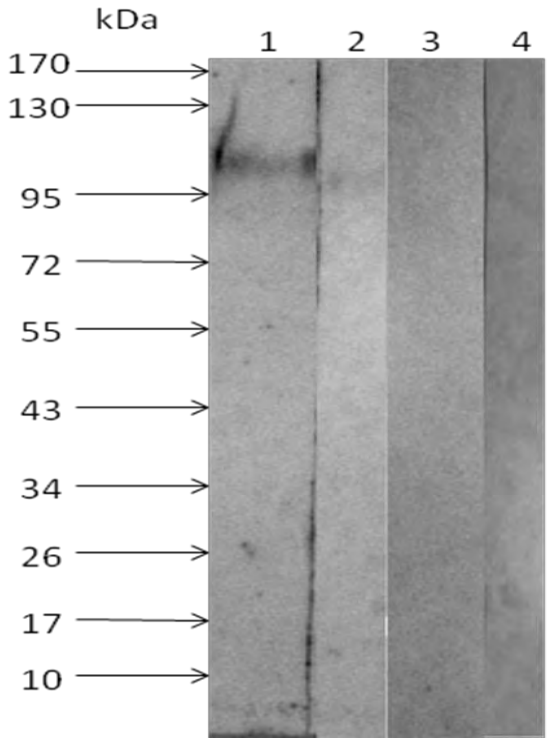

Figure 3.8: Characterization of rat anti-mouse LAMP-1 and -2 antibodies using J774 macrophage and *M.smegmatis* homogenates.

J774 homogenates (lane 1 and 2) and *M.smegmatis* homogenates (lane 3 and 4) were probed with rat anti-mouse LAMP-1 [1:800] (lane 1 and 3) and rat anti-mouse LAMP-2 [1:1000] (lane 2 and 4), detected with goat anti-rat IgG (whole molecule)-alkaline phosphatase [1:5000] and developed in alkaline phosphatase substrate solution after separation on a 15% reducing Laemmli gel and transferred onto nitrocellulose. MWM (Page Ruler Protein ladder from Inqaba biotechnical industries) consisted of recombinant prokaryotic proteins.

The rat anti-mouse LAMP-1 and -2 monoclonal antibodies used to detect the presence of LAMP-1 and -2, respectively, in J774 cells labelled a single band of approximately 113 kDa and 110 kDa, respectively, in J774 macrophage homogenates (Figure 3.8, lane 1 and 2, respectively). These correspond to the reported molecular weight ranges for

mouse LAMP-1 and -2, that are approximately between 105-115 kDa and 100-110 kDa, respectively (Chen *et al*., 1986; Chen *et al*., 1985). Cross-reactivity of rat anti-mouse LAMP-1 and -2 with *M.smegmatis* was not detected, (Figure 3.8, lane 3 and 4, respectively).

3.10 DISCUSSION

One of the main aims for the current study, was to characterize cathepsin D-positive vesicles in *M.smegmatis*-infected J774 macrophages, to establish a potential association between these cathepsin D-positive vesicles and the killing of *M.smegmatis* by J774 macrophages, and any pattern of association of LAMP-1 and -2 with cathepsin D. To this end, cathepsin D antibodies that do not cross-react with mycobacteria were required.

Amongst other requirements, the production of antibodies requires a suitable adjuvant that would ultimately enhance the reaction to a specific antigen and increase the level of antibody response (titre), avidity and duration of antibody production at a high level. More than one hundred adjuvants have been described and categorized in terms of their mode of action, route of administration and their components and preparations (Jennings *et al*., 1998; Rajput *et al*., 2007). Commonly used adjuvants include Ribi adjuvants (prepared as oil-in-water emulsions containing mycobacterial components), Montanide ISA adjuvants (adjuvants that contain different surfactants combined with either a non-metabolized mineral oil or a metabolized oil or a mixture of both), Gerbu (aqueous adjuvants that contain a soluble glycopeptide from the cell wall of the bacterial species *Lactobacillus bulgaricus*), Freund‟s Complete adjuvants (prepared as a water-in-oil emulsion of mineral oil, mannide monooleate and heat-killed *M.tuberculosis*), aluminium-containing adjuvants (particulate adjuvants that contain aluminium salts that bind to antigens via electrostatic forces), lipososome-type adjuvants (micelles made up of phopholipid bilayers separated by an aqueous compartment) and saponin-based adjuvants (steroid or triterpenoid glycosides that interact with cell membrane cholesterol resulting in the formation of pores in the membrane) (Eickhoff and Myers, 2002; Jennings, 1995; Rajput *et al*., 2007; Waghmare *et al*., 2009). Most of the commonly used adjuvants, therefore, contain an indigestible

oil or particulate base such as alum, that is insoluble, and, therefore, when mixed with an antigen is responsible for the slow release of the antigen. This is important because the other major component is usually a bacterial product which will bind and activate the toll-like receptors on APCs. Activated APCs move towards the site of injection or "depot" from which antigen is released and stimulate the release of cytokines that will activate uncommitted and committed T and B cells to stimulate the production of antibodies.

From the many types of adjuvants available, Freund‟s complete adjuvant was long considered as the "gold standard" as its immunostimulatory properties have been observed to be better than the majority of documented adjuvants in terms of increasing levels and titre of antibodies produced (Altman and Dixon, 1989; Stills, 2005).

Due to their mycobacterial components, adjuvants such as Freund‟s complete and Ribi adjuvants stimulate the immune response primarily via toll-like-receptor-dependent mechanisms, while releasing the antigen slowly in order to allow the stimulation of immune systems described. Toll-like receptors recognize and interact with components such as bacterial lipopolysaccharides, mycobacterial lipoprotein, lipoarabinomannans and lipomannans (mycobacterial cell wall components) that are contained in such adjuvants and ultimately influence the innate and adaptive immune response leading to antibody production in the host animal. Mycobacterial-containing adjuvants and adjuvants containing any other bacterial components or products could also not be used in the current study. Many of these are similar among organisms and antibodies stimulated would possibly not only recognize the antigen, cathepsin D, but may also interact with the components of *M.smegmatis*, thus confusing localization studies due to their lack of specificity in *M.smegmatis*-infected J774 macrophages.

Adjuvants that act via toll-like-receptor-independent mechanisms generally rely on the antigenicity of co-injected target protein and slow release of antigen due to their own indigestibility and lack of solubility. These include aluminium-containing adjuvants (that create a "depot" effect), liposome-type adjuvants (that protect antigens from rapid degradation, create a "depot" effect and transport the antigen to draining lymph nodes where they are exposed to APCs) and saponin-based adjuvants that remove cell

membrane cholesterol resulting in cell membrane-pore formation and the subsequent exposure of the antigen to MHC class I molecules and hence $CD8^+$ killer T cells (Jennings, 1995; Karanam *et al*., 2009; Rajput *et al*., 2007; Sjölander *et al*., 2001). This is generally not desirable where antibody product is desired, unless killed and damaged cells are subsequently phagocytosed exposing the target antigen to macrophages and other APCs and hence stimulating B and T cell antigen presentation and antibody production.

The anti-porcine cathepsin D antibodies raised with saponin during this current study recognized mouse cathepsin D in J774 cells. The weak intensity of the bands (reactivity) observed after probing J774 cells with this antibody at a fairly high concentration (100 µg/ml) during western blot analysis indicates that the antigen-adjuvant combination of porcine cathepsin D-saponin elicits a weak immune response in chickens, but none the less, results in the production of antibodies that did not cross-react with *M.smegmatis*.

From previous studies done in our laboratory, the combination of porcine cathepsin D with another popular non-mycobacterial-containing adjuvant, alum, also resulted in a weak immune response. In chickens, alum and saponin used in combination, together with the antigen porcine cathepsin D were also inefficient in eliciting a strong antibody response. This suggests that the antigenicity of porcine cathepsin D in chickens may not be high enough and uptake by only a few APCs may have occurred. This would result in low level antigen presentation and stimulation of T and B cells, producing a weak polyclonal response. Future studies should include the use of other non-mycobacterial-containing adjuvants, for example, those containing fungal components such as fungal β-glucans that interact with dectin-1 receptors in host animals (Zhang and Mosser, 2008). It is possible that such adjuvants would work similarly to mycobacterial-containing adjuvants that interact with toll-like receptors of host animals and attract more cells to the depot site. Non-mycobacterial containing adjuvants that contain hormones or cytokines usually secreted by the host during infections such as (IL)-1β, (TNF- α) or IL-6 could also be used as alternatives (Blatteis, 2000; Coma *et al*., 2006; Patterson *et al*., 2002; Russell *et al*., 2009). Generally, however, these being soluble and easily lost from the injection site, are less effective.

It may also be important to examine the source of cathepsin D used to raise antibodies for studies involving J774 macrophages. The use of mouse cathepsin D to raise antibodies in chickens may be a better alternative for studies on murine cells. Production of antibodies that would better recognize mouse antigens while having better antigenicity in chickens than porcine cathepsin D may result. This seems to be indicated as sequence homology between mouse cathepsin D and chicken cathepsin D is 66%, while that of porcine cathepsin D is 68%. When inoculated into chicken, it was reasoned that this antigen may result in a higher titre immune response and more avid antibodies.

The use of the previously raised anti-human cathepsin D antibody (raised with alum) and anti-porcine cathepsin D antibodies (raised with saponin) in immunogold labelling resulted in the detection of cathepsin D in electron dense vesicles in LR White resin-embedded J774 cells. These electron-dense vesicles were similar in size and found close to larger translucent vesicles resembling early endosomes. Despite the weak reactions, immunogold labelling also showed that the anti-porcine and anti-human cathepsin D antibodies did not cross react with *M.smegmatis* organisms embedded in LR White resin and retained reactivity with fixed cathepsin D after fixation with 4% paraformaldehyde (a fixative often used for electron microscopy involving immunogold labelling). Thus these antibodies were deemed suitable for proposed immunofluorescence labelling where 3.7% paraformaldehyde fixation would be used. Both the anti-porcine and anti-human cathepsin D antibodies, therefore, seemed suitable for further studies for labelling, cathepsin-D positive vesicles in *M.smegmatis*-infected J774 macrophages, though only the anti-human antibodies cathepsin D antibodies were subsequently used.

Although the use of saponin during the current study resulted in the production of weak reactive antibodies, the chickens that were immunized with this adjuvant did not display the lesions or granulomas that have been associated with the use of FCA (Broderson, 1989; Leenaars *et al*., 1998; Stills, 2005). Furthermore, the number of eggs laid per day per chicken immunized with the saponin-containing adjuvant did not decrease during the period of immunization as often occurs with FCA Therefore, according to the current study, saponin may be considered as a safe adjuvant for use in chickens.

The characterization of cathepsin D-positive vesicles using LAMP-1 and -2 antibodies was considered as important for the current study as these have been used in several studies as late endosome-"lysosome" markers in macrophages and could possibly be used to establish the stage at which cathepsin D may be associated with the possible killing of *M.smegmatis* i.e. when found in late endosomal compartments (Bringer *et al*., 2006; Fuller *et al*., 2008; O'Brien and Melville, 2000; Sturgill-Koszycki *et al*., 1996). Since LAMP-1 and -2 have been associated with MHC II antigen processing these markers could help in the analysis of the possible association of cathepsin D with mycobacterial antigen processing (Calafat *et al*., 1994; Dani *et al*., 2004; Zhou *et al*., 2005).

The antibodies characterized during the current study i.e. anti-human and anti-porcine cathepsin D antibodies and anti-LAMP-1 and -2 antibodies were deemed suitable for the detection and characterization of cathepsin D-positive vesicles in *M.smegmatis*-infected J774 cells. This will be discussed in Chapter four.

CHAPTER FOUR

ASSESSMENT OF THE ROLE OF CATHEPSIN D IN KILLING OF *Mycobacterium smegmatis*.

4.1 Introduction

As mentioned in chapter one, the killing of microorganisms by macrophages usually occurs within phagosomes and involves a series of fusion events, firstly between, early endosomes, followed by late endosomes and subsequently "lysosomes" (Section 1.4) (Raja, 2004; Singh *et al*., 2006; Vieira *et al*., 2002). In a highly dynamically interacting cell such as the macrophage, it is difficult to establish the exact sequence of fusion events that result in the killing of mycobacteria. Some studies have shown that one of the main events involves the fusion of "lysosomes" with the phagosome resulting in the discharge of certain lysosomal enzymes into the low pH phagosome where they are believed to be microbicidal (Anes *et al*., 2006; Lowrie *et al*., 1979; Silva *et al*., 1987; Sun *et al*., 2010). The studies on *M.smegmatis* by Anes *et al*. (2006) indicate that non-pathogenic mycobacteria seem to be mainly killed in early fusion events, possibly involving fusion with late endosomes and a compartment containing cathepsin D (or other lysosomal enzymes), at a pH on the limit of its optimal range for maximal catalytic activity. Bacterial cell numbers recover shortly, thereafter, however, as lysosomal enzymes are recycled out of the phagosome.

In order to survive killing, pathogenic mycobacteria have been shown to block various fusion events involving phagosomes and various endocytic bodies and "lysosomes". They may also prevent the assembly of various complexes required for the production of bacteriocidal products (Hart *et al*., 1987; Sturgill-Koszycki *et al*., 1994; Sun *et al*., 2010). Before the mechanisms for killing may be unravelled, the mechanisms by which non-pathogenic mycobacteria, such as *M.smegmatis*, have to be studied and the precise mechanisms of killing understood.

A comprehensive study by Anes *et al*. (2006) has mapped the dynamic sequence of events in the J774 macrophage killing of *M.smegmatis*. In order to conduct this study, internalization and pulse chase of colloidal gold conjugated to rhodamine was used to label first the endocytic pathway and later the late endosomes and last the "lysosomes". In addition, labelling for several endosomal markers/labels which are known or expected to be associated with late endocytic organelles, including LAMP-1, V-ATPase, LYAAT, CD63 and Hck, were used. Phagosomal pH (using LysoTracker Red-DND-99, which identifies organelles with a pH below 5.5-6), NO release, inducible NO synthase activity, and *M.smegmatis* growth using culture techniques were also assessed. Levels of a specific mitogen activated protein kinase (MAPK), p38, were also monitored and a role established using the specific inhibitor of this kinase (SB203580). Mitogen activated protein kinases (MAPKs) such as p38 were shown to mediate cellular responses such as assembly of actin, early endosome fusion, phagolysosome fusion, acidification and enhanced killing (Jahraus *et al*., 2001; Kjeken *et al*., 2004). It has been suggested that one of the ways in which MAPKs such as p38 do this is by promoting the production of cytokines such as IL-6, a key cytokine that is important for upregulating microbicidal activity in macrophages (Blumenthal *et al*., 2002; Zhou *et al*., 2010). Interestingly, p38 has been observed to be activated more during infection with non-pathogenic mycobacteria than pathogenic species, implying that pathogenic species may inhibit this map kinase in order to survive (Schorey and Cooper, 2003).

Additionally, the use of "lysosomal" protease inhibitors during this study allowed the phase during which lysosomal proteases were responsible for killing of mycobacteria to be established. This phase was established to be between one to four hours after infection (Section 1.6.2, Figure 1.5). To ensure that killing is being monitored at around this period of time (one to four hours post infection), it was decided that for the current study, colocalizations would be conducted five hours after infection.

In a dynamic, rapidly interacting cell, one of the most ideal ways to reveal interactions between various compartments and the phagosome is to use fluorescent substrates which may be visualized using confocal microscopy. These fluorescent substrates can also be used to show the activity of various enzymes and bactericidal compounds. Unfortunately, no such substrates are known to be available for cathepsin D, hence in

this study, there was a need for highly-specific anti-cathepsin D antibodies to detect cathepsin D.

In the study conducted by Anes *et al.* (2006), lysosomal enzymes were observed to play a role in the killing of *M.smegmatis* by J774 macrophages during the first four hours. The class of lysosomal enzyme responsible was not established. During this period, however, two interesting and crucial observations were made. Firstly, LAMP-1, an endosome-associated marker, was reported to recycle out of phagosomes which contain live but not dead mycobacteria. This indicates that the persistence of LAMP-1 may be associated with the presence of dead but not with live *M.smegmatis*. Secondly, the pH range of most phagosomes, during the early killing period (one to four hours post infection) reported by Anes *et al*. (2006), is approximately 5.5-6. This pH range is not usually associated with late endocytic organelles (i.e. where the pH is approximately 5 or less) but the early endosomes (Vieira *et al*., 2002). Cathepsin D has been reported to be active between pH 3.5-5.5, however (Barrett, 1970; Conus and Simon, 2010; Minarowska *et al*., 2008; Minarowska *et al*., 2007a) and may be active at a pH of 5.5 and be involved in the early killing phases during fusion with early/late endosomal compartments, within 4 hours (Lee, 2010; Piguet *et al*., 1999). Cathepsin D has also been reported to be the most prominent protease in mycobacterial phagosomes (Singh *et al*., 2006). In a study conducted by Singh *et al*. (2006) it was shown that this protease is involved in the processing of a mycobacterial antigen referred to as Ag85B. This involvement of cathepsin D in mycobacterial antigen processing may also imply a possible role in macrophage killing. Though Anes *et al*. (2006) have not shown which of the lysosomal proteases play a role in the killing of *M.smegmatis*, it now seems increasingly likely that cathepsin D may be involved.

Killing may also require cathepsin D of an intermediately processed form and a pH like that of the early endosome, and not fully processed cathepsin D, that is active between a pH of 3.5-5.5. Cathepsin D has been found to play a role in many pathological conditions, such as breast cancer, where it has been shown be secreted and function as a growth factor in its procathepsin D form (Ohri *et al*., 2007; Zaidi *et al*., 2008). This seems to be another possible example of how various processing forms of cathepsin D may play unanticipated roles.

In order to use confocal fluorescence microscopy to test the possibility that cathepsin D is involved in the killing, it was necessary to detect the presence of cathepsin D in phagosomes containing dead *M.smegmatis*. Anti-cathepsin D antibodies, that did not cross-react with mycobacteria, and a method of assessing bacterial viability were required. It was also important that the cathepsin D-containing-vesicles that play a role in the killing of *M.smegmatis* in macrophages be identified. This, it was speculated, could be achieved using labelling of vesicles for cathepsin D and for lysosomal associated membrane protein-1 and -2 (LAMP-1 and -2), late endosome-"lysosome" vesicle markers. Together with confocal microscopy these were used to visualize the localization of cathepsin D in relation to LAMP-1 and -2 and acidic compartments, the latter visualized using a fluorescent pH indicator, LysoTracker Red DND-99

The availability of GFP-tagged *M.smegmatis* (strain mc2155, which harbours a p19-long-lived EGFP plasmid) was also convenient and seemed a promising method by which visualization of "live" bacteria could be achieved in the current study. A marker for judging and confirming the presence of "dead" mycobacteria, in a similar manner, using confocal microscopy-based visualization, was required. Whereas in the study conducted by Anes *et al*. (2006), bacterial culture was used to monitor the decrease in *M.smegmatis* numbers, in the current study, loss of GFP fluorescence confirmed by uptake of PI by non-viable cells, was used to monitor bacterial death. Whether the loss of GFP fluorescence, could be used as an indicator of loss *M.smegmatis* cell viability in the phagosome was uncertain but seemed to be a reliable method as inducible GFP has been recently used to assess the metabolic activity of *M.tuberculosis* in the acidified macrophage phagosome (Lee *et al*., 2008a). Propidium iodide as an indicator of bacterial cell death or lack of viability in studies on *Mycobacterium leprae* proved also to be reliable (Lahiri *et al*., 2005). The reported shortcomings of both methods will now be described.

4.2 Green fluorescent protein (GFP) and propidium iodide for studying phagosomal killing

Green fluorescent protein (GFP), a 238 amino acid fluorescent protein, first isolated from the jellyfish *Aequorea Victoria*, produces a greenish luminescence due to the presence of GFP and another protein called aequorin (Toca-Herrera *et al*., 2006). When aequorin binds to Ca^{2+}, it undergoes an intramolecular reaction to produce a blue fluorescent protein in the singlet excited state. This protein transfers its energy by resonance to a chromophore acceptor in GFP. This chromophore is made up of an imidazolone ring structure and is formed as a product of a posttranslational modification of the primary structure, involving an auto-cyclodehydration of the tripeptide segment, –Ser65-Tyr66-Gly67-, and an autoxidation of the resulting dihydro-ring system (Nishiuchi *et al*., 1998; Niwa *et al*., 1996; Toca-Herrera *et al*., 2006). The group responsible for the emission of fluorescence is the phenolate anion of the chromophore (Niwa *et al.*, 1996).

GFP can form a functional fluorophore without cofactors and thus allows the visualization of fluorescent fusion proteins and protein expression and localization to be monitored (Brewis *et al.*, 2000; Ilk *et al.*, 2004). GFP has been observed to have two absorbance/excitation peaks namely one at 395 nm and another at 475 nm. Its emission peak has been observed at 508 nm (Heim *et al.*, 1994). Over the years several GFP mutants have been created as a result of genetic manipulations. These mutants have displayed excitation and emission spectra which are different from those of wild type GFP (Patterson *et al.*, 1997). Examples of GFP mutants include the enhanced green fluorescent protein (EGFP), S65T, EBFP and αGFP (Patterson *et al.*, 1997; Toca-Herrera *et al.*, 2006).

Two factors that have shown to have a major effect on GFP fluorescence include pH and temperature (Bizzarri *et al*., 2009; Kneen *et al*., 1998; Ogawa *et al*., 1995; Patterson *et al*., 1997).

Due to the phenol group on the chromophore of GFP, its fluorescence has been reported to be very sensitive to changes in pH both *in vitro* and *in vivo* (Bizzarri *et al.*, 2009; Kneen *et al.*, 1998). Patterson *et al*. (1997) conducted a study in which they showed the

effect that changes in pH had on the fluorescence of wild type GFP and four of its variants, αGFP, S65T, EBFP and EGFP. The fluorescence of wild type GFP and αGFP remained constant as the pH dropped from 9 to 6 but decreased below pH 6 while the fluorescence of S65T, EBFP and EGFP decreased below pH 7. Toca-Herrera *et al*. (2006) also showed that the fluorescence of EGFP reached a maximum value between pH 7 and 9 and began to decrease below pH 7 with no fluorescence being observed at pH 4. During the current study, the pH range of the environment in which EGFP-transfected *M.smegmatis* would be exposed in the macrophage would be a range from approximately 5.5-6.5 in the early endosome to 4.5-5.5 in the late endosome. It was, therefore, possible that GFP fluorophores would not be visible at lower pHs in later endocytic organelles. This, however, does not seem to be a problem as GFP-tagged *M.smegmatis* were observed to be visible in all low pH compartments in all studies which previously used the EGFP- *M.smegmatis* strain to be used in the current study (the *M.smegmatis* mc2155 harbouring a p19-(long-lived) EGFP plasmid) (Anes *et al*., 2003; Anes *et al*., 2006; Velaz-Faircloth *et al*., 1999).

The stability of GFP fluorescence at 37°C was also uncertain as studies have also shown that GFP fluorescence also depends on temperature. In a study by Ogawa *et al*. (1995), it was reported that when COS-1 and embryonic chicken retina cells were transfected with the plasmid pCMX-GFP, the fluorescence of GFP obtained after incubation at 37°C was barely detectable. However, stronger fluorescent intensity was detected at 30°C. Another study conducted by Patterson *et al*. (1997), showed that the chromophore formation of wild type GFP, S65T, EGFP and αGFP was efficient at 28°C. At 37°C, however, 25%, 30%, 95% and 100% of wild type GFP, S65T, EGFP and αGFP, respectively were expressed. This not only showed that temperature plays a role in GFP fluorescence but that certain mutants of GFP are more suitable to certain temperatures than others. Over the years GFP mutants which display a certain degree of "thermo-stability" have been produced. Such mutants are beneficial for experiments which require incubation temperatures around 37°C. An example of such a mutant is GFPA which has been shown to have reduced sensitivity to relatively high temperatures as it contains amino acid substitutions which prevent misfolding of GFP, a phenomenon that is believed to occur at high temperatures (Siemering *et al*., 1996). The GFP to be used

in the current study was EGFP and it seems that this form of GFP is one of the most suitable forms of GFP for infection studies in macrophages, except for visualizing mycobacteria in low pH-compartments. This, however, did not seem to be a problem with the *M.smegmatis* mc2155-EGFP strain used here (Anes *et al*., 2003; Anes *et al*., 2006; Gutierrez *et al*., 2008; Velaz-Faircloth *et al*., 1999).

GFP is non-toxic, requires no substrates or cofactors and has not been reported to induce any biological disturbance, allowing its use in living systems and microbial infection studies (Zhao *et al.*, 2001). In spite of the possible loss of fluorescence in low pH compartments Zhao *et al*. (2001) used *Escherichia coli* transfected with a variant of the *Renilla mulleri* (RMV)-GFP (a high-expression plasmid) for whole-body imaging visualization of an *E.coli* infection in mice. Sugawara *et al*. (2006) used a strain of *Mycobacterium tuberculosis*, H37Rv transformed with a BCG-hsp60 GFP promoter, to obtain a GFP-H37Rv mutant that was used to infect the lungs of mice and guinea pigs and study the formation of granulomas using a photon imager. None of these researchers mentioned a loss of GFP fluorescence being a problem in their studies.

However, Anes *et al*. (2006), used mycobacterial culture and PI staining of mycobacteria, after infected macrophages were lysed to release *M.smegmatis*, to confirm loss of viability. PI staining was not applied directly in labelling studies, as was intended in this current study. Additional indicators of mycobacterial cell death were also needed as GFP fluorescence may be quite stable and there was a possibility that EGFP-tagged mycobacteria may, fluoresce regardless of their viability (Lowder *et al*., 2000). During conditions of nutrient starvation, bacteria may also digest their own proteins in order to obtain energy as well as amino acids needed for protein synthesis under stressful conditions (Kuroda, 2006; Lowder *et al*., 2000).

Viablity studies are also often problematic as there are no absolute definitions of when a cell may be judged as “dead”. There are, however, characterisitcs which have been used. These include the loss of cell membrane integrity and the lack of ability to culture such organisms (Jepras *et al.*, 1995). Propidium iodide (PI), a membrane-impermeable intercalating fluorescent stain that binds to the DNA of cells or bacteria whose membranes have been permeabilized was, therefore, chosen in this study to enable

visualization of both cathepsin D, live and dead bacteria in the same compartment, to gain indirect evidence that cathepsin D may be responsible for killing *M.smegmatis* (Cui *et al*., 2003 ; Shi *et al*., 2007; Unal Cevik and Dalkara, 2003).

PI is excitated between 494 and 536 nm, emits at approximately 617 nm and intercalates between base pairs of DNA with little or no particular sequence preference, but in a ratio of one dye molecule per four to five DNA base pairs, producing a red fluorescence (Sigaut *et al*., 2009; Suzuki *et al*., 1997; Unal Cevik and Dalkara, 2003). Although several studies have used PI-based methods to determine bacterial viability, the reliability of such methods with certain bacterial species is still questionable. In a study conducted by Shi *et al*. (2007), 40% of a gram$^-$ *Sphingomonas* sp. LB126 and *Mycobacterium frederiksbergense* LB501T, stained with PI during early exponential growth, but were subsequently found to be culturable. In the above mentioned study, however, the bacterial species were exposed to PI for 10 minutes while in the current study *M.smegmatis* was exposed to PI for 2 minutes. Therefore, in the study conducted by Shi *et al*. (2007), the length of time that the bacterial species were exposed to PI may have contributed to false staining whereas PI labelling was found to absolutely correlate with loss of viability of *M.leprae*, judged via metabolic labelling and PI staining (Lahiri *et al*., 2005).

4.3 Infection studies in J774 macrophages

As the main aim of this current study was to extend the studies of Anes *et al*. (2006) and determine whether cathepsin D is involved in the J774 macrophage-killing of *M.smegmatis*, it was decided that a direct imaging approach using confocal microscopy-based visualization and a superior method of representing colocalization known as colocalization analysis (Section 2.7), a novel aspect of this study, would be used. One of the main requirements of this approach is the availability of appropriate markers located in the appropriately distinguishable or resoluble fluorophores, and highly specific antibodies. This prompted the production of anti-cathepsin D antibodies which did not cross-react with mycobacteria (Section 3.7). A second aim of this study was to characterize cathepsin D–positive vesicles. To do this, it was decided to label cathepsin D-positive vesicles for the presence of well-characterized endosomal markers, LAMP-1 and -2, were used and LysoTracker, a fluorescent pH indicator to detect acidic vesicles.

To visualize *M.smegmatis* in cathepsin D, LAMP-1 or -2 labelled vesicles, in J774 macrophages, it was decided to use EGFP-tagged *M.smegmatis*. A third aim of this current study was to determine if cathepsin D, LAMP-1 and -2–positive vesicles were associated with live and dead *M.smegmatis*. In the study conducted by Anes, *et al*. (2006), the relationship between LAMP-1 and live and dead *M.smegmatis* was explored, however, the association of cathepsin D and LAMP-2 with live and dead *M.smegmatis* was not determined. This is, therefore, a novel aspect of the current study. To analyze these associations, a direct visual indicator of mycobacterial cell death was sought and the impermeable fluorescent stain, propidium iodide, which binds to the DNA of membrane damaged cells, was used additionally for confocal studies. This was yet another novel aspect. Even though fluorescently-labelled-antibodies/markers enabled the visualization of cathepsin D, LAMP-1 and LAMP-2 positive vesicles, with live and dead *M.smegmatis*, (a means of analyzing the degree of colocalization) was explored using colocalization analysis (Section 2.7) in order to give a less subjective, more statistical means of establishing and expressing colocalization. This too was a novel aspect of the current study.

For this current study, intracellular antigen detection was required. This required the permeabilization of the cell membrane to allow antibodies to gain access to these antigens. The agent used to permeabilize cell membranes was saponin, a detergent-like molecule which intercalates into the cell membrane by removing the cholesterol contained within the membrane resulting in the formation of membrane pores. (Bangham *et al*., 1962; Schroeder *et al*., 1998). Although saponin-action results in the permeabilization of cell membranes, it is important to note that membrane integrity is largely preserved and such permeabilization did not affect the cell wall of mycobacteria (Anes *et al*., 2006; Jacob *et al*., 1991).

4.3.1 Reagents

PBS, pH 7.4 [8 mM Na_2HPO_4, 1.5 mM KH_2PO_4, 137 mM NaCl, 2.7 mM KCl, 1 mM $CaCl_2.2H_2O$ and 0.5 mM $MgCl_2.6H_2O$, pH 7.4]. Na_2HPO_4 (1.145 g), KH_2PO_4 (0.2 g), NaCl (7.99), KCl (0.1998 g), $CaCl_2.2H_2O$ (0.147 g) and $MgCl_2.6H_2O$ (0.1016 g) were dissolved in 1 l of dH_2O. The pH of the solution was verified to be pH 7.4 before being filtered through Whatman No. 1 filter paper and stored at 4ºC.

Paraformaldehyde (PFA) stock solution [16% (m/v) in dH_2O]. PFA (16 g) was dissolved in dH_2O (80 ml) and heated to 60ºC. The solution was cleared with the drop wise addition of a 1M NaOH solution. After the solution was cooled, it was made up to 100 ml, aliquoted and stored at -20ºC.

PFA-PBS [3.7% (m/v) in PBS, pH 7.4]. PFA stock solution (6 ml) was added to PBS (20 ml).

Saponin-PBS [0.1% (m/v) in PBS, pH 7.4]. Saponin (0.1 g) was dissolved in PBS (100 ml). The solution was then filtered through Whatman No.1 filter paper. The solution was made up just before use.

BSA-PBS [1% (m/v) in PBS, pH 7.4]. BSA (1 g) was dissolved in PBS (100 ml).

Moviol mounting medium [10% Moviol, 23 M glycerol in 0.1 M Tris, pH 8.5]. Moviol (2.4 g), was added to 0.2 M Tris (12 ml) in a closed container that was covered with foil and stirred overnight. Glycerol (6 g) and dH_2O (6 ml) were added to the solution and stirred overnight. The solution was then centrifuged (500 x g, 15 min), aliquoted and stored at -20ºC.

Hoechst stock solution. Hoechst (bis Benzimide H33342 trihydrochloride) (0.025 g) was dissolved in dH_2O (2.5 ml).

Hoechst working solution. Hoechst stock solution (1 µl) was dissolved in 10 ml dH_2O.

LysoTracker working solution [2 nM LysoTracker Red DND-99 in (DMEM) with 10% (v/v) decomplemented FCS]. LysoTracker stock solution (100 µ1, 1 mM) was diluted in DMEM (4 ml) with 10% (v/v) decomplemented FCS.

Propidium iodide stock solution [0.1% (m/v)]. Propidium iodide (0.001 g) was dissolved in dH_2O (1 ml).

Propidium iodide working solution. Propidium iodide stock solution (2.5 µl) was dissolved in dH_2O (1ml).

Antibodies. Anti-porcine cathepsin D antibodies, raised as described in Section 3.7.2, and anti-human cathepsin D antibodies, previously raised with alum by Mkhwanazi (2009) were used.

J774 cell and EGFP-tagged *M.smegmatis* culture. This was conducted using reagents described in Sections 2.2.1 and 2.6.1, respectively.

4.3.2 Procedure

For fluorescence microscopy studies, J774 macrophages and EGFP-tagged *M.smegmatis* culture were performed as described in Sections 2.2.2 and 2.6.2, respectively.

In order to determine whether propidium iodide (PI) could be used as an indicator of *M.smegmatis* cell death and confirm that live EGFP-tagged *M.smegmatis* would not take up PI, nor that GFP would survive in heat-killed cells, log-phase culture of *M.smegmatis* ($O.D_{600}$ 0.1) (2.5 ml) was heat-killed by autoclaving at 121°C and propidium iodide working solution (5 µl) was added to the heat-killed culture (2.5 ml) and to live culture (2.5 ml) and left to incubate for 2 min at RT. Both cultures were subsequently washed with new Middlebrook 7H9 broth medium and centrifuged (120 x g, 2 min, RT, 6 x). Both live and heat-killed cultures were then placed onto glass slides and viewed by confocal microscopy as described in Section 2.7.

For the immunofluorescence labelling of J774 macrophages sterile cover slips were placed into each well of a 24 well Multidish plate. J774 macrophages were trypsinized and resuspended in DMEM supplemented with 10% decomplemented FCS (15 ml). The

J774 cell suspension (250 µl/well) was added to the cover slips and the Multidish plate was placed into a Nuaire US Autoflow CO_2 water-jacket incubator for 15 min. Once cells adhered to the coverslips, DMEM supplemented with 10% decomplemented FCS (250 µl/well) was added to each coverslip-containing well. The cells were grown overnight until approximately 70% confluency was reached.

The infection of J774 macrophages was performed according to Blokpoel *et al*. (2005) and Anes *et al*., (2006) with minor modifications. After culturing of *M.smegmatis* as described in Section 2.6.2, log-phase cultures of *M.smegmatis* ($O.D_{600}$ 0.1) were centrifuged (120 x g, 2 min) and resuspended in DMEM. Infections were performed at a multiplicity of infection (MOI) of 100 bacteria per macrophage (100:1) so that more than 5 bacilli per macrophage would be taken up after one hour of infection. The infection process was conducted for 5 hours at 37ºC. After the infection period, infected cells were washed with PBS (400 µl/well). Both infected and uninfected J774 macrophages were thereafter fixed with PFA-PBS (400 µl/well, 10 min, RT). For studies in which acidic areas were identified, LysoTracker Red DND-99 working solution (150 µl) was added to cells and incubated for 30 min at 37ºC prior to fixation. After fixation, cells were washed with PBS (400 µl/well, 3 x, RT) and non-specific binding sites were blocked by incubating cells in BSA-PBS (400 µl/well, 1 h, RT). The BSA-PBS was subsequently removed, the cells were incubated in primary antibody diluted in saponin-PBS (150 µl/well, 1 h, RT) and washed in saponin-PBS (400 µl/well, 6 x, RT). This was followed by the incubation of the cells in BSA-PBS (400 µl/well, 1 h, RT), followed by their incubation in secondary antibody diluted in saponin-PBS (150 µl/well, 1 h, RT).

From this point onwards, the 24 well Multidish plate was covered with foil as fluorescent probes are sensitive to light. The cells were washed again with saponin-PBS (400 µl/well, 6 x, RT). If double immunolabelling was conducted, the labelling procedure was repeated. If not, the cells were incubated with Hoechst working solution (50 µl in 400 µl PBS/ per well) for 5 min and thereafter washed with PBS (400 µl/well, 6 x, RT). The cells were fixed with PFA-PBS (400 µl/well, 10 min, RT), thereafter washed with PBS (400 µl/well, 6 x, RT) and finally washed with dH_2O (400 µl/well, 3 x, RT). For J774 cells that were infected with *M.smegmatis*, propidium iodide working

solution (5 µl) was added to each well before fixation (2 min) and thereafter washed thoroughly with PBS (400 µl/well, 6 x, RT).

The coverslips of infected and uninfected cells were removed from the wells, air dried, mounted with moviol (3 µl) and sealed with clear nail varnish. Fluorescent labelling was viewed using a Zeiss 710 confocal laser scanning microscope (Heidelberg, Germany). Single confocal images were taken with a scanning mode format of 1024 x 1024 pixels in line-averaging mode and a scanning speed of 6, with a pinhole setting of 1 Airy unit (AU). As colour is not a feature of the signal from fluorophores captured with charge-coupled device (CCD) cameras or photomultiplier tubes (PMTS), in their representation where relevant, the colour assigned to signals may be falsely assigned so that the signals from two different fluorophores could be distinguished. This was done in the current study, where the signal of one fluorophore was designated a green colour while the other was designated a red colour. This allowed for the simultaneous visualization of fluorophores that emit light in the far red, near red and green-yellow part of the spectrum. Once captured, images were exported as Red-Green-Blue (RGB) images and image processing was performed using ImageJ software (http://rsbweb.nih.gov/ij/). Colocalization analysis was performed using the ImageJ plugin JACoP (Just Another Co-localization Plugin) (http://rsb.info.nih.gov/ij/plugins/track/jacop.html) as described in Section 2.7.1 and colocalizations were also represented so that colocalized pixels were coloured white for ease of visualization and representation of colocalization.

4.3.3 Results

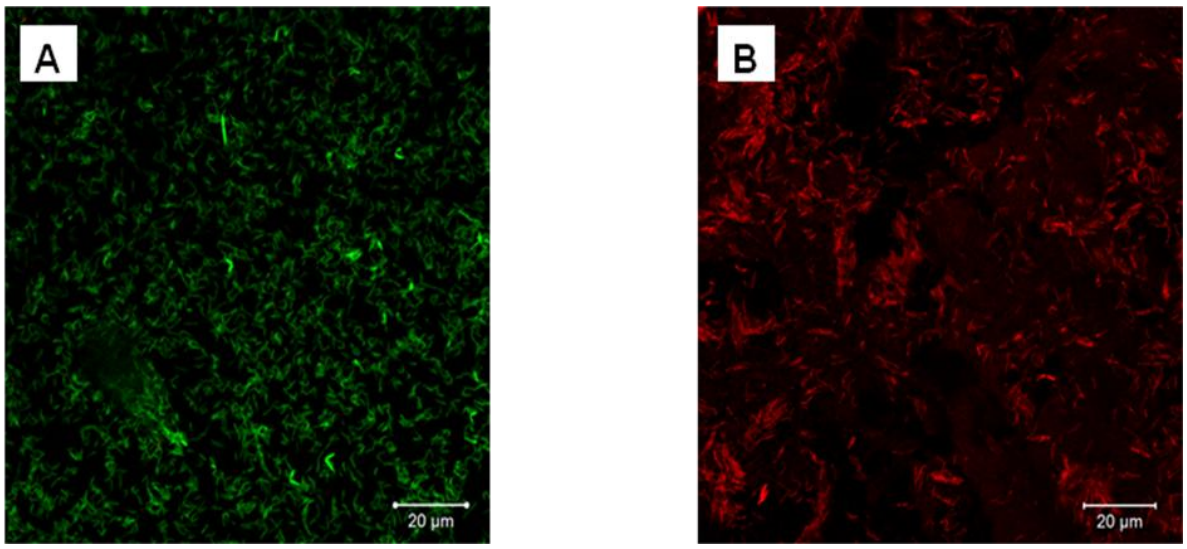

Figure 4.1: Live/dead assay of GFP-tagged *M.smegmatis*.

Log-phase culture of *M.smegmatis* ($O.D_{600}$ 0.1) (2.5 ml) was heat-killed (121 °C), Propidium iodide (0.0025 µg/µl) was added to heat-killed culture (B) and to 2.5 ml of live culture (A) (2 min). Cultures were then washed with new Middlebrook 7H9 broth medium and centrifuged (120 x g, 2 min 6 x). Both live and heat-killed cultures were then placed onto glass slides and viewed using a Zeiss 710 confocal laser scanning microscope (Heidelberg, Germany).

Heat-killed *M.smegmatis* mc2155 harbouring a p19-(long-lived) EGFP were shown to no longer fluoresce (Figure 4.1, B). Propidium iodide (PI) was observed to be a suitable indicator of cell death as it allowed the visualization of the heat-killed *M.smegmatis* (Figure 4.1, B) but did not label viable *M.smegmatis* (Figure 4.1, A).

After comparing results obtained with anti-human and anti-porcine cathepsin D antibodies, (not shown), it was observed that more satisfactory results were obtained using anti-human cathepsin D antibodies.

A

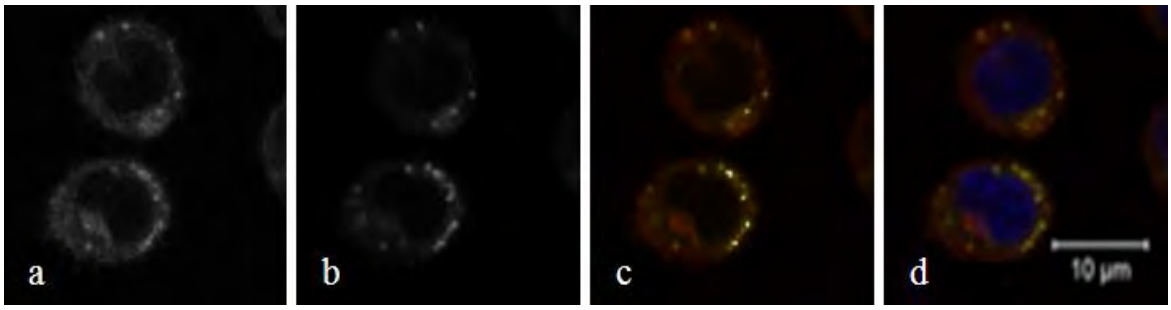

B

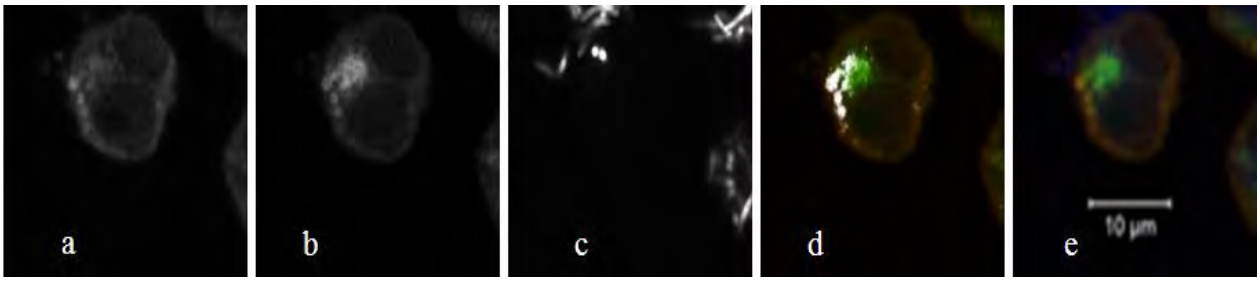

Figure 4.2: Uninfected- (A) and infected J774 macrophages (B) immunolabelled for cathepsin D and LysoTracker.

Uninfected- (A*)* and GFP-tagged *M.smegmatis* infected cells (B) were immunolabelled with chicken anti-human cathepsin D [10 µg/ml], detected with donkey anti-chicken CY5 [0.5 µg/ml] (Panel A and B, a), and LysoTracker working solution (150 µl, 2 nM) (Panel A and B, b), after overnight growth on coverslips and infection (of one set of coverslips) with GFP-tagged *M.smegmatis* (5 h), followed by fixation with 3.7% (m/v) PFA and permeablization with 0.1% (m/v) saponin in PBS. Images representing cathepsin D (Panel A and B, a), LysoTracker (Panel A and B, b) and GFP-tagged *M.smegmatis* (Panel B, c) were converted from RGB (Red Green Blue) to single images (only one channel displayed) and thereafter to 8-bit black and white images for simplicity of representation as colocalization can only use the red and green channels. Colocalization of cathepsin D (red) and LysoTracker (false green), together with labelling of the nucleus with Hoechst (blue) (Panel A and B, d and e, respectively) is shown by combining images in three channels (Panel A and B, d and e, respectively). As colocalization (usually shown as yellow as a result of overlaying of the two channels) is difficult to visualize (as is evident) (Panel A and B, d and e, respectively), images were also analyzed using Image J colocalization highlighter software, where colocalizing pixels are depicted as white (Panel A and B, images c and d, respectively). For completeness, GFP-tagged *M.smegmatis* was represented as a single 8-bit black and white image (Panel B, c), however, GFP-tagged *M.smegmatis* was omitted from the combined colocalization overlay image (Panel B, e).

The traditional overlay method of colocalization in which red labels are overlayed by green, giving rise to yellow, rendered colocalization difficult to visualize (Figure 4.2, Panel **A**, d and Panel **B**, e). However, by using ImageJ‟s colocalization highlighter tool (in which colocalizing flurophores are rendered white) it was clearly observed that there

is greater colocalization between cathepsin D vesicles and acidic vesicles in *M.smegmatis* infected J774 cells than in uninfected cells (Figure 4.2, Panel **A**, c and Panel **B**, d). This was also confirmed by the Pearson‟s and Manders‟ Overlap coefficients for infected cells (Table 4.1, 0.86 and 0.88, respectively) that are higher than for uninfected cells (Table 4.1, 0.73 and 0.77, respectively), and fall within the range for valid colocalization (0.5-1 for Pearson‟s coefficient and 0.6-1 for Manders‟ Overlap coefficient). These results were further validated by overlay coefficients where the differences between the values for k_1 and k_2 for both uninfected and infected cells are relatively small (0.11 for uninfected and 0.05 for infected, a requirement for valid colocalization, Table 4.1) but the difference between k_1 and k_2 for infected cells was smaller than that of uninfected cells, also indicating the greater colocalization between cathepsin D and acidity in vesicles of infected cells. Colocalization coefficients M_1 and M_2 values for infected cells (Table 4.1, 0.51 and 0.77, respectively) are also higher than that of uninfected cells (Table 4.1, 0.5 and 0.6, respectively), both being greater than 0.5 also validating colocalization results. Using the Costes‟ analysis approach, a P-value of 100% (Table 4.1) was calculated for both infected and uninfected cells suggesting that the calculated Pearson‟s coefficient is highly probable and not due to random overlap. The ICQ value for infected cells (0.44) is higher than that of uninfected cells (0.4), thus indicating and substantiating a greater colocalization in infected cells and in both cases, the ICQ values are positive and much greater than 0 validating colocalization.

As cathepsin D colocalizes more with LysoTracker in infected cells (Figure 4.2, Panel **A**, c and Panel **B**, d and Table 4.1), this suggests that cathepsin D is activated to a greater degree in infected cells since acidic conditions are required for activation and optimal cathepsin D activity (Minarowska *et al*., 2008). This suggests a possible role for active cathepsin D in the response and killing of non-pathogenic mycobacteria such as *M.smegmatis* by J774 cells. The presence of *M.smegmatis* in colocalized vesicles where cathepsin D should be active seems difficult to visualize, however, possibly due to the low pH of the compartment as observed in Figure 4.2, Panel **B**, c and d. The *M.smegmatis* (Figure 4.2, Panel **B**, c) which occupy the position in which cathepsin D colocalizes with LysoTracker (displayed by the white colour in Figure 4.2, Panel **B**, d)

seems to fluoresce less than mycobacteria that are not associated with cathepsin D and LysoTracker, possibly as the pH of the environment decreases, so does the GFP fluorescence (Toca-Herrera *et al*., 2006). This may explain the results observed (Fig 4.2, B) but may also imply that mycobacteria in low pH compartments are possibly being killed due to exposure to cathepsin D and this may be reflected in the loss of GFP fluorescence. This, however, needs to be verified via another method of indicating mycobacterial cell death. Propidium iodide (PI) could have been employed but PI and LysoTracker Red DND-99 fluorophores (available for this study) have similar excitation and emission wavelengths i.e. PI excitation occurs at 536 nm and emission at 617 nm, while LysoTracker Red DND-99 occurs at 577 nm and emission at 590 nm, respectively) (Freundt *et al*., 2007; Vogt and Schmid-Schönbein, 2001). This could, therefore, not be distinguished easily using confocal detection systems due to emission spectral overlap and therefore, these fluorophores could not be used simultaneously. There also, however, seems to be less overall cathepsin D in infected cells (Figure 4.2, Panel **A**, as compared to Panel **B**, a).

A

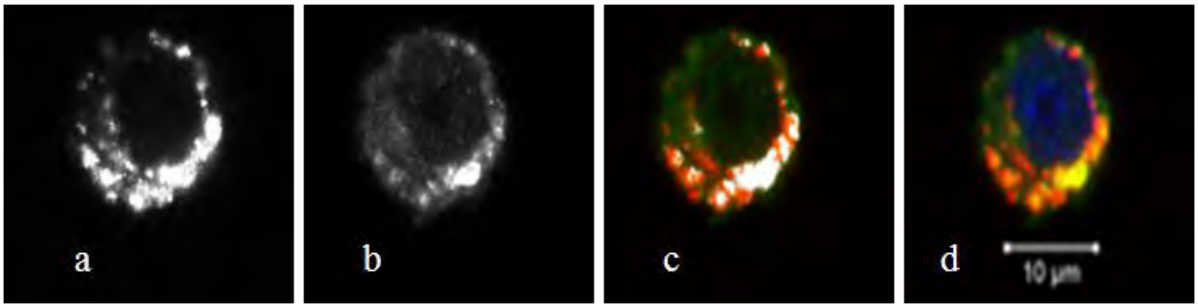

B

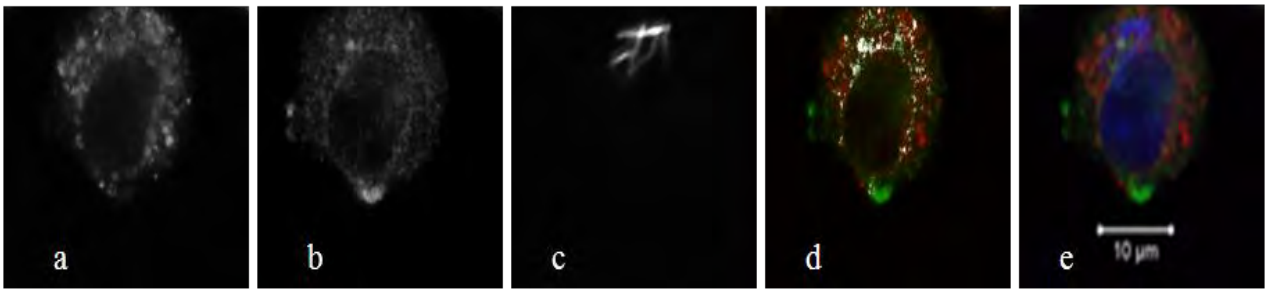

Figure 4.3: Uninfected- (A) and infected J774 macrophages (B) immunolabelled for LAMP-1 and cathepsin D.

Uninfected- (A) and GFP-tagged *M.smegmatis* infected cells (B) were immunolabelled with rat anti-mouse LAMP-1 [1:2000] (Panel A and B, a) and chicken anti-human cathepsin D [10 µg/ml] (Panel A and B, b) and labelling detected with donkey anti-rat CY5 [0.3 µg/ml] and donkey anti-chicken CY3 [0.5 µg/ml], respectively, after overnight growth on coverslips and infection (of one set of coverslips) with GFP-tagged *M.smegmatis* (5 h), followed by fixation with 3.7% (m/v) PFA and permeablization with 0.1% (m/v) saponin in PBS. Images representing LAMP-1 (Panel A and B, a), cathepsin D (Panel A and B, b) and GFP-tagged *M.smegmatis* (Panel B, c) were converted from RGB (Red Green Blue) to single images (only one channel displayed) and thereafter to 8-bit black and white images for simplicity of representation as colocalization can only use the red and green channels. Colocalization of LAMP-1 (red) and cathepsin D (false green), together with labelling of the nucleus with Hoechst (blue) (Panel A and B, d and e, respectively) is shown by combining images in three channels (Panel A and B, d and e, respectively). As colocalization (usually shown as yellow as a result of overlaying of the red and green channels) is difficult to visualize (as is evident) (Panel A and B, d and e, respectively), images were also analyzed using Image J colocalization highlighter software, where colocalizing pixels are depicted as white (Panel A and B, images c and d, respectively). For completeness, GFP-tagged *M.smegmatis* was represented as a single 8-bit black and white image (Panel B, c), however, GFP-tagged *M.smegmatis* was omitted from the combined colocalization overlay image (Panel B, e).

A

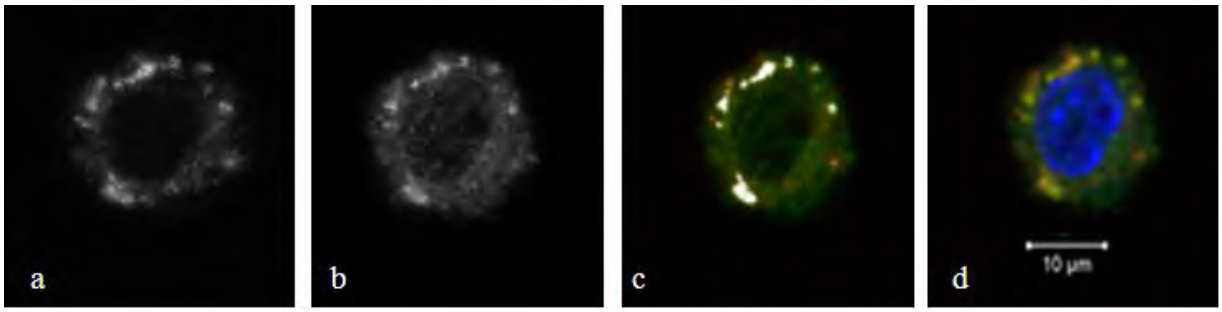

B

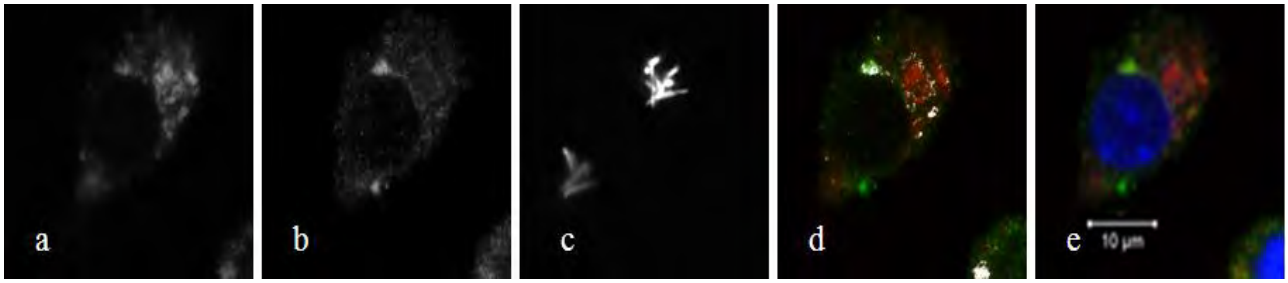

Figure 4.4: Uninfected- (A) and infected J774 macrophages (B) immunolabelled for LAMP-2 and cathepsin D.

Uninfected- (A) and GFP-tagged *M.smegmatis* infected cells (B) were immunolabelled with rat anti-mouse LAMP-2 [1:2000] (Panel A and B, a) and chicken anti-human cathepsin D [10 µg/ml] (Panel A and B, b) and labelling detected with donkey anti-rat CY5 [0.3 µg/ml] and donkey anti-chicken CY3 [0.5 µg/ml], respectively, after overnight growth on coverslips and infection (of one set of coverslips) with GFP-tagged *M.smegmatis* (5 h), followed by fixation with 3.7% (m/v) PFA and permeablization with 0.1% (m/v) saponin in PBS. Images representing LAMP-2 (Panel A and B, a), cathepsin D (Panel A and B, b) and GFP-tagged *M.smegmatis* (Panel B, c) were converted from RGB (Red Green Blue) to single images (only one channel displayed) and thereafter to 8-bit black and white images for simplicity of representation as colocalization can only use the red and green channels. Colocalization of LAMP-2 (red) and cathepsin D (false green), together with labelling of the nucleus with Hoechst (blue) (Panel A and B, d and e, respectively) is shown by combining images in three channels (Panel A and B, d and e, respectively). As colocalization (usually shown as yellow) is difficult to visualize (as is evident) (Panel A and B, d and e, respectively), images were also analyzed using Image J colocalization highlighter software, where colocalizing pixels are depicted as white (Panel A and B, images c and d, respectively). For completeness, GFP-tagged *M.smegmatis* was represented as a single 8-bit black and white image (Panel B, c), however, GFP-tagged *M.smegmatis* was omitted from the combined colocalization overlay image (Panel B, e).

Using the classical red-green overlay method of colocalization, there appears to be a greater amount of colocalization between cathepsin D and LAMP-1 (Figure 4.3 Panel **A**, d and Panel **B**, e), and cathepsin D and LAMP-2 (Figure 4.4 Panel **A**, d and Panel **B**, e) in uninfected cells than in infected cells. This was also observed using ImageJ‟s

colocalization highlighter tool (Figure 4.3, Panel **A**, c and Panel **B,** d) and (Figure 4.4, Panel **A**,c and Panel **B,**d), respectively. There also, however, appears to be less cathepsin D in infected cells generally (Figure 4.3, Pranel **A**, b and **B**, b) and (Figure 4.4, Pranel **A**, b and **B**, b) and this may suggest that cathepsin D is secreted out of the cell during infection. This, however, needs to be confirmed by western blot analysis.

Colocalization analysis calculated using the JACoP plugin confirms the greater amount of colocalization between cathepsin D and LAMP-1 in uninfected cells than in infected cells (Table 4.1). Pearson‟s and Manders‟ Overlap coefficients for uninfected cells for colocalization of cathepsin D with LAMP-1 (Table 4.1, 0.84 and 0.85, respectively) and cathepsin D with LAMP-2 (Table 4.1, 0.76 and 0.78, respectively) were higher than for cathepsin D and LAMP-1 in (Table 4.1, 0.69 and 0.75, respectively) and cathepsin D and LAMP-2 in infected cells (Table 4.1, 0.64 and 0.7, respectively) thus confirming a greater colocalization in both cases in uninfected cells. Both coefficients for both cases in infected and uninfected cells were within the range that indicates colocalization (namely 0.5-1 for Pearson‟s coefficient, and 0.6-1 for Manders‟ Overlap coefficient).

Differences in overlap coefficients k_1 and k_2 for cathepsin D with LAMP-1 in infected and uninfected cells (0.22 and 0.05, respectively) and cathepsin D with LAMP-2 for infected and uninfected cells (0.24 and 0.22, respectively) were relatively small also validating colocalization. The difference between k_1 and k_2 for cathepsin D with LAMP-1 and cathepsin D with LAMP-2 was smaller for uninfected cells than for infected cells, indicating a greater degree of colocalization in both cases for uninfected cells as compared to infected cells.

The values for M_1 and M_2 for cathepsin D with LAMP-1 (Table 4.1, 0.65 and 0.94, respectively) and cathepsin D with LAMP-2 in uninfected cells (Table 4.1, 0.74 and 0.59, respectively) are higher than that of cathepsin D with LAMP-1 (Table 4.1, 0.51 and 0.64, respectively) and cathepsin D with LAMP-2 in infected cells (Table 4.1, 0.52 and 0.58, respectively) thus also indicating a greater degree of colocalization in both cases in uninfected cells. The values for M_1 and M_2 in both cases were greater than 0.5, also indicating colocalization. Using the Costes‟ analysis approach, a P-value of 100% (Table 4.1) was calculated for both cathepsin D with LAMP-1 and cathepsin D with

LAMP-2 in infected and uninfected cells suggesting that the calculated Pearson‟s coefficient is highly probable and not due to random overlap.

The ICQ values calculated for cathepsin D with LAMP-1 for infected and uninfected cells (Table 4.1, 0.39 and 0.43, respectively) and cathepsin D with LAMP-2 for infected and uninfected cells (Table 4.1, 0.42 and 0.46, respectively) are positive, and much greater than 0, indicating colocalization in both cases, (Bolte and Cordelières, 2006; Li *et al*., 2004). In both cases, the ICQ value for uninfected cells is greater than that calculated for infected cells further suggesting a greater degree of colocalization for cathepsin D and LAMP-1 and cathepsin D and LAMP-2 in uninfected cells.

From the analyzed colocalization data, it can be established that cathepsin D colocalizes with LAMP-1 and -2 positive vesicles in both uninfected and infected cells, but there is a greater degree of colocalization in uninfected J774 cells. This may suggest that upon infection, cathepsin D is released from LAMP-1 and -2 positive vesicles. The smaller degree of colocalization of cathepsin D with LAMP-1 in infected cells as compared to uninfected cells could also be explained by the observation made by Anes *et al*. (2006) that indicated that LAMP-1 is recycled out of phagosomes containing live but not dead *M.smegmatis*. The difference in the degree of colocalization between LAMP-1 and cathepsin D in infected and uninfected cells is relatively small. This may be due to only a few mycobacteria being taken up by each cell, thus only a few vesicles would contain live or killed bacteria. Therefore, if this is so, recycling of LAMP-1 out of phagosomes containing live *M.smegmatis* would result in the recycling of LAMP-1 from a few phagosomes.

The colocalization analyses of cathepsin D with LAMP-1 and LAMP-2 in infected and uninfected cells are similar and this may suggest that LAMP-1 and -2 may label similar endosomal or “lysosomal” compartments.

A

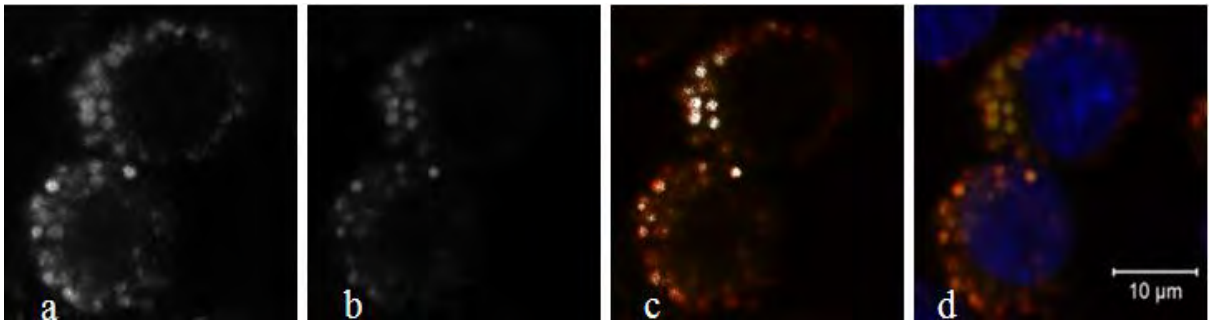

B

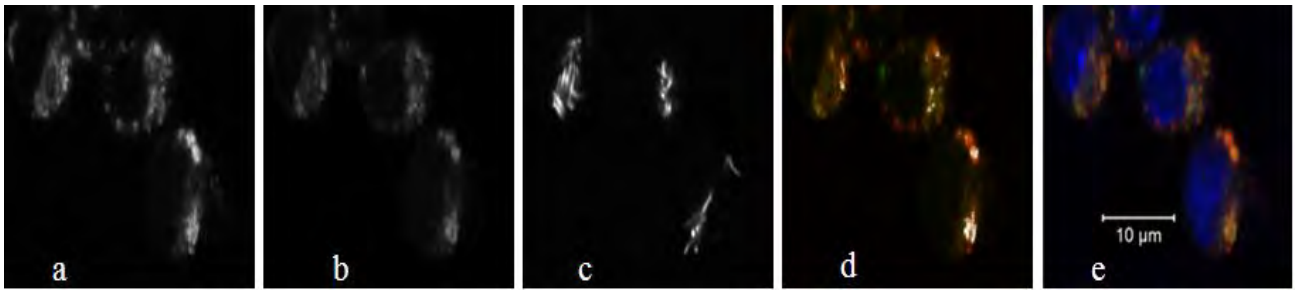

Figure 4.5: Uninfected- (A) and infected J774 macrophages (B) immunolabelled for LAMP-1 and LysoTracker.

Uninfected- (A) and GFP-tagged *M.smegmatis* infected cells (B) were immunolabelled with rat anti-mouse LAMP-1 [1:2000], detected with donkey anti-rat CY5 [0.3 µg/ml] (Panel A and B, a), and LysoTracker working solution (150 µl, 2 nM) (Panel A and B, b), after overnight growth on coverslips and infection (of one set of coverslips) with GFP-tagged *M.smegmatis* (5 h), followed by fixation with 3.7% (m/v) PFA and permeablization with 0.1% (m/v) saponin in PBS. Images representing LAMP-1 (Panel A and B, a), LysoTracker (Panel A and B, b) and GFP-tagged *M.smegmatis* (image c, Panel B) were converted from RGB (Red Green Blue) to single images (only one channel displayed) and thereafter to 8-bit black and white images for simplicity of representation as colocalization can only use the red and green channels. Colocalization of LAMP-1 (red) and LysoTracker (false green), together with labelling of the nucleus with Hoechst (blue) (Panel A and B, d and e, respectively) is shown by combining images in three channels (Panel A and B, d and e, respectively). As colocalization (usually shown as yellow) is difficult to visualize (as is evident) (Panel A and B, d and e, respectively), images were also analyzed using Image J colocalization highlighter software, where colocalizing pixels are depicted as white (Panel A and B, images c and d, respectively). For completeness, GFP-tagged *M.smegmatis* was represented as a single 8-bit black and white image (Panel B, c), however, GFP-tagged *M.smegmatis* was omitted from the combined colocalization overlay image (Panel B, e).

A

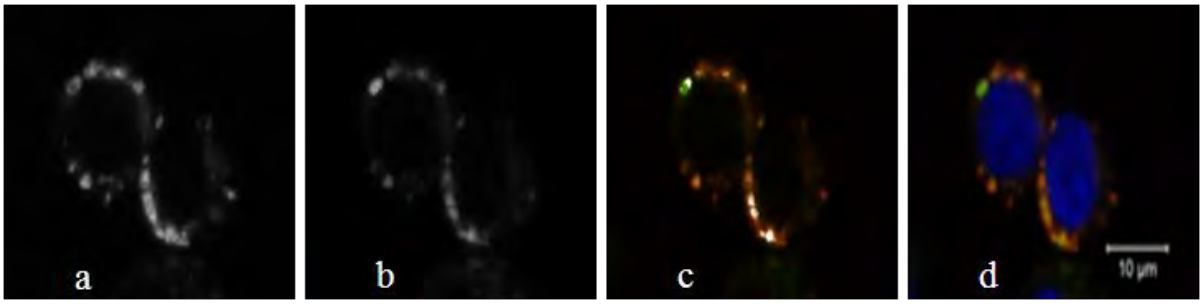

B

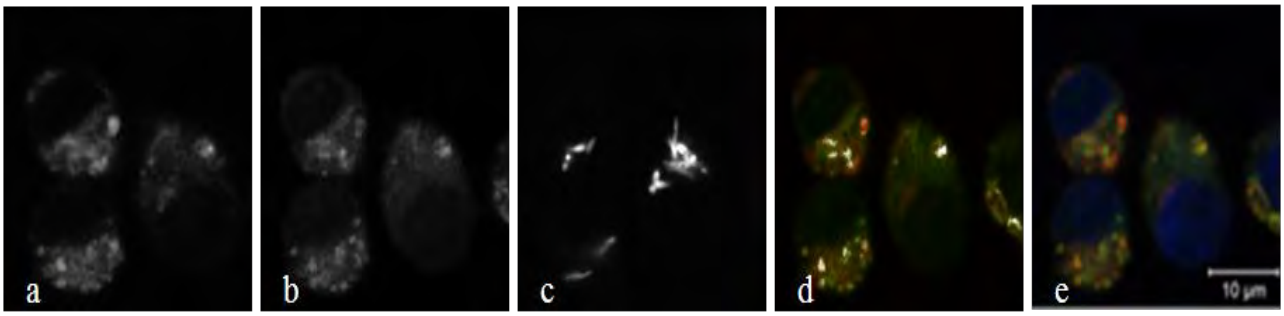

Figure 4.6: Uninfected- (A) and infected J774 macrophages (B) immunolabelled for LAMP-2 and LysoTracker.

Uninfected- (A) and GFP-tagged *M.smegmatis* infected cells (B) were immunolabelled with rat anti-mouse LAMP-2 [1:2000], detected with donkey anti-rat CY5 [0.3 µg/ml] (Panel A and B, a), and LysoTracker working solution (150 µl, 2 nM) (Panel A and B, b), after overnight growth on coverslips and infection (of one set of coverslips) with GFP-tagged *M.smegmatis* (5 h), followed by fixation with 3.7% (m/v) PFA and permeablization with 0.1% (m/v) saponin in PBS. Images representing LAMP-2 (Panel A and B, a), LysoTracker (Panel A and B, b) and GFP-tagged *M.smegmatis* (Panel B, c) were converted from RGB (Red Green Blue) to single images (only one channel displayed) and thereafter to 8-bit black and white images for simplicity of representation as colocalization can only use the red and green channels. Colocalization of LAMP-2 (red) and LysoTracker (false green), together with labelling of the nucleus with Hoechst (blue) (Panel A and B, d and e, respectively) is shown by combining images in three channels (Panel A and B, d and e, respectively). As colocalization (usually shown as yellow) is difficult to visualize (as is evident) (Panel A and B, d and e, respectively), images were also analyzed using Image J colocalization highlighter software, where colocalizing pixels are depicted as white (Panel A and B, images c and d, respectively). For completeness, GFP-tagged *M.smegmatis* was represented as a single 8-bit black and white image (Panel B, c), however, GFP-tagged *M.smegmatis* was ommitted from the combined colocalization overlay image (Panel B, e).

The classical Red-green overlay method of colocalization representation did not clearly show the difference in colocalization between LAMP-1 and LysoTracker and LAMP-2 and LysoTracker in infected and uninfected cells, (Figure 4.5, Panel **A**, d and Panel **B**, e) and (Figure 4.6, Panel **A**, d and Panel **B**, e), respectively. Similarly, ImageJ‟s

colocalization highlighter tool was unable to show the difference in colocalization between LAMP-1 and LysoTracker (Figure 4.5 Panel **A**, c and Panel **B,** d) and between LAMP-2 and LysoTracker (Figure 4.6 Panel **A**, c and Panel **B,** d), in infected and uninfected cells. The colocalization analysis data generated for both cases using the JACoP plugin only showed a slight difference (Table 4.1).

Pearson‟s coefficient for LAMP-1 and LysoTracker was slightly higher in uninfected cells than in infected cells (0.82 and 0.79, respectively). This was similar to Manders‟ Overlap coefficient for uninfected and infected cells (0.87 and 0.86, respectively). The Pearson‟s coefficient for LAMP-2 and LysoTracker was slightly higher in infected cells than in uninfected cells (0.8 and 0.79, respectively) while Manders‟ Overlap coefficient was higher for uninfected cells as compared to infected cells (0.91 and 0.9, respectively). The Pearson‟s and Manders‟ Overlap coefficients for LAMP-1 and -2 with LysoTracker in both infected and uninfected cells were within the range that indicates valid colocalization i.e. 0.5-1 for Pearson‟s coefficient and 0.6-1 for Manders‟ Overlap coefficients.

Differences in Overlap coefficient values, k_1 and k_2 for LAMP-1 and LysoTracker in infected and uninfected cells (calculated from Table 4.1, 0.2 and 0.16, respectively) and LAMP-2 and LysoTracker in infected and uninfected cells (0.1 and 0.12, respectively) were small indicating colocalization in both cases. The difference between k_1 and k_2 for LAMP-1 and LysoTracker was slightly higher for infected cells while the difference between these values for LAMP-2 and LysoTracker was slightly higher in uninfected cells.

The values for M_1 and M_2 for LAMP-1 and LysoTracker for infected cells (Table 4.1, 0.52 and 0.61, respectively) were lower than that of uninfected cells (Table 4.1, 0.62 and 0.71, respectively), while for LAMP-2 and LysoTracker, the value for M_1 for infected cells (Table 4.1, 0.81) was higher than for uninfected cells (Table 4.1, 0.72), while the value for M_2 in both cases was the same. For both LysoTracker with LAMP-1 and LAMP-2, in infected and uninfected cells, the M_1 and M_2 values were higher than 0.5, indicating colocalization.

Using the Costes‟ analysis approach, a P-value of 100% was calculated (Table 4.1) for both LysoTracker with LAMP-1 and LysoTracker with LAMP-2 in infected and uninfected cells suggesting that the calculated Pearson‟s coefficient is highly probable and not due to random overlap. The ICQ values for LysoTracker with LAMP-1 for infected cells (Table 4.1, 0.36) was lower than for uninfected cells (Table 4.1, 0.38), while in the case of LysoTracker with LAMP-2, this value was the same for infected and uninfected cells (Table 4.1, 0.35). The ICQ values for LysoTracker with LAMP-1 and -2 for infected and uninfected cells were positive and much greater than 0, indicating colocalization.

From the colocalization analysis data, it may be suggested that there is a slightly greater degree of colocalization between LAMP-1 and LysoTracker in uninfected cells as compared to infected cells. This difference in colocalization may be due to the recycling of LAMP-1 out of phagosomes containing live *M.smegmatis* as described by Anes *et al*. (2006) and may also imply that acidic vesicles that colocalize with LAMP-1 would be more likely to contain dead *M.smegmatis*.

However, using the data generated, it is unclear whether there is a greater degree of colocalization between LysoTracker and LAMP-2 in infected or in uninfected cells.

The colocalization analysis data suggests that LAMP-1 and -2 may label similar endosomal or “lysosomal” compartments as both markers have been observed to colocalize with acidic vesicles in both infected and uninfected cells.

Table 4.1: Colocalization analysis in infected and uninfected cells using intensity correlation coefficient-based tools with significant values/ ranges indicating colocalization in brackets.

	Pearson's Coefficient (values between 0.5 and 1)		Manders' Overlap Coefficient (values between 0.6 and 1)		Overlap coefficient expressed as two parameters (values that are close to each other, e.g. 0.5 and 0.6)				M_1 (values > 0.5)		M_2 (values > 0.5)		Costes' analysis approach P-value		ICQ 0 < ICQ values < 0.5		Colocalization present	
					k_1	k_2	k_1	k_2										
	I	U	I	U	I	I	U	U	I	U	I	U	I	U	I	U	I	U
Cathepsin D and Lysotracker	0.86	0.73	0.88	0.77	0.85	0.9	0.99	0.88	0.51	0.5	0.77	0.6	100%	100%	0.44	0.4	Yes	Yes
Cathepsin D and LAMP-1	0.69	0.84	0.75	0.85	0.6	0.82	0.55	0.6	0.51	0.65	0.64	0.94	100%	100%	0.39	0.43	Yes	Yes
Cathepsin D and LAMP-2	0.64	0.76	0.7	0.78	0.67	0.91	0.9	0.68	0.52	0.74	0.58	0.59	100%	100%	0.42	0.46	Yes	Yes
LAMP-1 and Lysotracker	0.79	0.82	0.86	0.87	0.63	0.83	0.68	0.84	0.52	0.62	0.61	0.71	100%	100%	0.36	0.38	Yes	Yes
LAMP-2 and Lysotracker	0.8	0.79	0.9	0.91	0.8	0.9	0.93	0.81	0.81	0.72	0.7	0.7	100%	100%	0.35	0.35	Yes	Yes

- I= *M.smegmatis*-infected J774 macrophages
- U= Uninfected macrophages
- Colocalization data presented represent the average values calculated for six images.
- ICQ = Intensity correlation quotient
- Costes" analysis approach P-value > 95% indicates that the Pearson"s coefficient is true and not due to random overlap.
- Threshold setting: Red channel = 40
  Green channel =55

A

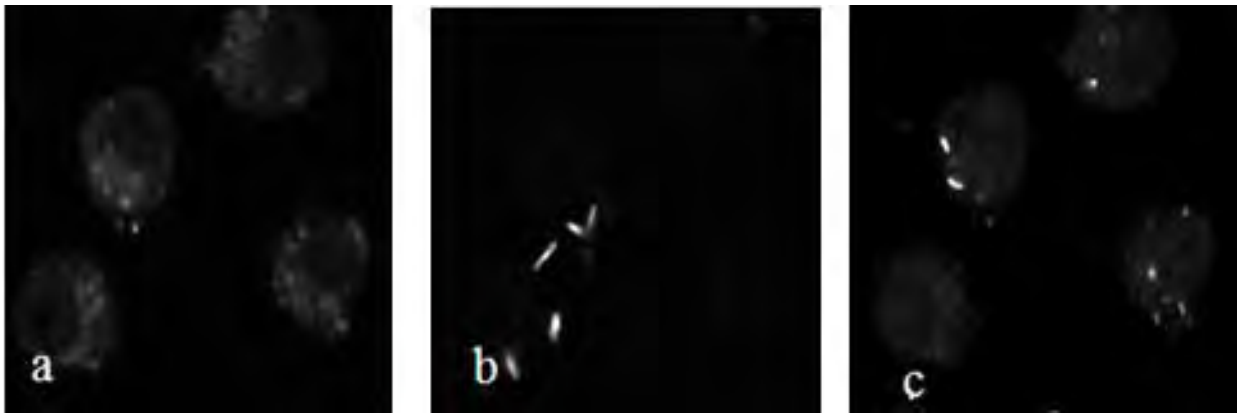

B

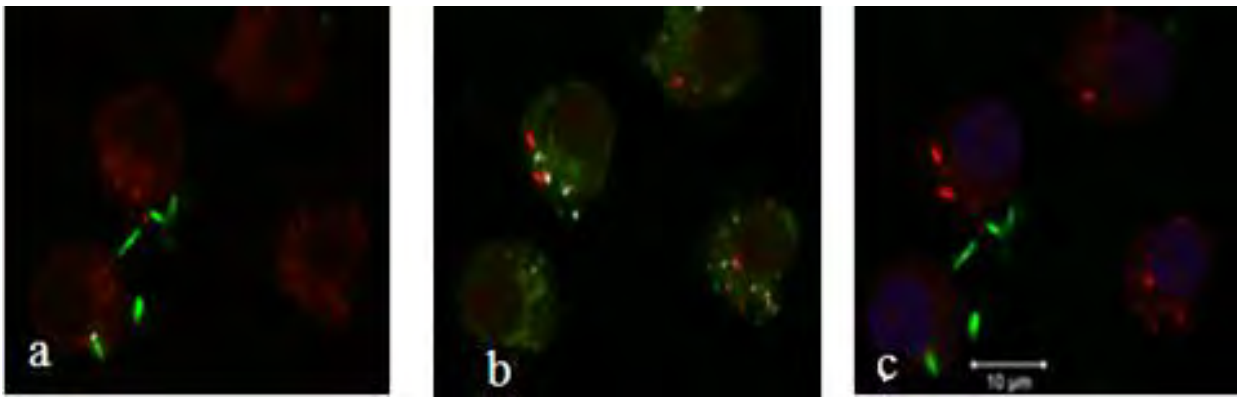

Figure 4.7: Immunofluorescent labelling of cathepsin D and propidium iodide in GFP expressing *M.smegmatis* infected J774 macrophages.

GFP-tagged *M.smegmatis* infected cells were immunolabelled with chicken anti-human cathepsin D [10 µg/ml], detected with donkey anti-chicken CY5 [0.5 g/ml] (Panel A, a) after overnight growth on coverslips and infection with GFP-tagged *M.smegmatis* (5 h), followed by fixation with 3.7% (m/v) PFA and permeablization with 0.1% (m/v) saponin in PBS. Cells were thereafter stained with propidium iodide so that dead GFP-tagged *M.smegmatis* could be visualised (Panel A, c). Images representing cathepsin D (Panel A, a), live GFP-tagged *M.smegmatis* (Panel A, b) and dead GFP-tagged *M.smegmatis* stained with propidium iodide (Panel A, c) were converted from RGB (Red Green Blue) to single images (only one channel displayed) and thereafter to 8-bit black and white images for simplicity of representation as colocalization can only use the red and green channels. ImageJ"s colocalization highlighter tool was used to display points of colocalization (displayed in white) between cathepsin D and live GFP-tagged *M.smegmatis* (Panel B, a) and cathepsin D and propidium iodide stained dead *M.smegmatis* (Panel B, b). For visualization purposes, cathepsin D was assigned a red colour to distinguish this antigen from GFP-tagged *M.smegmatis* which was assigned a green colour (Panel B, a). Similarly, cathepsin D was assigned a green colour to distinguish this antigen from dead *M.smegmatis* that was stained with propidium iodide and which was assigned a red colour (Panel B, b). This was necessary because at present, colocalization can only be conducted with two different colours representing two different fluorophores. The nucleus which was labelled with Hoechst, live GFP-tagged *M.smegmatis* and dead GFP-tagged *M.smegmatis* which was stained with propidium iodide were displayed in one image (Panel B, c) for purposes of distinguishing live from dead *M.smegmatis* in a single image.

A

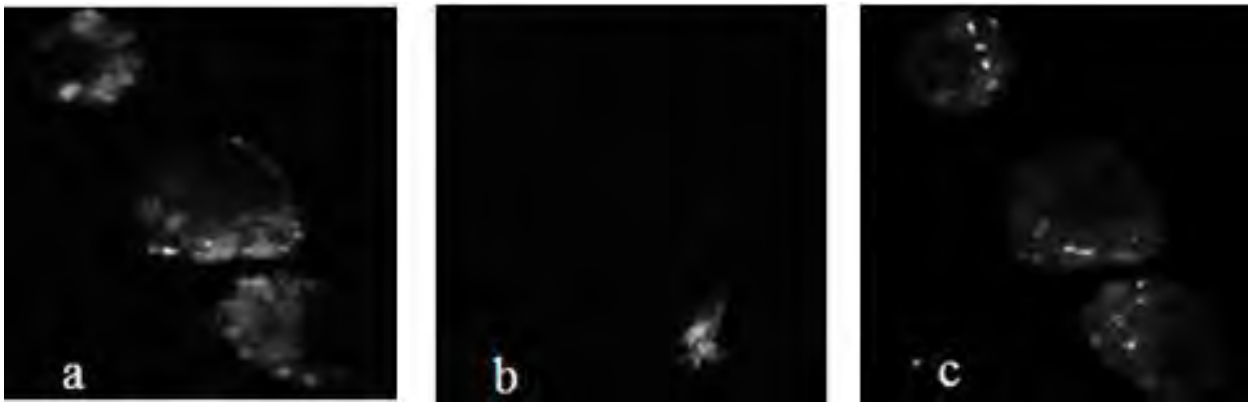

B

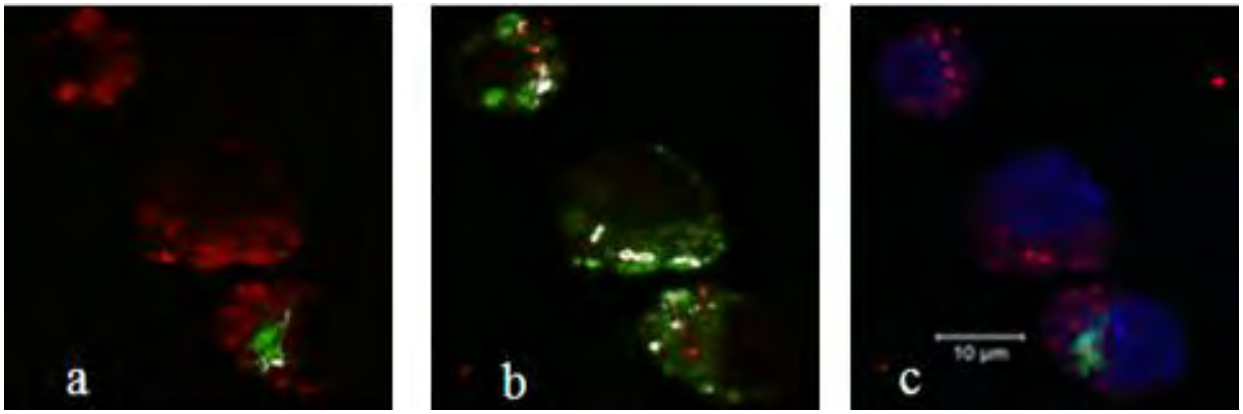

Figure 4.8: Immunofluorescent labelling of LAMP-1 in GFP expressing *M.smegmatis* infected J774 macrophages.

GFP-tagged *M.smegmatis* infected cells were immunolabelled with chicken rat anti-mouse LAMP-1 [1:2000], detected, with donkey anti-rat CY5 [0.3 µg/ml] (Panel A, a) after overnight growth on coverslips and infection with GFP-tagged *M.smegmatis* (5 h), followed by fixation with 3.7% (m/v) PFA and permeablization with 0.1% (m/v) saponin in PBS. Cells were thereafter stained with propidium iodide so that dead GFP-tagged *M.smegmatis* could be visualised (Panel A, c). Images representing LAMP-1 (Panel A, a), live GFP-tagged *M.smegmatis* (Panel A, b) and dead GFP-tagged *M.smegmatis* stained with propidium iodide (Panel A, c) were converted from RGB (Red Green Blue) to single images (only one channel displayed) and thereafter to 8-bit black and white images for simplicity of representation as colocalization can only use the red and green channels. ImageJ˝s colocalization highlighter tool was used to display points of colocalization (displayed in white) between LAMP-1 and live GFP-tagged *M.smegmatis* (Panel B, a) and LAMP-1 and propidium iodide stained dead *M.smegmatis* (Panel B, b). For visualization purposes, LAMP-1 was assigned a red colour to distinguish this antigen from GFP-tagged *M.smegmatis* which was assigned a green colour (Panel B, a). Similarly, LAMP-1 was assigned a green colour to distinguish this antigen from dead *M.smegmatis* that was stained with propidium iodide and which was assigned a red colour (Panel B, b). This was necessary because at present, colocalization can only be conducted with two different colours representing two different fluorophores. The nucleus which was labelled with Hoechst, live GFP-tagged *M.smegmatis* and dead GFP-tagged *M.smegmatis* which was stained with propidium iodide were displayed in one image (Panel B, c) for purposes of distinguishing live from dead *M.smegmatis* in a single image.

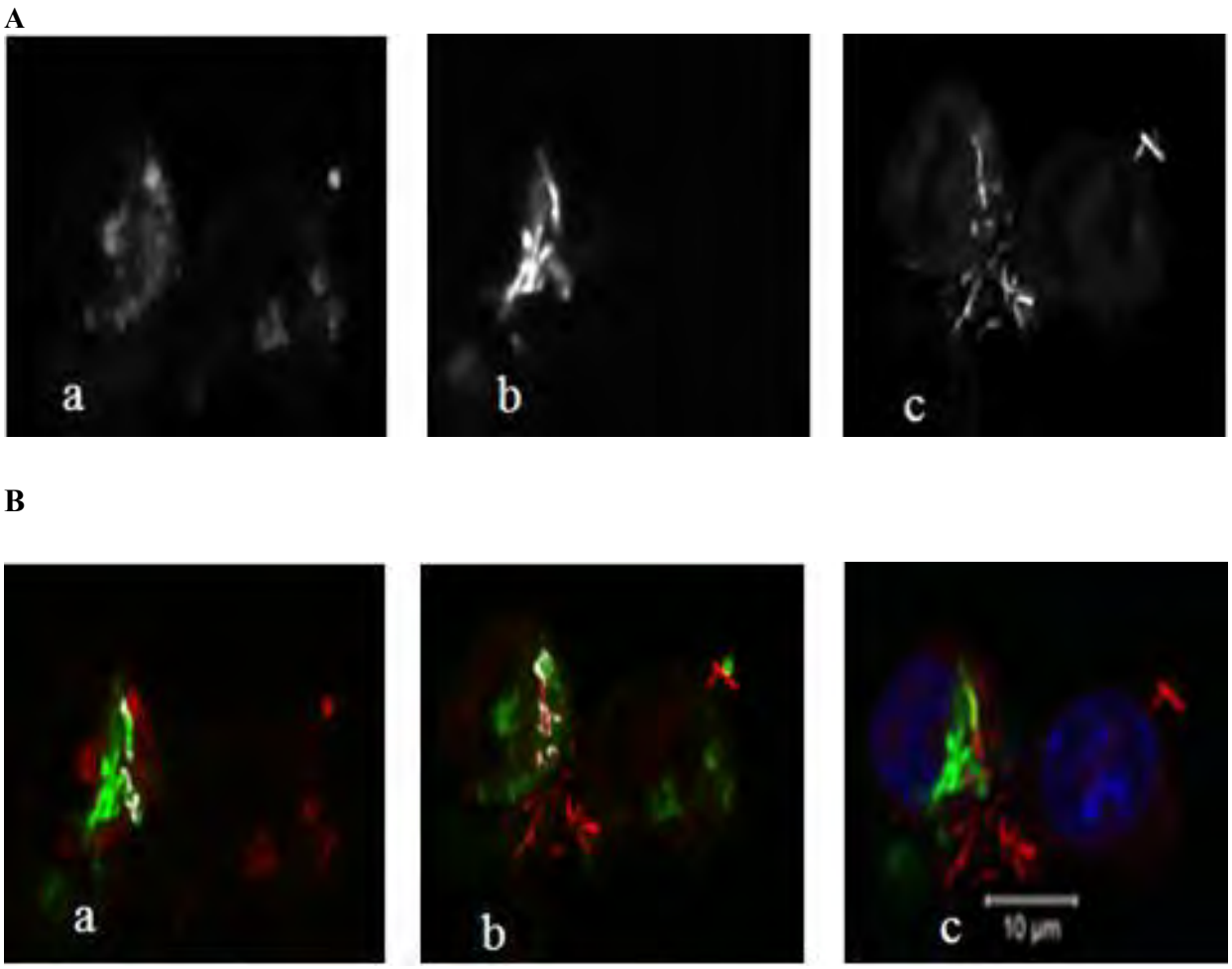

Figure 4.9: Immunofluorescent labelling of LAMP-2 and propidium iodide in GFP expressing *M.smegmatis* infected J774 macrophages.

GFP-tagged *M.smegmatis* infected cells were immunolabelled with chicken rat anti-mouse LAMP-2 [1:2000], detected, with donkey anti-rat CY5 [0.3 µg/ml] (Panel A, a) after overnight growth on coverslips and infection with GFP-tagged *M.smegmatis* (5 h), followed by fixation with 3.7% (m/v) PFA and permeablization with 0.1% (m/v) saponin in PBS. Cells were thereafter stained with propidium iodide so that dead GFP-tagged *M.smegmatis* could be visualised (Panel A, c). Images representing LAMP-2 (Panel A, a), live GFP-tagged *M.smegmatis* (Panel A, b) and dead GFP-tagged *M.smegmatis* stained with propidium iodide (Panel A, c) were converted from RGB (Red Green Blue) to single images (only one channel displayed) and thereafter to 8-bit black and white images for simplicity of representation as colocalization can only use the red and green channels. ImageJ"s colocalization highlighter tool was used to display points of colocalization (displayed in white) between LAMP-2 and live GFP-tagged *M.smegmatis* (Panel B, a) and LAMP-2 and propidium iodide stained dead *M.smegmatis* (Panel B, b). For visualization purposes, LAMP-2 was assigned a red colour to distinguish this antigen from GFP-tagged *M.smegmatis* which was assigned a green colour (Panel B, a). Similarly, LAMP-2 was assigned a green colour to distinguish this antigen from dead *M.smegmatis* that was stained with propidium iodide and which was assigned a red colour (Panel B, b). This was necessary because at present, colocalization can only be conducted with two different colours representing two different fluorophores. The nucleus which was labelled with Hoechst, live GFP-tagged *M.smegmatis* and dead GFP-tagged *M.smegmatis* which was stained with propidium iodide were displayed in one image (Panel B, c) for purposes of distinguishing live from dead *M.smegmatis* in a single image.

The colocalization images of cathepsin D, live GFP-tagged- and propidium iodide labelled *M.smegmatis* were converted to single 8-bit black and white images for colocalization analysis (Figure 4.7, Panel **A**, a, b, c, respectively). As colocalization analysis can only be conducted using two colours, cathepsin D, assigned a red colour and live GFP-tagged *M.smegmatis*, assigned a green colour allowed colocalization analysis using ImageJ‟s colocalization highlighter tool to be conducted (Figure 4.7, Panel **B**, a) and subsequently cathepsin D was assigned a green colour so that the association between cathepsin D and propidium iodide labelled *M.smegmatis* (dead *M.smegmatis*), assigned a red colour could be visualized in the same way (Figure 4.7, Panel **B**, b). From the images generated by ImageJ‟s colocalization highlighter tool for cathepsin D with live- and propidium iodide-labelled *M.smegmatis* (Figure 4.7, Panel **B**, a and b, respectively), it was observed that there was very low/ almost no colocalization between cathepsin D and live (GFP fluorescent) and dead (propidium iodide labelled) *M.smegmatis*. Though there is slightly greater colocalization between cathepsin D and propidium iodide-labelled *M.smegmatis* (Figure 4.7, Panel **B**, b) than live *M.smegmatis*. Live and dead *M.smegmatis* single images of GFP fluorescence (live *M.smegmatis*) and propidium iodide fluorescence (dead *M.smegmatis*) allow assessment of signal overlap between the live and dead mycobacteria signals (Figure 4.7, Panel **B**, c) and from these images, it was observed that the green fluorescence (live GFP-tagged *M.smegmatis*) and red fluorescence (dead GFP-tagged *M.smegmatis*) did not overlap (Figure 4.7, Panel **B**, c) so live GFP-tagged *M.smegmatis* did not take up propidium iodide and the reverse was true i.e. *M.smegmatis* that did not emit a green fluorescence were labelled using propidium iodide (Figure 4.7, Panel **B**, c). This seems to indicate that the detection of GFP fluorescence may be used to locate live *M.smegmatis* and propidium iodide labelling may be used to detect dead mycobacteria reliably.

Colocalization data generated using the JACoP plugin, however, indicated that there was no valid colocalization between cathepsin D, and live or dead *M.smegmatis*. The Pearson‟s and Manders‟ Overlap coefficients for the colocalization of cathepsin D with live (Table 4.2, 0.094 and 0.28, respectively) and dead *M.smegmatis* (Table 4.2, 0.36 and 0.42, respectively) were not within the ranges that indicate colocalization, namely 0.5-1 for Pearson‟s coefficient and 0.6-1 for Manders‟ Overlap coefficient. Furthermore,

the differences between the k_1 and k_2 values for both colocalization analyses (as calculated from Table 4.2) were large i.e. 0.46 for cathepsin D with live *M.smegmatis* and 0.36 for cathepsin D with dead *M.smegmatis*, not supporting valid colocalization but indicating an absence of colocalization. The values for M_1 and M_2 for both colocalization analyses were lower than 0.5, also indicating an absence of colocalization.

A P-value of 100% was calculated using the Costes‟ analysis approach, indicating that the calculated Pearson‟s coefficient is highly probable and not due to random overlap.

The ICQ values calculated for both colocalization analyses (Table 4.2) were positive and much greater than 0 indicating colocalization. This observation does not correlate with the other values that were calculated using the JACoP plugin which largely indicated a lack of colocalization, though slight colocalization is visible both between cathepsin D and live *M.smegmatis* (Figure 4.7, Panel **B**, a) and cathepsin D and dead *M.smegmatis* (Figure 4.7, Panel **B**, b). The presence of colocalization visually as well as the ICQ colocalization data seem to suggest that ICQ values are much more compatible with a low level of colocalization, whereas, perhaps due to the low infection/ dose of *M.smegmatis* in J774 cells, the other assessment parameters are not suitable. This is similar to the observation made in a study conducted by Fuller *et al*. (2008) in which the low concentration of bacteria in cells was believed to impact on colocalization calculations between the bacteria and LAMP-1.

Similar results were obtained for the colocalization analysis of LAMP-1 and -2 with live and dead *M.smegmatis*. The colocalization images of LAMP-1 (Figure 4.8, Panel **A**, a) and LAMP-2 (Figure 4.9, Panel **A**, a) live GFP-tagged *M.smegmatis* (Figure 4.8 and 4.9, Panel **A**, b) and propidium iodide labelled organisms (Figure 4.8 and 4.9, Panel **A**, c) were converted to single 8-bit black and white images for colocalization analysis. As in the case with cathepsin D, LAMP-1 and -2 were assigned a red colour and live GFP-tagged *M.smegmatis* assigned a green colour allowing for colocalization analysis using ImageJ‟s colocalization highlighter tool to be conducted (Figure 4.8, Panel **B**, a) and (Figure 4.9, Panel **B**, a), respectively. Subsequently, LAMP-1 and -2 were assigned a green colour so that the association between LAMP-1 and -2 and propidium iodide

stained mycobacteria could also be detected (Figure 4.8, Panel **B**, b) and (Figure 4.9, Panel **B**, b), respectively. As was the case with cathepsin D (Figure 4.7 Panel **B**, a and b) the images generated by ImageJ‟s colocalization highlighter tool for LAMP-1 and -2 with live GFP-tagged *M.smegmatis* and propidium iodide stained mycobacteria (Figure 4.8 Panel **B**, a and b, respectively) and (Figure 4.9 Panel **B**, a and b, respectively), showed very low/ but visible colocalization between LAMP-1 and -2 with live GFP-tagged *M.smegmatis* and propidium iodide stained mycobacteria.

The images in which the fluorescence signals from live GFP-tagged *M.smegmatis* and propidium iodide stained mycobacteria are contained within a single image (Figure 4.8 and Figure 4.9, Panel **B**, c) show that live GFP-tagged *M.smegmatis* did not take up the propidium iodide stain while the mycobacteria that were stained with propidium iodide did not emit a green fluorescence once again indicating that GFP fluorescence may be used to visualize live bacteria and that propidium iodide uptake by mycobacteria may be used to detect dead *M.smegmatis*.

As with cathepsin D, the data generated using the JACoP plugin indicated that there was no valid colocalization between LAMP-1 and -2 with live GFP-tagged *M.smegmatis* and propidium iodide stained/ dead *M.smegmatis*. The Pearson‟s and Manders‟ Overlap coefficients for LAMP-1 with live GFP-fluorescent *M.smegmatis* (Table 4.2, 0.2 and 0.35, respectively) and propidium iodide stained *M.smegmatis* (Table 4.2, 0.39 and 0.54, respectively) and LAMP-2 with live GFP-tagged *M.smegmatis* (Table 4.2, 0.42 and 0.58, respectively) and propidium iodide stained *M.smegmatis* (Table 4.2, 0.43 and 0.56, respectively) were all below the ranges that are considered for valid colocalization i.e. 0.5-1 for Pearson‟s coefficient and 0.6-1 for Manders‟ Overlap coefficients. Also, the differences between k_1 and k_2 for LAMP-1 with live GFP-tagged *M.smegmatis* and propidium iodide stained *M.smegmatis* (Table 4.2, 0.38 and 0.27, respectively) and LAMP-2 with live GFP-tagged *M.smegmatis* and propidium iodide stained *M.smegmatis* (Table 4.2, 0.43 and 0.32, respectively) were large and not indicative of colocalization. The values for M_1 and M_2 for LAMP-1 with live GFP-tagged *M.smegmatis* (Table 4.2, 0.052 and 0.36, respectively) and propidium iodide stained *M.smegmatis* (Table 4.2, 0.17 and 0.38, respectively) and LAMP-2 with live GFP-tagged *M.smegmatis* (Table 4.2, 0.2 and 0.32, respectively) and propidium iodide

stained *M.smegmatis* (Table 4.2, 0.19 and 0.33, respectively) were lower than 0.5 which also indicates an absence of colocalization.

The P-values (calculated using Coste‟s analysis approach) of 100% for both LAMP-1 and -2 with live GFP-tagged *M.smegmatis* and propidium iodide stained *M.smegmatis* indicated that the Pearson‟s coefficients that were calculated was not due to random overlap. The calculated ICQ values were positive and much greater than 0, indicating colocalization. This, once again, does not correlate with the other colocalization values generated using the JACoP plugin (Table 4.2) and is similar to the colocalization of cathepsin D with live GFP-tagged *M.smegmatis* and propidium iodide stained *M.smegmatis*.

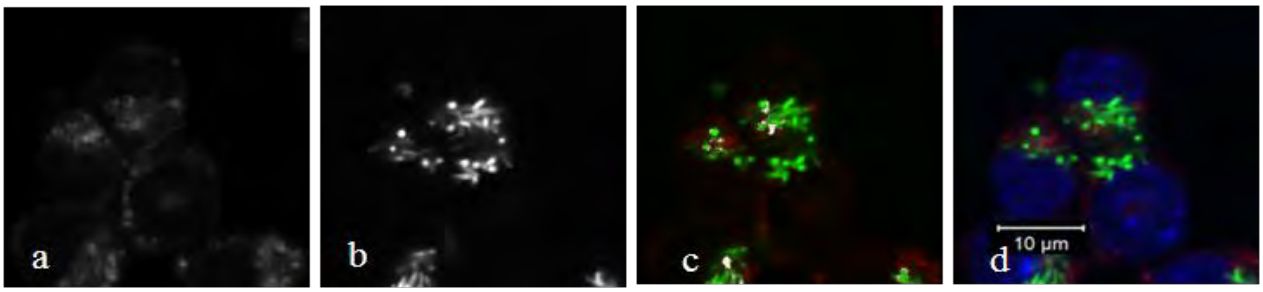

Figure 4.10: Immunofluorescent labelling of LysoTracker in GFP expressing *M.smegmatis* infected J774 macrophages.

GFP-tagged *M.smegmatis* infected cells were labelled with LysoTracker working solution (150 µl, 2 nM) (a) after overnight growth on coverslips and infection with GFP-tagged *M.smegmatis* (5 h), followed by fixation with 3.7% (m/v) PFA and permeablization with 0.1% (m/v) saponin in PBS. Images representing LysoTracker (a) and GFP-tagged *M.smegmatis* (b) were converted from RGB (Red Green Blue) to 8-bit black and white images for simplicity of representation. Colocalization of LysoTracker and GFP-tagged *M.smegmatis* together with labelling of the nucleus with Hoechst (blue) (d) is shown by combining images in three channels. As colocalization (usually shown as yellow) is difficult to render visible (as is evident), images were also analyzed using Image J colocalization highlighter software, where colocalizing pixels are depicted as white (c).

GFP, LysoTracker Red DND-99 and propidium iodide fluorophores cannot be simultaneously distinguished using confocal detection systems as LysoTracker Red DND-99 and PI fluorophores have similar excitation and emission wavelengths i.e. excitation and emission wavelengths of propidium iodide are 536 and 617 nm, respectively, while that of LysoTracker Red DND-99 are 577 and 590 nm (Freundt *et al*., 2007; Vogt and Schmid-Schönbein, 2001).

For this reason only LysoTracker and GFP images were finally colocalized. LysoTracker Red DND-99 and GFP-tagged *M.smegmatis* images were converted to single 8-bit black and white images after colocalization analysis (Figure 4.10, a and b, respectively). The traditional overlay red-green method of colocalization representation (Figure 4.10, d) as well the colocalization image created using ImageJ‟s colocalization highlighter tool (Figure 4.10, c) indicated that very little/ almost no colocalization was present.

Most of the data generated using the JACoP plugin also indicated that there was little/ almost no colocalization present between LysoTracker and live GFP-tagged *M.smegmatis*. The Pearson‟s and Manders‟ Overlap coefficients (Table 4.2, 0.49 and 0.58, respectively) were below the ranges that are considered for valid colocalization i.e. 0.5-1 and 0.6-1 for Pearson‟s and Manders‟ Overlap coefficients, respectively. The difference between the k_1 and k_2 values (Table 4.2, 0.07) was relatively small which may be an indication of colocalization. The M_1 and M_2 values (Table 4.2, 0.34 and 0.39, respectively) were below 0.5, indicating an absence of colocalization. The P-value was 100% indicating that the Pearson‟s coefficient calculated was not based on random overlap. The ICQ value (Table 4.2, 0.3) was positive and much greater than 0, indicating colocalization. From the colocalization data generated using JACoP, it is unclear whether colocalization between LysoTracker and live GFP-tagged *M.smegmatis* occurred. Visually this appears to be extremely limited (Figure 4.10, c) as would be anticipated.

Table 4.2: Colocalization analysis in J774 cells containing live and dead *M.smegmatis* using intensity correlation coefficient-based tools with significant values/ ranges indicating colocalization in brackets.

	Pearson's Coefficient (values between 0.5 and 1)		Manders' Overlap Coefficient (values between 0.6 and 1)		Overlap coefficient expressed as two parameters (values that are close to each other, e.g. 0.5 and 0.6)				M_1 (values > 0.5)		M_2 (values > 0.5)		Costes' analysis approach P-value		ICQ 0 < ICQ values <0.5		Colocalization present	
					k_1	k_2	k_1	k_2										
	L	D	L	D	L	L	D	D	L	D	L	D	L	D	L	D	L	D
Cathepsin D	0.094	0.36	0.28	0.42	0.27	0.73	0.43	0.79	0.012	0.2	0.046	0.31	100%	100%	0.13	0.16	No	No
LAMP-1	0.2	0.39	0.35	0.54	0.23	0.61	0.718	0.45	0.052	0.17	0.36	0.38	100%	100%	0.01	0.28	No	No
LAMP-2	0.42	0.43	0.58	0.56	0.26	0.69	0.63	0.31	0.2	0.19	0.32	0.33	100%	100%	0.32	0.3	No	No
Lysotracker	0.49	ND	0.58	ND	0.3	0.23	ND	ND	0.34	ND	0.39	ND	100%	ND	0.3	ND	uncertain	ND

- L = Live *M.smegmatis* which were not stained by propidium iodide
- D =Dead *M.smegmatis* which were stained by propidium iodide
- ND= not determined
- Colocalization data presented represent the average values calculated for six images.
- ICQ = Intensity correlation quotient
- Costes" analysis approach P-value > 95% indicates that the Pearson"s coefficient is true and not due to random overlap.
- Threshold setting: Red channel = 40
  Green channel =55

4.4 *In vitro* microbicidal activity of cathepsin D

As colocalization analysis gave inconclusive results as to whether cathepsin D was present in phagosomes containing killed mycobacteria, it was decided to re-determine if cathepsin D does play a direct role in the killing of *M.smegmatis* via a more direct means. An *in vitro* microbicidal assay, involving the addition of porcine cathepsin D directly to the microorganism, was conducted. Prior to this experiment, the proteolytic activity of the available porcine cathepsin D to be used in the microbicidal assay was assessed to ensure its activity.

Protease activity is often determined by monitoring, spectrophotometrically or fluorometrically (depending on the substrate) the breakdown of a suitable substrate (Dennison, 2003c; Sarath *et al*., 1989). Two substrates which have been used by several researchers to measure cathepsin D activity are haemoglobin and serum albumin (Levy *et al*., 1989; Minarowska *et al*., 2007b; Rojas-Espinosa *et al*., 1973). For the current study, haemoglobin was used, as the substrate of choice, in an assay that was based on the method described by Anson, (1938). In this assay, acid-denatured haemoglobin is digested and the undigested haemoglobin is precipitated with trichloroacetic acid (TCA), allowing the amount of unprecipitated protein to be monitored as indication of protease activity. This was measured spectrophotometrically by quantifying the total amount of product that has separated from the original substrate protein (Anson, 1938).

4.4.1 Reagents

Haemoglobin substrate [5% (m/v) in dH_2O]. Bovine haemoglobin powder (0.5 g) was dissolved in dH_2O (10 ml) by gentle stirring.

Assay buffer [250 mM sodium citrate buffer, pH 3.5]. Citric acid (5.26 g) was dissolved in dH_2O (approximately 80 ml), titrated with NaOH to pH 3.5 and made up to 100 ml with dH_2O.

Trichloroacetic acid (TCA) [5% (m/v) in dH_2O]. Trichloroacetic acid (5 g) was dissolved in dH_2O and made up to 100 ml.

Middlebrook 7H10 agar and Middlebrook 7H9 broth. This was prepared as described in Section 2.6.1.

Ringer‟s solution [0.25% (m/v) in dH_2O]. Ringer‟s (2.5 g) was dissolved in dH_2O (1 l).

Porcine cathepsin D stock solution [0.57 mg/ml]. was previously purified by Fortgens, (1996) from porcine spleen essentially according to Takahashi and Tang, (1981), but also using three-phase partitioning (TPP) prior to pepstatin affinity chromatography.

Porcine cathepsin D working solution [0.5 µg/ml]. Porcine cathepsin D stock solution (0.9 µl) was diluted in assay buffer (999.2 µl) just before use.

4.4.2 Procedure

Triplicate assays were carried out for both test samples as well as the controls and for this current study, 1 unit of activity was defined as the quantity of enzyme that produces an increase in absorbance of 1.0 as compared to the control in a time period of 60 min (Barrett, 1970).

In order to establish the levels of active enzyme contained in the porcine cathepsin D sample an activity assay using the method described by Anson, (1938) and Jacobs *et al*. (1989) was used with minor modifications. A reaction mixture was prepared by combining assay buffer (506 µl), haemoglobin substrate (133 µl) and the porcine cathepsin D stock solution (26 µl, containing 14.82 µg of enzyme). The reaction mixture was subsequently incubated at 37ºC for 30 min following which a sample of the reaction mixture (300 µl) was added to TCA (240 µl). A zero time control was prepared by mixing a sample of the reaction mixture (300 µl) with TCA (240 µl) immediately after the addition of the cathepsin D enzyme sample to the reaction mixture. The reaction mixture, zero time control and blank were centrifuged, the absorbance (A_{280nm}) of supernatants read against the blank supernatant and the amount of cathepsin D, as compared to the control, that would give an increase in absorbance of 1 in 60 minutes, calculated. This allowed the specific enzyme activity of the porcine cathepsin D sample

to be established and expressed in terms units/ml of final reaction mixture and subsequently used in the *in vitro* killing assay involving cathepsin D.

Determination of the *in vitro* bactericidal potential of cathepsin D was based on the method described by Maclvor *et al*. (1999) with minor modifications. Middlebrook 7H9 broth medium was inoculated with a single *M.smegmatis* mc2155 colony and culture grown at 37ºC with shaking (200 r.p.m) in a New Brunswick Scientific controlled environment incubator shaker. *M.smegmatis* organisms in a log phase of growth (100 µl, $O.D_{600}$ 0.1, ~10^5) were incubated in porcine cathepsin D working solution (100 µl, containing 0.057 µg of enzyme with a specific activity of 0.0196 units/ml, giving a final concentration of 0.0098 units/ml and incubated (37ºC for 4 h).

Controls were prepared similarly, however, one of the controls did not contain the enzyme and assay buffer, while the other control did not contain the enzyme but did contain the assay buffer. Serial dilutions of the controls as well as the test sample was prepared in Ringer‟s solution and 1 ml of both controls and the test sample were spread on Middlebrook 7H10 agar plates using the standard hockey stick inoculation method. Triplicate plates were prepared for each serial dilution. The number of colony forming units (CFUs) were determined after a 48 h incubation period and used to calculate .the number of organisms killed by the addition of 0.0098 units/ml of cathepsin D and whether incubation in assay buffer had any effect. This was done by expressing the CFUs of the buffer control and test as a percentage of the Ringer‟s solution control.

4.4.3 Results

Porcine cathepsin D stock solution (26 µl, containing 14.82 µg) was observed to have a total activity of 0.256 units in 30 min and therefore 0.512 units in 60 min i.e. the sample had a specific activity of 19.6 units/ml. The growth or survival rate (in CFUs) of the buffer control, Ringers solution control and sample of log phase *M.smegmatis* treated with a final concentration of 0.0098 units/ml are as recorded in Table 4.3.

Table 4.3: Number of CFUs observed after the incubation of *M.smegmatis* with test and control solutions.

Serial Dilution	Control 1 (prepared in Ringer‟s solution)	Control 2 (prepared in Ringer‟s solution and assay buffer)	Test (prepared in Ringer‟s solution assay buffer)
10^{-4}	298	262	165
10^{-5}	250	232	141
10^{-6}	153	142	54
10^{-7}	10	10	0
Average value of CFUs/ ml	6×10^7 CFUs/ml	5.6×10^7 CFUs/ml	2.3×10^7 CFUs/ml

- Triplicate plates were prepared for each serial dilution, and the average values for each serial dilution were calculated.
- Plates which had <30, and >300 colonies were disregarded.

The highest number of CFUs (6×10^7/ml) were observed in control 1 (Table 4.3, prepared in Ringer‟s solution without assay buffer and cathepsin D). The second highest number of CFUs (5.6×10^7/ml) was observed after the incubation of *M.smegmatis* with control 2 (Table 4.3, prepared in Ringer‟s solution and assay buffer without cathepsin D) and showed that the assay buffer depressed growth by about 1%. The assay buffer CFU was, therefore, used as for the test in which the bacteriocidal capacity of cathepsin D was tested. This showed that 59% of the *M.smegmatis* were killed using 0.0098 units/ml of cathepsin D at a pH of 3.5 in 4 hours.

4.5. Discussion

During the current study, immunofluorescence detected by confocal microscopy was used to detect the presence of LAMP-1 and -2, cathepsin D, GFP-tagged *M.smegmatis*, propidium iodide stained *M.smegmatis* and LysoTracker-positive vesicles in J774 macrophages so that colocalization analysis could be used to analyze the relationships between the above mentioned. Colocalization analysis was represented using two methods; visual representation of colocalization using the traditional overlay method in which the red and green channels are overlayed so that colocalized pixels are depicted in yellow and colocalization images created using ImageJ‟s colocalization highlighter tool in which colocalized pixels are depicted in white as well as a quantitative representation of colocalization using colocalization data that were generated using the ImageJ plugin, JACoP. In most cases, the representation of colocalization using ImageJ‟s colocalization highlighter tool rendered colocalization more easily and reliably visible than the classical red-green overlay method.

To ensure colocalization is non-variably represented i.e. colour intensities and hues, that may be subject to alteration, for example, in digital printers and personal computer monitors, potentially altering the amount of perceptible colocalization (i.e. yellow) as one colour, for example, green is adjusted to a greater intensity than, for example, red. It was, therefore, decided that during the current study, ImageJ‟s colocalization highlighter tool (which is insensitive to intensity and hue settings and only represents pixels found in the same pixel location in two channels as colocalized and subsequently colours them white) should be used.

Generally the ImageJ analysis JACoP plugin was useful in representing colocalization reproducibly and without bias as it generates quantitative colocalization data in a non-subjective fashion automatically, after background adjustment is completed. The only problem encountered, however, was during infection studies where most of the ICCB tools did not detect faintly visible colocalization while the ICQ values did verify the faintly visible colocalization. It, therefore, appears that the ICQ values are a more reliable indication of colocalization at low levels of colocalization.

One of the challenges for the current study was finding a means of detecting and visualizing dead *M.smegmatis*. Several studies have defined cell death as a loss of cell membrane integrity and uptake of fluorescent stains such as propidium iodide that are not able to cross intact cell membranes at low concentrations (Jepras *et al*., 1995). During the current study, fluorescent GFP-tagged *M.smegmatis* was observed not to take up the propidium iodide stain while those mycobacteria that did take up this stain did not show green fluorescence. This was observed during the heat-killing of *M.smegmatis* (Figure 4.1, A and B) as well as in the single images that included the fluorescence of both GFP-tagged *M.smegmatis* and propidium iodide stained *M.smegmatis* (Figure 4.7, 4.8, 4.9, Panel **B**, c). Although propidium iodide staining seemed to be a suitable method for detecting dead mycobacteria, it could not be detected simultaneously with LysoTracker Red DND-99 due to similar excitation and emission wavelengths. Therefore, the relationship between LysoTracker-positive/ acidic vesicles and dead *M.smegmatis* could not be established by checking colocalization of dead mycobacteria in low pH compartments. Future studies should include alternate methods for the detection of acidic vesicles.

To allow simultaneous detection of acidity and cell death, LysoTracker Blue DND-22, and propidium iodide could be used (Al Gadban *et al*., 2010). However, all LysoTracker probes do not indicate the exact pH of a particular organelle. These probes only indicate that vesicles have a pH below a certain value. Oregon Green 488 dextran, however, may be an alternative for the visualization of acidic vesicles with a range of pHs as this fluorescent pH marker has excitation and emission wavelengths of 493 and 520 nm, respectively, and exhibits different fluorescent intensities and colours at different pHs. The most intense red fluorescence is observed at pH 4 while at pH 5 a yellow fluorescence is exhibited and at pH 5.5 fluorescence appears to become green with the most intense green fluorescence observed at pH 6.5 (Jackson, 2005; Lee *et al*., 2008b). However, this in turn creates a problem in the choice of fluorescent labels as the emissions of the Oregon Green 488 dextran at various pHs have to be different from that of the other probes used to prevent “bleed through” or overlap of emitted spectra as the colour of the Oregon Green 488 dextran changes from green to red as the pH increases in acidity and “shifts” into the emission spectrum of the second probe. An

alternative to this would be to use the uptake of 3-(2,4-dinitroanilino)-3'-amino-N-methyldipropylamine (DAMP), a probe that enables the visualization of acidic organelles by electron microscopy (Anderson *et al*., 1984). This would give a definitive pH value but in turn would lead to the problem of assessing viability of bacteria at the EM level as propidium iodide and GFP could no longer be used as indicators of organism death or viability.

From the colocalization analysis between cathepsin D and LysoTracker, it was observed that there was a greater degree of colocalization between cathepsin D and LysoTracker in *M.smegmatis*-infected J774 macrophages than in uninfected macrophages. This possibly indicates that more of the active cathepsin D in infected macrophages as acidic conditions are required for the processing of cathepsin D (Minarowska *et al*., 2008) and the pH of organelles in which colocalization occurs is at least pH 5.5. LysoTracker, however, cannot be used to determine whether one vesicle is more acidic than another below pH 5.5. For this reason Anes *et al*. (2006) cannot categorically state that during the first killing phase (1-4 hours after infection) vesicles were mildly acidic or that during the second and third killing phases vesicles were more acidic based on results generated using LysoTracker. This posed a problem when deciding the pH at which to conduct *in vitro* killing experiments using cathepsin D. The literature in general suggests that a pH of about 5.5 may be relevant at early killing stages, however (Jensen and Bainton, 1973; McNeil *et al*., 1983; Vieira *et al*., 2002).

As cathepsin D colocalizes with LysoTracker in *M.smegmatis* infected-J774 macrophages this seems to indicate that this non-pathogenic species does not prevent the processing of cathepsin D from its proenzyme form into its active form, as does a pathogen such as *Mycobacterium avium* (Sturgill-Koszycki *et al*., 1996; Weiss and Souza, 2008). Sturgill-Koszycki *et al*. (1996) observed that cathepsin D was retained in its unactive/ proenzyme form in *M.avium*-containing phagosomes even in phagosomes isolated and stored for nine days post-infection. This appears to indicate that the enzyme had not been exposed to acidic conditions due to prevention of the acidification of *M.avium*-containing phagosomes and is a mechanism used by pathogens to escape killing.

GFP-tagged *M.smegmatis* appeared to fluoresce less in regions where cathepsin D and LysoTracker were colocalized. In a study conducted by Lee *et al*. (2008a), an isopropyl β-D-1-thiogalactopyranoside (IPTG)-inducible GFP expression system in *M.tuberculosis* was used as an indicator of mycobacterial viability as well as of phagosomal maturation. In this study, mycobacteria which responded to IPTG-induction of GFP expression and fluorescence were considered as metabolically active and were located in non-acidified phagosomes that had not fused with "lysosomes". However, those mycobacteria that did not express GFP in response to IPTG, and were subsequently considered as metabolically inactive, were located in acidified phagosomes that had fused with "lysosomes" (observed as lysosomes were pre-labelled with Texas red dextran). Therefore, in the current study, GFP-tagged *M.smegmatis* that no longer gave off a green fluorescence may be considered as dead. On the other hand, however, the low pH compartments in which these mycobacteria were located (indicated by the presence of LysoTracker) may have caused a reduction in the fluorescence of the GFP as environmental pH has been reported to have an influence on GFP fluorescence (Toca-Herrera *et al*., 2006).

Propidium idodide has been observed to be taken up by certain bacterial species such as *Mycobacterium frederiksbergense* LB501T and *Sphingomonas* sp. LB126 during exponential growth (i.e. by live bacteria) (Shi *et al*., 2007). This was not the case in the current study, however, as *M.smegmatis* that were stained with propidium iodide (i.e. indicating dead bacteria) did not also show simultaneous green fluorescence (i.e. indicating viability) and hence propidium iodide did not label live bacteria at anytime during the current study. Reciprocally, *M.smegmatis* which showed green fluorescence (i.e. were viable) did not take up propidium iodide (indicating dead bacteria) and hence GFP fluorescence appears to be a reliable indicator of mycobacterial viability. Furthermore, the permeabilization of J774 cells with saponin did not appear to have affected the viability of *M.smegmatis*.

The greater degree of colocalization observed between cathepsin D and LAMP-1 and -2 in uninfected cells as compared to infected cells may have several implications. It is possible that cathepsin D is secreted out of LAMP-1 and -2 positive vesicles into the extracellular environment. This suggests that *M.smegmatis* infection may influence the

association between cathepsin D and LAMP-1 and -2 in macrophages, and, since LAMP-2 deficiency in mice has been associated with elevated lysosomal enzyme secretion and incorrect cathepsin D trafficking, it may be possible that *M.smegmatis* infection affects cathepsin D trafficking by affecting the relationship between LAMP-2 and cathepsin D (Eskelinen *et al*., 2002; Huynh *et al*., 2007a).

The colocalization between cathepsin D and LAMP-1 and -2 in both uninfected and infected cells also indicates that this protease is involved in antigen processing and presentation since LAMP-1 and -2 have been associated with antigen processing and presentation via MHC class II molecules (Büning *et al*., 2006; Calafat *et al*., 1994; Dani *et al*., 2004; Zhou *et al*., 2005). Since cathepsin D appears to colocalize with LysoTracker, LAMP-1 and -2 in infected and uninfected cells, cathepsin D-positive vesicles may be classified as acidic vesicles that are also LAMP-1 and -2 positive. The colocalization of cathepsin D with LAMP-1 and -2 together with the colocalization of LAMP-1 and -2 with LysoTracker in uninfected and infected cells suggests that LAMP-1 and -2 may label the same organelles/vesicles.

Future studies should also include the study of the possible association between LAMP-3 (CD63) (a member of the tetraspanin protein family) with LAMP-1 and -2 and cathepsin D as LAMP-3 has been observed to be found in late endocytic organelles and has also been implicated in antigen internalization and antigen processing and presentation via MHC class II molecules (Mantegazza *et al*., 2004). It may be important to determine whether LAMP-1, -2 and -3 label the same vesicles/organelles/compartments in infected and uninfected cells as different late endocytic organelles and "lysosome" populations have been observed in previous studies (Anes *et al*., 2006; Burton and Lloyd, 1976; Deng *et al*., 1991; Selmi and Rousset, 1988).

The decrease in colocalization between cathepsin D and LAMP-1, and LysoTracker and LAMP-1, in infected cells, may be explained by the observation made by Anes *et al*. (2006) where LAMP-1 was found to be recycled out of vacuoles that contain live *M.smegmatis*. A similar observation was made for LAMP-2 in the current study i.e. a decrease in colocalization between cathepsin D and LAMP-2 and LysoTracker and

LAMP-2 in infected cells. Whether there is a general decrease in total LAMP-1 and -2 in infected cells is unknown. However, one would expect an increase in the total amount of these proteins in infected cells as they have been observed to be essential for phagosomal maturation (Huynh *et al*., 2007a). In a study conducted by Gutierrez *et al*. (2008), LAMP-2 was found to be up-regulated in *M.smegmatis* infected J774 cells, and, in another study conducted by Torres *et al*. (2006), the phagosomes isolated from *M.tuberculosis* infected human macrophages were observed to have an increased level of LAMP-1 as compared to uninfected cells, supporting the above hypothesis.

The absence of colocalization/low colocalization observed between cathepsin D, LAMP-1 and -2 with live and dead *M.smegmatis* may, however, have been due to low infection rates/concentrations of *M.smegmatis* in J774 cells. These low concentrations may have influenced the generation of the colocalization analysis data as well as the visual representation of colocalization. Future studies should, therefore, ensure that a greater multiplicity of infection (MOI) of *M.smegmatis* per macrophage is achieved.

The generation of the colocalization data for the colocalization of cathepsin D, LAMP-1 and -2 with live and dead *M.smegmatis* is also an aspect that should be closely analyzed to explain the lack of colocalization between these markers and live and dead *M.smegmatis*. Although intensity correlation coefficient-based (ICCB) analyses, used in the current study is one of the main ways in which colocalization is analyzed, this method of analysis is based on individual pixel coincidence analysis where each pixel is considered as part of an image and not part of a unique structure (Bolte and Cordelières, 2006). Therefore it is possible that the morphological and spatial properties of fluorescent objects such as GFP-tagged *M.smegmatis* and propidium iodide stained *M.smegmatis* are not properly considered during this type of colocalization analysis and this may be as a result of the way in which images are captured during confocal microscopy i.e. images are usually acquired at a single optical depth to produce a two-dimensional image. It is possible that some portions of irregular shaped fluorescent objects may be omitted from consideration due to the optical depth at which the image is acquired. Therefore, for a true reflection of colocalization, various images of the same object should be taken at several optical depths and this should be followed by the construction of a single three-dimensional image and subsequently, a colocalization

analysis program which is able to analyze the colocalization of three-dimensional objects should be used.

Not many studies have focussed on the *in vitro* microbicidal activities of lysosomal enzymes. However, in a study conducted by MacIvor *et al*. (1999), the direct addition of cathepsin G to *Escherichia coli, Klebsiella pneumoniae* and *Staphylococcus aureus* showed that cathepsin G did not affect the growth of test microorganisms. In a study conducted by Thorne *et al*. (1976), cathepsin D was observed to bring about the highest amount of lysis of *S.aureus*, as compared to other proteases, including cathepsins B and G, lysozyme and lysosomal elastase. The greatest amount of lysis of *S.aureus*, by cathepsin D, was observed to occur at pH 6.4 (which is not within the classically determined optimal pH range for cathepsin D activity i.e. from pH 3.5-5.5). No lysis was observed at pH 4, a pH value supposedly optimal for cathepsin D activity (Barrett, 1970; Dorer *et al*., 1978; Minarowska *et al*., 2008). In the current study, however, due to the limited amount of available cathepsin D the microbicidal *in vitro* assay was conducted using an assay buffer of pH 3.5, a pH classically considered optimal for activity, although it was realised that this may represent the minimal number of organisms that may be killed if the results of Thorne *et al*. (1976) are valid and best bacteriocidal activity was achieved at a higher pH. Killing assays at higher pHs should, however, be performed in the future. The current assay also used far less active enzyme, (~ 20 times less active) than the study by Thorne *et al*. (1976), though the amount of active cathepsin D used in the current study is possibly more representative of what might be found in the phagosome.

CHAPTER 5

DISCUSSION

Tuberculosis (TB) is one of the leading causes of mortality in South Africa, but the precise number of deaths due to this disease alone is often difficult to determine as infection is often due to a compromised immune system due to prior infection with Human Immunodeficiency Virus (HIV). The number of people infected with HIV in South Africa was observed to increase dramatically between 1990 and 2007 and was accompanied by an increase in the number of TB infections, with more than 100 000 people being diagnosed with this disease per year (Cohen *et al*., 2010). Of most concern is the rise in the number of people suffering with drug-resistant forms of this disease, with one in ten cases being reported as multi-drug resistant (McGaw *et al*., 2008; Migliori *et al*., 2010).

Multidrug- and extensively drug-resistant forms of TB have made the treatment of this disease, using standard drugs, ineffective and thus new methods of dealing with TB infection are required (Cohen *et al*., 2010). One method would be to target the cells that are involved in the killing of pathogenic species such as *M.tuberculosis* (the microorganism that causes TB). Macrophages are examples of such cells and although much progress has been made in understanding the mechanism by which killing is achieved, there is a great deal still unknown. Understanding of the mechanisms by which phagosomes undergo a maturation process that results in the creation of a hostile environment in which phagocytosed microorganisms are usually killed, and how these are blocked by pathogenic species such as *M.tuberculosis*, will facilitate the development of therapies that target such pathogens and will also enable a greater understanding of how 10% of humans who carry *M.tuberculosis* develop TB while 90% of the infected population do not (Flynn and Chan, 2001a).

The direct study of how pathogenic species such as *M.tuberculosis* are killed may be complicated by the existence of multiple strains that may have different mechanisms for evading killing. The use of non-pathogenic mycobacterial species such as *Mycobacterium smegmatis*, that share several characteristics with pathogenic species,

has been used by several researchers to first understand the way in which macrophages kill non-pathogenic mycobacteria (He and De Buck, 2010; Shiloh and DiGiuseppe Champion, 2010).

Our study, as well as that of Anes *et al*. (2006) and others have shown that, one of the key events during phagosome maturation, in the macrophages infected with non-pathogenic *M.smegmatis*, is the fusion of late endocytic organelles, often called "lysosomes" and the delivery of lysosomal proteases to the mycobacterium-containing phagosome (Nepal *et al*., 2006; Sturgill-Koszycki *et al*., 1994). This seems to be borne out by killing studies in which lysosomal protease inhibitors have been found to negatively affect the ability of macrophages to kill *M.smegmatis* during early killing stages (Anes *et al*., 2006). The production of nitric oxide (NO) is another mechanism used by macrophages for the killing of microorganisms. Pathogens such as *M.tuberculosis* and *M.avium* have, however, been observed to prevent the fusion of "lysosomes" and phagosomes, as well as the release of NO, and subsequently survive within phagosomes, largely in an NFκB-dependent manner (Flynn and Chan, 2003; Gutierrez *et al*., 2008; Russell, 2001)

Although the fusion of lysosomal enzymes and production of NO appear to be the main mechanisms in which macrophages eliminate mycobacterial infections, knowledge of the periods at which these mechanisms are employed, post infection and knowledge of the various changes that take place in the phagosome is extremely limited. A study by Anes *et al*. (2006) represents one of the major and most complete attempts to describe the periodicity of killing as well as the changes observed in non-pathogenic-mycobacterium-containing phagosomes. A well established model system involving GFP-tagged *M.smegmatis* (a non-pathogenic species) and J774 mouse macrophages was used in this, as well during the current study.

In the study conducted by Anes *et al*. (2006), it was observed that the initial killing by macrophages (0-1 hours after infection) was brought about by NO release. From 1-4 hours after infection, mycobacteria were found to be eliminated by the activity of lysosomal enzymes at a mild pH following the fusion of phagosomes with late endocytic organelles described as "lysosomes". Two subsequent phases in which

mycobacteria were killed (9-12 hours) and (12 -24 hours) after infection were characterized by the lowering of phagosomal pH.

Lysosomal enzymes only seemed to be responsible for *M.smegmatis* killing 1-4 hours post infection and did not seem to have an effect during the later killing phases. From the current study, it is speculated that this may be due to the possible secretion of lysosomal enzymes, such as cathepsin D, prior to the later killing phases i.e. (9-12 hours) and (12-24 hours) after infection. Such a hypothesis, however, needs to be confirmed via western blot analysis. Anes *et al*. (2006) suggests that the production of NO, lysosomal enzyme activity and the lowering of phagosomal pH do not occur all at once, but rather at distinct periods post infection. Killing may, therefore, be attributed to bacteriocidal systems at different time periods post infection.

Although Anes *et al*. (2006) showed, using lysosomal protease inhibitors, that lysosomal proteases activity may play a role in the early killing stage, whether a specific lysosomal enzyme or a group of lysosomal enzymes working in tandem at different pHs are responsible for killing was not shown. The protease inhibitors used by Anes *et al*. (2006) included leupeptin, aprotinin and pepstatin which inhibit cysteine, serine and aspartyl proteases, respectively. As cathepsin D, one of the lysosomal enzymes inhibited by pepstatin, is known to have bactericidal properties, its role in the macrophage killing of *M.smegmatis* formed the basis of this current study (del Cerro-Vadillo *et al*., 2006; Singh *et al*., 2006; Thorne *et al*., 1976).

Cathepsin D does seem be involved in the killing of *M.smegmatis,* according to our *in vitro* killing experiments which show a 59% killing rate. Whether the effect of cathepsin D on *M.smegmatis* viability would be enhanced after NO release or in combination with cathepsins Z and H, observed to be upregulated in a study by Gutierrez *et al*. (2008), is unknown. The target of cathepsin D proteolysis and the pH at which cathepsin D is involved in killing is similarly unknown. Similarly, the pH at which cathepsin D may be most active against mycobacteria seems unknown. Here killing was carried out at pH 3.5, the pH classically used for maximal cathepsin D activity, in classical enzyme assay buffer (Barrett, 1970; Minarowska *et al*., 2007b; Thorne *et al*., 1976).

The study by Anes *et al*. (2006), however, seems to suggest that cathepsin D is more active in killing at its higher limit of pH 5.5 (Barrett, 1970; Dorer *et al.*, 1978; Minarowska *et al.*, 2008). The study by Thorne *et al*. (1976) also showed greater killing at pH 6.4 as compared to a lower pH of 4, though test bacteria did not include mycobacteria. Further studies should, therefore, include killing experiments conducted at a higher pH, especially around pH 5.5, instead of pH 3.5 assessed during the current study. Also, different buffer systems should be tested as the requirement for- or effect of different ions on killing is similarly unknown as is the number of units of active cathepsin D present in the phagosome. In the current study, the *in vitro* killing of *M.smegmatis* was conducted using 0.0098 units/ml of active cathepsin D, whereas in a study by Thorne *et al*. (1976), 0.2 units/ml of active enzyme was used. Neverthless. A 59% kill rate in 4 hours was achieved with approximately one fortieth the amount of enzyme shown to lyze *Staphylococcus aureus*.

To visually assess the possible association of cathepsin D with *M.smegmatis* in J774 cells and hence its possible role in killing, confocal studies were employed. This required the use of antibodies against cathepsin D which would not cross-react with *M.smegmatis* antigens due to the use of adjuvants containing bacterial products, especially Freund‟s complete adjuvant. Saponin, an adjuvant that is believed to induce antibody production via the MHC class I pathway of antigen presentation was chosen in spite of an MHC class II response and antibody production being required. This adjuvant was chosen as previous experiments had shown that some antibody production was achieved when using this adjuvant. Though antibodies raised against porcine cathepsin D, in chickens, showed only weak recognition of mouse cathepsin D antigens, they did not cross-react with *M.smegmatis.* Eggs from week 8 post inoculation were, however, used for the current study, without checking whether this batch of eggs showed the highest titre. This is usually, but not always the case, and was used as a selection criterion in the current study due to the lack of availability of large amounts of antigen for ELISA assays to allow assessment of which week‟s eggs should be chosen (for the highest titre). Which eggs did give the best response, at which week, should, however, be established before any pronouncement on the suitability of saponin or alum as an adjuvant for the production of anti-cathepsin D antibodies may be made.

The production of polyclonal antibodies that do not cross-react with mycobacteria for use in mycobacterial-infection studies is not an aspect that has been widely researched. Methods have to be developed and form a significant barrier to microscopy-based investigations, especially using electron microscopy. Most researchers overlook this aspect during mycobacterial-infection studies and very few researchers seem to check the cross-reactivity of antibodies that they use with mycobacterial antigens. For raising anti-cathepsin D and similar antibodies for mycobacterial studies, future studies should involve the exploration of different non-bacterial containing adjuvants. Saponin seems to generate an inflammatory response, and possibly allow penetration of antigens into cells, and alum has the advantage of facilitating slow release of adsorbed antigen, for maximal exposure of the immune system. The missing component in such adjuvants, compared to Freund‟s-like adjuvants, is the content of bacterial antigens that also stimulate the toll-like receptors and assist in priming APC cells. Antigens from a different microbial source, for example, those from yeast or fungi may be suitable components, as long such studies do not involve yeast or fungi. Such adjuvants could contain fungal β-glucans and zymosan that interact with dectin-1 receptors in host animals (Zhang and Mosser, 2008).

Other non-mycobacterial and non-bacterial product containing adjuvants may be those that contain hormones or cytokines such as those usually secreted by the host during infections. These may include (IL)-1β, TNF-α or IL-6 and may also be useful alternatives for the production of antibodies that do not cross-react with *M.smegmatis* and other mycobacterial species (Blatteis, 2000; Coma *et al*., 2006; Patterson *et al*., 2002; Russell *et al*., 2009).

The use of confocal and colocalization studies appears to be a promising method for studying various aspects of mycobacterial infection. The aspect of finding an appropriate system to visually detect live and dead *M.smegmatis* during confocal studies was one of the main aims and hurdles in the current study. Although there were certain initial reservations about using propidium iodide as a means of visually detecting dead mycobacteria due to a report by Shi *et al*. (2007) in which mycobacteria were reported to take up PI during exponential growth (i.e. while being very much alive), this was found not to be the case in the current study. *M.smegmatis* that were stained with

propidium iodide (i.e. indicating dead mycobacteria) did not also exhibit simultaneous green fluorescence (i.e. indicating viability). Propidium iodide, therefore, did not stain live bacteria at anytime during the current study. Also, *M.smegmatis* which exhibited green fluorescence (i.e. indicating viablity) did not take up propidium iodide (indicating non-viability). Thus GFP and propidium idodide fluorescence seemed to be an appropriate method for confocal fluorescence detection of live and dead *M.smegmatis*, respectively, though detection of viability should also possibly have been assessed using culture techniques.

From the analysis of the visual methods used to represent colocalization the traditional red-green overlay method, where colocalized regions are represented in yellow, seemed to be inferior for representing colocalization as compared to those created using ImageJ‟s colocalization highlighter tool, where colocalized pixels are represented in white. This is due to the fact that intensities and hues of colours such as green and red may be subject to alteration on personal computer monitors and printers and this may alter the amount of perceived colocalization i.e. yellow coloured regions. ImageJ‟s colocalization highlighter tool, however, is not sensitive to intensity and hue settings as it only represents pixels found in the same pixel location in the two channels (i.e. red and green channels) as colocalized and subsequently colours such pixels white, and is hence superior for definitively representing colocalization.

A means of quantifying the amount/intensity of colocalization was also required during the current study and this was achieved using ImageJ‟s colocalization plugin, JACoP which calculates various intensity correlation coefficient-based (ICCB) values. The use of the JACoP plugin allowed for the representation of colocalization without bias, and was found to be a useful tool, although problems were encountered during infection studies where most of the ICCB analysis tools were unable to detect faintly visible colocalization while ICQ values did validate faintly visible colocalization. Therefore, it seems as though ICQ values are a more reliable indication of colocalization when low levels of colocalization are present.

As ICCB analysis is based on individual pixel coincidence analysis where each pixel is considered as part of an image and therefore not part of a unique structure, the

morphological and spatial characteristics of fluorescent objects are not taken into account and, therefore, future colocalization studies should also include the use of programs that take into consideration these characteristics (Bolte and Cordelières, 2006).

Confocal studies conducted in real time, and the use of substrates that fluorescence specifically upon proteolytic activity of specific lysosomal proteases would also be extremely useful for future studies. Also, it would be interesting to further develop the use of GFP and propidium iodide as a method of detecting live and dead mycobacteria and one of the ways that this can be done is to determine the effect that different environmental factors such as changes in pH have on the fluorescence of these fluorescent substances.

Indirect evidence gathered from confocal and colocalization studies, as well as direct evidence provided from the *in vitro* killing of *M.smegmatis,* seem to suggest that cathepsin D does play a role in the killing of *M.smegmatis*. Whether this protease has greater microbicidal properties compared to other lysosomal proteases is unknown, however, evidence seems to suggest that the combined activity of several lysosomal proteases such as cathepsins B, Z, G and H are important for the elimination of mycobacteria (Gutierrez *et al*., 2008). By further developing the live/dead detection system and the *in vitro* method for detecting activity of lysosomal enzymes, it may be possible to compare the microbicidal properties of such enzymes.

Overcoming barriers to fusion of bacteriocidal systems with the phagosome may be the most optimal way forward in patients where both the innate and adaptive immune systems seem to be paralysed, and resistance to antibiotics is developed by several strains of *M.tuberculosis* (Cohen *et al*., 2010; Hanekom *et al*., 2010). It is hoped that, by developing a greater understanding of the mechanisms used by macrophages in killing, such mechanisms can be discovered and manipulated in the future so that the killing by macrophages may be enhanced. For this reason studies into the fundamental cell biology and signalling of infected cells remain vital.

In summary, at the beginning of this study one of the aims was to establish whether the lysosomal protease, cathepsin D, may play a role in killing *M.smegmatis* in J774

macrophages, To this end, confocal and other visualization studies were chosen and polyclonal antibodies that do not cross-react with mycobacteria were identified to be required, and a chicken host and alum and saponin adjuvants chosen as adjuvants. Antibodies raised against porcine cathepsin D, using saponin, and previously raised with alum, against human cathepsin D, were compared for reactivity. Though similar, the anti-human cathepsin D antibodies raised with alum were chosen for final confocal work.

The organelles containing cathepsin D, characterized using the lysosomal associated membrane proteins-1 and 2 (LAMP-1 and -2) and LysoTracker, showed that cathepsin D colocalized with the above markers in both *M.smegmatis*-infected and uninfected J774 macrophages. There was a greater degree of colocalization between cathepsin D and LysoTracker in infected cells than in uninfected cells possibly indicating killing of *M.smegmatis*. One of the challenges of this study, however, was finding a way in which dead *M.smegmatis* could be visually distinguished from live *M.smegmatis*. Propidium iodide (PI) labelling and loss of GFP fluorescence appears to be reliable indicators of *M.smegmatis* death or viability as myobacteria that took up this stain also lost green fluorescence, while *M.smegmatis* that exhibited green fluorescence (viable) were not observed to take up propidium iodide (dead). Faint colocalization between cathepsin D, LAMP-1 and -2 with dead, and to a lesser extent with live *M.smegmatis,* therefore, seems to support the idea that cathepsin D in an acidic (LysoTracker positive) compartment may be involved in killing and tests of the bacteriocidal activity of cathespin D (in assay buffer at pH 3.5) on a logarithmically growing culture in a 4 hour treatment period (equivalent to the phase indicated by Anes *et al*. (2006) to be the period in which cathepsin D may be involved in killing) showed that this protease brought about a 59% rate killing of *M.smegmatis*. The results presented, therefore, appear to indicate that cathepsin D does have a possible role in the macrophage killing of *M.smegmatis*.

Future studies should also include the use of other markers for the characterization of cathepsin D-containing vesicles in infected and uninfected cells. These include markers for LAMP-3 (CD63) and MHC class I and II. Studies assessing whether the secretion of cathepsin D is induced as a means of escaping killing should also be conducted.

REFERENCES

Adams, D. O. and Hamilton, T. A. (1984). The cell biology of macrophage activation. *Annu Rev Immunol.* **2**, 283-318.

Agranoff, D., Monahan, I. M., Mangan, J. A., Butcher, P. D. and Krishna, S. (1999). Mycobacterium tuberculosis expresses a novel pH-dependent divalent cation transporter belonging to the Nramp family. *J Exp Med.* **190**, 717-724.

Aguilar, R. C., Boehm, M., Gorshkova, I., Crouch, R. J., Tomita, K., Saito, T., Ohno, H. and Bonifacino, J. S. (2001). Signal-binding specificity of the mu4 subunit of the adaptor protein complex AP-4. *J Biol Chem.* **276**, 13145-13152.

Al Gadban, M. M., Smith, K. J., Soodavar, F., Piansay, C., Chassereau, C., Twal, W. O., Klein, R. L., Virella, G., Lopes-Virella, M. F. and Hammad, S. M. (2010). Differential trafficking of oxidized LDL and oxidized LDL immune complexes in macrophages: impact on oxidative stress. *PLoS One.* **5**, e12534-e12543.

Allen, L. A. and Aderem, A. (1996a). Mechanisms of phagocytosis. *Curr Opin Immunol.* **8**, 36-40.

Allen, L. A. and Aderem, A. (1996b). Molecular definition of distinct cytoskeletal structures involved in complement- and Fc receptor-mediated phagocytosis in macrophages. *J Exp Med.* **184**, 627-637.

Allen, R. C. (1994). Role of oxygen in phagocyte microbicidal action. *Environ Health Perspect.* **102** 201-208.

Altman, A. and Dixon, F. J. (1989). Immunomodifiers in vaccines. *Adv Vet Sci Comp Med* **33**, 301-343.

Anderson, R. G., Falck, J. R., Goldstein, J. L. and Brown, M. S. (1984). Visualization of acidic organelles in intact cells by electron microscopy. *Proc Natl Acad Sci U S A.* **81**, 4838-4842.

Andrejewski, N., Punnonen, E. L., Guhde, G., Tanaka, Y., Lüllmann-Rauch, R., Hartmann, D., von Figura, K. and Saftig, P. (1999). Normal lysosomal morphology and function in LAMP-1-deficient mice. *J Biol Chem.* **274**, 12692-12701.

Andrew, S. M. and Titus, J. A. (2000). Purification of immunoglobulin G. *Curr Protoc Cell Biol.* **Supplement 5**, 16.3.1-16.3.12.

Anes, E., Kühnel, M. P., Bos, E., Moniz-Pereira, J., Habermann, A. and Griffiths, G. (2003). Selected lipids activate phagosome actin assembly and maturation resulting in killing of pathogenic mycobacteria. *Nat Cell Biol.* **5**, 793-802.

Anes, E., Peyron, P., Staali, L., Jordao, L., Gutierrez, M. G., Kress, H., Hagedorn, M., Maridonneau-Parini, I., Skinner, M. A., Wildeman, A. G. *et al.* (2006). Dynamic life and death interactions between Mycobacterium smegmatis and J774 macrophages. *Cell Microbiol.* **8**, 939-960.

Anson, M. L. (1938). The estimation of pepsin, trypsin, papain, and cathepsin with hemoglobin. *J Gen Physiol.* **22**, 79-89.

Appelberg, R. (2006). Macrophage nutriprive antimicrobial mechanisms. *J Leukoc Biol.* **79**, 1117-1128.

Arens, R. and Schoenberger, S. P. (2010). Plasticity in programming of effector and memory CD8 T-cell formation. *Immunol Rev.* **235**, 190-205.

Aucouturier, J., Dupuis, L. and Ganne, V. (2001). Adjuvants designed for veterinary and human vaccines. *Vaccine.* **19**, 2666-2672.

Bals, R. (2000). Epithelial antimicrobial peptides in host defense against infection. *Respir Res.* **1**, 141-150.
Bandyopadhyay, S., Soto-Nieves, N. and Macián, F. (2007). Transcriptional regulation of T cell tolerance. *Semin Immunol.* **19**, 180-187.
Bangham, A. D., Horne, R. W., Glauert, A. M., Dingle, J. T. and Lucy, J. A. (1962). Action of saponins on biological membranes. *Nature* **196**, 952-955.
Barbieri, M. A., Roberts, R. L., Mukhopadhyay, A. and Stahl, P. D. (1996). Rab5 regulates the dynamics of early endosome fusion. *Biocell.* **20**, 331-338.
Barrett, A. J. (1970). Cathepsin D. Purification of isoenzymes from human and chicken liver. *Biochem J.* **117**, 601-607.
Barth, R. and Afting, E. G. (1984). Cathepsin D from pig myometrium. Characterization of the proteinase. *Biochem J.* **219**, 899-904.
Barton, C. H., Biggs, T. E., Baker, S. T., Bowen, H. and Atkinson, P. G. (1999). Nramp1: a link between intracellular iron transport and innate resistance to intracellular pathogens. *J Leukoc Biol.* **66**, 757-762.
Baschong, W., Suetterlin, R. and Laeng, R. H. (2001). Control of autofluorescence of archival formaldehyde-fixed, paraffin-embedded tissue in confocal laser scanning microscopy (CLSM). *J Histochem Cytochem.* **49**, 1565-1572.
Bateman, J. F., Cole, W. G., Pillow, J. J. and Ramshaw, J. A. (1986). Induction of procollagen processing in fibroblast cultures by neutral polymers. *J Biol Chem.* **261**, 4198-4203.
Baylor, N. W., Egan, W. and Richman, P. (2002). Aluminum salts in vaccines--US perspective. *Vaccine.* **20** S18-S23.
Bedoui, S., Kupz, A., Wijburg, O. L., Walduck, A. K., Rescigno, M. and Strugnell, R. A. (2010). Different bacterial pathogens, different strategies, yet the aim is the same: evasion of intestinal dendritic cell recognition. *J Immunol.* **184**, 2237-2242.
Belizaire, R. and Unanue, E. R. (2009). Targeting proteins to distinct subcellular compartments reveals unique requirements for MHC class I and II presentation. *Proc Natl Acad Sci U S A.* **106**, 17463-17468.
Bendayan, M., Nanci, A. and Kan, F. W. (1987). Effect of tissue processing on colloidal gold cytochemistry. *J Histochem Cytochem.* **35**, 983-996.
Benes, P., Vetvicka, V. and Fusek, M. (2008). Cathepsin D--many functions of one aspartic protease. *Crit Rev Oncol Hematol.* **68**, 12-28.
Beyenbach, K. W. and Wieczorek, H. (2006). The V-type H+ ATPase: molecular structure and function, physiological roles and regulation. *J Exp Biol.* **209**, 577-589.
Bizzarri, R., Serresi, M., Luin, S. and Beltram, F. (2009). Green fluorescent protein based pH indicators for in vivo use: a review. *Anal Bioanal Chem.* **393**, 1107-1122.
Blatteis, C. M. (2000). The afferent signalling of fever. *J Physiol.* **526**, 653-661.
Blokpoel, M. C., Murphy, H. N., O'Toole, R., Wiles, S., Runn, E. S., Stewart, G. R., Young, D. B. and Robertson, B. D. (2005). Tetracycline-inducible gene regulation in mycobacteria. *Nucleic Acids Res.* **33**, e22-e28.
Blumenthal, A., Ehlers, S., Ernst, M., Flad, H. D. and Reiling, N. (2002). Control of mycobacterial replication in human macrophages: roles of extracellular signal-regulated kinases 1 and 2 and p38 mitogen-activated protein kinase pathways. *Infect Immun.* **70**, 4961-4967.

Boehm, M., Aguilar, R. C. and Bonifacino, J. S. (2001). Functional and physical interactions of the adaptor protein complex AP-4 with ADP-ribosylation factors (ARFs). *EMBO J.* **20**, 6265-6276.
Bohn, W. (1978). A fixation method for improved antibody penetration in electron microscopical immunoperoxidase studies. *J Histochem Cytochem.* **26**, 293-297.
Bohsali, A., Abdalla, H., Velmurugan, K. and Briken, V. (2010). The non-pathogenic mycobacteria M. smegmatis and M. fortuitum induce rapid host cell apoptosis via a caspase-3 and TNF dependent pathway. *BMC Microbiol.* **10**, 237-248.
Bolland, S. (2008). An innate path to human B cell tolerance. *Immunity.* **29**, 667-669.
Bolte, S. and Cordelières, F. P. (2006). A guided tour into subcellular colocalization analysis in light microscopy. *J Microsc.* **224**, 213-232.
Bonifacino, J. S. and Traub, L. M. (2003). Signals for sorting of transmembrane proteins to endosomes and lysosomes. *Annu Rev Biochem.* **72**, 395-447.
Brewis, N., Phelan, A., Webb, J., Drew, J., Elliott, G. and O'Hare, P. (2000). Evaluation of VP22 spread in tissue culture. *J Virol.* **74**, 1051-1056.
Bright, N. A., Reaves, B. J., Mullock, B. M. and Luzio, J. P. (1997). Dense core lysosomes can fuse with late endosomes and are re-formed from the resultant hybrid organelles. *J Cell Sci.* **110**, 2027-2040.
Bringer, M. A., Glasser, A. L., Tung, C. H., Méresse, S. and Darfeuille-Michaud, A. (2006). The Crohn's disease-associated adherent-invasive *Escherichia coli* strain LF82 replicates in mature phagolysosomes within J774 macrophages. *Cell Microbiol.* **8**, 471-484.
Brode, S. and Macary, P. A. (2004). Cross-presentation: dendritic cells and macrophages bite off more than they can chew! *Immunology.* **112**, 345-351.
Broderson, J. R. (1989). A retrospective review of lesions associated with the use of Freund's adjuvant. *Lab Anim Sci.* **39**, 400-405.
Brown, E. J. (1986). The role of extracellular matrix proteins in the control of phagocytosis. *J Leukoc Biol.* **39**, 579-591.
Buendía, A. J., Nicolás, L., Ortega, N., Gallego, M. C., Martinez, C. M., Sanchez, J., Caro, M. R., Navarro, J. A. and Salinas, J. (2007). Characterization of a murine model of intranasal infection suitable for testing vaccines against C. abortus. *Vet Immunol Immunopathol.* **115**, 76-86.
Büning, J., Hundorfean, G., Schmitz, M., Zimmer, K. P., Strobel, S., Gebert, A. and Ludwig, D. (2006). Antigen targeting to MHC class II-enriched late endosomes in colonic epithelial cells: trafficking of luminal antigens studied in vivo in Crohn's colitis patients. *FASEB J.* **20**, 359-361.
Burton, R. and Lloyd, J. B. (1976). Latency of some glycosidases of rat liver lysosomes. *Biochem J.* **160**, 631-638.
Calafat, J., Nijenhuis, M., Janssen, H., Tulp, A., Dusseljee, S., Wubbolts, R. and Neefjes, J. (1994). Major histocompatibility complex class II molecules induce the formation of endocytic MIIC-like structures. *J Cell Biol.* **126**, 967-977.
Camacho, C., Coulouris, G., Avagyan, V., Ma, N., Papadopoulos, J., Bealer, K. and Madden, T. L. (2009). BLAST+: architecture and applications. *BMC Bioinformatics.* **10**, 421-429.
Cameron, C. H. S. and Toner, P. G. (1992). Electron microscopic immunocytochemistry in histopathology. In *Electron Microscopic*

Immunocytochemistry., (ed. J. M. Polak and J. V. Priestley), pp. 11-50. New York: Oxford University Press.
Carroll, S. B. and Stollar, B. D. (1983). Antibodies to calf thymus RNA polymerase II from egg yolks of immunized hens. *J Biol Chem.* **258**, 24-26.
Casella, C. R. and Mitchell, T. C. (2008). Putting endotoxin to work for us: monophosphoryl lipid A as a safe and effective vaccine adjuvant. *Cell Mol Life Sci.* **65**, 3231-3240.
Cellier, M. F., Bergevin, I., Boyer, E. and Richer, E. (2001). Polyphyletic origins of bacterial Nramp transporters. *Trends Genet.* **17**, 365-370.
Chacon, O., Feng, Z., Harris, N. B., Cáceres, N. E., Adams, L. G. and Barletta, R. G. (2002). *Mycobacterium smegmatis* D-Alanine Racemase Mutants Are Not Dependent on D-Alanine for Growth. *Antimicrob Agents Chemother.* **46**, 47-54.
Chan, E. D., Chan, J. and Schluger, N. W. (2001). What is the role of nitric oxide in murine and human host defense against tuberculosis?Current knowledge. *Am J Respir Cell Mol Biol.* **25**, 606-612.
Chan, J. and Flynn, J. (2004). The immunological aspects of latency in tuberculosis. *Clin Immunol.* **110**, 2-12.
Chang, Z. L. (2009). Recent development of the mononuclear phagocyte system: in memory of Metchnikoff and Ehrlich on the 100th Anniversary of the 1908 Nobel Prize in Physiology or Medicine. *Biol Cell.* **101**, 709-721.
Chao, H. H., Waheed, A., Pohlmann, R., Hille, A. and von Figura, K. (1990). Mannose 6-phosphate receptor dependent secretion of lysosomal enzymes. *EMBO J.* **9**, 3507-3513.
Chavali, S. R. and Campbell, J. B. (1987a). Adjuvant effects of orally administered saponins on humoral and cellular immune responses in mice. *Immunobiology.* **174**, 347-359.
Chavali, S. R. and Campbell, J. B. (1987b). Immunomodulatory effects of orally-administered saponins and nonspecific resistance against rabies infection. *Int Arch Allergy Appl Immunol.* **84**, 129-134.
Chen, J. W., Chen, G. L., D'Souza, M. P., Murphy, T. L. and August, J. T. (1986). Lysosomal membrane glycoproteins: properties of LAMP-1 and LAMP-2. *Biochem Soc Symp.* **51**, 97-112.
Chen, J. W., Murphy, T. L., Willingham, M. C., Pastan, I. and August, J. T. (1985). Identification of two lysosomal membrane glycoproteins. *J Cell Biol.* **101**, 85-95.
Chien, Y. H. and Bonneville, M. (2006). Gamma delta T cell receptors. *Cell Mol Life Sci.* **63**, 2089-2094.
Chugani, D. C., Rome, L. H. and Kedersha, N. L. (1993). Evidence that vault ribonucleoprotein particles localize to the nuclear pore complex. *J Cell Sci.* **106**, 23-29.
Claus, V., Jahraus, A., Tjelle, T., Berg, T., Kirschke, H., Faulstich, H. and Griffiths, G. (1998). Lysosomal enzyme trafficking between phagosomes, endosomes, and lysosomes in J774 macrophages. Enrichment of cathepsin H in early endosomes. *J Biol Chem.* **273**, 9842-9851.
Claussen, M., Kübler, B., Wendland, M., Neifer, K., Schmidt, B., Zapf, J. and Braulke, T. (1997). Proteolysis of insulin-like growth factors (IGF) and IGF binding proteins by cathepsin D. *Endocrinology.* **138**, 3797-3803.

Clemens, D. L. and Horwitz, M. A. (1995). Characterization of the Mycobacterium tuberculosis phagosome and evidence that phagosomal maturation is inhibited. *J Exp Med.* **181**, 257-270.
Cogswell, C. J. and Larkin, K. G. (1995). The specimen illumination path and its effect on image quality. In *Handbook of Biological Confocal Microscopy.*, (ed. J. B. Pawley), pp. 127-138. New York: Plenum Press.
Cohen, T., Murray, M., Wallengren, K., Alvarez, G. G., Samuel, E. Y. and Wilson, D. (2010). The prevalence and drug sensitivity of tuberculosis among patients dying in hospital in KwaZulu-Natal, South Africa: a postmortem study. *PLoS Med.* **7**, e1000296-e1000303.
Collins, C. A., De Mazière, A., van Dijk, S., Carlsson, F., Klumperman, J. and Brown, E. J. (2009). Atg5-independent sequestration of ubiquitinated mycobacteria. *PLoS Pathog.* **5**, e1000430-e1000444.
Collins, T. J. (2007). ImageJ for microscopy. *Biotechniques.* **43**, 25-30.
Coma, G., Peña, R., Blanco, J., Rosell, A., Borras, F. E., Esté, J. A., Clotet, B., Ruiz, L., Parkhouse, R. M. and Bofill, M. (2006). Treatment of monocytes with interleukin (IL)-12 plus IL-18 stimulates survival, differentiation and the production of CXC chemokine ligands (CXCL)8, CXCL9 and CXCL10. *Clin Exp Immunol.* **145**, 535-544.
Conus, S. and Simon, H. U. (2010). Cathepsins and their involvement in immune responses. *Swiss Med Wkly.* **140**, w13042-w13048.
Conyers, S. M. and Kidwell, D. A. (1991). Chromogenic substrates for horseradish peroxidase. *Anal Biochem.* **192**, 207-211.
Cooper, M. D., Gabrielsen, A. E. and Good, R. A. (1967). Role of the thymus and other central lymphoid tissues in immunological disease. *Annu Rev Med.* **18**, 113-138.
Cortese, K., Diaspro, A. and Tacchetti, C. (2009). Advanced correlative light/electron microscopy: current methods and new developments using Tokuyasu cryosections. *J Histochem Cytochem.* **57**, 1103-1112.
Costes, S. V., Daelemans, D., Cho, E. H., Dobbin, Z., Pavlakis, G. and Lockett, S. (2004). Automatic and quantitative measurement of protein-protein colocalization in live cells. *Biophys J.* **86**, 3993-4003.
Cox, J. C. and Coulter, A. R. (1997). Adjuvants--a classification and review of their modes of action. *Vaccine.* **15**, 248-256.
Crowley, J. E., Scholz, J. L., Quinn, W. J., Stadanlick, J. E., Treml, J. F., Treml, L. S., Hao, Y., Goenka, R., O'Neill, P. J., Matthews, A. H. *et al.* (2008). Homeostatic control of B lymphocyte subsets. *Immunol Res.* **42**, 75-83.
Cui, H. H., Valdez, J. G., Steinkamp, J. A. and Crissman, H. A. (2003). Fluorescence lifetime-based discrimination and quantification of cellular DNA and RNA with phase-sensitive flow cytometry. *Cytometry A.* **52**, 46-55.
Cullander, C. (1999). Fluorescent Probes for Confocal Microscopy. In *Confocal Microscopy Methods and Protocols.*, (ed. S. W. Paddock), pp. 59-73. New Jersey: Humana Press.
Dai, J., Liu, B. and Li, Z. (2009). Regulatory T cells and Toll-like receptors: what is the missing link? *Int Immunopharmacol.* **9**, 528-533.
Dale, D. C., Boxer, L. and Liles, W. C. (2008). The phagocytes: neutrophils and monocytes. *Blood.* **112**, 935-945.

Dani, A., Chaudhry, A., Mukherjee, P., Rajagopal, D., Bhatia, S., George, A., Bal, V., Rath, S. and Mayor, S. (2004). The pathway for MHCII-mediated presentation of endogenous proteins involves peptide transport to the endo-lysosomal compartment. *J Cell Sci.* **117**, 4219-4230.
del Cerro-Vadillo, E., Madrazo-Toca, F., Carrasco-Marín, E., Fernandez-Prieto, L., Beck, C., Leyva-Cobián, F., Saftig, P. and Alvarez-Dominguez, C. (2006). Cutting edge: a novel nonoxidative phagosomal mechanism exerted by cathepsin-D controls Listeria monocytogenes intracellular growth. *J Immunol.* **176**, 1321-1325.
DeMali, K. A. and Burridge, K. (2003). Coupling membrane protrusion and cell adhesion. *J Cell Sci.* **116**, 2389-2397.
Demana, P. H., Fehske, C., White, K., Rades, T. and Hook, S. (2004). Effect of incorporation of the adjuvant Quil A on structure and immune stimulatory capacity of liposomes. *Immunol Cell Biol.* **82**, 547-554.
Deng, Y. P., Griffiths, G. and Storrie, B. (1991). Comparative behavior of lysosomes and the pre-lysosome compartment (PLC) in in vivo cell fusion experiments. *J Cell Sci.* **99**, 571-582.
Dennison, C. (2003a). Concentration of the extract. In *A guide to Protein Isolation*, (ed. R. Kaptein), pp. 58-88. Dordrecht: Kluwer Academic Publishers.
Dennison, C. (2003b). Electrophoresis. In *A Guide to Protein Isolation.*, (ed. R. Kaptein), pp. 139-160. Dordrecht. : Kluwer Academic Publishers.
Dennison, C. (2003c). An overview of protein isolation. In *A Guide to Protein Isolation.*, (ed. R. Kaptein), pp. 3-19. Dordrecht: Kluwer Academic Publishers.
Desjardins, M. (1995). Biogenesis of phagolysosomes: the 'kiss and run' hypothesis. *Trends Cell Biol.* **5**, 183-186.
Detmers, P. A., Wright, S. D., Olsen, E., Kimball, B. and Cohn, Z. A. (1987). Aggregation of complement receptors on human neutrophils in the absence of ligand. *J Cell Biol.* **105**, 1137-1145.
Diamond, G., Beckloff, N., Weinberg, A. and Kisich, K. O. (2009). The roles of antimicrobial peptides in innate host defense. *Curr Pharm Des.* **15**, 2377-2392.
Dice, J. F. (2007). Chaperone-mediated autophagy. *Autophagy.* **3**, 295-299.
Dietz, J. N. and Cole, B. C. (1982). Direct Activation of the J774.1 Murine Macrophage Cell Line by Mycoplasma arthritidis. *Infect Immun.* **37**, 811-819.
Diment, S., Leech, M. S. and Stahl, P. D. (1988). Cathepsin D is membrane-associated in macrophage endosomes. *J Biol Chem.* **263**, 6901-6907.
Dorer, F. E., Lentz, K. E., Kahn, J. R., Levine, M. and Skeggs, L. T. (1978). A comparison of the substrate specificities of cathepsin D and pseudorenin. *J Biol Chem.* **253**, 3140-3142.
Dunn, M. J. (1989). Initial Planning. In *Protein purification methods*, (ed. E. L. V. Harris and S. Angal), pp. 37-40. New York: Oxford University Press.
Dyer, D. W., West, E. P. and Sparling, P. F. (1987). Effects of serum carrier proteins on the growth of pathogenic neisseriae with heme-bound iron. *Infect Immun.* **55**, 2171-2175.
Eickhoff, T. C. and Myers, M. (2002). Workshop summary. Aluminum in vaccines. *Vaccine.* **20** S1-S4.
Eldred, W. D., Zucker, C., Karten, H. J. and Yazulla, S. (1983). Comparison of fixation and penetration enhancement techniques for use in ultrastructural immunocytochemistry. *J Histochem Cytochem.* **31**, 285-292.

Elhelu, M. A. (1983). The role of macrophages in immunology. *J Natl Med Assoc.* **75**, 314-317.
Eskelinen, E. L. (2006). Roles of LAMP-1 and LAMP-2 in lysosome biogenesis and autophagy. *Mol Aspects Med.* **27**, 495-502.
Eskelinen, E. L., Illert, A. L., Tanaka, Y., Schwarzmann, G., Blanz, J., Von Figura, K. and Saftig, P. (2002). Role of LAMP-2 in lysosome biogenesis and autophagy. *Mol Biol Cell.* **13**, 3355-3368.
Eskelinen, E. L., Schmidt, C. K., Neu, S., Willenborg, M., Fuertes, G., Salvador, N., Tanaka, Y., Lüllmann-Rauch, R., Hartmann, D., Heeren, J. *et al.* (2004). Disturbed cholesterol traffic but normal proteolytic function in LAMP-1/LAMP-2 double-deficient fibroblasts. *Mol Biol Cell.* **15**, 3132-3145.
Fabrino, D. L., Bleck, C. K., Anes, E., Hasilik, A., Melo, R. C., Niederweis, M., Griffiths, G. and Gutierrez, M. G. (2009). Porins facilitate nitric oxide-mediated killing of mycobacteria. *Microbes Infect.* **11**, 868-875.
Fahie-Wilson, M. and Halsall, D. (2008). Polyethylene glycol precipitation: proceed with care. *Ann Clin Biochem.* **45**, 233-235.
Feng, D., Marshburn, D., Jen, D., Weinberg, R. J., Taylor, R. M. and Burette, A. (2007). Stepping into the third dimension. *J Neurosci.* **27**, 12757-12760.
Ferrante, A., Anderson, M. W., Klug, C. S. and Gorski, J. (2008). HLA-DM mediates epitope selection by a "compare-exchange" mechanism when a potential peptide pool is available. *PLoS One.* **3**, 1-14.
Fikrig, E., Barthold, S. W. and Flavell, R. A. (1993). OspA vaccination of mice with established Borrelia burgdorferi infection alters disease but not infection. *Infect Immun.* **61**, 2553-2557.
Fleisher, T. A. (1997). Immune function. *Pediatr Rev.* **18**, 351-356.
Flynn, J. L. and Chan, J. (2001a). Immunology of tuberculosis. *Annu Rev Immunol.* **19**, 193-129.
Flynn, J. L. and Chan, J. (2001b). Tuberculosis: latency and reactivation. *Infect Immun.* **69**, 4195-4201.
Flynn, J. L. and Chan, J. (2003). Immune evasion by Mycobacterium tuberculosis: living with the enemy. *Curr Opin Immunol.* **15**, 450-455.
Foreman, A. L., Van de Water, J., Gougeon, M. L. and Gershwin, M. E. (2007). B cells in autoimmune diseases: insights from analyses of immunoglobulin variable (Ig V) gene usage. *Autoimmun Rev.* **6**, 387-401.
Forman, H. J. and Torres, M. (2002). Reactive oxygen species and cell signaling: respiratory burst in macrophage signaling. *Am J Respir Crit Care Med.* **166**, S4-S8.
Fortgens, P. (1996). Proteinases and extracellular matrix degradation in breast cancer. *Department of Biochemistry.* **PhD thesis**, University of Natal, Pietermaritzburg.
French, A. P., Mills, S., Swarup, R., Bennett, M. J. and Pridmore, T. P. (2008). Colocalization of fluorescent markers in confocal microscope images of plant cells. *Nat Protoc.* **3**, 619-628.
Freund, J. (1956). The mode of action of immunologic adjuvants. *Bibl Tuberc.* **10**, 130-148.
Freundt, E. C., Czapiga, M. and Lenardo, M. J. (2007). Photoconversion of Lysotracker Red to a green fluorescent molecule. *Cell Res.* **17**, 956-958.

Fu, G., Chen, Y., Yu, M., Podd, A., Schuman, J., He, Y., Di, L., Yassai, M., Haribhai, D., North, P. E. *et al.* (2010). Phospholipase C{gamma}1 is essential for T cell development, activation, and tolerance. *J Exp Med.* **207**, 309-318.
Fukuda, M. (1991). Lysosomal membrane glycoproteins. Structure, biosynthesis, and intracellular trafficking. *J Biol Chem.* **266**, 21327-21330.
Fuller, J. R., Craven, R. R., Hall, J. D., Kijek, T. M., Taft-Benz, S. and Kawula, T. H. (2008). RipA, a cytoplasmic membrane protein conserved among Francisella species, is required for intracellular survival. *Infect Immun.* **76**, 4934-4943.
Gacko, M., Minarowska, A., Karwowska, A. and Minarowski, Ł. (2007). Cathepsin D inhibitors. *Folia Histochem Cytobiol.* **45**, 291-313.
Gallagher, S. R. (2006). One-dimensional SDS gel electrophoresis of proteins. *Curr Protoc Immunol.* **Chapter 8**, Unit 8.4.
Gammon, S. T., Leevy, W. M., Gross, S., Gokel, G. W. and Piwnica-Worms, D. (2006). Spectral unmixing of multicolored bioluminescence emitted from heterogeneous biological sources. *Anal Chem.* **78**, 1520-1527.
Ganz, T. (2009). Iron in innate immunity: starve the invaders. *Curr Opin Immunol.* **21**, 63-67.
García-García, E. and Rosales, C. (2002). Signal transduction during Fc receptor-mediated phagocytosis. *J Leukoc Biol.* **72**, 1092-1108.
Garfin, D. E. (1990). One-dimensional gel electrophoresis. In *Guide to Protein Purification, Methods in Enzymology*, vol. 182 (ed. M. P. Deutscher), pp. 425-441. San Diego: Academic Press, Inc.
Garwicz, D., Lindmark, A., Persson, A. M. and Gullberg, U. (1998). On the role of the proform-conformation for processing and intracellular sorting of human cathepsin G. *Blood.* **92**, 1415-1422.
Giepmans, B. N. (2008). Bridging fluorescence microscopy and electron microscopy. *Histochem Cell Biol.* **130**, 211-217.
Girish, V. and Vijayalakshmi, A. (2004). Affordable image analysis using NIH Image/ImageJ. *Indian J Cancer.* **41**, 47.
Goldring, J. P. D. and Coetzer, T. H. T. (2003). Isolation of chicken immunoglobulins (IgY) from egg yolk. *Biochem Mol Biol Educ* **31**, 185-187.
Good, N. E., Winget, G. D., Winter, W., Connolly, T. N., Izawa, S. and Singh, R. M. (1966). Hydrogen ion buffers for biological research. *Biochemistry.* **5**, 467-477.
Goping, G., Kuijpers, G. A., Vinet, R. and Pollard, H. B. (1996). Comparison of LR White and Unicryl as embedding media for light and electron immunomicroscopy of chromaffin cells. *J Histochem Cytochem.* **44**, 289-295.
Gough, N. R., Zweifel, M. E., Martinez-Augustin, O., Aguilar, R. C., Bonifacino, J. S. and Fambrough, D. M. (1999). Utilization of the indirect lysosome targeting pathway by lysosome-associated membrane proteins (LAMPs) is influenced largely by the C-terminal residue of their GYXXphi targeting signals. *J Cell Sci.* **112**, 4257-4269.
Govoni, G. and Gros, P. (1998). Macrophage NRAMP1 and its role in resistance to microbial infections. *Inflamm Res.* **47**, 277-284.
Greenberg, S. (1999). Modular components of phagocytosis.
. *J Leukoc Biol.* **66**, 712-717.
Griffiths, G. (1993a). Embedding Media for Section Immunocytochemistry. In *Fine structure Immunocytochemistry*, pp. 90-136. Berlin: Springer-Verlag.

Griffiths, G. (1993b). Fixation for fine structure preservation and immunocytochemistry. In *Fine Structure Immunocytochemistry.*, pp. 26-89. Berlin: Springer-Verlag.
Griffiths, G. (1993c). Non-Immunological High-Affinity Interactions Used for Labelling. In *Fine Structure Immunocytochemistry.*, pp. 307-344. Berlin: Springer-Verlag.
Griffiths, G. (2004). On phagosome individuality and membrane signalling networks. *TRENDS in Cell Biology* **14**, 343-351.
Gruenberg, J. (2001). The endocytic pathway: a mosaic of domains. *Nat Rev Mol Cell Biol.* **2**, 721-730.
Gruenberg, J. and Maxfield, F. R. (1995). Membrane transport in the endocytic pathway. *Curr Opin Cell Biol.* **7**, 552-563.
Gruenheid, S., Canonne-Hergaux, F., Gauthier, S., Hackam, D. J., Grinstein, S. and Gros, P. (1999). The iron transport protein NRAMP2 is an integral membrane glycoprotein that colocalizes with transferrin in recycling endosomes. *J Exp Med.* **189**, 831-841.
Gu, F. and Gruenberg, J. (1999). Biogenesis of transport intermediates in the endocytic pathway. *FEBS Lett.* **452**, 61-66.
Guermonprez, P., Saveanu, L., Kleijmeer, M., Davoust, J., Van Endert, P. and Amigorena, S. (2003). ER-phagosome fusion defines an MHC class I cross-presentation compartment in dendritic cells. *Nature.* **425**, 397-402.
Gutierrez, M. G., Mishra, B. B., Jordao, L., Elliott, E., Anes, E. and Griffiths, G. (2008). NF-kappa B activation controls phagolysosome fusion-mediated killing of mycobacteria by macrophages. *J Immunol.* **181**, 2651-2663.
Hackam, D. J., Rotstein, O. D., Zhang, W., Gruenheid, S., Gros, P. and Grinstein, S. (1998). Host resistance to intracellular infection: mutation of natural resistance-associated macrophage protein 1 (Nramp1) impairs phagosomal acidification. *J Exp Med.* **188**, 351-364.
Hackam, D. J., Rotstein, O. D., Zhang, W. J., Demaurex, N., Woodside, M., Tsai, O. and Grinstein, S. (1997). Regulation of phagosomal acidification. Differential targeting of Na+/H+ exchangers, Na+/K+-ATPases, and vacuolar-type H+-atpases. *J Biol Chem.* **272**, 29810-29820.
Halliday, L. C., Artwohl, J. E., Hanly, W. C., Bunte, R. M. and Bennett, B. T. (2000). Physiologic and behavioral assessment of rabbits immunized with Freund's complete adjuvant. *Contemp Top Lab Anim Sci.* **39**, 8-13.
Hampton, M. B., Kettle, A. J. and Winterbourn, C. C. (1998). Inside the neutrophil phagosome: oxidants, myeloperoxidase, and bacterial killing. *Blood.* **92**, 3007-3017.
Hanekom, W. A., Lawn, S. D., Dheda, K. and Whitelaw, A. (2010). Tuberculosis research update. *Trop Med Int Health.* **15**, 981-989.
Hanly, W. C., Artwohl, J. E. and Bennett, B. T. (1995). Review of Polyclonal Antibody Production Procedures in Mammals and Poultry. *ILAR J.* **37**, 93-118.
Harrison, J. E. and Schultz, J. (1976). Studies on the chlorinating activity of myeloperoxidase. *J Biol Chem.* **251**, 1371-1374.
Hart, P. D., Young, M. R., Gordon, A. H. and Sullivan, K. H. (1987). Inhibition of phagosome-lysosome fusion in macrophages by certain mycobacteria can be explained by inhibition of lysosomal movements observed after phagocytosis. *J Exp Med.* **166**, 933-946.

Haskó, G., Pacher, P., Deitch, E. A. and Vizi, E. S. (2007). Shaping of monocyte and macrophage function by adenosine receptors. *Pharmacol Ther.* **113**, 264-275.
Hau, J. and Hendriksen, C. F. (2005). Refinement of polyclonal antibody production by combining oral immunization of chickens with harvest of antibodies from the egg yolk. *ILAR J.* **46**, 294-299.
Hayat, M. A. (2000a). Chemical Fixation. In *Principles and Techniques of Electron Microscopy.* , pp. 4-84. New York: Cambridge University Press.
Hayat, M. A. (2000b). Rinsing, Dehydration, and Embedding. In *Principles and Techniques of Electron Microscopy.*, pp. 85-137. New York: Cambridge University Press.
Hayat, M. A. (2000c). Sectioning. In *Principles and Techniques of Electron Microscopy.* , pp. 139-210. New York: Cambridge University Press.
He, Z. and De Buck, J. (2010). Cell wall proteome analysis of Mycobacterium smegmatis strain MC2 155. *BMC Microbiol.* **10**, 121-130.
Heale, J.-P. and Speert, D. P. (2002). Macrophages in bacterial infection. . In *The macrophage*, (ed. B. Burke and C. E. Lewis), pp. 210-224. Oxford: Oxford University Press, pp 210-252.
Heim, R., Prasher, D. C. and Tsien, R. Y. (1994). Wavelength mutations and posttranslational autoxidation of green fluorescent protein. *Proc Natl Acad Sci U S A.* **91**, 12501-12504.
Henneke, P. and Golenbock, D. T. (2004). Phagocytosis, innate immunity, and host-pathogen specificity. *J Exp Med.* **199**, 1-4.
Herman, B. (1998a). Applications of fluorescence microscopy. In *Fluorescence Microscopy*, (ed. J. Leonard), pp. 47-68. New York: BIOS Scientific Publishers Limited.
Herman, B. (1998b). Fluorescence microscopy. In *Fluorescence Microscopy*, (ed. J. Leonard), pp. 15-38. New York: Bios Scientific Publishers Limited.
Herman, B. (1998c). Fundamentals of fluorescence. In *Fluorescence Microscopy*, (ed. J. Leonard), pp. 1-12. New York: BIOS Scientific Publishers Limited.
Herman, B. (1998d). Single and multiphoton microscopy. In *Fluorescence Microscopy*, (ed. J. Leonard), pp. 89-99. New York: Bios Scientific Publishers Limited.
Heussen, C. and Dowdle, E. B. (1980). Electrophoretic analysis of plasminogen activators in polyacrylamide gels containing sodium dodecyl sulfate and copolymerized substrates. *Anal Biochem.* **102**, 196-202.
Hewitt, E. W. (2003). The MHC class I antigen presentation pathway: strategies for viral immune evasion. *Immunology.* **110**, 163-169.
Hinz, U. (2010). From protein sequences to 3D-structures and beyond: the example of the UniProt knowledgebase. *Cell Mol Life Sci.* **67**, 1049-1064.
Houde, M., Bertholet, S., Gagnon, E., Brunet, S., Goyette, G., Laplante, A., Princiotta, M. F., Thibault, P., Sacks, D. and Desjardins, M. (2003). Phagosomes are competent organelles for antigen cross-presentation. *Nature.* **425**, 402-406.
Hu, T., Simmons, A., Yuan, J., Bender, T. P. and Alberola-Ila, J. (2010). The transcription factor c-Myb primes CD4+CD8+ immature thymocytes for selection into the iNKT lineage. *Nat Immunol.* **11**, 435-441.
Huang, S., Gilfillan, S., Kim, S., Thompson, B., Wang, X., Sant, A. J., Fremont, D. H., Lantz, O. and Hansen, T. H. (2008). MR1 uses an endocytic pathway to activate mucosal-associated invariant T cells. *J Exp Med.* **205**, 1201-1211.

Hunter, R. L. (2002). Overview of vaccine adjuvants: present and future. *Vaccine.* **20** S7-S12.
Hunziker, W. and Geuze, H. J. (1996). Intracellular trafficking of lysosomal membrane proteins. *Bioessays.* **18**, 379-389.
Huynh, K. K., Eskelinen, E. L., Scott, C. C., Malevanets, A., Saftig, P. and Grinstein, S. (2007a). LAMP proteins are required for fusion of lysosomes with phagosomes. *EMBO J.* **26**, 313-324.
Huynh, K. K., Kay, J. G., Stow, J. L. and Grinstein, S. (2007b). Fusion, fission, and secretion during phagocytosis. *Physiology (Bethesda).* **22**, 366-372.
Ilk, N., Küpcü, S., Moncayo, G., Klimt, S., Ecker, R. C., Hofer-Warbinek, R., Egelseer, E. M., Sleytr, U. B. and Sára, M. (2004). A functional chimaeric S-layer-enhanced green fluorescent protein to follow the uptake of S-layer-coated liposomes into eukaryotic cells. *Biochem J.* **379**, 441-448.
Indik, Z. K., Park, J. G., Hunter, S. and Schreiber, A. D. (1995). The molecular dissection of Fc gamma receptor mediated phagocytosis. *Blood.* **86**, 4389-4399.
Inoue, S. (1995). Foundations of Confocal Scanned Imaging in Light Microscopy. In *Handbook of Biological Confocal Microscopy*, (ed. J. B. Pawley), pp. 1-17. New York: Plenum Press.
Jackson, J. G. (2005). Changes in endosome-lysosome pH accompanying pre-mailgnant transformation. *Department of Biochemistry.* **PhD thesis**, University of KwaZulu-Natal, Pietermaritzburg.
Jacob, M. C., Favre, M. and Bensa, J. C. (1991). Membrane cell permeabilization with saponin and multiparametric analysis by flow cytometry. *Cytometry.* **12**, 550-558.
Jacobs, G. R., Pike, R. N. and Dennison, C. (1989). Isolation of cathepsin D using three-phase partitioning in t-butanol/water/ammonium sulfate. *Anal Biochem.* **180**, 169-171.
Jacobsen, N. E., Fairbrother, W. J., Kensil, C. R., Lim, A., Wheeler, D. A. and Powell, M. F. (1996). Structure of the saponin adjuvant QS-21 and its base-catalyzed isomerization product by 1H and natural abundance 13C NMR spectroscopy. *Carbohydr Res.* **280**, 1-14.
Jahraus, A., Egeberg, M., Hinner, B., Habermann, A., Sackman, E., Pralle, A., Faulstich, H., Rybin, V., Defacque, H. and Griffiths, G. (2001). ATP-dependent membrane assembly of F-actin facilitates membrane fusion. *Mol Biol Cell.* **12**, 155-170.
Jahreiss, L., Menzies, F. M. and Rubinsztein, D. C. (2008). The itinerary of autophagosomes: from peripheral formation to kiss-and-run fusion with lysosomes. *Traffic.* **9**, 574-587.
Jain, E., Bairoch, A., Duvaud, S., Phan, I., Redaschi, N., Suzek, B. E., Martin, M. J., McGarvey, P. and Gasteiger, E. (2009). Infrastructure for the life sciences: design and implementation of the UniProt website. *BMC Bioinformatics.* **10**, 136-150.
Janeway, C., Travers, P., Walport, M. and Schlomchik, M. J. (2005a). The adaptive immune response. In *Immuno Biology*, (ed. E. Lawrence G. Bushell M. Morales and B. Goatly), pp. 319-409. New York: Garland Science Publishing.
Janeway, C., Travers, P., Walport, M. and Schlomchik, M. J. (2005b). Basic concepts in Immunology. In *Immuno Biology* (ed. E. Lawrence G. Bushell M. Morales and B. Goatly), pp. 1-35. New York: Garland Science Publishing.
Janvier, K. and Bonifacino, J. S. (2005). Role of the endocytic machinery in the sorting of lysosome-associated membrane proteins. *Mol Biol Cell.* **16**, 4231-4242.

Jennings, R., Simms, J. R. and Heath, A. W. (1998). Adjuvants and delivery systems for viral vaccines--mechanisms and potential. *Dev Biol Stand.* **92**, 19-28.
Jennings, V. M. (1995). Review of Selected Adjuvants Used in Antibody Production. *ILAR J.* **37**, 119-125.
Jensen, M. S. and Bainton, D. F. (1973). Temporal changes in pH within the phagocytic vacuole of the polymorphonuclear neutrophilic leukocyte. *J Cell Biol.* **56**, 379-388.
Jensenius, J. C., Andersen, I., Hau, J., Crone, M. and Koch, C. (1981). Eggs: conveniently packaged antibodies. Methods for purification of yolk IgG. *J Immunol Methods.* **46**, 63-68.
Jepras, R. I., Carter, J., Pearson, S. C., Paul, F. E. and Wilkinson, M. J. (1995). Development of a Robust Flow Cytometric Assay for Determining Numbers of Viable Bacteria. *Appl Environ Microbiol.* **61**, 2696-2701.
Jie, Y. H., Cammisuli, S. and Baggliolini, M. (1984). Immunomodulatory effects of Panax ginseng CA Meyer in the mouse. *Agents Actions.* **15**, 386-391.
Johnson, M., Zaretskaya, I., Raytselis, Y., Merezhuk, Y., McGinnis, S. and Madden, T. L. (2008). NCBI BLAST: a better web interface. *Nucleic Acids Res.* **36**, W5-W9.
Jovic, M., Sharma, M., Rahajeng, J. and Caplan, S. (2010). The early endosome: a busy sorting station for proteins at the crossroads. *Histol Histopathol.* **25**, 99-112.
Kaiko, G. E., Horvat, J. C., Beagley, K. W. and Hansbro, P. M. (2008). Immunological decision-making: how does the immune system decide to mount a helper T-cell response? *Immunology.* **123**, 326-338.
Kaniuk, A. S., Lortan, J. E. and Monteil, M. A. (1992). Specific IgG subclass antibody levels and phagocytosis of serotype 14 pneumococcus following immunization. *Scand J Immunol Suppl.* **11**, 96-98.
Karanam, B., Gambhira, R., Peng, S., Jagu, S., Kim, D. J., Ketner, G. W., Stern, P. L., Adams, R. J. and Roden, R. B. (2009). Vaccination with HPV16 L2E6E7 fusion protein in GPI-0100 adjuvant elicits protective humoral and cell-mediated immunity. *Vaccine.* **27**, 1040-1049.
Karttunen, T., Sormunen, R., Risteli, L., Risteli, J. and Autio-Harmainen, H. (1989). Immunoelectron microscopic localization of laminin, type IV collagen, and type III pN-collagen in reticular fibers of human lymph nodes. *J Histochem Cytochem.* **37**, 279-286.
Kaufmann, S. H. (2010). Future vaccination strategies against tuberculosis: thinking outside the box. *Immunity.* **33**, 567-577.
Kempf, E. K. (1973). Transmission electron microscopy of fossil spores. *Palaeontology* **16**, 787-797.
Kenney, R. T., Sacks, D. L., Sypek, J. P., Vilela, L., Gam, A. A. and Evans-Davis, K. (1999). Protective immunity using recombinant human IL-12 and alum as adjuvants in a primate model of cutaneous leishmaniasis. *J Immunol.* **163**, 4481-4488.
Kensil, C. R. (1996). Saponins as vaccine adjuvants. *Crit Rev Ther Drug Carrier Syst.* **13**, 1-55.
Kensil, C. R., Patel, U., Lennick, M. and Marciani, D. (1991). Separation and characterization of saponins with adjuvant activity from *Quillaja* saponaria Molina cortex. *J Immunol.* **146**, 431-437.

Kensil, C. R., Wu, J. Y., Anderson, C. A., Wheeler, D. A. and Amsden, J. (1998). QS-21 and QS-7: purified saponin adjuvants. *Dev Biol Stand.* **92**, 41-47.
Kersey, J. H. and Gajl-Peczalska, J. (1975). T and B lymphocytes in humans. A review. *Am J Pathol.* **81**, 446-458.
Killisch, I., Steinlein, P., Römisch, K., Hollinshead, R., Beug, H. and Griffiths, G. (1992). Characterization of early and late endocytic compartments of the transferrin cycle. Transferrin receptor antibody blocks erythroid differentiation by trapping the receptor in the early endosome. *J Cell Sci.* **103**, 211-232.
Kim, Y. J., Wang, P., Navarro-Villalobos, M., Rohde, B. D., Derryberry, J. and Gin, D. Y. (2006). Synthetic studies of complex immunostimulants from Quillaja saponaria: synthesis of the potent clinical immunoadjuvant QS-21Aapi. *J Am Chem Soc.* **128**, 11906-11915.
Kjeken, R., Egeberg, M., Habermann, A., Kuehnel, M., Peyron, P., Floetenmeyer, M., Walther, P., Jahraus, A., Defacque, H., Kuznetsov, S. A. *et al.* (2004). Fusion between phagosomes, early and late endosomes: a role for actin in fusion between late, but not early endocytic organelles. *Mol Biol Cell.* **15**, 345-358.
Klebanoff, S. J. (2005). Myeloperoxidase: friend and foe.
. *J Leukoc Biol.* **77**, 598-625.
Kneen, M., Farinas, J., Li, Y. and Verkman, A. S. (1998). Green fluorescent protein as a noninvasive intracellular pH indicator. *Biophys J.* **74**, 1591-1599.
Kool, M., Soullié, T., van Nimwegen, M., Willart, M. A., Muskens, F., Jung, S., Hoogsteden, H. C., Hammad, H. and Lambrecht, B. N. (2008). Alum adjuvant boosts adaptive immunity by inducing uric acid and activating inflammatory dendritic cells. *J Exp Med.* **205**, 869-882.
Krishnan, J., Selvarajoo, K., Tsuchiya, M., Lee, G. and Choi, S. (2007). Toll-like receptor signal transduction. *Exp Mol Med.* **39**, 421-438.
Kundra, R. and Kornfeld, S. (1999). Asparagine-linked oligosaccharides protect Lamp-1 and Lamp-2 from intracellular proteolysis. *J Biol Chem.* **274**, 31039-31046.
Kuroda, A. (2006). A polyphosphate-lon protease complex in the adaptation of Escherichia coli to amino acid starvation. *Biosci Biotechnol Biochem.* **70**, 325-331.
Kyhse-Andersen, J. (1984). Electroblotting of multiple gels: a simple apparatus without buffer tank for rapid transfer of proteins from polyacrylamide to nitrocellulose. *J Biochem Biophys Methods.* **10**, 203-209.
Laemmli, U. K. (1970). Cleavage of structural proteins during the assembly of the head of bacteriophage T4. *Nature.* **227**, 680-685.
Lahiri, R., Randhawa, B. and Krahenbuhl, J. (2005). Application of a viability-staining method for *Mycobacterium leprae* derived from the athymic (nu/nu) mouse foot pad. *J Med Microbiol.* **54**, 235-242.
Lam, J., Herant, M., Dembo, M. and Heinrich, V. (2009). Baseline mechanical characterization of J774 macrophages. *Biophys J.* **96**, 248-254.
Lamberts, R. and Goldsmith, P. C. (1986). Fixation, fine structure, and immunostaining for neuropeptides: perfusion versus immersion of the neuroendocrine hypothalamus. *J Histochem Cytochem.* **34**, 389-398.
Landowski, C. P., Godfrey, H. P., Bentley-Hibbert, S. I., Liu, X., Huang, Z., Sepulveda, R., Huygen, K., Gennaro, M. L., Moy, F. H., Lesley, S. A. *et al.* (2001). Combinatorial use of antibodies to secreted mycobacterial proteins in a host immune system-independent test for tuberculosis. *J Clin Microbiol.* **39**, 2418-2424.

Langman, R. E. and Cohn, M. (2000). A minimal model for the self-nonself discrimination: a return to the basics. *Semin Immunol.* **12**, 189-195.
Latta, H. and Hartmann, J. F. (1950). Use of a glass edge in thin sectioning for electron microscopy. *Proc Soc Exp Biol Med.* **74**, 436-439.
Laurent-Matha, V., Derocq, D., Prébois, C., Katunuma, N. and Liaudet-Coopman, E. (2006). Processing of human cathepsin D is independent of its catalytic function and auto-activation: involvement of cathepsins L and B. *J Biochem.* **139**, 363-371.
Lawn, S. D., Wood, R. and Wilkinson, R. J. (2010). Changing concepts of "latent tuberculosis infection" in patients living with HIV infection. *Clin Dev Immunol.* **2011**, 1-9.
Lee, B. Y., Clemens, D. L. and Horwitz, M. A. (2008a). The metabolic activity of *Mycobacterium tuberculosis*, assessed by use of a novel inducible GFP expression system, correlates with its capacity to inhibit phagosomal maturation and acidification in human macrophages. *Mol Microbiol.* **68**, 1047-1060.
Lee, K. K. (2010). Architecture of a nascent viral fusion pore. *EMBO J.* **29**, 1299-1311.
Lee, S. J., Kim, S. J., Kim, E. S., Geroski, D. H., McCarey, B. E. and Edelhauser, H. F. (2008b). Trans-scleral permeability of Oregon green 488. *J Ocul Pharmacol Ther.* **24**, 579-586.
Leenaars, M. and Hendriksen, C. F. (2005). Critical steps in the production of polyclonal and monoclonal antibodies: evaluation and recommendations. *ILAR J.* **46**, 269-279.
Leenaars, P. P., Koedam, M. A., Wester, P. W., Baumans, V., Claassen, E. and Hendriksen, C. F. (1998). Assessment of side effects induced by injection of different adjuvant/antigen combinations in rabbits and mice. *Lab Anim.* **32**, 387-406.
Lehrer, R. I. and Ganz, T. (1990). Antimicrobial polypeptides of human neutrophils. *Blood.* **76**, 2169-2181.
Lemmon, S. K. and Traub, L. M. (2000). Sorting in the endosomal system in yeast and animal cells. *Curr Opin Cell Biol.* **12**, 457-466.
Levy, J., Kolski, G. B. and Douglas, S. D. (1989). Cathepsin D-like activity in neutrophils and monocytes. *Infect Immun.* **57**, 1632-1634.
Li, Q., Lau, A., Morris, T. J., Guo, L., Fordyce, C. B. and Stanley, E. F. (2004). A syntaxin 1, Galpha(o), and N-type calcium channel complex at a presynaptic nerve terminal: analysis by quantitative immunocolocalization. *J Neurosci.* **24**, 4070-4081.
Lin, C. Y. (2007). Production of cathepsin D antibodies for the use in studies on *Mycobacterium tuberculosis*. *Department of Biochemistry* **Honours dissertation.**, University of KwaZulu-Natal, Pietermaritzburg.
Lindskog, M., Rockberg, J., Uhlén, M. and Sterky, F. (2005). Selection of protein epitopes for antibody production. *Biotechniques.* **38**, 723-727.
Lippolis, J. D. (2008). Immunological signaling networks: integrating the body's immune response. *J Anim Sci.* **86**, E53-E63.
Liu, X. and Bosselut, R. (2004). Duration of TCR signaling controls CD4-CD8 lineage differentiation in vivo. *Nat Immunol.* **5**, 280-288.
Lowder, M., Unge, A., Maraha, N., Jansson, J. K., Swiggett, J. and Oliver, J. D. (2000). Effect of starvation and the viable-but-nonculturable state on green fluorescent protein (GFP) fluorescence in GFP-tagged Pseudomonas fluorescens A506. *Appl Environ Microbiol.* **66**, 3160-3165.

Lowrie, D. B. and Andrew, P. W. (1988). Macrophage antimycobacterial mechanisms. *Br Med Bull.* **44**, 624-634.
Lowrie, D. B., Andrew, P. W. and Peters, T. J. (1979). Analytical subcellular fractionation of alveolar macrophages from normal and BCG-vaccinated rabbits with particular reference to heterogeneity of hydrolase-containing granules. *Biochem J.* **178**, 761-767.
Ludwig, T., Griffiths, G. and Hoflack, B. (1991). Distribution of newly synthesized lysosomal enzymes in the endocytic pathway of normal rat kidney cells. *J Cell Biol.* **115**, 1561-1572.
Lukacs, G. L., Rotstein, O. D. and Grinstein, S. (1990). Phagosomal acidification is mediated by a vacuolar-type H(+)-ATPase in murine macrophages. *J Biol Chem.* **265**, 21099-21107.
MacIvor, D. M., Shapiro, S. D., Pham, C. T., Belaaouaj, A., Abraham, S. N. and Ley, T. J. (1999). Normal neutrophil function in cathepsin G-deficient mice. *Blood.* **94**, 4282-4293.
MacLennan, I. C., Gulbranson-Judge, A., Toellner, K. M., Casamayor-Palleja, M., Chan, E., Sze, D. M., Luther, S. A. and Orbea, H. A. (1997). The changing preference of T and B cells for partners as T-dependent antibody responses develop. *Immunol Rev.* **156**, 53-66.
Malik, Z. A., Denning, G. M. and Kusner, D. J. (2000). Inhibition of Ca(2+) signaling by *Mycobacterium tuberculosis* is associated with reduced phagosome-lysosome fusion and increased survival within human macrophages. *J Exp Med.* **191**, 287-302.
Mallon, F. M., Graichen, M. E., Conway, B. R., Landi, M. S. and Hughes, H. C. (1991). Comparison of antibody response by use of synthetic adjuvant system and Freund complete adjuvant in rabbits. *Am J Vet Res.* **52**, 1503-1506.
Manders, E. M. M., Verbeek, F. J. and Aten, J. A. (1992). Measurement of co-localization of objects in dual-colour confocal images. *J Microsc.* **169**, 375-382.
Mannhalter, J. W., Neychev, H. O., Zlabinger, G. J., Ahmad, R. and Eibl, M. M. (1985). Modulation of the human immune response by the non-toxic and non-pyrogenic adjuvant aluminium hydroxide: effect on antigen uptake and antigen presentation. *Clin Exp Immunol.* **61**, 143-151.
Mantegazza, A. R., Barrio, M. M., Moutel, S., Bover, L., Weck, M., Brossart, P., Teillaud, J. L. and Mordoh, J. (2004). CD63 tetraspanin slows down cell migration and translocates to the endosomal-lysosomal-MIICs route after extracellular stimuli in human immature dendritic cells. *Blood.* **104**, 1183-1190.
Martino, A., Sacchi, A., Volpe, E., Agrati, C., De Santis, R., Pucillo, L. P., Colizzi, V. and Vendetti, S. (2005). Non-pathogenic *Mycobacterium smegmatis* induces the differentiation of human monocytes directly into fully mature dendritic cells. *J Clin Immunol.* **25**, 365-375.
Mathews, P. M., Guerra, C. B., Jiang, Y., Grbovic, O. M., Kao, B. H., Schmidt, S. D., Dinakar, R., Mercken, M., Hille-Rehfeld, A., Rohrer, J. *et al.* (2002). Alzheimer's disease-related overexpression of the cation-dependent mannose 6-phosphate receptor increases Abeta secretion: role for altered lysosomal hydrolase distribution in beta-amyloidogenesis. *J Biol Chem.* **277**, 5299-5307.

Matsuo, H., Chevallier, J., Mayran, N., Le Blanc, I., Ferguson, C., Fauré, J., Blanc, N. S., Matile, S., Dubochet, J., Sadoul, R. *et al.* (2004). Role of LBPA and Alix in multivesicular liposome formation and endosome organization. *Science.* **303**, 531-534.
May, R. C. and Machesky, L. M. (2001). Phagocytosis and the actin cytoskeleton. *J Cell Sci.* **114**, 1061-1077.
McGaw, L. J., Lall, N., Meyer, J. J. and Eloff, J. N. (2008). The potential of South African plants against Mycobacterium infections. *J Ethnopharmacol.* **119**, 482-500.
McKee, A. S., Munks, M. W. and Marrack, P. (2007). How do adjuvants work? Important considerations for new generation adjuvants. *Immunity.* **27**, 687-690.
McNally, J. G., Karpova, T., Cooper, J. and Conchello, J. A. (1999). Three-dimensional imaging by deconvolution microscopy. *Methods.* **19**, 373-385.
McNeil, P. L., Tanasugarn, L., Meigs, J. B. and Taylor, D. L. (1983). Acidification of phagosomes is initiated before lysosomal enzyme activity is detected. *J Cell Biol.* **97**, 692-702.
Merighi, A. (1992). Post-embedding electron microscopic immunocytochemistry. In *Electron Microscopic Immunocytochemistry Principles and Practice*, (ed. J. M. Polak and V. P. John), pp. 51-89. New York: Oxford University Press.
Merril, C. R. (1990). Gel-staining techniques. In *Guide to Protein Purification, Methods in Enzymology.*, vol. 182 (ed. M. P. Deutscher), pp. 477-488. San Diego: Academic Press, Inc.
Mickelsen, P. A. and Sparling, P. F. (1981). Ability of *Neisseria gonorrhoeae, Neisseria meningitidis*, and commensal Neisseria species to obtain iron from transferrin and iron compounds. *Infect Immun.* **33**, 555-564.
Middlebrook, G. and Cohn, M. L. (1958). Bacteriology of tuberculosis: laboratory methods. *Am J Public Health Nations Health.* **48**, 844-853.
Migliori, G. B., Dheda, K., Centis, R., Mwaba, P., Bates, M., O'Grady, J., Hoelscher, M. and Zumla, A. (2010). Review of multidrug-resistant and extensively drug-resistant TB: global perspectives with a focus on sub-Saharan Africa. *Trop Med Int Health.* **15**, 1052-1066.
Minarowska, A., Gacko, M., Karwowska, A. and Minarowski, Ł. (2008). Human cathepsin D. *Folia Histochem Cytobiol.* **46**, 23-38.
Minarowska, A., Minarowski, L., Karwowska, A. and Gacko, M. (2007a). Regulatory role of cathepsin D in apoptosis. *Folia Histochem Cytobiol.* **45**, 159-163.
Minarowska, A., Minarowski, L., Karwowska, A., Sands, D. and Dabrowska, E. (2007b). The activity of cathepsin D in saliva of cystic fibrosis patients. *Folia Histochem Cytobiol.* **45**, 165-168.
Minsky, M. (1988). Memoir on inventing the confocal scanning microscope. *Scanning* **10**, 128-138.
Mkhwanazi, B. (2009). Cathepsin D antibodies for use in studies on macrophage killing of mycobacteria. *Department of Biochemistry.* **Honours dissertation**, University of KwaZulu-Natal, Pietermaritzburg.
Mohrmann, K. and van der Sluijs, P. (1999). Regulation of membrane transport through the endocytic pathway by rabGTPases. *Mol Membr Biol.* **16**, 81-87.
Moorewood, C. R., Elliott, E., Dennison, C. and Bruton, A. G. (1992). Further modification of the LKB 7800 series knifemaker for improved reproducibility in breaking 'cryo' knives. *J Microsc.* **168**, 111-114.

Morton, D. B. and Griffiths, P. H. (1985). Guidelines on the recognition of pain, distress and discomfort in experimental animals and an hypothesis for assessment. *Vet Rec.* **116**, 431-436.
Moura, R., Agua-Doce, A., Weinmann, P., Graça, L. and Fonseca, J. E. (2008). B cells from the bench to the clinical practice. *Acta Reumatol Port.* **33**, 137-154.
Mukherjee, S., Ghosh, R. N. and Maxfield, F. R. (1997). Endocytosis. *Physiol Rev.* **77**, 759-803.
Mutasa, H. C. (1989). Applicability of using acrylic resins in post-embedding ultrastructural immunolabelling of human neutrophil granule proteins. *Histochem J.* **21**, 249-258.
Nathan, C. F. (1987). Secretory products of macrophages. *J Clin Invest.* **79**, 319-326.
Nepal, R. M., Mampe, S., Shaffer, B., Erickson, A. H. and Bryant, P. (2006). Cathepsin L maturation and activity is impaired in macrophages harboring *M. avium* and *M. tuberculosis*. *Int Immunol.* **18**, 931-939.
Newman, G. R. and Hobot, J. A. (1987). Modern acrylics for post-embedding immunostaining techniques. *J Histochem Cytochem.* **35**, 971-981.
Ninfa, A. J. and Ballou, D. P. (1998). Gel electrophoresis of proteins. In *Fundamental Laboratory Approches for Biochemistry and Biotechnology.* , pp. 125-145. Maryland: Fitzgerald Science Press, Inc.
Nishida, N., Walz, T. and Springer, T. A. (2006). Structural transitions of complement component C3 and its activation products. *Proc Natl Acad Sci U S A.* **103**, 19737-19742.
Nishiuchi, Y., Inui, T., Nishio, H., Bódi, J., Kimura, T., Tsuji, F. I. and Sakakibara, S. (1998). Chemical synthesis of the precursor molecule of the Aequorea green fluorescent protein, subsequent folding, and development of fluorescence. *Proc Natl Acad Sci U S A.* **95**, 13549-13554.
Niwa, H., Inouye, S., Hirano, T., Matsuno, T., Kojima, S., Kubota, M., Ohashi, M. and Tsuji, F. I. (1996). Chemical nature of the light emitter of the Aequorea green fluorescent protein. *Proc Natl Acad Sci U S A.* **93**, 13617-13622.
Noble, A. (2000). Review article: molecular signals and genetic reprogramming in peripheral T-cell differentiation. *Immunology.* **101**, 289-299.
Novotny, L., Halouzka, R., Matlova, L., Vavra, O., Bartosova, L., Slany, M. and Pavlik, I. (2010). Morphology and distribution of granulomatous inflammation in freshwater ornamental fish infected with mycobacteria. *J Fish Dis.* **33**, 946-955.
O'Brien, D. K. and Melville, S. B. (2000). The anaerobic pathogen *Clostridium perfringens* can escape the phagosome of macrophages under aerobic conditions. *Cell Microbiol.* **2**, 505-519.
Oberholzer, M., Ostreicher, M., Christen, H. and Brühlmann, M. (1996). Methods in quantitative image analysis. *Histochem Cell Biol.* **105**, 333-355.
Oda, K., Matsuda, H., Murakami, T., Katayama, S., Ohgitani, T. and Yoshikawa, M. (2000). Adjuvant and haemolytic activities of 47 saponins derived from medicinal and food plants. *Biol Chem.* **381**, 67-74.
Ogawa, H., Inouye, S., Tsuji, F. I., Yasuda, K. and Umesono, K. (1995). Localization, trafficking, and temperature-dependence of the Aequorea green fluorescent protein in cultured vertebrate cells. *Proc Natl Acad Sci U S A.* **92**, 11899-11903.

Ohri, S. S., Vashishta, A., Proctor, M., Fusek, M. and Vetvicka, V. (2007). Depletion of procathepsin D gene expression by RNA interference: a potential therapeutic target for breast cancer. *Cancer Biol Ther.* **6**, 1081-1087.
Ohshita, T. and Hiroi, Y. (2006). Cathepsin L plays an important role in the lysosomal degradation of L-lactate dehydrogenase. *Biosci Biotechnol Biochem.* **70**, 2254-2261.
Opie, E. L. and Freund, J. (1937). An experimental study of protective inoculation with heat killed tubercle bacilli. *J Exp Med.* **66**, 761-788.
Ornstein, L. (1964). Disc electrophoresis. I. Background and theory. *Ann NY Acad Sci.* **121**, 321-349.
Oxvig, C., Lu, C. and Springer, T. A. (1999). Conformational changes in tertiary structure near the ligand binding site of an integrin I domain. *Proc Natl Acad Sci U S A.* **96**, 2215-2220.
Paddock, S. W. (1999). An introduction to Confocal imaging. In *Confocal Microscopy Methods and Protocols.*, (ed. S. W. Paddock), pp. 1-34. New Jersey: Humana Press.
Pálffy, R., Gardlík, R., Behuliak, M., Kadasi, L., Turna, J. and Celec, P. (2009). On the physiology and pathophysiology of antimicrobial peptides. *Mol Med.* **15**, 51-59.
Palmieri, M. and Kiss, J. Z. (2005). A novel technique for flat-embedding cryofixed plant specimens in LR white resin. *Microsc Res Tech.* **68**, 80-84.
Pandey, K. N. (2009). Functional roles of short sequence motifs in the endocytosis of membrane receptors. *Front Biosci.* **14**, 5339-5360.
Parsons, R. F., Vivek, K., Redfield, R. R., Migone, T. S., Cancro, M. P., Naji, A. and Noorchashm, H. (2009). B-cell tolerance in transplantation: is repertoire remodeling the answer? *Expert Rev Clin Immunol.* **5**, 703-738.
Patterson, A. M., Schmutz, C., Davis, S., Gardner, L., Ashton, B. A. and Middleton, J. (2002). Differential binding of chemokines to macrophages and neutrophils in the human inflamed synovium. *Arthritis Res.* **4**, 209-214.
Patterson, G. H., Knobel, S. M., Sharif, W. D., Kain, S. R. and Piston, D. W. (1997). Use of the green fluorescent protein and its mutants in quantitative fluorescence microscopy. *Biophys J.* **73**, 2782-2790.
Pearson, C. M., Waksman, B. H. and Sharp, J. T. (1961). Studies of arthritis and other lesions induced in rats by injection of mycobacterial adjuvant. V. Changes affecting the skin and mucous membranes. Comparison of the experimental process with human disease. *J Exp Med.* **113**, 485-510.
Penna, A. and Cahalan, M. (2007). Western Blotting Using the Invitrogen NuPage Novex Bis Tris MiniGels. *J Vis Exp.* **264**, 1-3.
Perkins-Balding, D., Ratliff-Griffin, M. and Stojiljkovic, I. (2004). Iron transport systems in *Neisseria meningitidis*. *Microbiol Mol Biol Rev.* **68**, 154-171.
Pettegrew, C. J., Jayini, R. and Islam, M. R. (2009). **Transfer buffer containing methanol can be reused multiple times in protein electrotransfer.** *J Biomol Tech.* **20**, 93-95.
Piguet, V., Gu, F., Foti, M., Demaurex, N., Gruenberg, J., Carpentier, J. L. and Trono, D. (1999). Nef-induced CD4 degradation: a diacidic-based motif in Nef functions as a lysosomal targeting signal through the binding of beta-COP in endosomes. *Cell.* **97**, 63-73.
Pillion, D. J., Amsden, J. A., Kensil, C. R. and Recchia, J. (1996). Structure-function relationship among *Quillaja* saponins serving as excipients for nasal and ocular delivery of insulin. *J Pharm Sci.* **85**, 518-524.

Pitt-Rivers, R. and Impiombato, F. S. (1968). The binding of sodium dodecyl sulphate to various proteins. *Biochem J.* **109**, 825-830.
Pitt, A., Mayorga, L. S., Stahl, P. D. and Schwartz, A. L. (1992). Alterations in the protein composition of maturing phagosomes. *J Clin Invest.* **90**, 1978-1983.
Ploegh, H. L. (2007). Bridging B cell and T cell recognition of antigen. *J Immunol.* **179**, 7193-7193.
Polak, J. M. and Van Noorden, S. (1997). Introduction. In *Introduction to Immunocytochemistry.*, (ed. P. Goldby), pp. 1-3. New York: BIOS Scientific Publishers.
Polson, A., Coetzer, T., Kruger, J., von Maltzahn, E. and van der Merwe, K. J. (1985). Improvements in the isolation of IgY from the yolks of eggs laid by immunized hens. *Immunol Invest.* **14**, 323-327.
Polson, A., von Wechmar, M. B. and Fazakerley, G. (1980). Antibodies to proteins from yolk of immunized hens. *Immunol Commun.* **9**, 495-514.
Pommier, C. G., Inada, S., Fries, L. F., Takahashi, T., Frank, M. M. and Brown, E. J. (1983). Plasma fibronectin enhances phagocytosis of opsonized particles by human peripheral blood monocytes. *J Exp Med.* **157**, 1844-1854.
Prada-Delgado, A., Carrasco-Marin, E., Bokoch, G. M. and Alvarez-Dominguez, C. (2001). Interferon-gamma listericidal action is mediated by novel Rab5a functions at the phagosomal environment. *J Biol Chem.* **276**, 19059-19065.
Rabb, H. (2002). The T cell as a bridge between innate and adaptive immune systems: implications for the kidney. *Kidney Int.* **61**, 1935-1946.
Raja, A. (2004). Immunology of tuberculosis. *Indian J Med Res.* **120**, 213-232.
Rajput, Z. I., Hu, S. H., Xiao, C. W. and Arijo, A. G. (2007). Adjuvant effects of saponins on animal immune responses. *J Zhejiang Univ Sci B.* **8**, 153-161.
Ralph, P. and Nakoinz, I. (1977). Antibody-dependent killing of erythrocyte and tumor targets by macrophage-related cell lines: enhancement by PPD and LPS. *J Immunol.* **119**, 950-954.
Ramachandra, L., Noss, E., Boom, W. H. and Harding, C. V. (2001). Processing of *Mycobacterium tuberculosis* antigen 85B involves intraphagosomal formation of peptide-major histocompatibility complex II complexes and is inhibited by live bacilli that decrease phagosome maturation. *J Exp Med.* **194**, 1421-1432.
Reeve, I., Hummel, D., Nelson, N. and Voss, J. (2002). Overexpression, purification, and site-directed spin labeling of the Nramp metal transporter from *Mycobacterium leprae*. *Proc Natl Acad Sci U S A.* **99**, 8608-8613.
Reifenrath, W. G., Prystowsky, S. D., Nonomura, J. H. and Robinson, P. B. (1985). Topical glutaraldehyde-percutaneous penetration and skin irritation. *Arch Dermatol Res.* **277**, 242-244.
Rennie, B., Filion, L. G. and Smart, N. (2010). Antibody response to a sterile filtered PPD tuberculin in *M. bovis* infected and *M. bovis* sensitized cattle. *BMC Vet Res.* **6**, 50-63.
Riezman, H., Woodman, P. G., van Meer, G. and Marsh, M. (1997). Molecular mechanisms of endocytosis. *Cell.* **91**, 731-738.
Rigdon, R. H. and Schadewald, T. (1972). Bacteriological and pathological study of animals given Freund adjuvant. *Appl Microbiol.* **24**, 634-637.
Riguera, R. (1997). Isolating bioactive compounds from marine organisms. *J. Marine Biotechnol.* **5**, 187-193.

Roberg, K. and Ollinger, K. (1998). A pre-embedding technique for immunocytochemical visualization of cathepsin D in cultured cells subjected to oxidative stress. *J Histochem Cytochem.* **46**, 411-418.
Rocha-de-Souza, C. M., Berent-Maoz, B., Mankuta, D., Moses, A. E. and Levi-Schaffer, F. (2008). Human mast cell activation by Staphylococcus aureus: interleukin-8 and tumor necrosis factor alpha release and the role of Toll-like receptor 2 and CD48 molecules. *Infect Immun.* **76**, 4489-4497.
Rocha, N. and Neefjes, J. (2008). MHC class II molecules on the move for successful antigen presentation. *EMBO J.* **27**, 1-5.
Rohrer, J., Schweizer, A., Russell, D. and Kornfeld, S. (1996). The targeting of Lamp1 to lysosomes is dependent on the spacing of its cytoplasmic tail tyrosine sorting motif relative to the membrane. *J Cell Biol.* **132**, 565-576.
Roitt, I. M. (2006). Antibodies. In *Roitt's Essential Immunology*, pp. 37-52. Oxford: Blackwell Publishing.
Rojas-Espinosa, O., Dannenberg, A. M., Murphy, P. A., Straat, P. A., Huang, P. C. and James, S. P. (1973). Purification and properties of the cathepsin D types proteinase from beef and rabbit lung and its identification in macrophages. *Infect Immun.* **8**, 1000-1008.
Romagnoli, P., Layet, C., Yewdell, J., Bakke, O. and Germain, R. N. (1993). Relationship between invariant chain expression and major histocompatibility complex class II transport into early and late endocytic compartments. *J Exp Med.* **177**, 583-596.
Roth, J. (1982). Applications of immunocolloids in light microscopy. Preparation of protein A-silver and protein A-gold complexes and their application for localization of single and multiple antigens in paraffin sections. *J Histochem Cytochem.* **30**, 691-696.
Roth, J., Bendayan, M. and Orci, L. (1978). Ultrastructural localization of intracellular antigens by the use of protein A-gold complex. *J Histochem Cytochem.* **26**, 1074-1081.
Rothman, J. E. and Orci, L. (1990). Movement of proteins through the Golgi stack: a molecular dissection of vesicular transport. *FASEB J* **4**, 1460-1468.
Rueden, C. T. and Eliceiri, K. W. (2007). Visualization approaches for multidimensional biological image data. *Biotechniques.* **43**, 33-36.
Russell, D. G. (2001). *Mycobacterium tuberculosis*: here today, and here tomorrow. *Nat Rev Mol Cell Biol.* **2**, 569-577.
Russell, D. G., Vanderven, B. C., Glennie, S., Mwandumba, H. and Heyderman, R. S. (2009). The macrophage marches on its phagosome: dynamic assays of phagosome function. *Nat Rev Immunol.* **9**, 594-600.
Sabatini, D. D., Bensch, K. and Barrnett, R. J. (1963). Cytochemistry and electron microscopy. The preservation of cellular ultrastructure and enzymatic activity by aldehyde fixation. *J Cell Biol.* **17**, 19-58.
Sagné, C., Agulhon, C., Ravassard, P., Darmon, M., Hamon, M., El Mestikawy, S., Gasnier, B. and Giros, B. (2001). Identification and characterization of a lysosomal transporter for small neutral amino acids. *Proc Natl Acad Sci U S A.* **98**, 7206-7211.
Sakai, Y., Hosaka, M., Hira, Y. and Watanabe, T. (2005). Addition of phosphotungstic acid to ethanol for dehydration improves both the ultrastructure and antigenicity of pituitary tissue embedded in LR White acrylic resin. *Arch Histol Cytol.* **68**, 337-347.

Sánchez-Mejorada, G. and Rosales, C. (1998). Signal transduction by immunoglobulin Fc receptors. *J Leukoc Biol.* **63**, 521-533.
Santama, N., Krijnse-Locker, J., Griffiths, G., Noda, Y., Hirokawa, N. and Dotti, C. G. (1998). KIF2beta, a new kinesin superfamily protein in non-neuronal cells, is associated with lysosomes and may be implicated in their centrifugal translocation. *EMBO J.* **17**, 5855-5867.
Sarath, G., De La Motte, R. S. and Wagner, F. W. (1989). Protease assay methods. In *Protelytic enzymes a practical approach.*, (ed. R. J. Beynon and J. S. Bond). Oxford: IRL Press.
Sasaki, S., Sumino, K., Hamajima, K., Fukushima, J., Ishii, N., Kawamoto, S., Mohri, H., Kensil, C. R. and Okuda, K. (1998). Induction of systemic and mucosal immune responses to human immunodeficiency virus type 1 by a DNA vaccine formulated with QS-21 saponin adjuvant via intramuscular and intranasal routes. *J Virol.* **72**, 4931-4939.
Savina, A., Jancic, C., Hugues, S., Guermonprez, P., Vargas, P., Moura, I. C., Lennon-Duménil, A. M., Seabra, M. C., Raposo, G. and Amigorena, S. (2006). NOX2 controls phagosomal pH to regulate antigen processing during crosspresentation by dendritic cells. *Cell.* **126**, 205-218.
Savino, W., de Moraes Mdo, C., Barbosa, S. D., Da Fonseca, E. C., De Almeida, V. C. and Hontebeyrie-Joscowicz, M. (1992). Is the thymus a target organ in infectious diseases? *Mem Inst Oswaldo Cruz.* **87**, 73-78.
Schaible, U. E., Sturgill-Koszycki, S., Schlesinger, P. H. and Russell, D. G. (1998). Cytokine activation leads to acidification and increases maturation of *Mycobacterium avium*-containing phagosomes in murine macrophages. *J Immunol.* **160**, 1290-1296.
Schalkwijk, C., Pfeilschifter, J., Märki, F. and van den Bosch, H. (1992). Interleukin-1 beta- and forskolin-induced synthesis and secretion of group II phospholipase A2 and prostaglandin E2 in rat mesangial cells is prevented by transforming growth factor-beta 2. *J Biol Chem.* **267**, 8846-8851.
Schechter, I. and Berger, A. (1967). On the size of the active site in proteases. I. Papain. *Biochem Biophys Res Commun.* **27**, 157-162.
Schmid, B., Schindelin, J., Cardona, A., Longair, M. and Heisenberg, M. (2010). A high-level 3D visualization API for Java and ImageJ. *BMC Bioinformatics.* **11**, 274-280.
Schorey, J. S. and Cooper, A. M. (2003). Macrophage signalling upon mycobacterial infection: the MAP kinases lead the way. *Cell Microbiol.* **5**, 133-142.
Schroeder, R. J., Ahmed, S. N., Zhu, Y., London, E. and Brown, D. A. (1998). Cholesterol and sphingolipid enhance the Triton X-100 insolubility of glycosylphosphatidylinositol-anchored proteins by promoting the formation of detergent-insoluble ordered membrane domains. *J Biol Chem.* **273**, 1150-1157.
Scully, C. M. and Lehner, T. (1979). Opsonization, phagocytosis and killing of Streptococcus mutans by polymorphonuclear leukocytes, in relation to dental caries in the rhesus monkey (Macaca mulatta). *Arch Oral Biol.* **24**, 307-312.
Segura, M. and Gottschalk, M. (2002). *Streptococcus suis* Interactions with the Murine Macrophage Cell Line J774: Adhesion and Cytotoxicity. *Infect Immun.* **70**, 4312–4322.
Selmi, S. and Rousset, B. (1988). Identification of two subpopulations of thyroid lysosomes: relation to the thyroglobulin proteolytic pathway. *Biochem J.* **253**, 523-532.

Sendide, K., Deghmane, A. E., Pechkovsky, D., Av-Gay, Y., Talal, A. and Hmama, Z. (2005). *Mycobacterium bovis* BCG attenuates surface expression of mature class II molecules through IL-10-dependent inhibition of cathepsin S. *J Immunol.* **175**, 5324-5332.
Seto, S., Matsumoto, S., Ohta, I., Tsujimura, K. and Koide, Y. (2009). Dissection of Rab7 localization on *Mycobacterium tuberculosis* phagosome. *Biochem Biophys Res Commun.* **387**, 272-277.
Shapiro, A. L., Viñuela, E. and Maizel, J. V. (1967). Molecular weight estimation of polypeptide chains by electrophoresis in SDS-polyacrylamide gels. *Biochem Biophys Res Commun.* **28**, 815-820.
Shaw, C. M., Alvord, E. C. and Kies, M. W. (1964). Straight chain hydrocarbons as substitutes for the oil in Freund's adjuvants in the porduction of experimental "Allergic" Encephalomyelitis in the Guinea Pig. *J Immunol.* **92**, 24-27.
Sheppard, C. J. R. and Shotton, D. M. (1997a). Image Processing of confocal image data sets. In *Confocal Laser Scanning Microscopy.*, pp. 45-60. New York: Bios Scientific Publishers.
Sheppard, C. J. R. and Shotton, D. M. (1997b). Introduction. In *Confocal Laser Scanning Microscopy*, pp. 1-10. New York: Bios Scientific Publishers.
Shi, L., Günther, S., Hübschmann, T., Wick, L. Y., Harms, H. and Müller, S. (2007). Limits of propidium iodide as a cell viability indicator for environmental bacteria. *Cytometry A.* **71**, 592-598.
Shi, Y., Liu, C. H., Roberts, A. I., Das, J., Xu, G., Ren, G., Zhang, Y., Zhang, L., Yuan, Z. R., Tan, H. S. *et al.* (2006). Granulocyte-macrophage colony-stimulating factor (GM-CSF) and T-cell responses: what we do and don't know. *Cell Res.* **16**, 126-133.
Shiloh, M. U. and DiGiuseppe Champion, P. A. (2010). To catch a killer. What can mycobacterial models teach us about *Mycobacterium tuberculosis* pathogenesis? *Curr Opin Microbiol.* **13**, 86-92.
Shim, J., Sternberg, P. W. and Lee, J. (2000). Distinct and redundant functions of mu1 medium chains of the AP-1 clathrin-associated protein complex in the nematode Caenorhabditis elegans. *Mol Biol Cell.* **11**, 2743-2756.
Shotton, D. M. (1989). Confocal scanning optical microscopy and its applications for biological specimens. *J Cell Sci.* **94**, 175-206.
Siemering, K. R., Golbik, R., Sever, R. and Haseloff, J. (1996). Mutations that suppress the thermosensitivity of green fluorescent protein. *Curr Biol.* **6**, 1653-1663.
Sigaut, S., Jannier, V., Rouelle, D., Gressens, P., Mantz, J. and Dahmani, S. (2009). The preconditioning effect of sevoflurane on the oxygen glucose-deprived hippocampal slice: the role of tyrosine kinases and duration of ischemia. *Anesth Analg.* **108**, 601-608.
Silva, C. L. and Faccioli, L. H. (1992). Tumor necrosis factor and macrophage activation are important in clearance of Nocardia brasiliensis from the livers and spleens of mice. *Infect Immun.* **60**, 3566-3570.
Silva, M. T., Appelberg, R., Silva, M. N. and Macedo, P. M. (1987). In vivo killing and degradation of *Mycobacterium aurum* within mouse peritoneal macrophages. *Infect Immun.* **55**, 2006-2016.
Singh, C. R., Moulton, R. A., Armitige, L. Y., Bidani, A., Snuggs, M., Dhandayuthapani, S., Hunter, R. L. and Jagannath, C. (2006). Processing and presentation of a mycobacterial antigen 85B epitope by murine macrophages is

dependent on the phagosomal acquisition of vacuolar proton ATPase and in situ activation of cathepsin D. *J Immunol.* **177**, 3250-3259.
Singh, N., Agrawal, S. and Rastogi, A. K. (1997). Infectious diseases and immunity: special reference to major histocompatibility complex. *Emerg Infect Dis.* **3**, 41-49.
Sisson, S. P. and Vernier, R. L. (1980). Methods for immunoelectron microscopy: Localization of antigens in rat kidney. *J Histochem Cytochem.* **28**, 441-452.
Sjölander, A., Drane, D., Maraskovsky, E., Scheerlinck, J. P., Suhrbier, A., Tennent, J. and Pearse, M. (2001). Immune responses to ISCOM formulations in animal and primate models. *Vaccine.* **19**, 2661-2665.
Smith, J., Manoranjan, J., Pan, M., Bohsali, A., Xu, J., Liu, J., McDonald, K. L., Szyk, A., LaRonde-LeBlanc, N. and Gao, L. Y. (2008). Evidence for pore formation in host cell membranes by ESX-1-secreted ESAT-6 and its role in *Mycobacterium marinum* escape from the vacuole. *Infect Immun.* **76**, 5478-5487.
Smith, R. M. and Curnutte, J. T. (1991). Molecular basis of chronic granulomatous disease. *Blood.* **77**, 673-686.
Smith, W. D. and Pettit, D. M. (2004). Immunization against sheep scab: preliminary identification of fractions of Psoroptes ovis which confer protective effects. *Parasite Immunol.* **26**, 307-314.
Somsel Rodman, J. and Wandinger-Ness, A. (2000). Rab GTPases coordinate endocytosis. *J Cell Sci.* **113**, 183-192.
Stahlberg, H. and Walz, T. (2008). Molecular electron microscopy: state of the art and current challenges. *ACS Chem Biol.* **3**, 268-281.
Steblay, R. W. and Rudofsky, U. H. (1983). Experimental autoimmune glomerulonephritis induced by anti-glomerular basement membrane antibody. II. Effects of injecting heterologous, homologous, or autologous glomerular basement membranes and complete Freund's adjuvant into sheep. *Am J Pathol.* **113**, 125-133.
Steinberg, B. E., Huynh, K. K. and Grinstein, S. (2007). Phagosomal acidification: measurement, manipulation and functional consequences. *Biochem Soc Trans.* **35**, 1083-1087.
Steinberg, T. H. (2009). Protein gel staining methods: an introduction and overview. *Methods Enzymol.* **463**, 541-563.
Stills, H. F. (2005). Adjuvants and antibody production: dispelling the myths associated with Freund's complete and other adjuvants. *ILAR J.* **46**, 280-293.
Stockwin, L. H., McGonagle, D., Martin, I. G. and Blair, G. E. (2000). Dendritic cells: immunological sentinels with a central role in health and disease. *Immunol Cell Biol.* **78**, 91-102.
Straus, W. (1982). Imidazole increases the sensitivity of the cytochemical reaction for peroxidase with diaminobenzidine at a neutral pH. *J Histochem Cytochem.* **30**, 491-493.
Stuewart-Tull, D. E., Shimono, T., Kotani, S. and Knights, B. A. (1976). Immunosuppressive effect in mycobacterial adjuvant emulsions of mineral oils containing low molecular weight hydrocarbons. *Int Arch Allergy Appl Immunol.* **52**, 118-128.
Sturgill-Koszycki, S., Schaible, U. E. and Russell, D. G. (1996). Mycobacterium-containing phagosomes are accessible to early endosomes and reflect a transitional state in normal phagosome biogenesis. *EMBO J.* **15**, 6960-6968.
Sturgill-Koszycki, S., Schlesinger, P. H., Chakraborty, P., Haddix, P. L., Collins, H. L., Fok, A. K., Allen, R. D., Gluck, S. L., Heuser, J. and Russell, D. G. (1994).

Lack of acidification in Mycobacterium phagosomes produced by exclusion of the vesicular proton-ATPase. *Science.* **263**, 678-681.
Sugawara, I., Mizuno, S., Tatsumi, T. and Taniyama, T. (2006). Imaging of pulmonary granulomas using a photon imager. *Jpn J Infect Dis.* **59**, 332-333.
Sun-Wada, G. H., Wada, Y. and Futai, M. (2003). Lysosome and lysosome-related organelles responsible for specialized functions in higher organisms, with special emphasis on vacuolar-type proton ATPase. *Cell Struct Funct.* **28**, 455-463.
Sun, J., Song, X. and Hu, S. (2008). Ginsenoside Rg1 and aluminum hydroxide synergistically promote immune responses to ovalbumin in BALB/c mice. *Clin Vaccine Immunol.* **15**, 303-307.
Sun, J., Wang, X., Lau, A., Liao, T. Y., Bucci, C. and Hmama, Z. (2010). Mycobacterial nucleoside diphosphate kinase blocks phagosome maturation in murine RAW 264.7 macrophages. *PLoS One.* **5**, e8769-e8780.
Suzuki, T., Fujikura, K., Higashiyama, T. and Takata, K. (1997). DNA staining for fluorescence and laser confocal microscopy. *J Histochem Cytochem.* **45**, 49-53.
Swanson, J. A. and Hoppe, A. D. (2004). The coordination of signaling during Fc receptor-mediated phagocytosis. *J Leukoc Biol.* **76**, 1093-1103.
Switzer, R. and Garrity, L. (1999). Electrophoresis. In *Experimental biochemistry*, pp. 61-77. New York: W.H. Freeman and Company.
Tabel, H. and Ingram, D. G. (1971). Effect of Freund's adjuvant on standard dark and pastel mink. *Can J Comp Med.* **35**, 115-120.
Takagi, A., Matsui, M., Ohno, S., Duan, H., Moriya, O., Kobayashi, N., Oda, H., Mori, M., Kobayashi, A., Taneichi, M. *et al.* (2009). Highly efficient antiviral CD8+ T-cell induction by peptides coupled to the surfaces of liposomes. *Clin Vaccine Immunol.* **16**, 1383-1392.
Takahashi, T. and Tang, J. (1981). Cathepsin D from porcine and bovine spleen. *Methods Enzymol.* **80**, 565-581.
Takayama, K. and Kilburn, J. O. (1989). Inhibition of synthesis of arabinogalactan by ethambutol in *Mycobacterium smegmatis*. *Antimicrob Agents Chemother* **33**, 1493-1499.
Tanaka, Y., Guhde, G., Suter, A., Eskelinen, E. L., Hartmann, D., Lüllmann-Rauch, R., Janssen, P. M., Blanz, J., von Figura, K. and Saftig, P. (2000). Accumulation of autophagic vacuoles and cardiomyopathy in LAMP-2-deficient mice. *Nature* **406**, 902-906.
Tell, L. A., Woods, L. and Cromie, R. L. (2001). Mycobacteriosis in birds. *Rev Sci Tech.* **20**, 180-203.
Thilo, L., Stroud, E. and Haylett, T. (1995). Maturation of early endosomes and vesicular traffic to lysosomes in relation to membrane recycling. *J Cell Sci.* **108**, 1791-1803.
Thorne, K. J., Oliver, R. C. and Barrett, A. J. (1976). Lysis and killing of bacteria by lysosomal proteinases. *Infect Immun.* **14**, 555-563.
Toca-Herrera, J. L., Küpcü, S., Diederichs, V., Moncayo, G., Pum, D. and Sleytr, U. B. (2006). Fluorescence emission properties of S-Layer enhanced green fluorescent fusion protein as a function of temperature, pH conditions, and guanidine hydrochloride concentration. *Biomacromolecules.* **7**, 3298-3301.
Torres, M., Ramachandra, L., Rojas, R. E., Bobadilla, K., Thomas, J., Canaday, D. H., Harding, C. V. and Boom, W. H. (2006). Role of phagosomes and major

histocompatibility complex class II (MHC-II) compartment in MHC-II antigen processing of *Mycobacterium tuberculosis* in human macrophages. *Infect Immun.* **74**, 1621-1630.
Towbin, H., Staehelin, T. and Gordon, J. (1979). Electrophoretic transfer of proteins from polyacrylamide gels to nitrocellulose sheets: procedure and some applications. *Proc Natl Acad Sci U S A.* **76**, 4350-4359.
Tufariello, J. M., Chan, J. and Flynn, J. L. (2003). Latent tuberculosis: mechanisms of host and bacillus that contribute to persistent infection. *Lancet Infect Dis.* **3**, 578-590.
Turk, V., Turk, B. and Turk, D. (2001). Lysosomal cysteine proteases: facts and opportunities. *EMBO J.* **20**, 4629-4633.
Ulanova, M., Tarkowski, A., Hahn-Zoric, M. and Hanson, L. A. (2001). The Common vaccine adjuvant aluminum hydroxide up-regulates accessory properties of human monocytes via an interleukin-4-dependent mechanism. *Infect Immun.* **69**, 1151-1159.
Unal Cevik, I. and Dalkara, T. (2003). Intravenously administered propidium iodide labels necrotic cells in the intact mouse brain after injury. *Cell Death Differ.* **10**, 928-929.
Unanue, E. R. (1976). Secretory function of mononuclear phagocytes: a review. *Am J Pathol.* **83**, 396-418.
Unanue, E. R., Beller, D. I., Calderon, J., Kiely, J. M. and Stadecker, M. J. (1976). Regulation of immunity and inflammation by mediators from macrophages. *Am J Pathol.* **85**, 465-478.
Utermöhlen, O., Karow, U., Löhler, J. and Krönke, M. (2003). Severe impairment in early host defense against *Listeria monocytogenes* in mice deficient in acid sphingomyelinase. *J Immunol.* **170**, 2621-2628.
van den Eertwegh, A. J., Laman, J. D., Noelle, R. J., Boersma, W. J. and Claassen, E. (1994). In vivo T-B cell interactions and cytokine-production in the spleen. *Semin Immunol.* **6**, 327-336.
van Egmond, M., Hanneke van Vuuren, A. J. and van de Winkel, J. G. (1999). The human Fc receptor for IgA (Fc alpha RI, CD89) on transgenic peritoneal macrophages triggers phagocytosis and tumor cell lysis. *Immunol Lett.* **68**, 83-87.
Van Ginderachter, J. A., Movahedi, K., Hassanzadeh Ghassabeh, G., Meerschaut, S., Beschin, A., Raes, G. and De Baetselier, P. (2006). Classical and alternative activation of mononuclear phagocytes: picking the best of both worlds for tumor promotion. *Immunobiology.* **211**, 487-501.
van Lookeren Campagne, M., Wiesmann, C. and Brown, E. J. (2007). Macrophage complement receptors and pathogen clearance. *Cell Microbiol.* **9**, 2095-2102.
van Meel, E. and Klumperman, J. (2008). Imaging and imagination: understanding the endo-lysosomal system. *Histochem Cell Biol.* **129**, 253-266.
van Noort, J. M. and van der Drift, A. C. (1989). The selectivity of cathepsin D suggests an involvement of the enzyme in the generation of T-cell epitopes. *J Biol Chem.* **264**, 14159-14164.
Vandal, O. H., Pierini, L. M., Schnappinger, D., Nathan, C. F. and Ehrt, S. (2008). A membrane protein preserves intrabacterial pH in intraphagosomal *Mycobacterium tuberculosis*. *Nat Med.* **14**, 849-854.

Veerapandian, B., Cooper, J. B., Sali, A., Blundell, T. L., Rosati, R. L., Dominy, B. W., Damon, D. B. and Hoover, D. J. (1992). Direct observation by X-ray analysis of the tetrahedral "intermediate" of aspartic proteinases. *Protein Sci.* **1**, 322-328.
Veillette, A., Zúñiga-Pflücker, J. C., Bolen, J. B. and Kruisbeek, A. M. (1989). Engagement of CD4 and CD8 expressed on immature thymocytes induces activation of intracellular tyrosine phosphorylation pathways. *J Exp Med.* **170**, 1671-1680.
Velaz-Faircloth, M., Cobb, A. J., Horstman, A. L., Henry, S. C. and Frothingham, R. (1999). Protection against *Mycobacterium avium* by DNA vaccines expressing mycobacterial antigens as fusion proteins with green fluorescent protein. *Infect Immun.* **67**, 4243-4250.
Vergne, I., Chua, J., Singh, S. B. and Deretic, V. (2004). Cell biology of *mycobacterium tuberculosis* phagosome. *Annu Rev Cell Dev Biol.* **20**, 367-394.
Vieira, O. V., Botelho, R. J. and Grinstein, S. (2002). Phagosome maturation: aging gracefully. *Biochem J.* **366**, 689-704.
Viret, C. and Janeway, C. A. (1999). MHC and T cell development. *Rev Immunogenet.* **1**, 91-104.
Vogt, C. J. and Schmid-Schönbein, G. W. (2001). Microvascular endothelial cell death and rarefaction in the glucocorticoid-induced hypertensive rat. *Microcirculation.* **8**, 129-139.
Waghmare, A., Deopurkar, R. L., Salvi, N., Khadilkar, M., Kalolikar, M. and Gade, S. K. (2009). Comparison of Montanide adjuvants, IMS 3012 (Nanoparticle), ISA 206 and ISA 35 (Emulsion based) along with incomplete Freund's adjuvant for hyperimmunization of equines used for production of polyvalent snake antivenom. *Vaccine.* **27**, 1067-1072.
Wagner, D., Maser, J., Moric, I., Boechat, N., Vogt, S., Gicquel, B., Lai, B., Reyrat, J. M. and Bermudez, L. (2005). Changes of the phagosomal elemental concentrations by *Mycobacterium tuberculosis* Mramp. *Microbiology.* **151**, 323-332.
Wallace, J., Sanford, J., Smith, M. W. and Spencer, K. V. (1990). The assessment and control of the severity of scientific procedures on laboratory animals. *Lab Anim.* **24**, 97-130.
Wang, L. and Bosselut, R. (2009). CD4-CD8 lineage differentiation: Thpok-ing into the nucleus. *J Immunol.* **183**, 2903-2910.
Weber, K. and Osborn, M. (1969). The reliability of molecular weight determinations by dodecyl sulfate-polyacrylamide gel electrophoresis. *J Biol Chem.* **244**, 4406-4412.
Weiss, D. J. and Souza, C. D. (2008). Review paper: modulation of mononuclear phagocyte function by *Mycobacterium avium* subsp. paratuberculosis. *Vet Pathol.* **45**, 829-841.
Wilkinson, P. C. (1976). Recognition and response in mononuclear and granular phagocytes. *Clin Exp Immunol.* **25**, 355-366.
Wille, A., Gerber, A., Heimburg, A., Reisenauer, A., Peters, C., Saftig, P., Reinheckel, T., Welte, T. and Bühling, F. (2004). Cathepsin L is involved in cathepsin D processing and regulation of apoptosis in A549 human lung epithelial cells. *Biol Chem.* **385**, 665-670.
Willson, P. J., Rossi-Campos, A. and Potter, A. A. (1995). Tissue reaction and immunity in swine immunized with *Actinobacillus pleuropneumoniae* vaccines. *Can J Vet Res.* **59**, 299-305.

Willstätter, R. and Bamann, E. (1929). Uber die proteasen der magenschleimhaut. *Hoppe-Seyler's Z. Physiol. Chem.* **180**, 127–143.
Wilson, T. (1995). The role of the pinhole in confocal imaging system. In *Handbook of Biological Confocal Microscopy*, (ed. J. B. Pawley), pp. 167-182. New York: Plenum Press.
Woodman, P. G. (2000). Biogenesis of the sorting endosome: the role of Rab5. *Traffic* **1**, 695-701.
Xu, S., Cooper, A., Sturgill-Koszycki, S., van Heyningen, T., Chatterjee, D., Orme, I., Allen, P. and Russell, D. G. (1994). Intracellular trafficking in *Mycobacterium tuberculosis* and *Mycobacterium avium*-infected macrophages. *J Immunol.* **153**, 2568-2578.
Yamamoto, T. (2006). Bacterial strategies for escaping the bactericidal mechanisms by macrophage. *Yakugaku Zasshi.* **126**, 1235-1243.
Yanagawa, M., Tsukuba, T., Nishioku, T., Okamoto, Y., Okamoto, K., Takii, R., Terada, Y., Nakayama, K. I., Kadowaki, T. and Yamamoto, K. (2007). Cathepsin E deficiency induces a novel form of lysosomal storage disorder showing the accumulation of lysosomal membrane sialoglycoproteins and the elevation of lysosomal pH in macrophages. *J Biol Chem.* **282**, 1851-1862.
Ye, J., McGinnis, S. and Madden, T. L. (2006). BLAST: improvements for better sequence analysis. *Nucleic Acids Res.* **34**, W6-W9.
Yokota, A., Yukawa, K., Yamamoto, A., Sugiyama, K., Suemura, M., Tashiro, Y., Kishimoto, T. and Kikutani, H. (1992). Two forms of the low-affinity Fc receptor for IgE differentially mediate endocytosis and phagocytosis: identification of the critical cytoplasmic domains. *Proc Natl Acad Sci U S A.* **89**, 5030-5034.
Yonezawa, S., Takahashi, T., Wang, X. J., Wong, R. N., Hartsuck, J. A. and Tang, J. (1988). Structures at the proteolytic processing region of cathepsin D. *J Biol Chem.* **263**, 16504-16511.
Yoshiki, Y., Kudou, S. and Okubo, K. (1998). Relationship between chemical structures and biological activities of triterpenoid saponins from soybean. *Biosci Biotechnol Biochem.* **62**, 2291-2299.
Young, H. A. (2006). Unraveling the pros and cons of interferon-gamma gene regulation. *Immunity.* **24**, 506-507.
Zabrenetzky, V. and Gallin, E. K. (1988). Inositol 1,4,5-trisphosphate concentrations increase after adherence in the macrophage-like cell line J774.1. *Biochem J.* **255**, 1037-1043.
Zaidi, N., Maurer, A., Nieke, S. and Kalbacher, H. (2008). Cathepsin D: a cellular roadmap. *Biochem Biophys Res Commun.* **376**, 5-9.
Zamechnik, P. C. and Stephenson, M. L. (1945). Distribution of Catheptic Enzymes in the Hog Kidney. *J. Biol. Chem.* **159**, 625-629.
Zamecnik, P. C. and Stephenson, M. L. (1945). Distribution of Catheptic Enzymes in the Hog Kidney. *J. Biol. Chem.* **159**, 625-629.
Zasloff, M. (2002). Antimicrobial peptides of multicellular organisms. *Nature.* **415**, 389-395.
Zasloff, M. (2007). Antimicrobial peptides, innate immunity, and the normally sterile urinary tract. *J Am Soc Nephrol.* **18**, 2810-2816.
Zerial, M. and McBride, H. (2001). Rab proteins as membrane organizers. *Nat Rev Mol Cell Biol.* **2**, 107-117.

Zhang, X. and Mosser, D. M. (2008). Macrophage activation by endogenous danger signals. *J Pathol.* **214**, 161-178.
Zhao, M., Yang, M., Baranov, E., Wang, X., Penman, S., Moossa, A. R. and Hoffman, R. M. (2001). Spatial-temporal imaging of bacterial infection and antibiotic response in intact animals. *Proc Natl Acad Sci U S A.* **98**, 9814-9818.
Zhou, B., He, Y., Zhang, X., Xu, J., Luo, Y., Wang, Y., Franzblau, S. G., Yang, Z., Chan, R. J., Liu, Y. *et al.* (2010). Targeting mycobacterium protein tyrosine phosphatase B for antituberculosis agents. *Proc Natl Acad Sci U S A.* **107**, 4573-4578.
Zhou, D., Li, P., Lin, Y., Lott, J. M., Hislop, A. D., Canaday, D. H., Brutkiewicz, R. R. and Blum, J. S. (2005). Lamp-2a facilitates MHC class II presentation of cytoplasmic antigens. *Immunity.* **22**, 571-581.
Ziegler, K. and Unanue, E. R. (1981). Identification of a macrophage antigen-processing event required for I-region-restricted antigen presentation to T lymphocytes. *J Immunol.* **127**, 1869-1875.
Zinchuk, V. and Zinchuk, O. (2008). Quantitative colocalization analysis of confocal fluorescence microscopy images. *Curr Protoc Cell Biol.* **39**, 4.19.1-4.19.16.
Zinchuk, V., Zinchuk, O. and Okada, T. (2007). Quantitative Colocalization Analysis of Multicolor Confocal ImmunofluorescenceMicroscopy Images: Pushing Pixels to Explore Biological Phenomena. *Acta Histochem Cytochem.* **40**, 101-111.